Molekulare und funktionelle Charakterisierung der Typ III-Effektoren XopB, XopL und XopS aus *Xanthomonas campestris* pv. *vesicatoria*

Dissertation

zur Erlangung des
Doktorgrades der Naturwissenschaften (Dr. rer. nat.)

der

Naturwissenschaftlichen Fakultät I
– Biowissenschaften –

der Martin-Luther-Universität
Halle-Wittenberg,

vorgelegt
von
Herrn Sebastian Schulze

geb. am 23.04.1982 in Sangerhausen

Gutachter:

Prof. Dr. U. Bonas

Prof. Dr. D. Scheel

Prof. Dr. M. Göttfert

Verteidigung: 11.10.2013

Inhaltsverzeichnis

Abbildungs- und Tabellenverzeichnis

Abbildungen:

Tabellen:

Abkürzungsverzeichnis

aa	*amino acid*; Aminosäure
Abb.	Abbildung
ATP	Adenosintriphosphat
Avr	Avirulenz
BAK1	*brassinosteroid insensitive kinase* 1
bp	Basenpaar
CDPK	*calcium-dependent protein kinase*
cv.	*cultivar;* Kultivar
DNA	*deoxyribonucleic acid*; Desoxyribonukleinsäure
DAPI	4′,6-Diamidin-2-phenylindol
ECW	*Early Californian Wonder*; Capsicum annuum-Kultivar
EFR	EF-Tu Rezeptor
EF-Tu	Elongationsfaktor Tu
EPS	extrazelluläre Polysaccharide
ER	endoplasmatisches Retikulum
ETI	*effector-triggered immunity*
ETS	*effector-triggered susceptibility*
FLS2	*flagellin-sensing* 2
FRK1	*flg22-induced receptor kinase* 1
GFP	grün-fluoreszierendes Protein
Hop	*Hrp outer Protein*
hpa	*hrp-associated*
hrc	*hrp-conserved*
hrp	*hypersensitive response and pathogenicity*
KBE	Kolonie-bildende Einheiten
kDa	Kilodalton
LRR	Leuzin-reiche Region
LUC	Luciferase
LV	*Leervektor*
MAPK/MPK	Mitogen-aktivierte Proteinkinase
MAPKK/MKK	MAP Kinase-Kinase
NHL10	*NDR1/ HIN1-LIKE 10*
OD	optische Dichte

PAGE	Polyacrylamidgelelektrophorese
PAMP	*pathogen associated molecular pattern*
PCD	*plant cell death*
PCR	*polymerase chain reaction*; Polymerasekettenreaktion
PHI-1	*phosphate-induced* 1
PIP	plant-inducible promoter
PR	*pathogenesis-related*
PRR	*pattern recognition receptor*
PTI	*PAMP triggered immunity*
pv.	Pathovar
R	Resistenz
RNA	*ribonucleic acid*; Ribonukleinsäure
ROS	*reactive oxygen species;* reaktive Sauerstoffspezies
SCF	Skp, Cullin und F-Box
SDS	Natriumdodecylsulfat
SnRK1	*sucrose nonfermenting* 1-*related kinase* 1
Sop	*Salmonella outer protein*
spp.	*species pluralis*; Subspezies
SUMO	*small ubiquitin-related modifier*
T3E	Typ III-Effektor
T3S	Typ III-Sekretion
T3SS	Typ III-Sekretionssystem
TAL	*transcription activator-like*
Ub	Ubiquitin
UMP	Uridinmonophosphat
UPA	upregulated by AvrBs3
VIGS	Virus-induziertes Gen-*silencing*
X.	*Xanthomonas*
Xac	*Xanthomonas axonopodis* pv. *citri*
Xcc	*Xanthomonas campestris* pv. *campestris*
Xcv	*Xanthomonas campestris* pv. *vesicatoria*
Xoc	*Xanthomonas oryzae* pv. *oryzicola*
Xoo	*Xanthomonas oryzae* pv. *oryzae*
Xop	*Xanthomonas outer protein*
Yop	*Yersinia outer protein*

1. Einleitung

1.1 Interaktion von Pflanzen und pathogenen Mikroorganismen

Organismen eines Ökosystems stehen in ständiger Interaktion miteinander. Die Interaktionen können zum gegenseitigen Nutzen (Mutualismus, Symbiose), aber auch zum Nachteil eines Organismus sein (Parasitismus, Räuber-Beute-Beziehung, (Long und Staskawicz, 1993). Parasiten schädigen den besiedelten Organismus (Wirt), was oft zur Ausbildung von Krankheiten führt.

Pathogene, die Pflanzen befallen und Krankheiten auslösen, werden als Phytopathogene bezeichnet. Hierzu zählen Pilze, Oomyzeten, Nematoden, Viren und Bakterien. Pflanzenkrankheiten führen zu schweren Schäden an Nutzpflanzen und bewirken damit erhebliche Ernteverluste, was wiederum einen dramatischen Einfluss auf die Landwirtschaft haben kann (Dodds und Rathjen, 2010).

Jedoch stellen nicht alle Krankheitserreger eine Gefahr für Pflanzen dar. Die meisten Pflanzenspezies sind Nicht-Wirts-Organismen und können nicht von Parasiten oder Pathogenen befallen werden (Nicht-Wirts-Resistenz; Heath, 2000).

Die erfolgreiche Infektion einzelner Pflanzenspezies ist somit eine Ausnahme. Nur spezialisierte phytopathogene Pilze, Oomyzeten und Bakterien sind in der Lage den Stoffwechsel der Pflanzen zum eigenen Nutzen zu manipulieren und Krankheiten auszulösen (Thordal-Christensen, 2003). Gram-negative Bakterien der Gattungen *Xanthomonas*, *Pseudomonas*, *Agrobacterium* und *Erwinia* stehen besonders im Fokus der Wissenschaft. Die genannten Bakteriengattungen sind leicht zugänglich für molekularbiologische Untersuchungen und ermöglichen detaillierte Charakterisierungen von Pflanzen-Pathogen-Interaktionen. Analysen dieser Interaktionen erlauben nützliche Einblicke in pflanzliche Abwehrprozesse und deren Manipulation durch phytopathogene Bakterien. Diese Erkenntnisse liefern neue biotechnologische Möglichkeiten, um Nutzpflanzen effizient zu schützen (Dodds und Rathjen, 2010).

Pflanzen besitzen im Wesentlichen zwei Mechanismen, um phytopathogene Bakterien zu erkennen (Chisholm *et al.*, 2006; Jones und Dangl, 2006). Ein Mechanismus beruht auf der Erkennung von bestimmten Molekülen, die unter den meisten phytopathogenen, aber auch nicht-pathogenen Bakterien konserviert sind. Die zweite Möglichkeit ist die spezifische Erkennung bakterieller Virulenzfaktoren, welche direkt oder indirekt erfolgen kann, indem die durch Virulenzfaktoren bedingten Veränderungen von der Pflanze registriert werden (Dodds und Rathjen, 2010).

1.2 Die basale Abwehr der Pflanze

Die Basis der pflanzlichen Abwehr umfasst sowohl passive Barrieren wie Wachsschichten der Kutikula und die pflanzliche Zellwand, als auch induzierbare Abwehrreaktionen (Nürnberger und Lipka, 2005). Die Aktivierung der Abwehrmechanismen erfolgt nach Erkennung von konservierten pathogen-assoziierten Molekülen. Diese sogenannten PAMPs (*pathogen-associated molecular patterns*) sind essentielle und hochkonservierte Komponenten, die unter Pathogenen weit verbreitet sind. Zu den PAMPs Gram-negativer Bakterien gehören beispielsweise das Flagellin (Bestandteil des bakteriellen Flagellums), der Elongationsfaktor EF-Tu und Kälteschockproteine (Felix *et al.*, 1999; Felix und Boller, 2003; Kunze *et al.*, 2004). Nach Erkennung dieser Moleküle durch spezifische Rezeptoren (*pattern recognition receptors*, PRRs) an der Oberfläche der Pflanzenzelle (Boller und Felix, 2009) wird die PAMP-induzierte Abwehr aktiviert (*PAMP-triggered immunity*, PTI; Abb. 1-1).
PAMP-Rezeptoren sind meist Rezeptor-ähnliche Kinasen mit einer N-terminalen Domäne, bestehend aus Leuzin-reichen Sequenzwiederholungen (*leucin-rich-repeat*, LRR) zur Bindung der Liganden, einer Transmembrandomäne und einer zytoplasmatischen Kinasedomäne, die der Signalweiterleitung dient (Zipfel, 2008). Die PRRs FLS2 (*flagellin sensing* 2) und EFR (*EF-Tu receptor*) zählen zu den am besten charakterisierten Rezeptorkinasen.
Nach Erkennung der PAMPs interagieren viele PRRs mit der Rezeptorkinase BAK1 (*brassinosteroid insensitive kinase* 1), wodurch Abwehrprozesse der Pflanze aktiviert werden (Chinchilla *et al.*, 2007). In Folge dessen kommt es zur Erhöhung des Ca^{2+}-Level im Zytoplasma, Aktivierung von Mitogen-aktivierten Proteinkinasen (*mitogen-activated protein kinases*, MAPK) und Transkriptionsfaktoren sowie Änderungen der Expression von Wirtsgenen (Blume *et al.*, 2000; Nürnberger und Scheel, 2001; Asai *et al.*, 2002; Thilmony *et al.*, 2006). Dadurch induzierte Abwehrreaktionen sind u.a. die Synthese reaktiver Sauerstoffspezies, antimikrobieller Substanzen wie Phytoalexine und PR-Proteine (*pathogenesis-related*) sowie Kalloseeinlagerungen in die pflanzliche Zellwand (Zellwand-basierte Abwehr; Darvill, 1984; Gomez-Gomez *et al.*, 1999; Kitajima und Sato, 1999; Chinchilla *et al.*, 2007; Sels *et al.*, 2008). Bei Kalloseeinlagerungen handelt es sich um lokale Verdickungen der Zellwand, Papillen genannt, die an der Kontaktstelle zwischen Pathogen und Pflanze durch *de novo* Synthese von Zellwandbestandteilen entstehen (Kwon *et al.*, 2008). Über das endoplasmatische Retikulum (ER) und den Golgi-Apparat werden zusätzlich antimikrobielle Substanzen sekretiert, die innerhalb der Papille einen für das Pathogen toxischen „Cocktail“ bilden (Kwon *et al.*, 2008). Die genannten Reaktionen können das mikrobielle Wachstum hemmen und dadurch die Kolonisierung der Pflanze behindern.

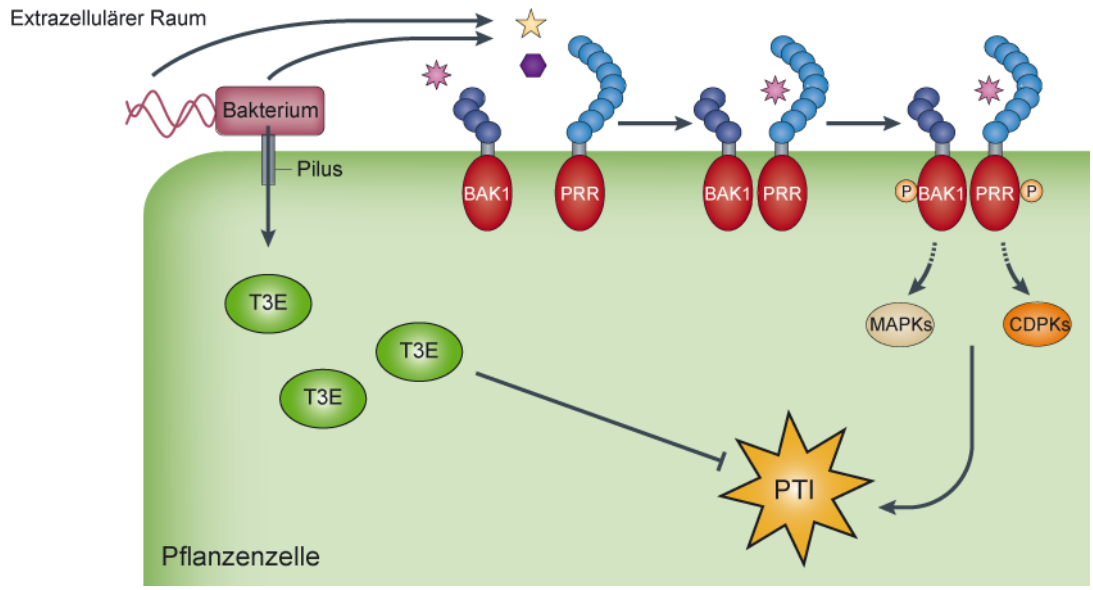

Abbildung 1-1: Aktivierung der PTI durch phytopathogene Bakterien.
Bakterien vermehren sich im extrazellulären Raum von Pflanzenzellen. PAMPs der Pathogene, wie Flagellin oder Elongationsfaktor Tu, werden von Rezeptoren (PRR) an der Zelloberfläche erkannt. PRRs besitzen eine extrazelluläre Leuzin-reiche Repeat-Region (*leucin rich repeat*, LRR, blau), eine Transmembrandomäne (grau) und eine zytoplasmatische Kinasedomäne (rot). Zur Aktivierung der PTI-Signalwege interagieren PRRs oft mit *brassinosteroid insensitive kinase* 1 (BAK1). Die Signalweiterletung erfolgt über MAP-Kinasen (MAPK) und/oder CDPKs (*calcium-dependent protein kinase*) und führt zur Aktivierung von Abwehreaktionen der PTI. Phytopathogene Bakterien translozieren Effektorproteine (T3E) über das Typ III-Sekretionssystem (Pilus) in die Wirtszelle. Einige T3E unterdrücken die PTI und tragen dadurch zur Virulenz des Bakteriums bei. Modifiziert nach Dodds und Rathjen (2010).

1.3 Virulenzfaktoren Gram-negativer Bakterien

Um die pflanzliche Abwehr zu umgehen und eine erfolgreiche Besiedlung des Wirtes zu gewährleisten, nutzen Gram-negative Bakterien zahlreiche Virulenzfaktoren. Hierzu zählen beispielsweise extrazelluläre Polysaccharide (EPS; Denny, 1995; Dharmapuri und Sonti, 1999), Adhäsine (Ray *et al.*, 2002), Toxine (Bender *et al.*, 1999; Strange, 2007) und zellwandabbauende Enzyme (Toth und Birch, 2005). Extrazelluläre Polysaccharide bilden eine Kapsel oder Schleimhülle um die Bakterienzelle und schützen diese vor der Austrocknung. Außerdem fördern EPS die Anhäufung von Nährstoffen und wirken sich aufgrund ihrer adhäsiven Eigenschaften positiv auf die Anheftung des Bakteriums an die Wirtszelle aus. Des Weiteren können EPS die Suszeptibilität der Pflanze erhöhen und das Bakterium vor Toxinen schützen (Denny, 1995; Ray *et al.*, 2002). Zellwandabbauende Enzyme, wie Zellulasen und Pektinasen, erleichtern phytopathogenen Bakterien das Durchdringen der pflanzlichen Zellwand. Dabei werden die Hauptbestandteile der Zellwand (Zellulose, Hemizellulose und Pektin) abgebaut, wodurch die Stabilität der Zellwand beeinträchtigt wird. Die durch den Abbau entstehenden Einfachzucker dienen den Bakterien wiederum als Nährstoffe (Lagaert *et al.*, 2009).

Die genannten Substanzen werden über spezielle Sekretionssysteme aus der Bakterienzelle heraustransportiert. Das Typ I-Sekretionssystem dient dem Transport von Toxinen, Proteasen und Lipasen (Holland *et al.*, 2005). Über das Typ II-System werden ebenfalls Toxine und hydrolytische Enzyme sekretiert (Sandkvist, 2001), während das Typ IV-System zum Transport von DNA oder Proteinen dient (Christie und Cascales, 2005). Das Typ III-Sekretionssystem (T3SS) transportiert Typ III-Effektorproteine (T3E) direkt in das Innere der Wirtszelle (Büttner und Bonas, 2010).

1.3.1 Das Typ III-Sekretionssystem

Das Typ III-Sekretionssystem (T3SS) spielt eine Schlüsselrolle beim Transport von Proteinen und ist für die Pathogenität der meisten Gram-negativen Bakterien essentiell (Tampakaki *et al.*, 2004). Ausnahmen sind *Agrobacterium* spp. und *Xylella fastidiosa*, die kein T3SS besitzen (Simpson *et al.*, 2000; Wood *et al.*, 2001). Das T3SS transportiert Proteine über beide bakterielle Membranen in das extrazelluläre Milieu (Sekretion) oder zusätzlich über die pflanzliche Zellwand und -membran direkt in das Zytosol der Pflanzenzelle (Translokation), ähnlich einer molekularen Spritze (Tampakaki *et al.*, 2004; Büttner und Bonas, 2006). Das T3SS besteht aus einem Membran-durchspannenden Basalapparat und einem extrazellulären Pilus. Über das T3SS sekretierte Translokonproteine bilden vermutlich eine Pore in der pflanzlichen Zellmembran und ermöglichen dadurch die „Injektion“ von Effektorproteinen (Ghosh, 2004; Büttner und He, 2009).

In pflanzenpathogenen Bakterien werden die Komponenten des T3SS vom *hrp*-Gencluster (*hypersensitive response and pathogenicity*) kodiert, welches sowohl für die Pathogenität in anfälligen Pflanzen als auch die Induktion der hypersensitiven Reaktion (HR) in resistenten Pflanzen essentiell ist (Bonas *et al.*, 1991; He *et al.*, 2004). Das *hrp*-Gencluster des in dieser Arbeit untersuchten Pathogens *Xanthomonas campestris* pv. *vesicatoria* (*Xcv*) besteht aus mehr als 20 Genen, die in Transkriptionseinheiten organisiert sind (Büttner und Bonas, 2002). Die Regulation der Expression des *hrp*-Clusters unterscheidet sich zwischen verschiedenen Gram-negativen Pflanzenpathogenen. Im Fall von *Xcv* sind der OmpR-ähnliche Regulator HrpG sowie HrpX, ein transkriptioneller Aktivator des AraC-Typs, für die Aktivierung der Expression des *hrp*-Genclusters verantwortlich. Bei Kontakt mit der Pflanzenzelle aktiviert ein bislang unbekanntes Signal HrpG, welches wiederum die Expression von *hrpX* aktiviert (Wengelnik und Bonas, 1996; Wengelnik *et al.*, 1996a; Wengelnik *et al.*, 1996b; Noël *et al.*, 2001). HrpX bindet an die *cis*-regulatorischen PIP-Boxen (*plant-inducible promoter*) in den Promotoren von *hrp*- und anderen Typ III-assoziierten Genen und aktiviert deren Expression (Koebnik *et al.*, 2006).

Elf der im *hrp*-Cluster kodierten Proteine sind in Pflanzen- und Tierpathogenen konserviert und werden als Hrc (*hrp-conserved*) bezeichnet (Bogdanove *et al.*, 1996). Sie bilden vermutlich den Kern des Typ III-Basalapparates (He *et al.*, 2004; Tampakaki *et al.*, 2004). Neben den *hrc*-Genen sind auch die nicht konservierten *hrp*-Gene für die Pathogentität von *Xcv* essentiell. Unter den Hrp-Proteinen sind HrpE als Hauptbestandteil des extrazellulären Pilus und HrpF als Hauptkomponente des

Translokons maßgeblich an der Translokation von Effektoren beteiligt (Büttner *et al.*, 2002; Weber *et al.*, 2005). Einige Komponenten des T3SS von *Xcv* werden von *hrp*-assoziierten Genen (*hrp-associated, hpa*) kodiert, welche zur Interaktion mit der Wirtspflanze beitragen (Huguet *et al.*, 1998; Büttner *et al.*, 2004). Ein Beispiel ist das Typ III-Chaperon HpaB, welches für die effiziente Translokation der T3E benötigt wird und daher für die Pathogenität von *Xcv* essentiell ist. Typ III-Chaperone binden spezifisch an ihre Substrate und fördern deren Stabilität und/oder Sekretion und Translokation (Parsot *et al.*, 2003; Wilharm *et al.*, 2007). Da die Translokation einzelner Effektoren von *Xcv* in unterschiedlichem Maß von HpaB abhängig ist, werden die Effektoren in zwei Klassen unterteilt. Während die Translokation von Klasse A-T3E HpaB-abhängig ist, werden Effektoren der Klasse B auch in Abwesenheit von HpaB transloziert, wenn auch in geringeren Mengen (Büttner *et al.*, 2004; Büttner *et al.*, 2006).

Generell ist das Vorhandensein spezieller Signale im N-terminalen Bereich der T3E für die erfolgreiche Sekretion und Translokation in die Wirtszelle essentiell. Die T3S-Signale sind jedoch nicht konserviert und über ihren genauen Aufbau ist bislang wenig bekannt. Wahrscheinlich ist die Zusammensetzung und die amphipathische Natur der Aminosäuren essentiell (Büttner und He, 2009).

1.4 Unterdrückung der PTI durch Typ III-Effektoren

Über das T3SS können Bakterien Effektorproteine direkt in das Zytosol der Pflanzenzelle transportieren (siehe 1.3.1). Typ III-Effektoren von *Xanthomonas* werden als *Xanthomonas outer protein* (Xop) und in *Pseudomonas* als *Hrp outer protein* (Hop) bezeichnet. Im Zellinneren manipulieren die Effektoren Wirtszellprozesse und unterdrücken die Pflanzenabwehr (Abb. 1-1). Dadurch tragen T3E zur Virulenz und zum Wachstum der Bakterien bei (Büttner und Bonas, 2010; Block und Alfano, 2011). Die Mechanismen, die zur Suppression der PAMP-induzierten Abwehr führen, konnten für einige Effektoren von *Pseudomonas* und *Xanthomonas* geklärt werden (Brown *et al.*, 1995; Nomura *et al.*, 2005). Die T3E greifen sämtliche Schritte der PTI an, von der PAMP-Erkennung und der Expression PTI-assoziierter Gene bis zu induzierten Abwehrreaktionen. Die PAMP-Erkennung durch PRRs wird beispielsweise durch AvrPtoB und AvrPto aus *Pseudomonas* verhindert. AvrPtoB bindet BAK1 und bewirkt die Dissoziation des FLS2/BAK1-Komplexes (Shan *et al.*, 2008). Außerdem wird FLS2 durch die E3-Ligasedomäne von AvrPtoB ubiquitiniert und Proteasom-vermittelt abgebaut (Göhre *et al.*, 2008). Die Interaktion von AvrPto und dessen Zielproteinen wird momentan kontrovers diskutiert. So postulierten Shan und Kollegen, dass AvrPto, ähnlich wie AvrPtoB, die FLS2/BAK1-Komplexbildung verhindert, indem es an BAK1 bindet (Shan *et al.*, 2008). In späteren Studien wurde gezeigt, dass diese Interaktion eher ein indirekter Effekt ist. Xiang und Kollegen fanden heraus, dass AvrPto mit FLS2 interagiert und die Interaktion zwischen AvrPto und BAK1 nur in Gegenwart von FLS2 erfolgt und vermutlich auf die räumliche Nähe von FLS2 und BAK1, im Zuge der Komplexbildung beider PRRs, zurückzuführen ist (Xiang *et al.*, 2011).

Entsprechend dieser Daten wird angenommen, dass AvrPto an FLS2 bindet und dessen Kinaseaktivität inhibiert, wodurch die stromabwärts-gelegene PTI-Signalweiterleitung unterbunden wird (Xiang *et al.*, 2011). Dieses Modell berücksichtigt frühere Ergebnisse der Autoren, in denen die Inhibierung der Kinaseaktivität von FLS2 in Gegenwart von AvrPto gezeigt wurde (Xiang *et al.*, 2008).
Die Signalweiterleitung über MAPK-Kaskaden wird beispielsweise durch HopF2 und HopAI1 gestört. HopF2 interagiert mit der MAP-Kinase-Kinase MKK5 und verhindert deren Phosphorylierung (Wang *et al.*, 2010). HopAI1 dagegen besitzt Phosphothreoninlyase-Aktivität und dephosphoryliert die MAP-Kinasen MPK3 und MPK6. In Folge dessen wird die transkriptionelle Aktivierung von Abwehrgenen sowie Kalloseablagerungen und Produktion reaktiver Sauerstoffspezies unterdrückt (Zhang *et al.*, 2007). Neben HopAI1 und HopF2 greift auch HopAO1 in die Zellwand-basierte Abwehr ein (Guo *et al.*, 2009).
Ähnliches wurde auch für Effektoren aus *Xanthomonas* gezeigt. So unterdrücken XopD, XopJ, XopN und AvrBsT die PTI-induzierte Genexpression und/oder Kalloseeinlagerungen in die pflanzliche Zellwand (Kim *et al.*, 2008; Bartetzko *et al.*, 2009; Kim *et al.*, 2009; Kim *et al.*, 2010). Da die Suppression der PTI die Vermehrung der Bakterien begünstigt, spricht man deshalb von Effektor-induzierter Suszeptibilität (*effector-triggered susceptibility*, ETS; Abb. 1-2; Jones und Dangl, 2006).
Diese Daten belegen, dass T3E verschiedener phytopathogener Bakterien im Allgemeinen ähnliche Prozesse der Pflanze manipulieren. Allerdings gibt es doch vielfältige Unterschiede in deren Wirkungsweise und Beitrag zur Virulenz der Bakterien (s. Abschnitt 1.6).

1.5 Spezifische Resistenz durch Erkennung von Typ III-Effektoren

Pflanzen haben neben der Erkennung von PAMPs einen weiteren Mechanismus, um die Kolonisierung durch phytopathogene Bakterien zu verhindern. Einige bakterielle Effektorproteine, die zur ETS beitragen, werden spezifisch von der Pflanze erkannt. Diese spezifische Resistenz (*effector-triggered immunity*, ETI) basiert auf Resistenz (*R*)-Genen oder -Proteinen, die die Anwesenheit oder Aktivität eines bestimmten Effektors spezifisch erkennen. Diese Effektoren werden auch als Avirulenz (Avr)-Proteine bezeichnet. In den meisten Fällen erfolgt eine direkte oder indirekte Erkennung der Avr-Proteine durch Rezeptorproteine bestehend aus einer N-terminalen TIR- (Toll, Interleukin-1 Rezeptor) bzw. CC- (*coiled-coil*) Domäne, einer zentralen Nukleotid-Bindedomäne (*nucleotide binding*, NB) und einer C-terminalen LRR-Domäne (van Ooijen *et al.*, 2007).
Während die LRR-Domäne die Spezifität bestimmt, ist die NB-Region vermutlich für die Signalweiterleitung verantwortlich (van Ooijen *et al.*, 2007). Als Beispiel sei hier die Erkennung des Effektors AvrPtoB aus *P. syringae* genannt. AvrPtoB interagiert mit den Kinasen Fen und Pto aus Tomate. Fen und Pto sind R-Proteine, besitzen jedoch selbst keine Transmembran- und extrazelluläre LRR-Domänen. Die Aktivierung der ETI ist deshalb vom NB-LRR-Protein Prf abhängig, welches mit

Pto interagiert (Kim *et al.*, 2002; Abramovitch *et al.*, 2003; Rosebrock *et al.*, 2007; Gimenez-Ibanez *et al.*, 2009).

T3E können auch auf Promotoren von Resistenz- oder Suszeptibilitätsgenen wirken. AvrBs3 von *Xanthomonas* wirkt als Transkriptionsfaktor und aktiviert Promotoren im Zellkern von Paprikapflanzen (Kay *et al.*, 2007; Römer *et al.*, 2007). In anfälligen Pflanzen induziert AvrBs3 die Zellvergrößerung (Hypertrophie) durch Bindung und Aktivierung des Promotors von *UPA20* (*upregulated by AvrBs3*), einem Hauptregulator der Zellgröße (Kay *et al.*, 2007). In resistenten Pflanzen bindet AvrBs3 zusätzlich an den Promotor von *Bs3* und aktiviert das *Bs3-R*-Gen, welches für eine Flavinmonooxygenase kodiert (Römer *et al.*, 2007).

Die Erkennung der Avr-Proteine durch entsprechende R-Proteine oder *R*-Gene führt zur Expression verschiedener Gene und zur Aktivierung von Signalwegen, die denen der PAMP-induzierten Abwehr ähnlich sind (Tao *et al.*, 2003; Pitzschke *et al.*, 2009). Dazu zählen die Erhöhung des zytosolischen Ca^{2+} Level, die Produktion reaktiver Sauerstoffspezies und die Aktivierung von MAPK-Kaskaden. Allerdings erfolgt die Immunantwort der ETI viel schneller und stärker als die der PTI und führt oftmals zur Ausbildung der HR, einer lokal-begrenzten Zelltodreaktion, die das Wachstum der Bakterien behindert (Tao *et al.*, 2003; Greenberg und Yao, 2004; Thilmony *et al.*, 2006).

1.5.1 Unterdrückung der spezifischen Resistenz

Phytopathogene Bakterien besitzen einige Effektoren, die die spezifische Erkennung anderer T3E unterdrücken können (Jones und Dangl, 2006). Ein Beispiel ist der Effektor AvrPphC von *P. syringae* pv. *phaseolicola*, der zwar selbst in verschiedenen Kultivaren der Bohne erkannt wird, aber auch die durch AvrPphF ausgelöste ETI supprimieren kann (Tsiamis *et al.*, 2000). AvrPtoB aus *P. syringae* pv. *tomato* kann dagegen die eigene Erkennung unterdrücken, indem es die Kinase Fen degradiert (Abramovitch *et al.*, 2006; Rosebrock *et al.*, 2007). Pto hingegen entgeht diesem Abbau, da es AvrPtoB phosphoryliert und damit inaktiviert (Ntoukakis *et al.*, 2009). Dadurch bleibt die Pto-vermittelte Resistenz bestehen. Darüber hinaus unterdrückt AvrPtoB auch die durch HopA1 und AvrRpm1 induzierten hypersensitiven Reaktionen (Guo *et al.*, 2009).

Diese Beispiele verdeutlichen die Ko-Evolution zwischen Pflanzen und phytopathogenen Bakterien, die in der Entwicklung neuer Angriffs- bzw. Abwehrmechanismen resultiert. Dieses „Wettrüsten“ ist im Zick-Zack-Modell nach Jones und Dangl in Abbildung 1-2 dargestellt und fasst die oben genannten Mechanismen zusammen (Jones und Dangl, 2006).

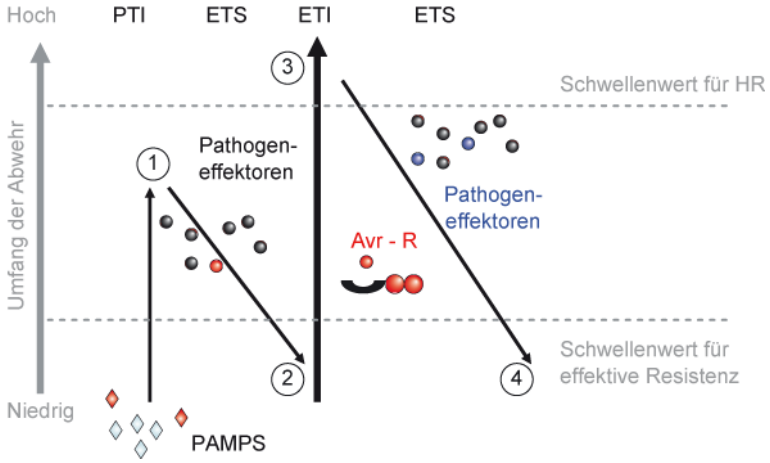

Abbildung 1-2: Das Zick-Zack-Modell illustriert die Ko-Evolution zwischen Pathogenen und Abwehrmechanismen der Pflanze.
In der 1. Phase der Immunantwort werden pathogen-assoziierte molekulare Muster (PAMPs, rote und weiße Diamanten) der Pathogene erkannt und aktivieren die PTI (*PAMP-triggered immunity*). Erfolgreiche Pathogene transportieren Effektorproteine in die Wirtszelle, welche die PTI unterdrücken (Phase 2). Dies erlaubt Wachstum und Vermehrung der Pathogene und resultiert in Effektor-induzierter Suszeptibilität (*effector-triggered susceptibility,* ETS). In Phase 3 wird ein Effektor (Avr, rot) durch korrespondierende Resistenzgene oder –proteine (R, rot) erkannt und die ETI (*effector-triggered immunity*) aktiviert, die oft zur Ausbildung einer hypersensitiven Reaktion (HR) führt. Manche Isolate eines Pathogens besitzen wiederum Effektoren, welche die ETI unterdrücken können und erneut ETS bewirken (Phase 4). Modifiziert nach Jones und Dangl (2006).

1.6 Wirkungsweise von Typ III-Effektoren

Die Zahl bakterieller Effektoren bzw. Effektorkandidaten hat in jüngster Zeit durch neue Genomdaten, funktionelle Analysen sowie Sequenz- und Strukturähnlichkeiten zu bekannten (Effektor-) Proteinen enorm zugenommen (White *et al.*, 2009). Des Weiteren konnte die biochemische Aktivität zahlreicher T3E bestimmt und deren pflanzliche Zielproteine identifiziert werden (Deslandes und Rivas, 2012). Effektoren mit gleicher biochemischer Aktivität bzw. Wirkungsweise wurden dabei zu „Effektorfamilien“ zusammengefasst (White *et al.*, 2009; Block und Alfano, 2011; Deslandes und Rivas, 2012).

Die TAL-Effektoren (*transcription activator-like*) repräsentieren die größte Effektorfamilie und kommen in *Xanthomonas* spp. und *Ralstonia solanacearum* vor (Scholze und Boch, 2011). Sie binden direkt an die Promotorregionen von pflanzlichen Zielgenen und wirken als Transkriptionsaktivatoren (s. Kapitel 1.5; Kay und Bonas, 2009; White *et al.*, 2009; Boch und Bonas, 2010).

Eine weitere große Gruppe umfasst die Effektoren der YopJ/AvrRxv/HopZ-Familie, die in verschiedenen tier-und pflanzenpathogenen Bakterien vorhanden sind. Sie besitzen Cysteinprotease- und/oder Acetyltransferase-Aktivität (Lewis *et al.*, 2011), welche auf einer konservierten Aminosäuretriade beruht und für die Funktionalität dieser Effektorproteine notwendig ist. (Shao *et al.*, 2003; Bonshtien *et al.*, 2005; Bartetzko *et al.*, 2009; Lee, AH *et al.*, 2012; Lee, J *et al.*, 2012). Die Cysteinprotease HopN1 ist ein Vertreter dieser Effektorfamilie und unterdrückt Kalloseablagerungen

und die Bildung reaktiver Sauerstoffspezies der PTI. Mutationen im katalytischen Zentrum von HopN1 führen sowohl zum Verlust der enzymatischen Aktivität als auch der Suppressionswirkung (Lopez-Solanilla *et al.*, 2004; Rodriguez-Herva *et al.*, 2012). XopD und AvrXv4 von *Xanthomonas* wirken ebenfalls als Cysteinproteasen und spalten posttranslationale SUMO-Modifikationen von Zielproteinen (*small ubiquitin-related modifier, SUMO*; Hotson und Mudgett, 2004; Roden, J *et al.*, 2004). Im Fall von XopD hat dies Veränderungen der Transkription von Wirtsgenen zur Folge und trägt zum bakteriellen Wachstum von *Xanthomonas* bei (Hotson *et al.*, 2003; Kim *et al.*, 2008; Canonne *et al.*, 2011).

Tier- und pflanzenpathogene Bakterien manipulieren auch den eukaryotischen Ubiquitin-vermittelten Proteinabbau, indem sie Schlüsselkomponenten, wie z. B. E3-Ubiquitin-Ligasen, imitieren (Janjusevic *et al.*, 2006; Singer *et al.*, 2008; Lin *et al.*, 2011). AvrPtoB und das in dieser Arbeit charakterisierte XopL sind die bislang einzig bekannten T3E phytopathogener Bakterien mit E3-Ligase-Aktivität (Abramovitch *et al.*, 2006; Janjusevic *et al.*, 2006; Singer *et al.*, 2013).

Weitere bekannte Enzymaktivitäten von Effektoren dienen der posttranslationalen Modifikation von Zielproteinen. So nutzt HopAO1 (früher HopPtoD2) seine Tyrosinphosphatase-Aktivität, um MAPK-Signalwege zu inhibieren (Espinosa *et al.*, 2003). Ein weiteres Beispiel sind die Effektorproteine HopF2 und HopU1, die als ADP-Ribosyltransferasen wirken. Während HopU1 das RNA-Bindeprotein GRP7 modifiziert, vermittelt HopF2 die ADP-Ribosylierung von MAPKKs, verhindert deren Phosphorylierung und inaktiviert dadurch die Signalweiterleitung der PTI (siehe Kapitel 1.4; Fu *et al.*, 2007; Wang *et al.*, 2010). Einen ähnlichen Mechanismus nutzt AvrAC aus *Xanthomonas*. AvrAC bindet an RLCKs (*receptor-like cytoplasmic kinases*) und blockiert deren Phosphorylierung, indem es mittels seiner Uridylyltransferase-Aktivität UMP auf die Serin- und Threoninreste des aktiven Zentrums der Kinasen überträgt. Dadurch wird Signalweiterleitung der PTI inhibiert und Abwehrreaktionen der Pflanze werden unterdrückt, was wiederum das Wachstum von *Xanthomonas* begünstigt (Feng *et al.*, 2012).

Effektoren manipulieren aber auch Wirtszellprozesse, um selbst in der Pflanze posttranslational modifiziert zu werden. Für die subzelluläre Lokalisierung an der pflanzlichen Plasmamembran müssen einige Effektoren acyliert werden (Robert-Seilaniantz *et al.*, 2006; Thieme *et al.*, 2007; Lewis *et al.*, 2008; Dowen *et al.*, 2009). AvrPto wird hingegen phosphoryliert und trägt nur im phosphorylierten Zustand zu Krankheitssymptomen und bakteriellem Wachstum in anfälligen Tomatenpflanzen bei (Anderson *et al.*, 2006). Der Effektor AvrRpt2 wird erst durch einen pflanzlichen Faktor aktiviert. Das Cyclophilin ROC1 aus Arabidopsis bindet an AvrRpt2 und bewirkt dessen korrekte Faltung, so dass AvrRpt2 als Protease wirken kann (Coaker *et al.*, 2005; Coaker *et al.*, 2006).

1.7 Die Gattung *Xanthomonas*

Vertreter der Gattung *Xanthomonas* sind Gram-negative, stäbchenförmige γ-Proteobakterien. Sie ernähren sich hemibiotroph und befallen eine Vielzahl von landwirtschaftlichen Kulturpflanzen und verursachen dadurch erhebliche Ernteverluste. Aufgrund ihres unterschiedlichen Wirtsspektrums werden sie in Pathovare (pv.) eingeteilt. *X. axonopodis* pv. *citri* (*Xac*) löst den Zitruskrebs auf verschiedenen Zitruspflanzen aus (Abb. 1-3 a), die Adernschwärze auf Brassicaceen wird durch *X. campestris* pv. *campestris* (*Xcc*) hervorgerufen (Abb. 1-3 b) und *X. axonopodis* pv. *glycines* bewirkt die bakterielle Pustelkrankheit auf Soja (Abb. 1-3 c). Eine besondere Bedeutung haben auch die Reispathogene *X. oryzae* pv. *oryzae* (*Xoo*) und *X. oryzae* pv. *oryzicola* (*Xoc*), welche die Weißblättrigkeit bzw. bakterielle Streifenkrankheit (Abb. 1-3 d) auslösen und besonders in Afrika und Asien zu hohen Ernteausfällen führen (Nino-Liu *et al.*, 2006).
Die Bakterien dringen über natürliche Öffnungen wie Stomata und Hydathoden oder Verwundungen in die Wirtspflanzen ein und vermehren sich systemisch durch Verbreitung im Xylem wie im Fall von *Xoo*, oder lokal wie *Xoc* (Nino-Liu *et al.*, 2006).

1.7.1 *Xanthomonas campestris* pv. *vesicatoria*

Xanthomonas campestris pv. *vesicatoria* oder auch *X. euvesicatoria* (Jones *et al.*, 2004) ist der Erreger der bakteriellen Fleckenkrankheit (*bacterial spot disease*) in Paprika (*Capsicum annuum*) und Tomate (*Solanum lycopersicum*) (Doidge, 1920; Higgins, 1922). Charakteristische Symptome sind wässrige Läsionen an Blättern und Früchten, die später nekrotisch werden (Abb. 1-3 e-h). Die bakterielle Fleckenkrankheit tritt weltweit auf, führt aber besonders in tropischen und subtropischen Regionen zu hohen Ernteverlusten (Cox, 1966; Jones *et al.*, 1998). Die Bakterien können in infizierten Paprika- oder Tomatenpflanzen, Saatgut und für kurze Dauer auch in befallenen Pflanzenteilen im Boden überdauern (Stall *et al.*, 2009). *Xcv* dringt über Stomata oder Wunden in das Pflanzengewebe ein und vermehrt sich im Apoplasten zu hohen Zelldichten. Die Ausbreitung von *Xcv* zwischen verschiedenen Pflanzen erfolgt hauptsächlich über Spritzwasser bei Regen (Pohronezny *et al.*, 1990). *Xcv* ist ein Modellorganismus für das Studium der Interaktion zwischen Pflanzen und phytopathogenen Bakterien. Bislang konnten mehr als 20 Effektoren bzw. Effektorkandidaten in *Xcv* identifiziert werden. Mit AvrBs1 und AvrBs2 wurden die ersten Effektoren aufgrund ihrer Avirulenzaktivität identifiziert (Ronald und Staskawicz, 1988; Minsavage *et al.*, 1990). Weitere T3E wurden durch genetische Studien und ausführliche „Effektorscreens“ gefunden (Roden, JA *et al.*, 2004). Die Entschlüsselung der Genomsequenz des *Xcv*-Stamms 85-10 lieferte weitere Effektoren bzw. Effektorkandidaten (Thieme *et al.*, 2005). Die bekannten Effektorproteine von *Xcv* 85-10 sind in Tabelle 1 zusammengefasst. Allerdings ist über deren Beitrag zur Virulenz von *Xcv* viel weniger bekannt als für Effektoren von *Pseudomonas*.

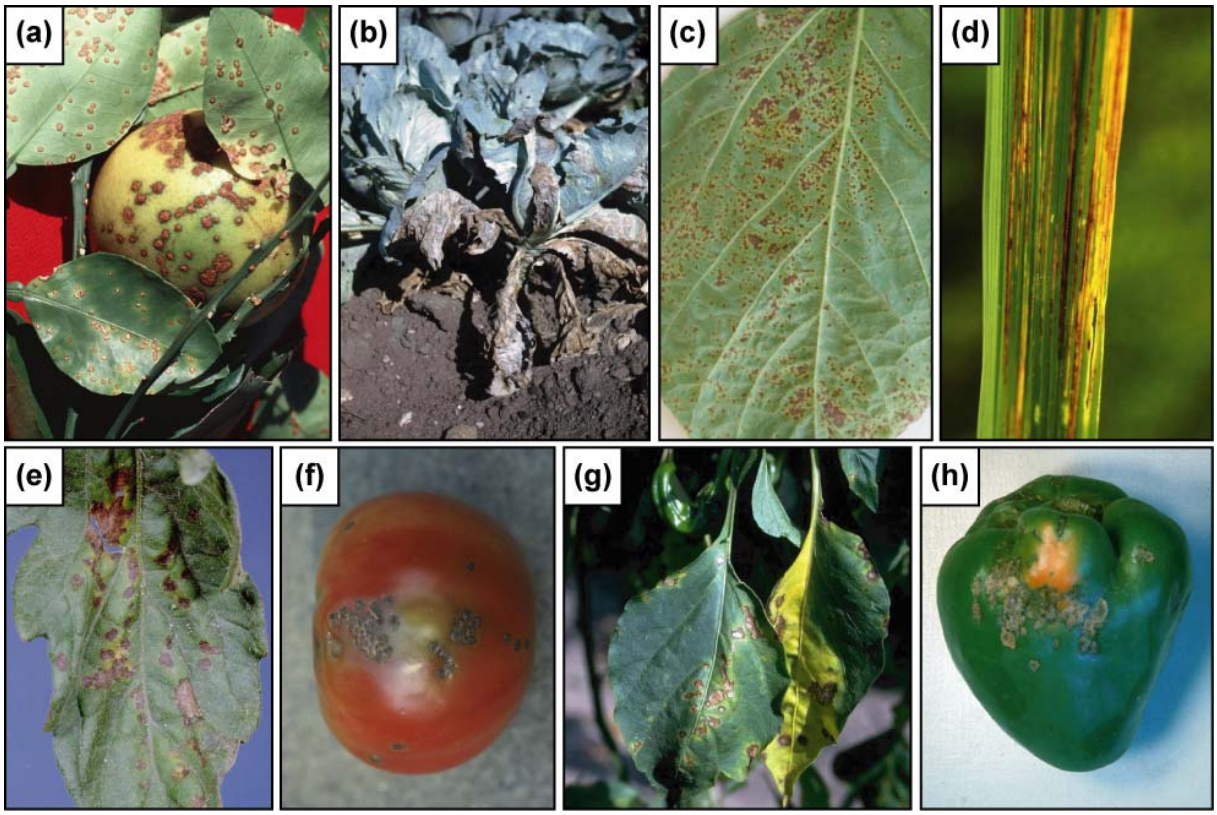

Abbildung 1-3: *Xanthomonas* spp. befallen verschiedene Pflanzenspezies.
(a) Symptome des Zitruskrebs auf Früchten und Blättern von Grapefruit ausgelöst durch *X. axonopodis* pv. *citri* (*Xac*), sichtbar als runde, bräunliche, korkartige Tumoren. **(b)** Durch *X. campestris* pv. *campestris* (*Xcc*) hervorgerufene Adernschwärze an Kohl zeigt sich als „V"-förmige Nekrosen der Blätter und Schwarzfärbungen der Gefäße. **(c)** *X. axonopodis* pv. *glycines* induziert bakterielle Pustelkrankheit in Soja und führt zur Ausbildung gelblich-brauner, wässriger Läsionen, die nekrotisieren. **(d)** Bakterielle Streifenkrankheit in Reisblättern wird von *X. oryzae* pv. *oryzicola* (*Xoc*) ausgelöst und zeigt sich als wässrige Läsionen, die sich parallel zu den Blattadern ausbreiten. **(e-h)** *X. campestris* pv. *vesicatoria* (*Xcv*) induziert die bakterielle Fleckenkrankheit in Blättern und Früchten von Tomate (e, f) bzw. Paprika (g, h). Charakteristische Symptome sind wässrige Läsionen, die später nekrotisch werden.
Bildquellen: T. Schubert, Florida Department of Agriculture and Consumer Services (a); R. W. Samson, Purdue University (b); D. Mueller, Iowa State University (c); D. Groth, Louisana State University (d); Clemson University (e); M. A. Hansen, Virginia Polytechnic Institute and State University (f); H. F. Schwartz, Colorado State University (g); Volcani Center Archive, Agriculture Research Organization (h)

Tabelle 1: Verifizierte Effektorproteine des Stamms *Xcv* 85-10 und deren biologische Funktion.

Effektor	**Vorhergesagte Funktion und Motive**	**Referenz**
AvrBs1	Unbekannt	(Ronald und Staskawicz, 1988; Escolar *et al.*, 2001)
AvrBs2	Glycerolphosphodiesterase	(Kearney und Staskawicz, 1990; Zhao *et al.*, 2011)
AvrRxv	Protease	(Whalen *et al.*, 1993; Whalen *et al.*, 2008)
XopB	Unbekannt	(Noël *et al.*, 2001)
XopC	Phosphoribosyltransferase	(Noël *et al.*, 2003)
XopD	SUMO-Protease	(Noël *et al.*, 2002; Hotson *et al.*, 2003)
XopE1	Transglutaminase, N-Myristoylierungsmotiv	(Thieme *et al.*, 2007)
XopE2	Transglutaminase, N-Myristoylierungsmotiv	(Thieme *et al.*, 2007)
XopF1	Unbekannt	(Roden, JA *et al.*, 2004)
XopF2	Unbekannt	(Roden, JA *et al.*, 2004)
XopG	Zink-Endopeptidase	(Potnis *et al.*, 2011)
XopH	Tyrosinphosphatase	(Schonsky, 2013)
XopI	F-Box Protein	(Schulze *et al.*, 2012)
XopJ	Protease/Acetyltransferase C55	(Noël *et al.*, 2003)
XopK	Unbekannt	(Schulze *et al.*, 2012)
XopL	E3-Ligase	(Singer *et al.*, 2013)
XopM	Unbekannt	(Schulze *et al.*, 2012)
XopN	Unbekannt	(Roden, JA *et al.*, 2004)
XopO	Unbekannt	(Roden, JA *et al.*, 2004)
XopP	Unbekannt	(Roden, JA *et al.*, 2004)
XopQ	Nukleosid-Hydrolase	(Roden, JA *et al.*, 2004)
XopR	Unbekannt	(Schulze *et al.*, 2012)
XopS	Unbekannt	(Schulze *et al.*, 2012)
XopV	Unbekannt	(Schulze *et al.*, 2012)
XopX	Unbekannt	(Metz *et al.*, 2005)
XopAA (Ecf)	*Early chlorosis factor*	(Morales *et al.*, 2005)

1.8 Vorarbeiten der Arbeit

Zu Beginn dieser Arbeit waren bereits 17 Effektorproteine von *Xcv* 85-10 experimentell verifiziert (Thieme *et al.*, 2007). Analysen der Genomsequenz ergaben weitere Effektorkandidaten aufgrund des Vorhandenseins von PIP-Boxen in den korrespondierenden Promotorregionen, Sequenzhomologien zu bekannten Effektoren oder vorhergesagten eukaryotischen Proteinmotiven. In früheren Arbeiten konnte bereits gezeigt werden, dass die Expression der Effektorkandidatengene *xopK*, *xopL*, *xopR*, *xopS* und *xopV* mit dem T3SS ko-reguliert ist (A. Krüger, M. Egler, R. Szczesny, F. Thieme und U. Bonas, unpubliziert). Außerdem wurde die Typ III-abhängige Sekretion und Translokation der Effektorkandidaten XopK, XopL, XopR und XopS in Vorarbeiten nachgewiesen bzw. ein entsprechendes AvrBs3Δ2-Reporterkonstrukt von XopV erstellt, um diese Analysen durchzuführen (Schonsky, 2013; M. Egler, R. Szczesny und U. Bonas, unpubliziert). In dieser Arbeit sollten Translokations-und Sekretionsstudien für XopV durchgeführt werden. Des Weiteren sollte die Translokation von Effektoren in Abhängigkeit vom Typ III-Chaperon HpaB durchgeführt werden und die T3E XopB, XopG, XopH, XopI, XopK, XopL, XopM, XopR, XopS und XopV klassifiziert werden (s. 1.3.1).

Genetische und biologische Analysen sollten Aufschluss über mögliche Funktionen von XopK, XopL, XopR, XopS und XopV und deren Beitrag zur Virulenz von *Xcv* liefern. Mikroskopische Analysen zur Lokalisierung der Effektoren sollten dabei Hinweise für mögliche Wirkungsorte der genannten Effektoren liefern. In vorangegangenen Studien wurde bereits gezeigt, dass XopL weder die Induktion von Krankheitssymptomen noch das bakterielle Wachstum von *Xcv* beeinflusst (M. Egler und U. Bonas, unpubliziert). Die biologische Funktion in der Pflanze und biochemische Aktivität von XopL waren bisher nicht bekannt.

In Vorarbeiten wurde mit der Charakterisierung des T3E XopB durch A. Schonsky begonnen. Ihre vorläufigen Daten deuteten darauf hin, dass XopB die durch andere Effektoren ausgelösten Zelltodreaktionen unterdrücken kann (Schonsky, 2013). Aufbauend auf den Vorarbeiten von A. Schonsky sollten detaillierte und weiterführende Studien durchgeführt werden. Durch Expressionsanalysen, Elektrolytmessungen zur Quantifizierung von Zelltodreaktionen und Ko-Lokalisierungsstudien von XopB und den entsprechenden Zelltod-auslösenden T3E, sollte die Suppressorwirkung von XopB genauer untersucht werden. Aufgrund der Suppression von Effektor-induzierten Zelltodreaktionen wurde ein Einfluss von XopB auf die pflanzliche Abwehr (PTI und ETI) vermutet. Dies wurde in der vorliegenden Arbeit ebenfalls untersucht.

2. Ergebnisse

2.1 Suppression der AvrBs1-induzierten HR durch AvrBsT

2.1.1 Publikation 1

Suppression of the AvrBs1-specific hypersensitive response by the YopJ effector homolog AvrBsT from *Xanthomonas* depends on a SNF1-related kinase

Robert Szczesny, Daniela Büttner, Lucia Escolar, Sebastian Schulze, Anja Seiferth and Ulla Bonas

Institute of Biology, Department of Genetics, Martin-Luther-University Halle-Wittenberg, D-06099 Halle (Saale), Germany

Author for correspondence:
Ulla Bonas
Tel: +49 345 5526290
Email: ulla.bonas@genetik.uni-halle.de

Received: *29 April 2010*
Accepted: *18 May 2010*

New Phytologist (2010)
doi: 10.1111/j.1469-8137.2010.03346.x

Key words: AvrRxv, bacterial spot disease, effectors, pepper, protease, transacetylase, YopJ.

Summary

- Pathogenicity of the Gram-negative plant pathogen *Xanthomonas campestris* pv. *vesicatoria* (*Xcv*) depends on a type III secretion system that translocates a cocktail of > 25 type III effector proteins into the plant cell.
- In this study, we identified the effector AvrBsT as a suppressor of specific plant defense. AvrBsT belongs to the YopJ/AvrRxv protein family, members of which are predicted to act as proteases and/or acetyltransferases.
- AvrBsT suppresses the hypersensitive response (HR) that is elicited by the effector protein AvrBs1 from *Xcv* in resistant pepper plants. HR suppression occurs inside the plant cell and depends on a conserved predicted catalytic residue of AvrBsT. Yeast two-hybrid based analyses identified plant interaction partners of AvrBs1 and AvrBsT, including a putative regulator of sugar metabolism, SNF1-related kinase 1 (SnRK1), as interactor of AvrBsT. Intriguingly, gene silencing experiments revealed that SnRK1 is required for the induction of the AvrBs1-specific HR.
- We therefore speculate that SnRK1 is involved in the AvrBsT-mediated suppression of the AvrBs1-specific HR.

Introduction

Plant pathogenic bacteria have evolved sophisticated strategies to exploit their corresponding host organisms. Pathogenicity of most members of the Gram-negative genera *Xanthomonas*, *Ralstonia* and *Pseudomonas* depends on a type III secretion (T3S) system, which spans both bacterial membranes and is associated with an extracellular pilus and a channel-like translocon in the eukaryotic plasma membrane (He *et al.*, 2004). The T3S system translocates a cocktail of type III effector proteins (T3Es) directly into the plant cell cytosol (Ghosh, 2004; Grant *et al.*, 2006; Block *et al.*, 2008). T3Es have diverse functions and target multiple host cellular pathways such as gene expression, hormone signaling, proteasome-dependent protein degradation and defense responses to the benefit of the pathogen (Speth *et al.*, 2007; Block *et al.*, 2008; Göhre & Robatzek, 2008; Lewis *et al.*, 2009). The main target of many T3Es appears to be the plant immune system. Plants defend themselves against microbial invaders by basal defense responses that include expression of pathogenesis-related genes, production of reactive oxygen species and callose deposition into the plant cell wall (Dangl & Jones, 2001; Bent & Mackey, 2007; de Wit, 2007). Basal plant defense is activated upon recognition of pathogen- (or microbe-) associated molecular patterns such as flagellin, lipopolysaccharides and elongation factor EF-Tu by specific receptors (Jones & Dangl, 2006). Furthermore, during coevolution with pathogens, plants have also evolved disease resistance (*R*) genes that detect individual T3Es. *R* gene-mediated recognition of T3Es (also designated avirulence (Avr) proteins) is often associated with the hypersensitive response (HR), a rapid programmed cell death at the infection site that restricts bacterial multiplication (Dangl & Jones, 2001). Successful pathogens often deliver T3Es that suppress basal plant defense responses or effector-triggered programmed cell death (Abramovitch & Martin, 2004).

In our laboratory, we study *Xanthomonas campestris* pv. *vesicatoria* (*Xcv*, also termed *Xanthomonas euvesicatoria* or *Xanthomonas axonopodis* pv. *vesicatoria*; Jones *et al.*, 2004), the causal agent of bacterial spot disease of pepper and tomato. The T3S system of *Xcv* is encoded by the

chromosomal *hrp* (hypersensitive response and pathogenicity) gene cluster, which is essential for disease in susceptible plants and the HR in resistant plants, and translocates *c.* 30 T3Es into the plant cell (Bonas *et al.*, 1991; Thieme *et al.*, 2007; White *et al.*, 2009). Efficient effector protein translocation depends on the cytoplasmic HpaB protein, a T3S chaperone (Büttner *et al.*, 2004, 2006; Lorenz *et al.*, 2008). T3S chaperones specifically bind to one or several T3S substrates and promote their secretion and/or stability (Feldman & Cornelis, 2003; Wilharm *et al.*, 2007). HpaB from *Xcv* has a broad substrate specificity and is required for the efficient secretion of all T3Es tested so far (Büttner *et al.*, 2006; J. Stuttmann *et al.*, unpublished). Notably, T3Es from *Xcv* differ in their HpaB dependency: class A T3Es depend on HpaB for translocation, whereas class B T3Es are translocated even in the absence of HpaB, albeit in reduced amounts (Büttner *et al.*, 2006). The differential contribution of HpaB to the translocation of T3Es suggests that there is a hierarchy in effector protein translocation and that class A and class B T3Es are translocated at a subsequent stage during infection (Büttner *et al.*, 2006).

Mutant studies of T3S system components revealed that translocation of the T3E arsenal is essential for pathogenicity of *Xcv* (Büttner *et al.*, 2002). However, most known T3Es from *Xcv* do not contribute significantly to the interaction with the host, presumably because of functional redundancies (Noël *et al.*, 2003; Roden *et al.*, 2004b; Thieme *et al.*, 2007; F Thieme *et al.*, unpublished). This is also true for numerous T3Es from other plant pathogenic bacteria (Vivian & Arnold, 2000; Cunnac *et al.*, 2009; Büttner & Bonas, 2010). Lack of mutant phenotypes has significantly hampered the identification and characterization of T3Es. Only in a few cases was a contribution of individual T3Es (e.g. AvrBs2, XopD and XopN) to bacterial virulence, symptoms and/or *in planta* bacterial growth reported (Marois *et al.*, 2002; Wichmann & Bergelson, 2004; Metz *et al.*, 2005; Morales *et al.*, 2005; Jiang *et al.*, 2008; Kim *et al.*, 2008, 2009).

In this study, we identified the T3E AvrBsT from *Xcv* as a suppressor of the HR elicited by AvrBs1 in resistant pepper plants. AvrBs1 promotes virulence of *Xcv* in pepper *Capsicum annuum* cv Early Cal Wonder (ECW) under field conditions and is recognized in ECW-10R pepper plants by the corresponding resistance gene *Bs1* (Ronald & Staskawicz, 1988; Wichmann & Bergelson, 2004). Transient expression studies showed that AvrBs1 induces chlorosis in the nonhost plant *Nicotiana benthamiana* and decreases the starch content in chloroplasts (Gürlebeck *et al.*, 2009). The C-terminal region of AvrBs1 is homologous to AvrA from *Pseudomonas syringae* pv. *glycinea* (Napoli & Staskawicz, 1987), but the function of AvrA and AvrBs1 is unknown (Escolar *et al.*, 2001). AvrBsT belongs to the clan CE of cysteine proteases with homology to YopJ (C55 family; YopP in *Yersinia enterocolitica*; Ciesiolka *et al.*, 1999). Members of the YopJ/AvrRxv protein family are present in many plant and animal pathogenic bacteria and include AvrRxv, AvrBsT, AvrXv4 and XopJ from *Xcv*, YopJ from *Yersinia* spp., AvrA from *Salmonella* spp. and T3Es from *Ralstonia solanacearum*, *P. syringae* and *Erwinia* spp. (Minsavage *et al.*, 1990; Keen & Buzzell, 1991; Whalen *et al.*, 1993; Galyov *et al.*, 1994; Astua-Monge *et al.*, 2000; Noël *et al.*, 2003; Shrestha *et al.*, 2005; Ma *et al.*, 2006). Most members of the YopJ family from animal pathogens contribute to the host–pathogen interaction; however, their biochemical function and impact on pathogenicity are a matter of debate (Mukherjee *et al.*, 2006; Sweet *et al.*, 2007). Several biochemical activities have been shown for members of the YopJ/AvrRxv family, that is isopeptidase (Orth *et al.*, 2000; Hotson & Mudgett, 2004; Ma *et al.*, 2006), acetyltransferase (Mukherjee *et al.*, 2006), and deubiquitination protease (Sweet *et al.*, 2007), all of which depend on a conserved catalytic triad consisting of histidine, aspartate or glutamate, and cysteine residues. One target of YopJ in animal cells is a mitogen-activated protein kinase kinase, MKK6, which is required for the activation of the transcription factor NF-κB, suggesting that YopJ interferes with signal transduction pathways (Mukherjee *et al.*, 2006). Mutant studies revealed that the Avr activities of the YopJ/AvrRxv family members from plant pathogens depend on the catalytic triad, suggesting that the enzymatic function is required for the recognition by corresponding plant R proteins (Orth *et al.*, 2000; Roden *et al.*, 2004a; Bonshtien *et al.*, 2005; Whalen *et al.*, 2008). Notably, a chimeric protein between the N-terminal region of AvrXv4 from *Xcv* and the C-terminal catalytic domain of YopP from *Y. enterocolitica* still exhibits Avr activity, suggesting a conservation of the catalytic activity of YopJ/AvrRxv homologs (Whalen *et al.*, 2008).

Here, we show that AvrBsT from *Xcv* suppresses the efficient induction of the AvrBs1-specific HR. Protein–protein interaction revealed that AvrBsT interacts with the SNF1-related kinase SnRK1 from pepper in the plant cell cytoplasm. Silencing of the *SnRK1* transcript leads to a severe reduction of the AvrBs1-specific HR, suggesting that SnRK1 is involved in the AvrBs1-induced plant immunity.

Materials and Methods

Bacterial strains and growth conditions

For bacterial strains and plasmids used in this study, see Table 1. Plasmids were introduced into *Escherichia coli* by electroporation and into *Xcv* and *Agrobacterium tumefaciens* by conjugation using pRK2013 as helper plasmid in triparental matings (Figurski & Helinski, 1979; Ditta *et al.*, 1980). *E. coli* strains were grown at 37°C in Lysogeny broth (LB) or Super medium (Qiagen). *Xcv* strains were cultivated at 30°C in nutrient-yeast-glycerol (NYG) (Daniels *et al.*,

Table 1 Bacterial strains and plasmids used in this study

	Relevant characteristics[a]	Reference or source
Xcv		
75-3	Tomato race 1; wild-type; Rif^r	Minsavage *et al.* (1990)
75-3Δ*avrBsT*	75-3 derivative deleted in *avrBsT*	This study
85-10	pepper-race 2; wild type; Rif^r	Canteros (1990); Kousik & Ritchie (1998)
85-10*xopJ*FS	*xopJ* frameshift mutant derivative of strain 85-10	Noël *et al.* (2003)
85-10Δ*avrRxv*	*avrRxv* deletion mutant derivative of strain 85-10	This study
85-10*xopJ*FSΔ*avrRxv*	*xopJ/avrRxv* double mutant derivative of strain 85-10	This study
85*	85-10 derivative containing the *hrpG** mutation	Wengelnik *et al.* (1999)
85*Δ*hpaB*	*hpaB* deletion mutant derivative of strain 85*	Büttner *et al.* (2004)
85*Δ*hrcV*	*hrcV* deletion mutant derivative of strain 85*	Rossier *et al.* (1999)
A. tumefaciens		
GV3101(pMP90)	Carries Ti plasmid pMP90; Rif^r; Gent^r	Van Larebeke *et al.* (1974)
E. coli		
Top10	F$^-$ *mcr*A Δ(*mrr-hsd*RMS-*mcr*BC) Φ80*lacZ*ΔM15 Δ*lac*X74 *rec*A1 *ara*D139 Δ(*araleu*) 7697 *gal*U *gal*K *rps*L (Str^R) *end*A1 *nup*G	Invitrogen
DB3.1	F$^-$ *gyr*A462 *end*A1 *gln*V44 Δ(sr1-*rec*A) *mcr*B *mrr hsd*S20(r_B^-, m_B^-) *ara*14 *gal*K2 *lac*Y1 *pro*A2 *rps*L20(Sm^r) *xyl*5 Δ*leu mtl*1	Invitrogen
BL21(DE3)	F$^-$ *omp*T *hsd*S_B (r_B^- m_B^-) *gal dcm* (DE3)	Stratagene, Heidelberg, Germany
DH5α	F$^-$ *recA hsdR17*(r_k^-, m_k^+) *Φ80dlacZ DM15*	Bethesda Research Laboratories, Bethesda, MD, USA
DH5α λpir	F$^-$ *recA hsdR17*(r_k^-, m_k^+) *Φ80dlacZ DM15* [λ*pir*]	Ménard *et al.* (1993)
Saccharomyces cerevisiae		
AH109	*MATa,trp1-901,leu2-3,112,ura3-52,his3-200,GAL4Δ, gal80Δ, LYS2::GAL1UAS- GAL1TATA-HIS3, GAL2UAS- GAL2TATAADE2, URA3::MEL1UAS-MEL1TATA-lacZ, MEL1*	Clontech, Heidelberg, Germany
Y187	*MATα,ura3-52,his3-200,ade2-101,trp1-901,leu2-3,112,GAL4Δ, met,gal80Δ, URA3::GAL1UAS- GAL1TATA- lacZ, MEL1*	Clontech
Plasmids		
pBlueskript(II) KS	Phagemid, pUC derivative; Ap^r	Stratagene
pDEST17	T7-His_6-*att*R1-Cm^r-*ccd*B-*att*R2, GATEWAY based *E. coli* expression vector	Invitrogen
pDSK602	Broad-host-range vector; contains triple *lacUV5* promoter; Sm^r	Murillo *et al.* (1994)
pENTR/D-TOPO	GATEWAY compatible directional cloning vector	Invitrogen
pGADT7	Yeast expression vector for the synthesis of proteins fused to a GAL4 activation domain, contains HA epitope-encoding sequence and *T7* promoter; Ap^r; *LEU2* nutritional marker	Clontech
pGADT7attR	Derivative of pGADT7 containing GATEWAY cassette	A Strauß & T Lahaye (unpublished)
pGBKT7	Yeast expression vector for the synthesis of proteins fused to a GAL4 DNA-binding domain, contains c-Myc epitope-encoding sequence and *T7* promoter; Km^r; *TRP1* nutritional marker	Clontech
pGBKT7attR	Derivative of pGBKT7 containing GATEWAY cassette	A Strauß & T Lahaye (unpublished)
pGWB2	Binary expression vector, contains *35S* promoter upstream of *attR1*-Cm^r-*ccdB-attR2*; Hm^r, Km^r	Nakagawa *et al.* (2007)
pGWB5	Binary *gfp* expression vector, contains *35S* promoter upstream of *attR1*-Cm^r-*ccdB-attR2-sgfp*; Hm^r, Km^r	Nakagawa *et al.* (2007)
pGWB6	Binary *gfp* expression vector, contains *35S* promoter upstream of *sgfp-attR1*-Cm^r-*ccdB-attR2*; Hm^r, Km^r	Nakagawa *et al.* (2007)
pGWB20	Binary expression vector, contains *35S* promoter upstream of *attR1*-Cm^r-*ccdB-attR2-20xc-myc*; Hm^r, Km^r	Nakagawa *et al.* (2007)
pGWB735/1	Derivative of pGWB2 encoding the C-terminal 86 aa of YFP	S Schornack and T Lahaye (unpublished)
pOK1	suicide vector; *sacB sacQ mobRK2* oriR6K; Sm^r	Huguet *et al.* (1998)
pRK2013	ColE1 replicon, TraRK$^+$ Mob$^+$; Km^r	Figurski & Helinski (1979)
pSPYNE	Gateway®-compatible derivative of pSPYNE-*35S* encoding the N-terminal 155 aa of YFP	Walter *et al.* (2004); Anand *et al.* (2007)
pTRV1	Vector for gene silencing, contains RNA1 encoding replicase proteins and movement protein of TRV	Liu *et al.* (2002a,b)

Table 1 (*Continued*)

	Relevant characteristics[a]	Reference or source
pTRV2a	GATEWAY-compatible tobacco rattle virus vector for gene silencing containing 2xCaMV promoter and RNA2 of TRV, derivative of pTRV2 containing ampicillin resistance cassette	Liu *et al.* (2002a,b) P Römer & T Lahaye (unpublished)
pUC119	ColE1 replicon; Ap^r	Vieira & Messing (1987)
Constructs		
pDD62avrBsT	Derivative of broad host range vector pDD62 containing *avrBsT*	Orth *et al.* (2000)
pDD62avrBsT$_{C222A}$	Derivative of pDD62 containing *avrBsT*$_{C222A}$	Orth *et al.* (2000)
pDEST17avrBsT	pDEST17 derivative containing *avrBsT*	This study
pDEST17avrBsT$_{C222A}$	Derivative of pDEST17 containing *avrBsT*$_{C222A}$	This study
pDEST17SnRK1	Derivative of pDEST17 containing *SnRK1*	This study
pDSF300	Derivative of pDSK602 containing *avrBs3*	Van den Ackerveken *et al.* (1996)
pDS400	Derivative of pDSK602 containing *avrBsT*	Escolar *et al.* (2001)
pENTR/DavrBs1	Derivative of pENTR/D-TOPO containing *avrBs1*	Gürlebeck *et al.* (2009)
pENTR/DavrBsT	Derivative of pENTR/D-TOPO containing *avrBsT*	This study
pENTR/DavrBsT$_{C222A}$	Derivative of pENTR/D-TOPO containing *avrBsT*$_{C222A}$	This study
pENTR/DSnRK1	Derivative of pENTR/D-TOPO containing *SnRK1*	This study
pGADT7tolib	Derivative of pGADT7 containing the tomato cDNA library	Gürlebeck (2007)
pGADT7attRpelib	Derivative of pGADT7attR containing the pepper cDNA library	This study
pGBKT7avrBs1	Derivative of pGBKT7attR containing *avrBs1* for yeast library screening	This study
pGBKT7attRavrBsT$_{C222A}$	Derivative of pGBKT7attR containing *avrBsT*$_{C222A}$ for yeast library screening	This study
pGWB2avrBs1	Derivative of pGWB2 containing *avrBs1*	Gürlebeck *et al.* (2009)
pGWB5avrBs1	Derivative of pGWB5 containing *avrBs1*	Gürlebeck *et al.* (2009)
pGWB5avrBsT	Derivative of pGWB5 containing *avrBsT*	This study
pGWB5avrBsT$_{C222A}$	Derivative of pGWB5 containing *avrBsT*$_{C222A}$	This study
pGWB5SnRK1	Derivative of pGWB5 containing *SnRK1*	This study
pGWB20SnRK1	Derivative of pGWB20 containing *SnRK1*	This study
pGWB735/1SnRK1	Derivative of pGWB735/1 containing *SnRK1*	This study
pO11	Derivative of pOK1 carrying flanking regions of *xopJ*	Noël *et al.* (2003)
pOKavrBsT	Derivative of pOK1 carrying flanking regions of *avrBsT*	This study
pOKavrRxv	Derivative of pOK1 carrying flanking regions of *avrRxv*	This study
pSPYNEavrBs1	Derivative of pSPYNE containing *avrBs1*	This study
pSPYNEavrBsT	Derivative of pSPYNE containing *avrBsT*	This study
pSPYNEavrBsT$_{C222A}$	Derivative of pSPYNE containing *avrBsT*$_{C222A}$	This study
pTRV2aSnRK1	Derivative of pTRV2a containing the first 343 bp of *SnRK1*	This study
pXV943	Derivative of pLAFR3 carrying a 4.3 kb *Pst*I fragment containing *avrBsT*	Minsavage *et al.* (1990)

[a]Ap, ampicillin; Hm, hygromycin; Km, kanamycin; Rif, rifampicin; Sm, spectinomycin; Str, streptomycin; Tc, tetracycline; r, resistant.

1984) or in minimal medium A (Ausubel *et al.*, 1996), which was supplemented with sucrose (10 mM) and casamino acids (0.3%) and *A. tumefaciens* strains at 30°C in yeast extract broth (YEB) medium. Antibiotics were added at the following final concentrations: ampicillin, 100 μg ml^{-1}; hygromycin, 50 μg ml^{-1}; kanamycin, 25 μg ml^{-1}; rifampicin, 100 μg ml^{-1}; and spectinomycin, 100 μg ml^{-1}.

Plant material and plant inoculations

The near-isogenic pepper cvs ECW, ECW-10R and ECW123 (Minsavage *et al.*, 1990; Stall & Minsavage, 1996) and tomato *Solanum lycopersicum* cv Moneymaker plants were grown at 25°C with *c.* 65% relative humidity and 16 h light. *Xcv* strains were hand-inoculated with a needleless syringe into the apoplast of leaves at 2×10^8 cfu ml^{-1} in 1 mM $MgCl_2$ if not stated otherwise. For *in planta* growth curves, bacteria were inoculated at a density of 10^4 cfu ml^{-1} and bacterial growth was determined as described in Bonas *et al.* (1991). For *in planta* transient expression studies and virus-induced gene silencing (VIGS), *A. tumefaciens* GV3101 was grown overnight in YEB medium, resuspended in inoculation medium (10 mM $MgCl_2$, 5 mM MES, pH 5.3, 150 μM acetosyringone) and inoculated into leaves at concentrations of 8×10^8 cfu ml^{-1}.

Generation of GATEWAY-compatible expression constructs

For the generation of *avrBs1*, *avrBsT*, *avrBsT*$_{C222A}$ and *SnRK1* expression constructs, corresponding coding sequences

Table 2 Primers used in this study

Name	Sequence (5′–3′)
aBs1-fe	CACCATGTCCGACATGAAAGTTAATTTC
aBs1-r	CTCTTACGCTTCTCCTGCATTTGTAAC
aBs1-rsl	CGCTTCTCCTGCATTTGTAACATG
aBsT-fe	CACCATGAAGAATTTTATGCGTTCAC
aBsT-r	CGAATTATGATTCAATAGTTTTCCTAATTTTC
aBsT-rsl	TGATTCAATAGTTTTCCTAATTTTCCTC
xpJ-fe	CACCATGGGTCTATGCGTTTCA
xpJ-rsl	TGACTGGCGATCAGAGATAGCTGTC
aRxv-fe	CACCATGTGCGACTCCATAAGAGTG
aRRxv-r	GGATTCTAAGGCGTGACGGA
CaSnVIGS-fe	CACCATGGATGGGTCAACAGTC
CaSnVIGS-r	GCAATCTGCCCTTCTCAACA
CaSn5race1	GATATAACCTCTGGGGCAGCATAGTTTGGAC
CaSn5race2	CAGGCCTAAGGTCTCTATGAACCACCATG
CaSn5race3	GAACCAAGGGTGCAGGCGAATCTCAG
CaSn5race4	CTTAACCACCTCCTGAAGAATCTCTTC
CaSnRK1-fe	CACCATGGATGGGTCAACAGTCCAAG
CaSnRK1-rs	TCAAAGGACCCGAAGCTGAGCAAG
CaSnRK1-rsl	AAGGACCCGAAGCTGAGCAAG
CaSnRKrt-f	TGCGCGATGGTCATTTTCTG
CaSnRKrt-r	GCAGGCGAATCTCAGGAATA
eEF1Art-f	AGTCAACTACCACTGGTCAC
eEF1Art-r	GTGCAGTAGTACTTAGTGGTC

were amplified by PCR and inserted into pENTR/D-TOPO and recombined into pDEST17, pGWB2, pGWB5, pGWB20, pSPYNE and pGWB735/1 using GATEWAY® technology (see Table 1). Primer sequences are listed in Table 2.

Generation of *avrBsT* and *avrRxv* deletion strains

To generate an *avrBsT* deletion mutant in *Xcv*, the 4.3 kb *Pst*I fragment from pXV943 containing *avrBsT* was cloned in pBluescript KS followed by digestion with *Sal*I and religation, resulting in pKSavrBsTLR. A 900 bp deletion and a frameshift in *avrBsT* (resulting in deletion of amino acids 14–314 out of 350) were introduced by *Bgl*II/*Bsr*B1 digestion of pKSavrBsTLR and religation. The resulting insert was cloned into the *Sal*I/*Xba*I sites of suicide vector pOK1 (Table 1) and introduced into the genome of *Xcv* strain 75-3 by homologous recombination as described in Huguet *et al.* (1998). To delete *avrRxv*, an *avrRxv*-containing cosmid isolated from a genomic cosmid library of *Xcv* strain 75-3 (Minsavage *et al.*, 1990) was digested with *Eco*RI and *Hin*dIII and a 6 kb fragment was cloned into pBluescript KS. The first 801 bp (corresponding to amino acids 1–267 out of 374) from *avrRxv* were deleted by *Bgl*II digestion and religation. The fragment containing the *avrRxv*-flanking regions was cloned into the *Bam*HI/*Sal*I sites of pOK1 and the resulting construct was conjugated into *Xcv* strain 85-10 to select for strain 85-10Δ*avrRxv*.

Yeast two-hybrid screening

For yeast two-hybrid (Y2H) screens we used the BD Matchmaker™ Library Construction & Screening Kit (Clontech, Heidelberg, Germany) according to the manufacturer's instructions. Screens were performed with a tomato cDNA library (Gürlebeck, 2007) and a pepper cDNA library that was generated from a mixture of leaf material of ECW-10R (untreated, inoculated with *Xcv* 85-10 and 85-10(pDS400), respectively) and of ECW-30R (untreated and inoculated with 85-10(pDSF300)).

RNA analysis and rapid amplification of cDNA ends (RACE)

For 5′-RACE, RNA was isolated from *C. annuum* ECW and ECW-10R with RNeasy Plant Mini Kit (Qiagen) and RACE was performed using a BD SMART RACE cDNA Amplification Kit (Clontech) according to the manufacturer's instructions.

For quantitative reverse-transcription PCR (qRT-PCR) analysis, RNA was extracted from 1.9 cm^2 leaf tissue using RNeasy Plant Mini Kit (Qiagen). cDNA was synthesized from 4.5 μg RNA using RevertAid™ H Minus First Strand cDNA Synthesis Kit (Fermentas, St Leon-Rot, Germany). qRT-PCR was performed on an iCycler (Bio-Rad) using ABsolute QPCR SYBR® Green Fluorescein Mix (ABgene Limited, Hamburg, Germany) and *c.* 9 ng of cDNA template as technical triplicates. PCR profiles are available upon request. For transcript abundance comparisons of different genes, the amplification efficiency for each gene was determined using a standard curve plot of a dilution series. Amplification specificity was determined by melting curve analysis. Transcript abundances of the constitutively expressed elongation factor 1A were used to account for differences in cDNA amounts as described in the user bulletin 2 (Applied Biosystems, Foster City, CA, USA).

Bimolecular fluorescence complementation

Bimolecular fluorescence complementation (BiFC) experiments were performed as described previously (Hu *et al.*, 2002) using pSPYNE and pGWB735/1 (Table 1).

Virus-induced gene silencing (VIGS)

Gene silencing in pepper ECW123 plants was performed as described previously (Liu *et al.*, 2002a; Chung *et al.*, 2004). At 21 d after initiation of silencing, plants were inoculated with *Xcv* at bacterial density of 8×10^8 cfu ml^{-1}. The silencing efficiency was determined by qRT-PCR.

Trypan blue staining and ion leakage measurements

For trypan blue staining, samples of inoculated leaf tissue were harvested 12 and 16 h post-inoculation (hpi), boiled 2 min in trypan blue solution (Koch & Slusarenko, 1990) and incubated overnight. After 2 d of bleaching in chloral hydrate (2.5 g ml^{-1} water), samples were incubated in 70% glycerol and analyzed by microscopy. For electrolyte leakage experiments, triplicates of 3.1 cm^2 infected leaf material were taken 2 and 16 hpi. Leaf discs were placed on the bottom of a 15 ml tube and covered with plastic screen. A total of 7 ml of deionized water was added to each tube and vacuum-infiltrated (1 min). Tubes were placed on to a rotary shaker at 100 rpm for 1 h and conductivity was determined (first reading) with a conductometer (Knick, Berlin, Germany). To determine maximum conductivity of the entire sample, conductivity was measured after boiling the samples for 30 min (Stall *et al.*, 1974).

Protein purification and biochemical assays

His-tagged derivatives of AvrBsT and $AvrBsT_{C222A}$ were expressed in *E. coli* BL21 and purified using nickel nitrilotriacetic acid (Ni-NTA) columns (Qiagen). Protein amounts were analyzed by SDS-PAGE and Coomassie staining and adsorbance was measured at 280 nm. Purified proteins were dialyzed in reaction buffer (100 mM Tris, pH 8.0, 150 mM NaCl, 1 mM Dithiothreitol (DTT) DTT) and protease activity of equal protein amounts was determined as described in Ma *et al.* (2006) using RediPlate 96 EnzChek Protease Assay Kit red fluorescence (Invitrogen) in a Tecan SpectraFluor Fluorescence Reader (Tecan Trading AG, Männedorf, Switzerland) at 630 nm.

For transacetylation assays, N-terminally His_6 epitope-tagged derivatives of AvrBsT and $AvrBsT_{C222A}$ were purified from *E. coli* under native conditions. Equal protein amounts were incubated with 5,5′-dithiobis-(2-nitrobenzoic acid) (DTNB) and acetyl-CoA (Williams *et al.*, 1975). The assay is based on a color change to yellow if the disulfide bond of DTNB is cleaved by thiols (e.g. from CoA-SH), resulting in 2-nitro-5-thiobenzoate (NTB). The absorbance was measured at 410 nm in a Tecan SpectraFluor Fluorescence Reader (Tecan Trading AG).

Results

The AvrBs1-specific HR in pepper ECW-10R plants is suppressed in the presence of AvrBsT

Genome sequence and Southern blot analyses revealed that the T3E gene *avrBs1* is present in the pepper-pathogenic *Xcv* strain 85-10 and in the tomato-pathogenic strain 75-3 (Ronald & Staskawicz, 1988; Escolar *et al.*, 2001; Hajri *et al.*, 2009). Notably, however, induction of the AvrBs1-specific HR in resistant ECW-10R pepper plants by strain 75-3 is significantly reduced when compared with strain 85-10, suggesting that AvrBs1 is not efficiently delivered by strain 75-3 or that the AvrBs1-specific HR is suppressed (Fig. 1a). The genome of strain 75-3 is not yet sequenced, but it was reported that strain 75-3 contains AvrBsT, which is absent from strain 85-10 (Ciesiolka *et al.*, 1999; Escolar *et al.*, 2001; Thieme *et al.*, 2005; Hajri *et al.*, 2009). We therefore wondered whether the reduction of the AvrBs1-specific HR was a result of the presence of AvrBsT. To investigate a potential influence of AvrBsT on the HR induction, we deleted *avrBsT* from the genome of strain 75-3 and inoculated the resulting deletion mutant strain 75-3Δ*avrBsT* into leaves of ECW-10R plants. In contrast to strain 75-3, strain 75-3Δ*avrBsT* induced a confluent HR in a similar manner to strain 85-10 (Fig. 1a). To confirm this finding, we introduced the expression construct pDD62avrBsT encoding AvrBsT into strain 85-10. Strain 85-10 (pDD62avrBsT) induced a significantly reduced HR when compared with strain 85-10 carrying the empty vector, suggesting that the presence of AvrBsT leads to a reduced AvrBs1-specific HR (Fig. 1a). We also investigated whether suppression of the AvrBs1-specific HR depends on the residues of the predicted catalytic triad of AvrBsT (H154, E173, C222). These residues are conserved in all YopJ/AvrRxv family members and were shown to be essential for the induction of the AvrBsT-specific HR in *N. benthamiana* and *Arabidopsis thaliana* (Orth *et al.*, 2000; Cunnac *et al.*, 2007). Notably, ectopic expression of $avrBsT_{C222A}$ in *Xcv* strain 85-10 did not interfere with the induction of the AvrBs1-specific HR (Fig. 1a).

Next, we analyzed whether suppression of the AvrBs1-induced HR occurs inside the plant cell. For this, *avrBs1* and *avrBsT* were transiently expressed in leaves of pepper ECW-10R plants via *Agrobacterium*-mediated T-DNA transfer. As expected, expression of *avrBs1* induced a confluent HR (Fig. 1b; Escolar *et al.*, 2001). Coexpression of *avrBs1* and *avrBsT* led to a significant reduction in HR induction, suggesting that the AvrBsT-dependent HR suppression occurs inside the plant cell (Fig. 1b). No HR suppression was observed upon coexpression of $avrBsT_{C222A}$ and *avrBs1*, which confirms our finding that the predicted catalytic cysteine residue of AvrBsT is crucial for the suppression of the AvrBs1-specific HR.

Analysis of the AvrBsT-mediated HR suppression by trypan blue staining and ion leakage assays

To characterize the suppression of the AvrBs1-specific HR by AvrBsT in more detail, plant cell death was monitored by trypan blue staining of infected tissue. Trypan blue is a vital stain that specifically stains dead cells but is not absorbed by cells with intact plasma membranes (Derenzis & Schechtman, 1973). *Xcv* strain 85-10 carrying the empty

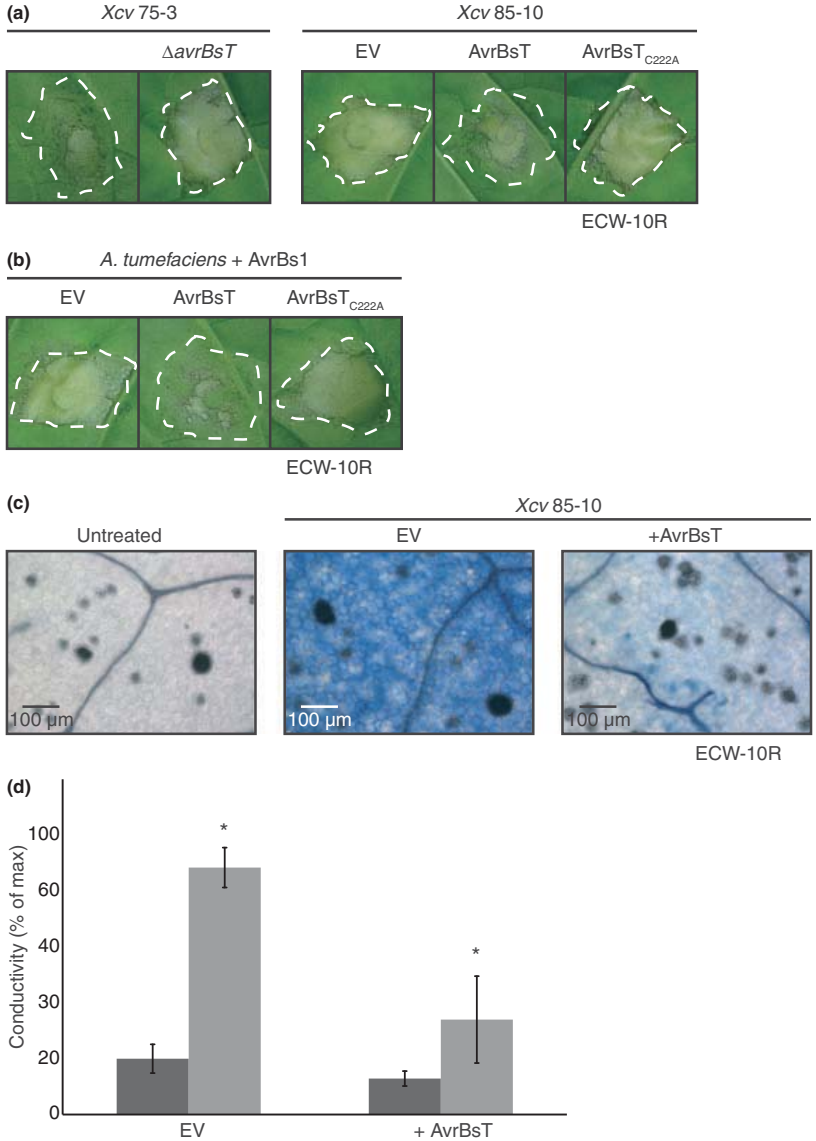

Fig. 1 The AvrBs1-specific hypersensitive response (HR) in pepper (*Capsicum annuum*) is suppressed by the YopJ-homolog AvrBsT. (a) *Xcv* strains 75-3 and 85-10 induce a reduced AvrBs1-specific HR in pepper in the presence of AvrBsT. *Xcv* 75-3, the *avrBsT* deletion mutant 75-3Δ*avrBsT* (Δ*avrBsT*) and strain 85-10 carrying the empty vector (EV) or expression constructs encoding AvrBsT or AvrBsT$_{C222A}$ were inoculated into leaves of AvrBs1-responsive ECW-10R pepper plants. Plant reactions were photographed 36 h post-inoculation (hpi). Dashed lines outline the inoculated areas. (b) AvrBsT-mediated suppression of the AvrBs1-specific HR occurs inside the plant cell. *Agrobacterium tumefaciens* strain GV3101(pMP90) carrying the EV or binary constructs encoding AvrBsT and AvrBsT$_{C222A}$ as indicated was co-inoculated with strain GV3101(pMP90) delivering *avrBs1* (+AvrBs1) at a bacterial density of 4×10^8 cfu ml^{-1} into leaves of ECW-10R pepper plants. Phenotypes were photographed 48 hpi. Dashed lines indicate the inoculated areas. (c) Trypan blue staining of infected tissue of AvrBs1-responsive ECW-10R plants reveals reduced cell death in the presence of AvrBsT. *Xcv* strain 85-10 carrying the EV or the *avrBsT* expression construct (+AvrBsT) was inoculated into leaves of pepper ECW-10R plants at a bacterial density of 2×10^8 cfu ml^{-1}. Samples of infected and untreated leaves were taken 12 hpi and stained with trypan blue. Dead plant cells stain blue. Grey and black spots represent calcium oxalate crystals. (d) Quantification of the AvrBs1-mediated HR by ion leakage measurements. *Xcv* strain 85-10 carrying the EV or the *avrBsT* expression construct (+AvrBsT) was inoculated into ECW-10R pepper plants at a bacterial density of 2×10^8 cfu ml^{-1}. Samples were taken 2 hpi (black bars) and 16 hpi (gray bars). Bars represent the average ion leakage measured for triplicates of five leaf discs each, and the error bars indicate the standard deviation thereof. The asterisks indicate a significant difference with $P < 0.05$ based on results of an unpaired Student's *t*-test. The experiment was repeated once with similar results.

vector or the *avrBsT* expression construct was inoculated into leaves of pepper ECW-10R plants. Samples from infected leaf tissue were collected 12 hpi, stained with trypan blue and analyzed by transmission light microscopy. In contrast to untreated leaf material that remained unstained, almost all cells were stained by trypan blue in tissue inoculated with strain 85-10 Fig. 1(c). In leaves inoculated with strain 85-10 expressing *avrBsT*, only a few cells were stained, which is in agreement with the reduced HR induction by this strain Fig. 1(c); see Fig. 1(a). Similar results were obtained 16 hpi (data not shown). Reduced staining of infected plant tissue was also observed after inoculation of strain 75-3Δ*avrBsT* when compared with strain 75-3 (data not shown).

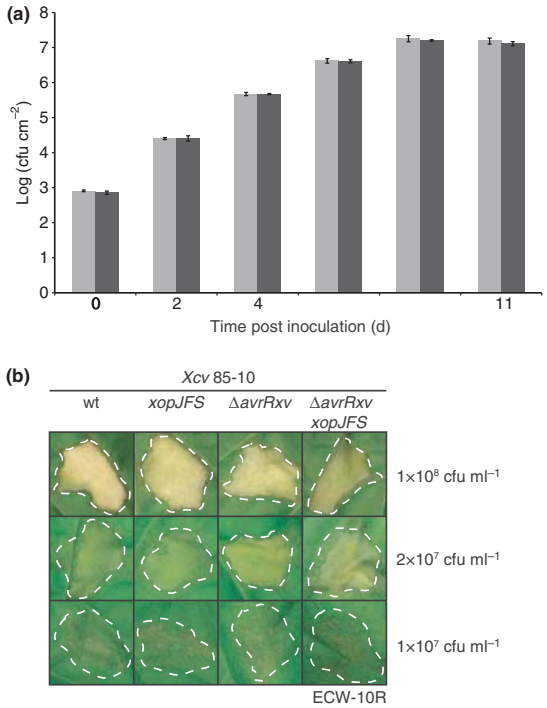

Fig. 2 AvrBsT does not significantly contribute to *in planta* bacterial growth. (a) *In planta* growth curve analyses with *Xcv* strains 75-3 (wt; gray bars) and 75-3Δ*avrBsT* (Δ*avrBsT*; black bars). Bacteria were inoculated into leaves of susceptible tomato (*Solanum lycopersicum*) plants cv Moneymaker, and bacterial numbers were determined over a period of 11 d post-inoculation (dpi). Values are the average of three samples from three different plants. Error bars represent standard deviations. Similar results were obtained in two repetitions of the experiment. (b) Mutation of *avrRxv* and *xopJ* in strain 85-10 does not affect the AvrBs1-specific hypersensitive response (HR). Strain 85-10 (wt) and derivatives mutated in *xopJ* (*xopJFS*) and/or *avrRxv* (Δ*avrRxv*) were inoculated into ECW-10R pepper (*Capsicum annuum*) plants at 1×10^8, 2×10^7 and 1×10^7 cfu ml^{-1} as indicated. Phenotypes were photographed 36 h post-inoculation (hpi). Dashed lines indicate the inoculated areas.

For the quantitative analysis of the HR suppression, we determined ion leakage in leaves infected with strain 85-10 carrying the empty vector or the *avrBsT* expression construct. Ion leakage is associated with cell death and leads to conductivity changes of samples in distilled water. As expected for an ongoing HR, conductivity increased in samples inoculated with *Xcv* strain 85-10 (Fig. 1d). In the presence of AvrBsT, however, ion leakage was reduced by *c.* 50% (Fig. 1d), which correlates well with the observed HR suppression by AvrBsT.

AvrBsT does not significantly contribute to bacterial virulence in tomato plants

Given the function of AvrBsT as HR suppressor, we wondered whether AvrBsT contributes to bacterial virulence. We therefore analyzed disease symptoms and growth of *Xcv* strains 75-3 and 75-3Δ*avrBsT* in leaves of susceptible tomato cv Moneymaker plants. No differences in disease symptoms were detected (data not shown). Furthermore, deletion of *avrBsT* from *Xcv* 75-3 did not alter bacterial growth *in planta*, suggesting that AvrBsT does not significantly contribute to bacterial virulence (Fig. 2a). It remains to be investigated whether the lack of an obvious virulence function of AvrBsT is a result of the presence of functionally redundant effector proteins. As mentioned earlier, AvrBsT belongs to the YopJ/AvrRxv protein family, which includes XopJ and AvrRxv, both present in strain 85-10. Notably, however, deletion mutant derivatives of strain 85-10 lacking *xopJ* and/or *avrRxv* induced the HR in ECW-10R pepper plants in a similar fashion to strain 85-10, suggesting that both do not suppress the AvrBs1-specific HR (Fig. 2b). Furthermore, *Agrobacterium*-mediated coexpression of *avrBs1* with *xopJ* or *avrRxv*, did not affect the HR in ECW-10R plants (data not shown). Thus, the suppression of the AvrBs1-specific HR is specifically caused by AvrBsT.

AvrBs1 and AvrBsT are class B effectors that are translocated in the absence of the general T3S chaperone HpaB

To confirm the T3S system-dependent translocation of AvrBs1 and AvrBsT into the plant cell, we generated fusion proteins between AvrBs1 and AvrBsT and the reporter protein AvrBs3Δ2, which is a derivative of the type III effector AvrBs3 lacking the translocation signal. However, AvrBs3Δ2 contains the effector domain and is recognized in AvrBs3-responsive ECW-30R pepper plants when fused to a functional T3S and translocation signal (Szurek *et al.*, 2002; Noël *et al.*, 2003). AvrBs3Δ2 reporter constructs were introduced into *Xcv* strains 85-10*hrpG** (85*), the T3S mutant 85-10*hrpG*ΔhrcV* (85*Δ*hrcV*), and the *hpaB* deletion mutant 85-10*hrpG*ΔhpaB* (85*Δ*hpaB*) (Büttner *et al.*, 2004). *hrpG** strains contain a constitutively active

derivative of the key regulator HrpG, which activates *hrp* gene expression and is essential for the translocation of class B T3Es in the *hpaB* deletion mutant (Wengelnik *et al.*, 1996, 1999; Büttner *et al.*, 2006). For *in vivo* translocation assays, bacteria were inoculated into leaves of AvrBs3-responsive ECW-30R plants. Derivatives of strain 85* delivering AvrBs1-AvrBs3Δ2 and AvrBsT-AvrBs3Δ2 induced the HR in ECW-30R, whereas no HR was observed with the T3S mutant 85*Δ*hrcV*, suggesting that both fusion proteins were translocated by the T3S system (Fig. 3a).

AvrBsT-AvrBs3Δ2 and AvrBs1-AvrBs3Δ2 both induced a partial HR when delivered by strain 85*Δ*hpaB*, suggesting that translocation occurred even in the absence of the global T3S chaperone HpaB, albeit in reduced amounts (Fig. 3a). This is in agreement with the previous finding that strain 85*Δ*hpaB* induces a partial AvrBs1-specific HR in ECW-10R plants (Fig. 3a; Büttner *et al.*, 2004). Differences in the HR were not the result of differences in protein stabilities, because similar amounts of AvrBsT-AvrBs3Δ2 and AvrBs1-AvrBs3Δ2 were detected in wild-type and *hpaB* deletion mutant strains (Fig. 3b). Our results therefore suggest that AvrBs1 and AvrBsT belong to class B of T3Es that are translocated in the absence of the global T3S chaperone HpaB (Büttner *et al.*, 2006). It is therefore tempting to speculate that AvrBs1 and AvrBsT are translocated at the same stage during infection.

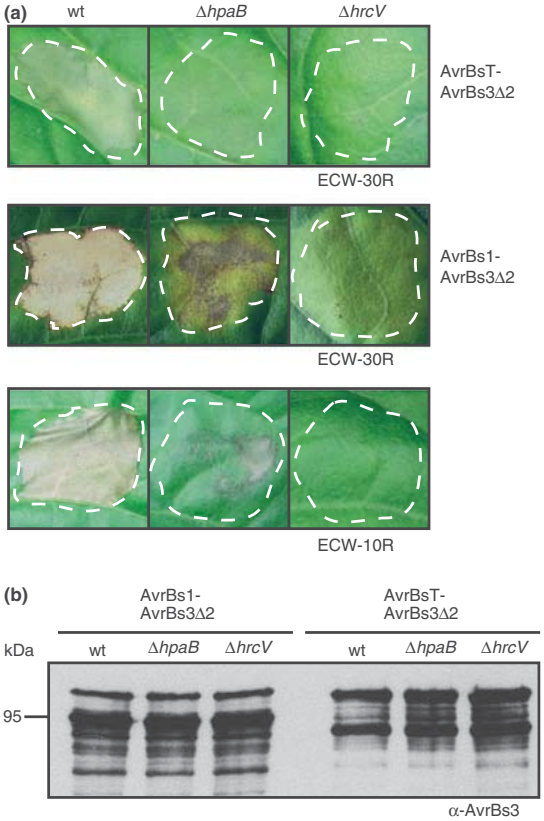

Fig. 3 AvrBs1 and AvrBsT are translocated in the absence of the general T3S chaperone HpaB. (a) AvrBs1-AvrBs3Δ2 and AvrBsT-AvrBs3Δ2 are translocated by the T3S system in the absence of the global T3S chaperone HpaB. *Xcv* strains 85* (wt), 85*Δ*hpaB* (Δ*hpaB*) and 85*Δ*hrcV* (Δ*hrcV*) encoding AvrBs1-AvrBs3Δ2 and AvrBsT-AvrBs3Δ2 from corresponding expression constructs were inoculated at 4×10^8 and 2×10^9 cfu ml^{-1}, respectively, into leaves of AvrBs3-responsive ECW-30R pepper (*Capsicum annuum*) plants. Similarly, strains 85* (wt), 85*Δ*hpaB* (Δ*hpaB*) and 85*Δ*hrcV* (Δ*hrcV*) encoding AvrBs1-AvrBs3Δ2 were inoculated into leaves of AvrBs1-responsive ECW-10R plants at 4×10^8 cfu ml^{-1}. Dashed lines indicate the inoculated areas. (b) Analysis of AvrBs1-AvrBs3Δ2 and AvrBsT-AvrBs3Δ2 protein accumulation. *Xcv* strains 85* (wt), 85*Δ*hpaB* (Δ*hpaB*) and 85*Δ*hrcV* (Δ*hrcV*) encoding AvrBs1-AvrBs3Δ2 and AvrBsT-AvrBs3Δ2 from respective expression constructs were grown in minimal medium. Protein extracts from equal amounts of bacterial cells were analyzed by immunoblotting using an AvrBs3-specific antibody. Upper bands represent AvrBs3Δ2 fusion proteins; lower bands correspond to degradation products.

Isolation of plant interaction partners of AvrBs1 and AvrBsT

To identify potential plant interaction partners of AvrBs1 and AvrBsT, we used AvrBs1 and the catalytic mutant $AvrBsT_{C222A}$ as baits in Y2H screens. $AvrBsT_{C222A}$ was chosen to ensure that interaction partners of AvrBsT are not proteolytically cleaved or modified. Since AvrBs1 and $AvrBsT_{C222A}$ did not auto-activate the reporter genes, yeast strains expressing these baits were mated with strains containing prey cDNA libraries. The latter were generated from mRNA isolated from leaves of pepper lines ECW and ECW-30R and tomato *Solanum lycopersicum* cv Moneymaker, respectively. We analyzed *c.* 10^8 clones per screen and identified potential interaction partners of AvrBs1 and $AvrBsT_{C222A}$ (Table 3). Potential interactors of AvrBs1 include, for example, proteins with homology to a tonoplast-intrinsic protein, a tyrosine kinase and a DNA-binding protein with basic helix-loop-helix motif. Proteins interacting with AvrBsT showed homology to elongation factor eEF1A, a subunit of the 26S proteasome, an ABC transporter and a sucrose nonfermenting 1 (SNF1)-related kinase 1 (SnRK1) (Fig. 4a). Reproducibility of the interactions was tested by retransforming prey and bait plasmids into yeast. Prey plasmids encoding potential interactors of AvrBs1 and $AvrBsT_{C222A}$ did not activate expression of reporter genes in yeast strains that contained Lamin C, suggesting that the interactions were specific (data not shown). We also tested whether interactors of AvrBs1 interact with $AvrBsT_{C222A}$ and vice versa; however, no common interacting protein was identified.

Table 3 Plant interactors of AvrBs1 and AvrBsT identified in yeast two-hybrid screens

Annotation[a]	TIGR entry	Amino acid identity (%)	Silencing phenotype[b]
AvrBs1 interacting proteins			
δ-tonoplast intrinsic protein	TC192986[c]	100	No
Tyrosine kinase	TC203725[c]	97	No
DNA-binding protein (bHLH)	TC203608[c]	90	No
Pentatricopeptide repeat-containing protein	TC207123[c]	96	nd
ATP/GTP-binding protein	TC194177[c]	99	nd
$AvrBsT_{C222A}$ interacting proteins			
Elongation factor-1A (eEF1A)	TC205961[c]	92	No
Unknown protein (GYF domain)	TC193387[c]	93	No
26S proteasome RPN8	TC197733[c]	91	nd
ABC transporter	TC12447[d]	70	No
SNF1-homologous protein	TC194482[c]	92	Reduction of AvrBs1-specific HR

[a]Interactors were isolated from a tomato cDNA-library. eEF1A and the SNF1-homologous protein were also isolated from the pepper cDNA library.
[b]A potential contribution to the induction of the AvrBs1-specific HR in ECW-10R pepper plants was analyzed by VIGS. No, no reduction in HR induction observed; nd, not determined.
[c]*Solanum lycopersicum* TIGR database (http://compbio.dfci.harvard.edu/tgi/).
[d]*Capsicum annuum* TIGR database (http://compbio.dfci.harvard.edu/tgi/).

The AvrBsT interactor SnRK1 is required for the efficient induction of the AvrBs1-specific HR

To test whether plant proteins interacting with AvrBsT or AvrBs1 are biologically relevant for the AvrBs1-specific HR, the corresponding genes were silenced in different AvrBs1-responsive pepper cultivars using VIGS. For VIGS, 300–500 bp fragments of the respective coding sequences were cloned into a tobacco rattle virus-silencing vector and expressed *in planta* using *Agrobacterium*-mediated T-DNA delivery. As negative control, plants were treated with *Agrobacterium* carrying the empty silencing vector. Two weeks later leaves were inoculated with *Xcv* strain 85-10. qRT-PCR analysis revealed that VIGS resulted in a > 70-fold reduction of the *SnRK1* transcript at this time-point (Fig. 4b).

Silencing of the *SnRK1* transcript led to a severe reduction of the AvrBs1-specific HR induced by strain 85-10 in ECW-10R and ECW123 (Fig. 4c,d). The AvrBs1-specific HR is visible as a white necrosis of the inoculated leaf area 4 d post-inoculation (dpi) (Fig. 4e). The partial necrosis in *SnRK1*-silenced ECW-10R and ECW123 plants after inoculation of strain 85-10 was presumably the result of residual recognition of AvrBs1, because in virus-treated control plants a similar phenotype was observed after inoculation with strain 85-10 carrying AvrBsT (Fig. 4c,d). Besides, AvrBs1 ECW123 also recognizes AvrBs3. Strain 85-10 carrying AvrBs3 elicited a white necrotic HR in virus-treated ECW123 controls, whereas *SnRK1*-silenced plants showed a reduced brownish HR (Fig. 4d). The brown necrosis was caused by recognition of AvrBs3 (compare also Fig. 4e), suggesting that SnRK1 is not essential for the Bs3-mediated HR. Therefore SnRK1 does not appear to be a general mediator of plant defense.

SnRK1 was isolated from both pepper and tomato and is homologous to *SNF1* from yeast. We determined the complete coding sequence from pepper ECW and ECW-10R plants by 5′-RACE. Both sequences were identical and share 95% DNA sequence identity with *Snf1* from tomato (accession number AF143743). Comparison of the corresponding proteins revealed 98% sequence identity. SnRK1 contains predicted serine/threonine kinase, ubiquitin-associated and kinase-associated domains.

SnRK1 and AvrBsT interact in the plant cell cytosol

To investigate the subcellular localization of AvrBs1, AvrBsT and SnRK1 in the plant cell, green fluorescent protein (GFP) fusions were synthesized in *N. benthamiana* after *Agrobacterium*-mediated gene delivery. We did not use pepper plants for these experiments because of the very low efficiency of *Agrobacterium*-mediated transformation of pepper (R Szczesny & U Bonas, unpublished). Since AvrBsT induces the HR in *N. benthamiana* 24 hpi (Orth *et al.*, 2000; data not shown), GFP fluorescence was analyzed 20 hpi. Confocal laser-scanning microscopy of infected plant tissue revealed that AvrBs1-GFP localized to the plant cell cytoplasm and was nuclear-excluded as reported previously (Fig. 5a; Gürlebeck *et al.*, 2009). By contrast, GFP fusions of AvrBsT and SnRK1 localized to both the cytoplasm and nuclei (Fig. 5a). Detection of GFP fluorescence in the nucleus was not a result of nuclear transport of GFP-containing protein degradation products since all GFP fusion proteins were stably synthesized (Fig. 5b). Our results therefore suggest that AvrBsT and SnRK1 localize to the same cellular compartments in the plant cell.

To confirm the interaction between AvrBsT and SnRK1 *in planta*, we performed BiFC (Hu *et al.*, 2002). BiFC is observed when translational fusions between the two non-fluorescent portions of the yellow fluorescent protein (YFP) to two potential interaction partners are brought into close proximity. We generated expression constructs encoding YFP_C-SnRK1 and AvrBsT-YFP_N and co-delivered the

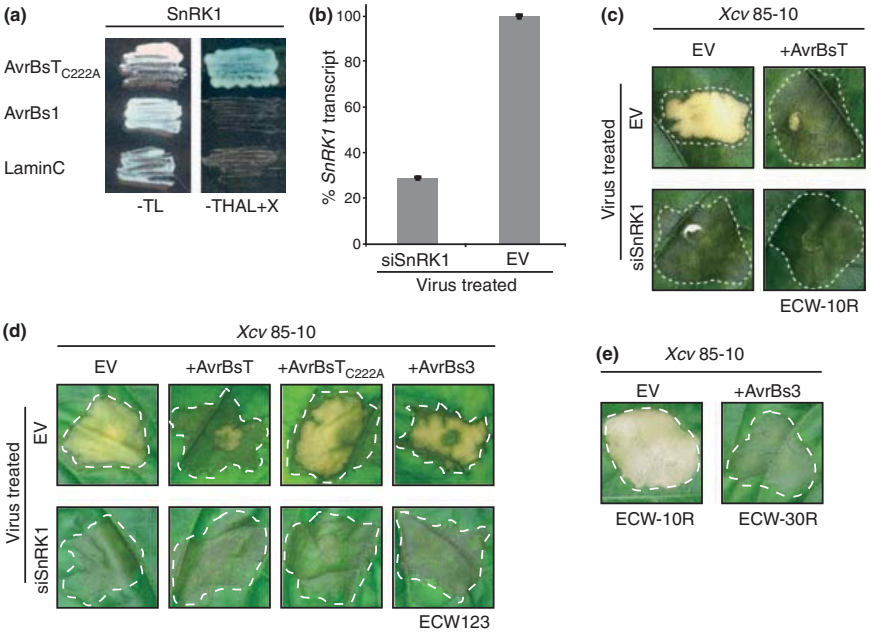

Fig. 4 AvrBsT interacts with SnRK1, which is required for the elicitation of the AvrBs1-specific hypersensitive response (HR) in pepper (*Capsicum annuum*). (a) AvrBsT interacts with SnRK1 in yeast. *Saccharomyces cerevisiae* transformants encoding AvrBsT$_{C222A}$, AvrBs1 and Lamin C as fusions to the GAL4 DNA-binding domain and a pepper protein with homology to the C-terminal region of SnRK1 fused to the GAL4-activation domain were grown on minimal synthetic defined (SD) dropout medium lacking tryptophan and leucine (−TL) or lacking adenine, tryptophan, histidin and leucine (−THAL) and containing 5-bromo-4 chloro-3-indolyl-alpha-D galactopyranosid (+X). Plates were photographed 3 days after plating. (b) Quantification of *SnRK1* transcript accumulation in *SnRK1*-silenced plants. For VIGS *C. annuum* ECW123 plants were co-inoculated with derivatives of *Agrobacterium tumefaciens* strain GV3101(pMP90) carrying pTRV1 and pTRV2aSnRK1 (siSNRK1). As negative control we used GV3101(pMP90) carrying empty pTRV2a (EV). *SnRK1* transcript abundances were determined 2 wk after silencing by quantitative reverse-transcription PCR (qRT-PCR). Bars represent transcript abundance of the average of five leaf discs; the error bars indicate the standard deviation between the samples. The experiment was repeated three times with similar results. Transcript abundance of constitutively expressed elongation factor 1α served to adjust differences in cDNA-amounts (data not shown). (c) VIGS reveals a role of pepper SnRK1 in the induction of the AvrBs1-specific HR. Virus-treated (EV) and *SnRK1*-silenced (siSnRK1) ECW-10R pepper plants were inoculated with *Xcv* strain 85-10 carrying empty vector (EV) or an expression construct encoding AvrBsT at 4×10^8 cfu ml^{-1}. Please note that the HR induction in virus-treated plants is generally delayed by at least 2 d compared with untreated plants. Phenotypes were photographed 4 dpi. Dashed lines indicate the inoculated areas. (d) Silencing of *SnRK1* transcript does not abolish the AvrBs3-specific HR. Virus-treated (EV) and *SnRK1*-silenced (siSnRK1) ECW123 pepper plants were inoculated with *Xcv* strain 85-10 carrying EV or expression constructs encoding AvrBsT, AvrBsT$_{C222A}$ and AvrBs3, respectively. Phenotypes were photographed 4 dpi. Dashed lines indicate the inoculated areas. The enhanced necrosis induced by strain 85-10 in the presence of AvrBsT is to the result of the recognition of AvrBsT, which elicits the HR in all ECW pepper lines. (e) Recognition of AvrBs1 induces a white necrosis of the infected leaf tissue. *Xcv* strains 85-10 (EV) and 85-10 encoding AvrBs3-FLAG (+AvrBs3) were inoculated into leaves of ECW-10R (AvrBs1 recognition) and ECW-30R (AvrBs3 recognition), respectively. Phenotypes were photographed 4 dpi. Dashed lines indicate the inoculated areas.

corresponding genes into leaves of *N. benthamiana* by *Agrobacterium*. Infected leaf material was analyzed by confocal laser-scanning microscopy; however, no fluorescent signal was detected 20 hpi (data not shown; note that AvrBsT induces the HR in *N. benthamiana* 24 hpi). Because this time-point might be too early to detect BiFC, we repeated the experiment with YFP$_C$-SnRK1 and the catalytic mutant AvrBsT$_{C222A}$-YFP$_N$, which does not induce the HR in *N. benthamiana* (Orth *et al.*, 2000; data not shown). Inspection of infected leaf material 48 hpi revealed YFP fluorescence in the plant cell cytoplasm (Fig. 5c). No fluorescence was observed for YFP$_C$-SnRK1 and AvrBs1-YFP$_N$ (Fig. 5c), which confirms that SnRK1 is a specific interactor of AvrBsT and does not interact with AvrBs1. Taken together, we conclude that AvrBsT and SnRK1 interact in the plant cell cytoplasm.

AvrBsT does not degrade or transacetylate SnRK1

AvrBsT belongs to the conserved YopJ/AvrRxv protein family, members of which were proposed to act as cysteine proteases (Orth, 2002). To test AvrBsT for proteolytic activity, His$_6$ epitope-tagged derivatives of AvrBsT and AvrBsT$_{C222A}$ were synthesized in *E. coli*, purified (see the

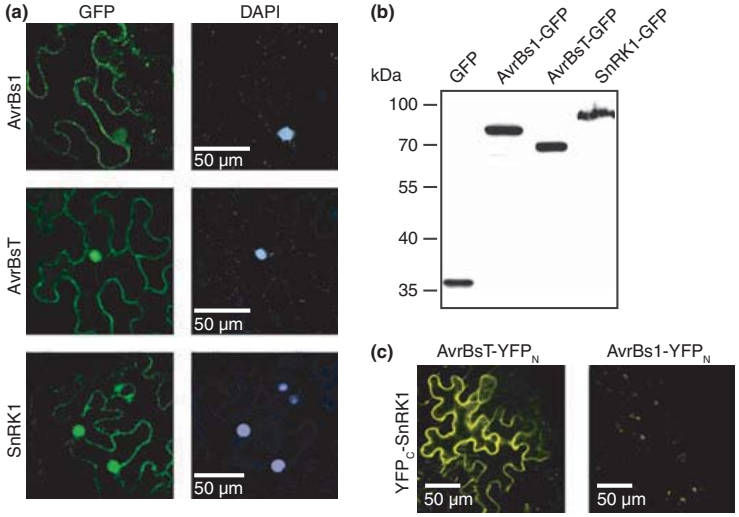

Fig. 5 AvrBsT and SnRK1 localize in the plant cell cytoplasm and interact *in planta*. (a) *In planta* localization of AvrBs1, AvrBsT and SnRK1. Leaves of *Nicotiana benthamiana* were inoculated with *Agrobacterium tumefaciens* strain GV3101(pMP90) delivering *gfp* (GFP), *avrBs1-gfp* (AvrBs1), *avrBsT-gfp* (AvrBsT) and *SnRK1-gfp* (SnRK1), respectively. Infected plant tissue was analyzed 20 h post-inoculation (hpi) by confocal laser scanning microscopy. The second panel shows diamidin-2-phenylindol (DAPI) staining of nuclei. (b) GFP and GFP fusion proteins are stably synthesized. Samples of infected leaf material of *N. benthamiana* plants inoculated with *A. tumefaciens* as described in (a) were analyzed 20 hpi by immunoblotting using a GFP-specific antibody. (c) AvrBsT and SnRK1 interact in the plant cell cytoplasm. YFP_C-SnRK1 was synthesized together with $AvrBsT_{C222A}$-YFP_N or AvrBs1-YFP_N as indicated in *N. benthamiana* leaves after *A. tumefaciens*-mediated gene delivery. Infected leaf material was inspected 48 hpi by confocal laser scanning microscopy using yellow fluorescent protein (YFP)-specific filters.

Materials and Methods section; Fig. 6a) and incubated with fluorescence-labeled casein as substrate. AvrBsT led to a weak increase of fluorescence indicative of a protease activity, which was dependent on the predicted catalytic cysteine residue at position 222 (Fig. 6b). We also investigated whether stability of SnRK1 is affected in the presence of AvrBsT. For this, genes encoding AvrBsT, $AvrBsT_{C222A}$ and AvrBs1 (used as control), and a c-Myc epitope-tagged derivative of SnRK1, were expressed under control of the cauliflower mosaic virus *35S* promoter in leaves of pepper ECW-10R after *Agrobacterium*-mediated gene delivery. Leaf material was harvested 1 dpi and analyzed by immunoblotting using a c-Myc specific antibody. Coexpression of *SnRK1* with either *avrBsT*, $avrBsT_{C222A}$ or *avrBs1* did not result in any obvious degradation of SnRK1 (Fig. 6c).

We also investigated a possible transacetylase activity of AvrBsT because the AvrBsT homolog YopJ acts as acetyltransferase (Mukherjee *et al.*, 2006). For this, derivatives of SnRK1, AvrBsT and $AvrBsT_{C222A}$ with N-terminal His_6 epitope tag were synthesized in *E. coli*, purified under native conditions (see the Materials and Methods section) and incubated with DTNB and acetyl-CoA (see the Materials and Methods section). With AvrBsT we observed a slight increase in absorbance indicative of the generation of NTB; however, similar results were obtained with the catalytic mutant $AvrBsT_{C222A}$ (Fig. 6d). Taken together, we conclude that AvrBsT does not cleave or transacetylate SnRK1 under the conditions tested.

Discussion

In this study, we identified the T3E AvrBsT from *Xcv* as a suppressor of the AvrBs1-specific HR in pepper plants. The HR suppression occurred when both AvrBsT and AvrBs1 were delivered by *Xcv* or were synthesized *in planta* after *Agrobacterium*-mediated gene delivery, suggesting that AvrBsT interferes with plant defense inside the plant cell. *In vivo* translocation assays revealed that both effectors are translocated by the T3S system even in the absence of the global T3S chaperone HpaB, suggesting that AvrBs1 and AvrBsT belong to class B of T3Es and are presumably translocated at a similar stage during infection. AvrBsT is homologous to members of the YopJ/AvrRxv family, which were predicted to act as cysteine proteases and/or acetyltransferases. Acetyltransferase activity was indeed demonstrated for YopJ from *Yersinia* spp. (Mukherjee *et al.*, 2006). By contrast, a weak protease activity was shown for the YopJ-homologs HopZ1 and HopZ2 from *Pseudomonas* (Ma *et al.*, 2006). Here, we show that AvrBsT from *Xcv* exhibits a weak *in vitro* protease activity, which depends on the conserved predicted catalytic cysteine residue of AvrBsT at position 222. Interestingly, cysteine 222 is also required for

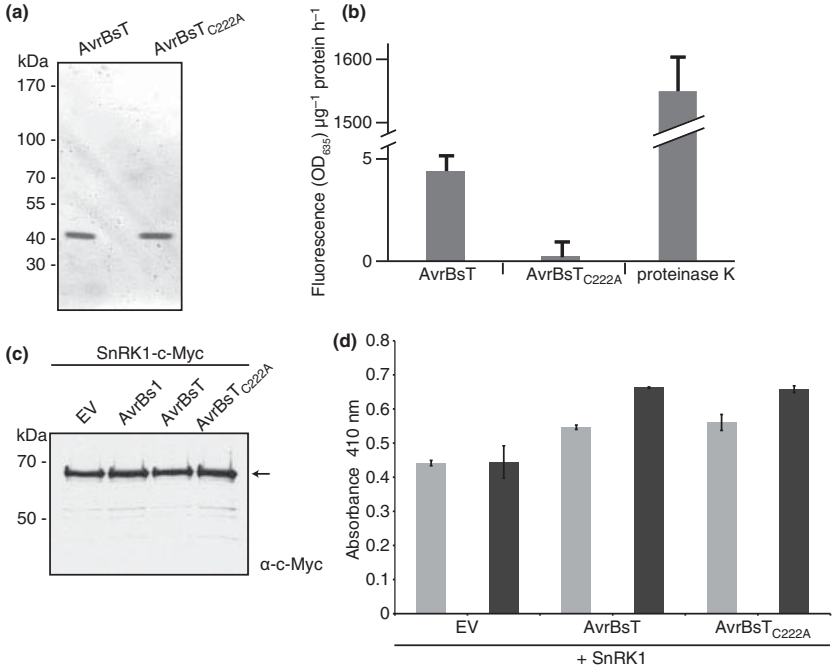

Fig. 6 Analysis of potential AvrBsT-mediated degradation or acetylation of SnRK1. (a) Purification of His_6-AvrBsT and His_6-$AvrBsT_{C222A}$ from *Escherichia coli*. Proteins were purified from *E. coli* using Ni-NTA agarose and analyzed by SDS-PAGE and Coomassie staining. (b) Protease assay with AvrBsT and $AvrBsT_{C222A}$. Protease activity was measured using casein as substrate. Bars represent fluorescence of five replicates 1 h post-inoculation (hpi). Proteinase K was used as a positive control. Error bars represent standard deviations. The experiment was repeated twice with similar results. (c) SnRK1 is not degraded by AvrBsT. *SnRK1-c-Myc* was coexpressed in ECW-10R with *avrBsT*, *avrBsT*$_{C222A}$ or *avrBs1* after *Agrobacterium*-mediated T-DNA transfer. Tissue was harvested 24 hpi and analyzed by western blot using a α-c-Myc antibody. (d) Analysis of a potential AvrBsT-mediated acetylation of SnRK1. Extracts from *E. coli* containing empty vector (EV), His_6-AvrBsT, His_6-$AvrBsT_{C222A}$ and His_6-SnRK1, respectively, were purified using Ni-NTA agarose under native conditions and incubated with acetyl-CoA and 5,5′-dithiobis-(2-nitrobenzoic acid) (DTNB). Absorbance was measured at 410 nm after 0 (gray bars) and 10 (black bars) min as indicated. The bars indicate the average of five reactions; error bars indicate the corresponding standard deviation.

the AvrBsT-dependent HR induction in pepper, *N. benthamiana* and *A. thaliana* ecotype Pi-0, which suggests that the induction of defense responses in AvrBsT-responsive plants depends on the predicted enzymatic activity of AvrBsT (Orth *et al.*, 2000; Cunnac *et al.*, 2007). Notably, the AvrBsT-HR in *A. thaliana* is suppressed by a carboxylesterase (Cunnac *et al.*, 2007).

To our knowledge, AvrBsT is the first member of the YopJ/AvrRxv family known to suppress effector-triggered plant immunity. Notably, we did not observe a suppression of the AvrBs1-specific HR by AvrBsT homologs such as XopJ or AvrRxv from *Xcv* that are both expressed in *Xcv* strain 85-10. However, it was previously shown that XopJ suppresses callose deposition in the plant cell wall, which is part of basal plant defense (Bartetzko *et al.*, 2009). Suppression of plant defense responses appears to be one of the major missions of T3Es from plant pathogenic bacteria and is often achieved by modulation of host protein turnover. Several T3Es that interfere with plant immunity act as proteases; for example, the cysteine proteases AvrPphB and AvrRpt2 from *P. syringae* and XopD from *Xcv*. AvrPphB cleaves the plant protein kinase PBS1 which is guarded by the R protein RPS5 (Shao *et al.*, 2003; Ade *et al.*, 2007). AvrRpt2, by contrast, degrades RIN4, which is a negative regulator of plant defense (Axtell *et al.*, 2003; Kim *et al.*, 2005). XopD presumably acts on small ubiquitin-like modifier (SUMO)-conjugated proteins in the plant cell nucleus (Hotson *et al.*, 2003). A function as SUMO protease was also proposed for the AvrBsT homolog YopJ; however, no specific host target proteins for de-SUMOylation by YopJ were identified (Orth *et al.*, 2000). Preliminary data suggest that AvrBsT from *Xcv* does not significantly alter the amounts of SUMO- or ubiquitin-associated proteins (R Szczesny *et al.*, unpublished).

To identify potential plant targets of AvrBsT we performed Y2H screens. Plant interactors of AvrBsT include a subunit of the 26S proteasome and SnRK1. We did not identify 14-3-3 proteins although a member of this large

protein family was previously shown to interact with AvrRxv from *Xcv* (Whalen *et al.*, 2008). It is conceivable that YopJ/AvrRxv family members differ in the choice of their host targets, which might also be reflected by differences in protein localization. Thus, in contrast to AvrRxv, which is in the cytoplasm (Bonshtien *et al.*, 2005), XopJ from *Xcv* is targeted to the plasma membrane (Thieme *et al.*, 2007), and AvrBsT localizes to both cytoplasm and nucleus (Fig. 5).

Given the finding that several T3Es exploit the host proteasome to modulate protein turnover, for example, by acting as ubiquitin ligase (Speth *et al.*, 2007), it will be interesting to investigate whether AvrBsT associates with the proteasome *in planta* and modifies its ubiquitination status. Thus far, we have not determined whether the predicted association of AvrBsT with the proteasome is required for the interference with plant immunity. However, our gene silencing experiments revealed that reduced transcript abundance of *SnRK1* lead to a severe reduction of the AvrBs1-specific HR. SnRK1 does not interact with AvrBs1 and is therefore presumably indirectly involved in the recognition of AvrBs1 by the cognate, as yet unknown *R* gene *Bs1* or in downstream signaling that leads to the HR-induction. It is unlikely that SnRK1 represents the R protein Bs1 because the *SnRK1* open reading frame is identical in susceptible ECW and resistant ECW-10R plants. We cannot exclude that resistance in ECW-10R depends on differences in the *SnRK1* promoter region. However, transient expression of *SnRK1* under control of the 35S promoter in ECW-10R pepper plants did not induce any detectable cell death reaction (data not shown), suggesting that enhanced transcript abundance of SnRK1 is not sufficient to trigger the HR.

SnRK1 is the plant ortholog of SNF1 from yeast and the AMP-activated protein kinase (AMPK) from mammals that are important regulators of sugar metabolism (Hardie, 2007; Hedbacker & Carlson, 2008; Halford & Hey, 2009). SnRK1 phosphorylates enzymes involved in primary metabolism and is a central regulator of reprogramming gene expression in response to environmental stresses (Halford & Hey, 2009). Similarly to SNF1 and AMPK, SnRK1 is presumably part of a heterotrimeric complex. The AMPK heterotrimer consists of a catalytic α subunit that is homologous to SNF1, and β and γ subunits (Davies *et al.*, 1994; Mitchelhill *et al.*, 1994). Homologs of the β and the γ subunits in yeast are encoded by *SNF4* and the related genes *SIP1*, *SIP2* and *GAL83*. Proteins with homology to SNF4, SIP1, SIP2 and GAL83 have been cloned from *A. thaliana*, *Solanum tuberosum* and maize and were shown to interact with SnRK1 (Bouly *et al.*, 1999; Lakatos *et al.*, 1999; Kleinow *et al.*, 2000; Lumbreras *et al.*, 2001). In agreement with this finding, we identified a protein from pepper with homology to GAL83 as interactor of pepper SnRK1 (R Szczesny & U Bonas, unpublished).

Interestingly, there is growing evidence for a role of SNF1 homologs in response to pathogens. First, SnRK1 was found to be induced in citrus plants after infection with *X. axonopodis* pv. *citri* (Cernadas *et al.*, 2008). Furthermore, the SnRK1 homolog AKIN1 from *N. benthamiana* is important for resistance against tomato golden mosaic virus and beet curly top virus (Hao *et al.*, 2003). The viral proteins AL2 and L2 interact with AKIN1, which in turn is inactivated (Sunter *et al.*, 2001). It remains to be investigated whether AvrBsT inhibits the function of pepper SnRK1 and thereby suppresses the AvrBs1-specific HR. In any case, the mere interaction of SnRK1 and AvrBsT is not sufficient for the HR-suppression because the catalytic core mutant $AvrBsT_{C222A}$ also binds SnRK1 but does not suppress the AvrBs1-induced HR. This suggests that the predicted catalytic activity of AvrBsT is essential for the HR suppression. Surprisingly, we did not detect degradation of SnRK1 in the presence of AvrBsT. Furthermore, *in vitro* assays did not reveal an obvious acetylation of SnRK1 by AvrBsT. We cannot, of course, exclude that AvrBsT has an as yet unknown enzymatic function or that degradation or acetylation of SnRK1 occurs under natural conditions but is not detectable *in vitro* or upon *in planta* overexpression of *SnRK1* and *avrBsT*. Furthermore, it is possible that AvrBsT degrades another subunit of the predicted SnRK1-containing trimeric complex, for example the GAL83 homolog that interacts with SnRK1.

Taken together, our findings suggest that the effector AvrBsT from *Xcv* targets pepper SnRK1, a regulator of sugar metabolism, which is required for AvrBs1-induced immunity. Future studies are needed to elucidate whether AvrBsT modifies the SnRK1 complex and, if so, which kind of modification occurs.

Acknowledgements

We are grateful to M. Schattat for contributing to microscopy studies, to M. B. Mudgett and to T. Lahye for providing plasmids, to P. Römer for contributing to the generation of the pepper Y2H library, to C. Kretschmer for sequencing, and to B. Rosinsky for glasshouse work. This work was supported by grants from the Deutsche Forschungsgemeinschaft (Sonderforschungsbereich 648 'Molekulare Mechanismen der Informationsverarbeitung in Pflanzen') to D.B. and U.B.

References

Abramovitch RB, Martin GB. 2004. Strategies used by bacterial pathogens to suppress plant defenses. *Current Opinion in Plant Biology* **7**: 356–364.

Ade J, DeYoung BJ, Golstein C, Innes RW. 2007. Indirect activation of a plant nucleotide binding site-leucine-rich repeat protein by a bacterial protease. *Proceedings of the National Academy of Sciences, USA* **104**: 2531–2536.

Anand A, Krichevsky A, Schornack S, Lahaye T, Tzfira T, Tang Y, Citovsky V, Mysore KS. 2007. *Arabidopsis* VIRE2 INTERACTING PROTEIN2 is required for *Agrobacterium* T-DNA integration in plants. *Plant Cell* **19**: 1695–1708.

Astua-Monge G, Minsavage GV, Stall RE, Vallejos CE, Davis MJ, Jones JB. 2000. *Xv4-avrXv4*: a new gene-for-gene interaction identified between *Xanthomonas campestris* pv. *vesicatoria* race T3 and the wild tomato relative *Lycopersicon pennellii*. *Molecular Plant-Microbe Interactions* **13**: 1346–1355.

Ausubel FM, Brent R, Kingston RE, Moore DD, Seidman JG, Smith JA, Struhl K. 1996. *Current protocols in molecular biology*. New York, NY, USA: John Wiley & Sons, Inc.

Axtell MJ, Chisholm ST, Dahlbeck D, Staskawicz BJ. 2003. Genetic and molecular evidence that the *Pseudomonas syringae* type III effector protein AvrRpt2 is a cysteine protease. *Molecular Microbiology* **49**: 1537–1546.

Bartetzko V, Sonnewald S, Vogel F, Hartner K, Stadler R, Hammes UZ, Bornke F. 2009. The *Xanthomonas campestris* pv. *vesicatoria* type III effector protein XopJ inhibits protein secretion: evidence for interference with cell wall-associated defense responses. *Molecular Plant-Microbe Interactions* **22**: 655–664.

Bent AF, Mackey D. 2007. Elicitors, effectors, and *R* genes: the new paradigm and a lifetime supply of questions. *Annual Review of Phytopathology* **45**: 399–436.

Block A, Li G, Fu ZQ, Alfano JR. 2008. Phytopathogen type III effector weaponry and their plant targets. *Current Opinion in Plant Biology* **11**: 396–403.

Bonas U, Schulte R, Fenselau S, Minsavage GV, Staskawicz BJ, Stall RE. 1991. Isolation of a gene-cluster from *Xanthomonas campestris* pv. *vesicatoria* that determines pathogenicity and the hypersensitive response on pepper and tomato. *Molecular Plant-Microbe Interactions* **4**: 81–88.

Bonshtien A, Lev A, Gibly A, Debbie P, Avni A, Sessa G. 2005. Molecular properties of the *Xanthomonas* AvrRxv effector and global transcriptional changes determined by its expression in resistant tomato plants. *Molecular Plant-Microbe Interactions* **18**: 300–310.

Bouly JP, Gissot L, Lessard P, Kreis M, Thomas M. 1999. *Arabidopsis thaliana* proteins related to the yeast SIP and SNF4 interact with AKINalpha1, an SNF1-like protein kinase. *Plant Journal* **18**: 541–550.

Büttner D, Bonas U. 2010. Regulation and secretion of *Xanthomonas* virulence factors. *FEMS Microbiology Reviews* **34**: 107–133.

Büttner D, Gürlebeck D, Noel LD, Bonas U. 2004. HpaB from *Xanthomonas campestris* pv. *vesicatoria* acts as an exit control protein in type III-dependent protein secretion. *Molecular Microbiology* **54**: 755–768.

Büttner D, Lorenz C, Weber E, Bonas U. 2006. Targeting of two effector protein classes to the type III secretion system by a HpaC- and HpaB-dependent protein complex from *Xanthomonas campestris* pv. *vesicatoria*. *Molecular Microbiology* **59**: 513–527.

Büttner D, Nennstiel D, Klüsener B, Bonas U. 2002. Functional analysis of HrpF, a putative type III translocon protein from *Xanthomonas campestris* pv. vesicatoria. *Journal of Bacteriology* **184**: 2389–2398.

Canteros BI. 1990. *Diversity of plasmids and plasmid-encoded phenotypic traits in* Xanthomonas campestris *pv.* vesicatoria. PhD thesis. University of Florida, Gainesville, FL, USA.

Cernadas RA, Camillo LR, Benedetti CE. 2008. Transcriptional analysis of the sweet orange interaction with the citrus canker pathogens *Xanthomonas axonopodis* pv. *citri* and *Xanthomonas axonopodis* pv. *aurantifolii*. *Molecular Plant Pathology* **9**: 609–631.

Chung E, Seong E, Kim YC, Chung EJ, Oh SK, Lee S, Park JM, Joung YH, Choi D. 2004. A method of high frequency virus-induced gene silencing in chili pepper (*Capsicum annuum* L. cv. Bukang). *Molecules and Cells* **17**: 377–380.

Ciesiolka LD, Hwin T, Gearlds JD, Minsavage GV, Saenz R, Bravo M, Handley V, Conover SM, Zhang H, Caporgno J *et al.* 1999. Regulation of expression of avirulence gene *avrRxv* and identification of a family of host interaction factors by sequence analysis of *avrBsT*. *Molecular Plant-Microbe Interactions* **12**: 35–44.

Cunnac S, Lindeberg M, Collmer A. 2009. *Pseudomonas syringae* type III secretion system effectors: repertoires in search of functions. *Current Opinion in Microbiology* **12**: 53–60.

Cunnac S, Wilson A, Nuwer J, Kirik A, Baranage G, Mudgett MB. 2007. A conserved carboxylesterase is a SUPPRESSOR OF AVRBST-ELICITED RESISTANCE in *Arabidopsis*. *Plant Cell* **19**: 688–705.

Dangl JL, Jones JDG. 2001. Plant pathogens and integrated defence responses to infection. *Nature* **411**: 826–833.

Daniels MJ, Barber CE, Turner PC, Sawczyc MK, Byrde RJW, Fielding AH. 1984. Cloning of genes involved in pathogenicity of *Xanthomonas campestris* pv. *campestris* using the broad host range cosmid pLAFR1. *EMBO Journal* **3**: 3323–3328.

Davies SP, Hawley SA, Woods A, Carling D, Haystead TAJ, Hardie DG. 1994. Purification of the AMP-activated protein kinase on ATP-γ-Sepharose and analysis of its subunit structure. *European Journal of Biochemistry* **223**: 351–357.

Derenzis FA, Schechtman A. 1973. Staining by neutral red and trypan blue in sequence for assaying vital and nonvital cultured cells. *Biotechnic & Histochemistry* **48**: 135–136.

Ditta G, Stanfield S, Corbin D, Helinski D. 1980. Broad host range DNA cloning system for gram-negative bacteria: construction of a gene bank of *Rhizobium meliloti*. *Proceedings of the National Academy of Sciences, USA* **77**: 7347–7351.

Escolar L, Van den Ackerveken G, Pieplow S, Rossier O, Bonas U. 2001. Type III secretion and *in planta* recognition of the *Xanthomonas* avirulence proteins AvrBs1 and AvrBsT. *Molecular Plant Pathology* **2**: 287–296.

Feldman MF, Cornelis GR. 2003. The multitalented type III chaperones: all you can do with 15 kDa. *FEMS Microbiology Letters* **219**: 151–158.

Figurski D, Helinski DR. 1979. Replication of an origin-containing derivative of plasmid RK2 dependent on a plasmid function provided *in trans*. *Proceedings of the National Academy of Sciences, USA* **76**: 1648–1652.

Galyov EE, Hakansson S, Wolf-Watz H. 1994. Characterization of the operon encoding the YpkA Ser/Thr protein kinase and the YopJ protein of *Yersinia pseudotuberculosis*. *Journal of Bacteriology* **176**: 4543–4548.

Ghosh P. 2004. Process of protein transport by the type III secretion system. *Microbiology and Molecular Biology Reviews* **68**: 771–795.

Göhre V, Robatzek S. 2008. Breaking the barriers: microbial effector molecules subvert plant immunity. *Annual Review Phytopathology* **46**: 189–215.

Grant SR, Fisher EJ, Chang JH, Mole BM, Dangl J. 2006. Subterfuge and manipulation: type III effector proteins of phytopathogenic bacteria. *Annual Review of Microbiology* **60**: 425–449.

Gürlebeck D. 2007. *Identifizierung und Analyse von Protein-Interaktionen des Typ III-Effektors AvrBs3 aus* Xanhomonas campestris *pv.* vesicatoria. PhD thesis. Martin-Luther University Halle-Wittenberg, Halle, Germany.

Gürlebeck D, Jahn S, Gürlebeck N, Szczesny R, Szurek B, Hahn S, Hause G, Bonas U. 2009. Visualization of novel virulence activities of the *Xanthomonas* type III effectors AvrBs1, AvrBs3 and AvrBs4. *Molecular Plant Pathology* **10**: 175–188.

Hajri A, Brin C, Hunault G, Lardeux F, Lemaire C, Manceau C, Boureau T, Poussier S. 2009. A ''repertoire for repertoire'' hypothesis: repertoires of type three effectors are candidate determinants of host specificity in *Xanthomonas*. *PLoS ONE* **4**: e6632.

Halford NG, Hey SJ. 2009. Snf1-related protein kinases (SnRKs) act within an intricate network that links metabolic and stress signalling in plants. *Biochemical Journal* **419**: 247–259.

Hao L, Wang H, Sunter G, Bisaro DM. 2003. Geminivirus AL2 and L2 proteins interact with and inactivate SNF1 kinase. *Plant Cell* **15**: 1034–1048.

Hardie DG. 2007. AMP-activated/SNF1 protein kinases: conserved guardians of cellular energy. *Nature Reviews Molecular Cell Biology* **8**: 774–785.

He SY, Nomura K, Whittam TS. 2004. Type III protein secretion mechanism in mammalian and plant pathogens. *Biochimica et Biophysica Acta* **1694**: 181–206.

Hedbacker K, Carlson M. 2008. SNF1/AMPK pathways in yeast. *Front Biosciences* **13**: 2408–2420.

Hotson A, Chosed R, Shu H, Orth K, Mudgett MB. 2003. *Xanthomonas* type III effector XopD targets SUMO-conjugated proteins *in planta*. *Molecular Microbiology* **50**: 377–389.

Hotson A, Mudgett MB. 2004. Cysteine proteases in phytopathogenic bacteria: identification of plant targets and activation of innate immunity. *Current Opinion in Plant Biology* **7**: 384–390.

Hu CD, Chinenov Y, Kerppola TK. 2002. Visualization of interactions among bZIP and Rel family proteins in living cells using bimolecular fluorescence complementation. *Molecular Cell* **9**: 789–798.

Huguet E, Hahn K, Wengelnik K, Bonas U. 1998. *hpaA* mutants of *Xanthomonas campestris* pv. *vesicatoria* are affected in pathogenicity but retain the ability to induce host-specific hypersensitive reaction. *Molecular Microbiology* **29**: 1379–1390.

Jiang BL, He YQ, Cen WJ, Wei HY, Jiang GF, Jiang W, Hang XH, Feng JX, Lu GT, Tang DJ *et al.* 2008. The type III secretion effector XopXccN of *Xanthomonas campestris* pv. *campestris* is required for full virulence. *Research in Microbiology* **159**: 216–220.

Jones JD, Dangl JL. 2006. The plant immune system. *Nature* **444**: 323–329.

Jones JB, Lacy GH, Bouzar H, Stall RE, Schaad NW. 2004. Reclassification of the Xanthomonads associated with bacterial spot disease of tomato and pepper. *Systematic and Applied Microbiology* **27**: 755–762.

Keen NT, Buzzell RI. 1991. New disease resistance genes in soybean against *Pseudomonas syringae* pv. *glycinea*: evidence that one of them interacts with a bacterial elicitor. *Theoretical and Applied Genetics* **81**: 133–138.

Kim MG, da Cunha L, McFall AJ, Belkhadir Y, DebRoy S, Dangl JL, Mackey D. 2005. Two *Pseudomonas syringae* type III effectors inhibit RIN4-regulated basal defense in *Arabidopsis*. *Cell* **121**: 749–759.

Kim JG, Li X, Roden JA, Taylor KW, Aakre CD, Su B, Lalonde S, Kirik A, Chen Y, Baranage G *et al.* 2009. *Xanthomonas* T3S effector XopN suppresses PAMP-triggered immunity and interacts with a tomato atypical receptor-like kinase and TFT1. *Plant Cell* **21**: 1305–1323.

Kim JG, Taylor KW, Hotson A, Keegan M, Schmelz EA, Mudgett MB. 2008. XopD SUMO protease affects host transcription, promotes pathogen growth, and delays symptom development in *Xanthomonas*-infected tomato leaves. *Plant Cell* **20**: 1915–1929.

Kleinow T, Bhalerao R, Breuer F, Umeda M, Salchert K, Koncz C. 2000. Functional identification of an Arabidopsis SNF4 ortholog by screening for heterologous multicopy suppressors of *snf4* deficiency in yeast. *Plant Journal* **23**: 115–122.

Koch E, Slusarenko A. 1990. *Arabidopsis* is susceptible to infection by a downy mildew fungus. *Plant Cell* **2**: 437–445.

Kousik CS, Ritchie DF. 1998. Response of bell pepper cultivars to bacterial spot pathogen races that individually overcome major resistance genes. *Plant Disease* **82**: 181–186.

Lakatos L, Klein M, Hofgen R, Banfalvi Z. 1999. Potato StubSNF1 interacts with StubGAL83: a plant protein kinase complex with yeast and mammalian counterparts. *Plant Journal* **17**: 569–574.

Lewis JD, Guttman DS, Desveaux D. 2009. The targeting of plant cellular systems by injected type III effector proteins. *Seminars in Cell and Developmental Biology* **20**: 1055–1063.

Liu Y, Schiff M, Dinesh-Kumar SP. 2002a. Virus-induced gene silencing in tomato. *Plant Journal* **31**: 777–786.

Liu Y, Schiff M, Marathe R, Dinesh-Kumar SP. 2002b. Tobacco *Rar1*, *EDS1* and *NPR1/NIM1* like genes are required for N-mediated resistance to tobacco mosaic virus. *Plant Journal* **30**: 415–429.

Lorenz C, Schulz S, Wolsch T, Rossier O, Bonas U, Büttner D. 2008. HpaC controls substrate specificity of the *Xanthomonas* type III secretion system. *PLoS Pathogens* **4**: e1000094.

Lumbreras V, Alba MM, Kleinow T, Koncz C, Pages M. 2001. Domain fusion between SNF1-related kinase subunits during plant evolution. *EMBO Report* **2**: 55–60.

Ma W, Dong FF, Stavrinides J, Guttman DS. 2006. Type III effector diversification via both pathoadaptation and horizontal transfer in response to a coevolutionary arms race. *PLoS Genetics* **2**: e209.

Marois E, Van den Ackerveken G, Bonas U. 2002. The *Xanthomonas* type III effector protein AvrBs3 modulates plant gene expression and induces cell hypertrophy in the susceptible host. *Molecular Plant-Microbe Interactions* **15**: 637–646.

Ménard R, Sansonetti PJ, Parsot C. 1993. Nonpolar mutagenesis of the *ipa* genes defines IpaB, IpaC, and IpaD as effectors of *Shigella flexneri* entry into epithelial cells. *Journal of Bacteriology* **175**: 5899–5906.

Metz M, Dahlbeck D, Morales CQ, Al Sady B, Clark ET, Staskawicz BJ. 2005. The conserved *Xanthomonas campestris* pv. *vesicatoria* effector protein XopX is a virulence factor and suppresses host defense in *Nicotiana benthamiana*. *Plant Journal* **41**: 801–814.

Minsavage GV, Dahlbeck D, Whalen MC, Kearny B, Bonas U, Staskawicz BJ, Stall RE. 1990. Gene-for-gene relationships specifying disease resistance in *Xanthomonas campestris* pv. *vesicatoria*–pepper interactions. *Molecular Plant-Microbe Interactions* **3**: 41–47.

Mitchelhill KI, Stapleton D, Gao G, House C, Michell B, GKatsis F, Witters LA, Kemp BE. 1994. Mammalian AMP activated protein kinase shares structural and functional homology with the catalytic domain of yeast Snf1 protein kinase. *Journal of Biological Chemistry* **269**: 2361–2364.

Morales CQ, Posada J, Macneale E, Franklin D, Rivas I, Bravo M, Minsavage J, Stall RE, Whalen MC. 2005. Functional analysis of the early chlorosis factor gene. *Molecular Plant-Microbe Interactions* **18**: 477–486.

Mukherjee S, Keitany G, Li Y, Wang Y, Ball HL, Goldsmith EJ, Orth K. 2006. *Yersinia* YopJ acetylates and inhibits kinase activation by blocking phosphorylation. *Science* **312**: 1211–1214.

Murillo J, Shen H, Gerhold D, Sharma A, Cooksey DA, Keen NT. 1994. Characterization of pPT23B, the plasmid involved in syringolide production by *Pseudomonas syringae* pv. *tomato* PT23. *Plasmid* **31**: 275–287.

Nakagawa T, Takayuki K, Hino T, Tanaka K, Kawamukai M, Niwa Y, Toyooka K, Matsuoka K, Jinbo T, Kimura T. 2007. Development of series of Gateway binary vectors, pGWBs, for realizing efficient construction of fusion genes for plant transformation. *Journal of Bioscience and Bioengineering* **104**: 34–41.

Napoli C, Staskawicz B. 1987. Molecular characterization and nucleic acid sequence of an avirulence gene from race 6 of *Pseudomonas syringae* pv. glycinea. *Journal of Bacteriology* **169**: 572–578.

Noël L, Thieme F, Gäbler J, Büttner D, Bonas U. 2003. XopC and XopJ, two novel type III effector proteins from *Xanthomonas campestris* pv. vesicatoria. *Journal of Bacteriology* **185**: 7092–7102.

Orth K. 2002. Function of the *Yersinia* effector YopJ. *Current Opinion in Microbiology* **5**: 38–43.

Orth K, Xu Z, Mudgett MB, Bao ZQ, Palmer LE, Bliska JB, Mangel WF, Staskawicz B, Dixon JE. 2000. Disruption of signaling by *Yersinia* effector YopJ, ubiquitin-like protein protease. *Science* **290**: 1594–1597.

Roden J, Eardley L, Hotson A, Cao Y, Mudgett MB. 2004a. Characterization of the *Xanthomonas* AvrXv4 effector, a SUMO protease

translocated into plant cells. *Molecular Plant-Microbe Interactions* **17**: 633–643.

Roden JA, Belt B, Ross JB, Tachibana T, Vargas J, Mudgett MB. 2004b. A genetic screen to isolate type III effectors translocated into pepper cells during *Xanthomonas* infection. *Proceedings of the National Academy of Sciences, USA* **101**: 16624–16629.

Ronald PC, Staskawicz BJ. 1988. The avirulence gene *avrBs1* from *Xanthomonas campestris* pv. *vesicatoria* encodes a 50-kDa protein. *Molecular Plant-Microbe Interactions* **1**: 191–198.

Rossier O, Wengelnik K, Hahn K, Bonas U. 1999. The *Xanthomonas* Hrp type III system secretes proteins from plant and mammalian pathogens. *Proceedings of the National Academy of Sciences, USA* **96**: 9368–9373.

Shao F, Golstein C, Ade J, Stoutemyer M, Dixon JE, Innes RW. 2003. Cleavage of Arabidopsis PBS1 by a bacterial type III effector. *Science* **301**: 1230–1233.

Shrestha R, Tsuchiya K, Baek SJ, Bae HN, Hwang I, Hur JH, Lim CK. 2005. Identification of the *dspEF*, *hrpW*, and *hrpN* loci and characterization of the $hrpN_{EP}$ gene in *Erwinia pyrifoliae*. *Journal of General Plant Pathology* **71**: 211–220.

Speth EB, Lee YN, He SY. 2007. Pathogen virulence factors as molecular probes of basic plant cellular functions. *Current Opinion in Plant Biology* **10**: 580–586.

Stall RE, Bartz JA, Cook AA. 1974. Decreased hypersensitivity to xanthomonads in pepper after inoculations with virulent cells of *Xanthomonas vesictoria*. *Phytopathology* **64**: 731–735.

Stall RE, Minsavage GV. 1996. Method for screening for bacterial spot resistance genes, Bs1, Bs2 and Bs3, in a single pepper plant. In: Maynard D, ed. *National pepper conference*. Naples, Italy: Citrus & Vegetables Magazine, 63–64.

Sunter G, Sunter JL, Bisaro DM. 2001. Plants expressing tomato golden mosaic virus AL2 or beet curly top virus L2 transgenes show enhanced susceptibility to infection by DNA and RNA viruses. *Virology* **285**: 59–70.

Sweet RC, Conlon J, Golenbock DT, Goguen J, Silverman N. 2007. YopJ targets TRAF proteins to inhibit TLR-mediated NF-κB, MAPK and IRF3 signal transduction. *Cellular Microbiology* **9**: 2700–2715.

Szurek B, Rossier O, Hause G, Bonas U. 2002. Type III-dependent translocation of the *Xanthomonas* AvrBs3 protein into the plant cell. *Molecular Microbiology* **46**: 13–23.

Thieme F, Koebnik R, Bekel T, Berger C, Boch J, Büttner D, Caldana C, Gaigalat L, Goesmann A, Kay S *et al.* 2005. Insights into genome plasticity and pathogenicity of the plant pathogenic bacterium *Xanthomonas campestris* pv. vesicatoria revealed by the complete genome sequence. *Journal of Bacteriology* **187**: 7254–7266.

Thieme F, Szczesny R, Urban A, Kirchner O, Hause G, Bonas U. 2007. New type III effectors from *Xanthomonas campestris* pv. *vesicatoria* trigger plant reactions dependent on a conserved N-myristoylation motif. *Molecular Plant-Microbe Interactions* **20**: 1250–1261.

Van den Ackerveken G, Marois E, Bonas U. 1996. Recognition of the bacterial avirulence protein AvrBs3 occurs inside the host plant cell. *Cell* **87**: 1307–1316.

Van Larebeke N, Engler G, Holsters M, Van den Elsacker S, Zaenen I, Schilperoort RA, Schell J. 1974. Large plasmid in *Agrobacterium tumefaciens* essential for crown gall-inducing ability. *Nature* **252**: 169–170.

Vieira J, Messing J. 1987. Production of single-stranded plasmid DNA. *Methods in Enzymology* **153**: 3–11.

Vivian A, Arnold DL. 2000. Bacterial effector genes and their role in host pathogen interactions. *Journal of Plant Pathology* **82**: 163–178.

Walter M, Chaban C, Schutze K, Batistic O, Weckermann K, Nake C, Blazevic D, Grefen C, Schumacher K, Oecking C *et al.* 2004. Visualization of protein interactions in living plant cells using bimolecular fluorescence complementation. *Plant Journal* **40**: 428–438.

Wengelnik K, Rossier O, Bonas U. 1999. Mutations in the regulatory gene *hrpG* of *Xanthomonas campestris* pv. vesicatoria result in constitutive expression of all *hrp* genes. *Journal of Bacteriology* **181**: 6828–6831.

Wengelnik K, Van den Ackerveken G, Bonas U. 1996. HrpG, a key *hrp* regulatory protein of *Xanthomonas campestris* pv. *vesicatoria* is homologous to two-component response regulators. *Molecular Plant-Microbe Interactions* **9**: 704–712.

Whalen M, Richter TE, Zakhareyvich K, Yoshikawa M, Al-Azzeh D, Adefioye A, Spicer G, Mendoza LL, Morales CQ, Klassen V *et al.* 2008. Identification of a host 14-3-3 protein that interacts with *Xanthomonas* effector AvrRxv. *Physiological and Molecular Plant Pathology* **72**: 46–55.

Whalen MC, Wang JF, Carland FM, Heiskell ME, Dahlbeck D, Minsavage GV, Jones JB, Scott JW, Stall RE, Staskawicz BJ. 1993. Avirulence gene *avrRxv* from *Xanthomonas campestris* pv. *vesicatoria* specifies resistance on tomato line Hawaii 7998. *Molecular Plant-Microbe Interactions* **6**: 616–627.

White FF, Potnis N, Jones JB, Koebnik R. 2009. The type III effectors of *Xanthomonas*. *Molecular Plant Pathology* **10**: 749–766.

Wichmann G, Bergelson J. 2004. Effector genes of *Xanthomonas axonopodis* pv. *vesicatoria* promote transmission and enhance other fitness traits in the field. *Genetics* **166**: 693–706.

Wilharm G, Dittmann S, Schmid A, Heesemann J. 2007. On the role of specific chaperones, the specific ATPase, and the proton motive force in type III secretion. *International Journal of Medical Microbiology* **297**: 27–36.

Williams JW, Langer JS, Northrop DB. 1975. A spectrophotometric assay for gentamicin. *The Journal of Antibiotics* **28**: 982–987.

de Wit PJ. 2007. How plants recognize pathogens and defend themselves. *Cellular and Molecular Life Sciences* **64**: 2726–2732.

2.1.2 Zusammenfassung der Ergebnisse

Die Suppression der AvrBs1-induzierten HR durch AvrBsT wurde in Publikation 1 analysiert. Der T3E AvrBs1 ist im Genom der beiden *Xcv*-Stämme 85-10 und 75-3 kodiert. Nach Infektion von AvrBs1-responsiven Paprikapflanzen (ECW-10R) wurde jedoch eine deutlich verzögerte HR für 75-3 im Vergleich zu 85-10 beobachtet. Es wurde untersucht, ob der T3E AvrBsT, welcher im Genom von 75-3, aber nicht von 85-10 kodiert wird, für die Suppression der AvrBs1-HR verantwortlich ist. In resistenten ECW-10R Pflanzen induzierte *Xcv* 75-3Δ*avrBsT* die AvrBs1-HR vergleichbar zu 85-10. Außerdem führte die ektopische Expression von *avrBsT* in *Xcv* 85-10 zur Suppression der AvrBs1-induzierten HR, ähnlich zum *Xcv* 75-3 Wildtyp-Stamm. Die Stärke der Zelltodreaktionen wurde mittels Elektrolytmessungen quantifiziert. Die *Agrobacterium*-vermittelte Ko-Expression von *avrBs1* und *avrBsT* führte ebenfalls zu einer deutlich verzögerten HR in ECW-10R Pflanzen. Diese Daten belegen, dass der T3E AvrBsT für die Suppression der AvrBs1-vermittelten HR verantwortlich ist.

AvrBsT gehört zur YopJ/AvrRxv Proteinfamilie, deren Aktivität auf einer aktiven katalytischen Triade beruht, die aus Histidin, Aspartat oder Glutamat und Cystein besteht. Eine intakte katalytische Triade von AvrBsT ist für dessen Wirkung als HR-Suppressor notwendig. Weder die ektopische Expression der Mutante $avrBsT_{C222A}$ in 85-10, noch die *Agrobacterium*-vermittelte Ko-Expression von $avrBsT_{C222A}$ und *avrBs1* führte zu einer Suppression der AvrBs1-vermittelten HR.

Da AvrBsT als HR-Suppressor wirkt, wurde untersucht, ob AvrBsT auch zur Virulenz von *Xanthomonas* beiträgt. Krankheitssymptome und bakterielles Wachstum von *Xcv* 75-3Δ*avrBsT* waren jedoch im Vergleich zum Wildtyp unverändert.

In Hefe-Di-Hybrid-Sichtungen einer Tomaten-cDNA-Bibliothek wurde u.a. SnRK1 (*sucrose nonfermenting* 1 (SNF1)-*related kinase* 1) als Interaktor von AvrBsT identifiziert. Durch bimolekulare Fluoreszenz-Komplementation wurde gezeigt, dass AvrBsT, jedoch nicht AvrBs1 mit SnRK1 im Zytoplasma der Pflanzenzelle interagiert. Mittels Virus-induziertem Gen-„Silencing“ von *SnRK1* wurde in verschiedenen AvrBs1-responsiven Paprika-Kultivaren nachgewiesen, dass SnRK1 für die Ausbildung der AvrBs1-vermittelten HR notwendig ist. Die bloße Interaktion zwischen AvrBsT und SnRK1 kann jedoch nicht für die Suppression der AvrBs1-HR verantwortlich sein, weil auch $AvrBsT_{C222A}$ mit SnRK1 interagierte. Aus diesem Grund wurde untersucht, ob SnRK1 durch AvrBsT posttranslational modifiziert oder degradiert wird.

In dieser Publikation wurde gereinigtes, rekombinantes AvrBsT bzw. $AvrBsT_{C222A}$ bezüglich dieser Enzymaktivitäten *in vitro* getestet. Für AvrBsT konnte in Abhängigkeit von dessen katalytischer Triade eine schwache Proteaseaktivität nachgewiesen werden. Deshalb wurde untersucht, ob SnRK1 durch AvrBsT proteolytisch degradiert wird. *In planta* konnte jedoch kein proteolytischer Abbau von SnRK1 in Gegenwart von AvrBsT nachgewiesen werden.

2.2 Identifizierung und Charakterisierung von Typ III-Effektoren aus *Xanthomonas campestris* pv. *vesicatoria*

2.2.1 Publikation 2

Analysis of new type III effectors from *Xanthomonas* uncovers XopB and XopS as suppressors of plant immunity

Sebastian Schulze[1], Sabine Kay[1], Daniela Büttner[1], Monique Egler[1], Lennart Eschen-Lippold[2], Gerd Hause[3], Antje Krüger[1], Justin Lee[2], Oliver Müller[1], Dierk Scheel[2], Robert Szczesny[1], Frank Thieme[1] and Ulla Bonas[1]

[1]Institute of Biology, Department of Genetics, Martin-Luther-University Halle-Wittenberg, Weinbergweg 10, D-06120 Halle (Saale), Germany; [2]Leibniz Institute of Plant Biochemistry, Weinberg 3, D-06120 Halle (Saale), Germany; [3]Biozentrum, Martin-Luther-University Halle-Wittenberg, Weinbergweg 22, D-06120 Halle (Saale), Germany

Author for correspondence:
Ulla Bonas
Tel: +49 345 5526290
Email: ulla.bonas@genetik.uni-halle.de

Received: *28 March 2012*
Accepted: *15 May 2012*

New Phytologist (2012)
doi: 10.1111/j.1469-8137.2012.04210.x

Key words: bacterial spot disease, *Capsicum annuum* (pepper), cell death suppression, effector, HpaB, type III secretion, vesicle trafficking, *Xanthomonas campestris*.

Summary

- The pathogenicity of the Gram-negative plant-pathogenic bacterium *Xanthomonas campestris* pv. *vesicatoria* (*Xcv*) is dependent on type III effectors (T3Es) that are injected into plant cells by a type III secretion system and interfere with cellular processes to the benefit of the pathogen.
- In this study, we analyzed eight T3Es from *Xcv* strain 85-10, six of which were newly identified effectors. Genetic studies and protoplast expression assays revealed that XopB and XopS contribute to disease symptoms and bacterial growth, and suppress pathogen-associated molecular pattern (PAMP)-triggered plant defense gene expression.
- In addition, XopB inhibits cell death reactions induced by different T3Es, thus suppressing defense responses related to both PAMP-triggered immunity (PTI) and effector-triggered immunity (ETI).
- XopB localizes to the Golgi apparatus and cytoplasm of the plant cell and interferes with eukaryotic vesicle trafficking. Interestingly, a XopB point mutant derivative was defective in the suppression of ETI-related responses, but still interfered with vesicle trafficking and was only slightly affected with regard to the suppression of defense gene induction. This suggests that XopB-mediated suppression of PTI and ETI is dependent on different mechanisms that can be functionally separated.

Introduction

Plants defend themselves against microbial invaders by basal defense responses including the production of reactive oxygen species, activation of mitogen-activated protein kinase (MAPK) cascades, expression of pathogenesis-related (*PR*) genes and callose deposition into the plant cell wall (Nürnberger *et al.*, 2004). Usually, these defense reactions are activated on recognition of pathogen-associated molecular patterns (PAMPs), such as flagellin, lipopolysaccharides and elongation factor EF-Tu, by specific receptors in the plant plasma membrane (Nürnberger *et al.*, 2004; Jones & Dangl, 2006). However, specialized bacterial pathogens have evolved sophisticated strategies to avoid or manipulate plant defense responses and to proliferate in the plant's apoplast. Essential for the pathogenicity of Gram-negative bacteria is often a type III secretion (T3S) system consisting of a complex membrane-spanning injection apparatus that is associated with an extracellular pilus and a channel-like translocon in the plant plasma membrane (Büttner & He, 2009). T3S systems translocate type III effectors (T3Es) directly into the host cell cytosol where they interfere with plant cell processes to the benefit of the pathogen, often leading to the suppression of PAMP-triggered immunity (PTI) (Jones & Dangl, 2006). However, individual effectors can also act as avirulence (Avr) proteins that are recognized in plants carrying a corresponding resistance (*R*) gene. Recognition leads to the elicitation of host defense reactions that often culminate in the hypersensitive response (HR), a rapid, localized programmed cell death reaction that restricts pathogen ingress (Klement & Goodman, 1967; Greenberg & Yao, 2004). To circumvent effector-triggered immunity (ETI), bacterial pathogens have evolved T3Es that interfere with the induction of *R* gene-mediated defense responses (Jones & Dangl, 2006).

Most phytopathogenic bacteria translocate 20–30 different T3Es into the plant cell (Büttner & Bonas, 2010; Hann *et al.*, 2010). Notably, the deletion of individual effector genes often does not lead to reduced virulence, presumably because of functional redundancies among T3Es (Büttner & Bonas, 2010; Hann *et al.*, 2010). Although the molecular functions of most T3Es inside the plant cell are still unknown, a number of T3Es from phytopathogenic bacteria have been shown to interfere with signaling cascades, proteasome-dependent protein degradation and the transcription machinery (Kay & Bonas, 2009; Block & Alfano, 2011).

Our laboratory studies the T3S system and T3Es from *Xanthomonas campestris* pv. *vesicatoria* (*Xcv*, also termed *X. euvesicatoria* (Jones *et al.*, 2004) and *X. axonopodis* pv. *vesicatoria* (Vauterin *et al.*, 2000)), the causal agent of bacterial spot disease on pepper and tomato. The T3S system of *Xcv* is encoded by the 23-kb chromosomal *hrp* (hypersensitive response and pathogenicity) gene cluster, which is essential for bacterial growth and disease symptoms on susceptible plants, as well as for HR induction in resistant host and nonhost plants (Bonas *et al.*, 1991). The expression of *hrp* genes is induced *in planta* by the OmpR-family regulator HrpG, which controls the expression of a genome-wide regulon (Noël *et al.*, 2001) including *hrpX*, which encodes an AraC-type transcriptional activator (Wengelnik & Bonas, 1996; Wengelnik *et al.*, 1996a). HrpX binds to *cis*-regulatory PIP (plant-inducible promoter) boxes in the promoter regions of *hrp* and other genes that contribute to virulence (Koebnik *et al.*, 2006).

In addition to a functional T3S apparatus, efficient translocation of effectors by the *Xcv* T3S system requires the T3S chaperone HpaB, which has a broad substrate specificity (Büttner *et al.*, 2004, 2006; Szczesny *et al.*, 2010a). T3S chaperones specifically bind T3S substrates and promote their secretion and/or stability (Parsot *et al.*, 2003; Wilharm *et al.*, 2007). Interestingly, T3Es in *Xcv* differ in their HpaB dependence and are therefore grouped into two classes. While class A effectors depend on HpaB for translocation, class B effectors are translocated even in the absence of HpaB, albeit in reduced amounts. It is conceivable that HpaB imposes a hierarchy on T3E translocation and that class A effectors are preferentially translocated during a certain stage of the infection process (Büttner *et al.*, 2006).

On the basis of experimental and bioinformatic analyses, individual *Xanthomonas* strains express 23–37 different T3Es (Büttner & Bonas, 2010). The largest effector class, although not present in all strains, is the AvrBs3/PthA family of transcription activator-like (TAL) effectors, which mimic eukaryotic transcription factors and induce the transcription of plant genes to support bacterial growth and dispersal (Marois *et al.*, 2002; Yang *et al.*, 2006; Kay *et al.*, 2007; Boch *et al.*, 2009; Antony *et al.*, 2010). Intriguingly, they can also activate *R* gene promoters leading to the induction of the HR (Gu *et al.*, 2005; Römer *et al.*, 2007). Plant transcript levels are also modulated by XopD (Xop, *Xanthomonas* outer protein) from *Xcv*, which negatively regulates the expression of defense- and senescence-related genes via ethylene response factor amphiphilic repression motifs (Kim *et al.*, 2008). In addition, XopD acts as a cysteine protease (Hotson *et al.*, 2003). All biochemical activities of XopD contribute to its virulence function, that is, a delay of plant chlorosis and necrosis and the promotion of bacterial multiplication in tomato (Kim *et al.*, 2008). Cysteine protease activity has also been demonstrated for effectors of the YopJ/AvrRxv family from plant- and animal-pathogenic bacteria (Orth *et al.*, 2000; Hotson & Mudgett, 2004; Ma *et al.*, 2006; Sweet *et al.*, 2007; Szczesny *et al.*, 2010a). Their exact mode of action, however, is a controversial issue because an acetyltransferase activity has also been described (Mukherjee *et al.*, 2006). Members of the YopJ/AvrRxv family, for example XopJ and AvrBsT from *Xcv*, are involved in the suppression of plant defense by the inhibition of cell wall-associated defense responses and ETI, respectively (Bartetzko *et al.*, 2009; Szczesny *et al.*, 2010a). A role in the suppression of plant immunity has also been proposed for other *Xcv* T3Es, including XopX and XopN (Metz *et al.*, 2005; Kim *et al.*, 2009). The latter presumably suppresses PTI by targeting an atypical receptor-like kinase in tomato involved in immune signaling (Kim *et al.*, 2009).

Our goal was the identification and analysis of new T3Es from the *Xcv* model strain 85-10, for which 16 T3Es have been identified and confirmed experimentally to date (Mudgett *et al.*, 2000; Escolar *et al.*, 2001; Noël *et al.*, 2002, 2003; Hotson *et al.*, 2003; Roden *et al.*, 2004; Metz *et al.*, 2005; Morales *et al.*, 2005; Lorenz *et al.*, 2008; Szczesny *et al.*, 2010a; Potnis *et al.*, 2011). Analysis of the genome sequence (Thieme *et al.*, 2005) revealed the presence of further effector candidates as a result of PIP boxes in the corresponding promoter, homology to known effectors and sequence motifs typically restricted to eukaryotic proteins. In this study, we analyzed eight T3Es, six of which were newly identified, using AvrBs3 as T3S reporter. Mutant and overexpression studies revealed that XopB and XopS contribute to disease symptoms and bacterial growth, and suppress plant defense gene expression. In addition, XopB inhibits cell death reactions triggered by different T3Es, thus suppressing both PTI- and ETI-related responses.

Materials and Methods

Bacterial strains and growth conditions

Escherichia coli cells were cultivated in LB (lysogeny broth) medium at 37°C. *Agrobacterium tumefaciens* was grown at 30°C in YEB (yeast extract broth) medium and *Xcv* at 30°C in NYG (nutrient yeast glycerol; Daniels *et al.*, 1984), *hrp* gene-inducing medium (XVM2; Wengelnik *et al.*, 1996b) or secretion medium (minimal medium A; Ausubel *et al.*, 1996) supplemented with 10 mM sucrose and 0.3% casamino acids. Plasmids were introduced into *E. coli* and *A. tumefaciens* by electroporation, and into *Xcv* by conjugation, using pRK2013 as helper plasmid in triparental matings (Figurski & Helinski, 1979). Bacterial strains and plasmids are listed in Supporting Information Table S1.

Plant material and inoculations

The near-isogenic pepper (*Capsicum annuum*) cultivars ECW, ECW-10R, ECW-20R and ECW-30R (Minsavage *et al.*, 1990), *Nicotiana benthamiana* and *N. tabacum* plants were grown at 25°C with 65% relative humidity and 16 h light. *Xcv* strains were hand-inoculated with a needleless syringe into the apoplast of leaves at 10^8 colony-forming units (cfu) ml^{-1} in 10 mM $MgCl_2$. For *in planta* growth curves, bacteria were inoculated at 10^4 cfu ml^{-1}, and bacterial growth was determined as described by Bonas *et al.* (1991). For *in planta* transient expression studies, *A. tumefaciens* strain GV3101 was grown overnight in YEB medium, resuspended in inoculation medium (10 mM $MgCl_2$, 5 mM MES, pH 5.3, 150 μM acetosyringone) and inoculated into

leaves at 4×10^8 cfu ml^{-1} for localization studies and 2×10^8 cfu ml^{-1} for secGFP secretion assays. For the analysis of cell death suppression, we used final bacterial densities of 4×10^8 cfu ml^{-1} (*Agrobacterium* delivering *avrBs1*, *avrBs2*, *avrBsT*, *avrRxv*, *xopG* and *xopJ*) and 6×10^8 cfu ml^{-1} (*Agrobacterium* delivering *xopS*, *xopB* and mutant derivatives), respectively. For fractionation studies, *Agrobacterium* strains were inoculated at 6×10^8 cfu ml^{-1}. For co-expression, *Agrobacterium* strains were mixed before inoculation.

RNA analysis

RNA extraction from *Xanthomonas*, cDNA synthesis and semi-quantitative reverse transcription polymerase chain reaction (RT-PCR) experiments were performed as described by Noël *et al.* (2001) and Thieme *et al.* (2007). For oligonucleotide sequences, see Table S2. Experiments were performed at least three times for each gene with two independent cDNA preparations each.

Protein analysis

Xanthomonas protein secretion experiments were performed as described by Rossier *et al.* (1999) and Büttner *et al.* (2002). Equal amounts of total bacterial cell extracts and culture supernatants were analyzed by sodium dodecylsulfate-polyacrylamide gel electrophoresis (SDS-PAGE) and immunoblotting following standard protocols. To check for bacterial lysis, blots were routinely reacted with an antibody specific for the intracellular protein HrcJ (data not shown; Rossier *et al.*, 2000). For *Agrobacterium*-mediated expression studies, two 0.64-cm^2 leaf disks per strain were frozen in liquid nitrogen, ground and resuspended in 100 μl of 8 M urea and 50 μl of 5 × Laemmli buffer, and boiled for 10 min. Proteins were separated by SDS-PAGE and analyzed by immunoblotting. We used specific polyclonal antibodies for the detection of AvrBs3 (Knoop *et al.*, 1991), GFP (green fluorescent protein; Invitrogen GmbH, Karlsruhe, Germany), RFP (red fluorescent protein; Antibodies-online GmbH, Aachen, Germany), cFBPase (Agrisera AB, Vaennaes, Sweden) and XopB (H. Berndt & U. Bonas, unpublished), and a monoclonal c-Myc-specific antibody (Roche Diagnostics, Mannheim, Germany). Horseradish peroxidase-labeled α-rabbit and α-mouse antibodies (Amersham Pharmacia Biotech, Piscataway, NJ, USA) were used as secondary antibodies. Antibody reactions were visualized by enhanced chemiluminescence (Amersham Pharmacia Biotech).

Golden Gate vectors

The suicide vector pOGG2 was derived from the suicide plasmid pOK1 (Huguet *et al.*, 1998) and contains a *lacZ* gene for blue–white selection. The binary vector pGGA1 contains the backbone of pBGWFS7 (Karimi *et al.*, 2005), a chloramphenicol resistance-*ccdB* selection cassette, and allows the expression of genes 3′ translationally fused to *GFP* under the control of the *35S* promoter. To allow cloning of DNA fragments by *Bsa*I/T4-ligase cut-ligation (Engler *et al.*, 2008), additional *Bsa*I restriction sites were removed during vector construction. Cloning details are available on request.

GATEWAY and Golden Gate expression constructs

To generate binary expression constructs, the coding sequences of *avrRxv*, *xopB*, $xopB_{A313V}$, $xopB_{K455R}$, *xopG*, *xopI*, *xopK*, *xopM*, *xopR*, *xopS* and *xopV* were amplified by PCR, cloned into pENTR/D-TOPO (Invitrogen) and recombined into pGWB5, pGWB17, pK7FWG2 and pK7WGF2 (Karimi *et al.*, 2005; Nakagawa *et al.*, 2007) using Gateway® technology (Invitrogen). Oligonucleotides are listed in Table S2.

For expression in *Xcv*, *xopS* was amplified from strain 85-10 and cloned into the Golden Gate-compatible expression vector pBRM (Szczesny *et al.*, 2010b). *xopB* and $xopB_{A313V}$ PCR amplicons were cloned downstream of *plac* into the Golden Gate-compatible expression vector pLAND, which allows the insertion of the cloned fragment into the genome by homologous recombination (C. Lorenz & D. Büttner, unpublished).

To generate *avrBs3Δ2* fusions, the promoters and 5′ coding sequences of *xopG*, *xopI*, *xopK*, *xopM*, *xopR*, *xopS* and *xopV* were amplified by PCR from genomic DNA of *Xcv* 85-10, cloned into pENTR/D-TOPO and recombined into pL6GW356 (Noël *et al.*, 2003). In the case of *xopM*, the complete coding region was amplified. For *xopB*, the 5′ coding sequence without promoter was amplified and cloned downstream of *plac* into pBR356, which allows a 3′ fusion of the gene to *avrBs3Δ2* encoding an N-terminally truncated AvrBs3 derivative with a C-terminal FLAG epitope (C. Lorenz & D. Büttner, unpublished).

For Arabidopsis protoplast assays, *xopB*, $xopB_{A313V}$ and *xopS* were cloned into pUGW14 (Nakagawa *et al.*, 2007) using the pENTR/D-TOPO constructs described above. *H2B* (At5g59910) was recombined into pUGW15 (Nakagawa *et al.*, 2007) using an available pDONR221 derivative (Feilner *et al.*, 2005).

secGFP, which contains a basic chitinase signal sequence at the N-terminus of GFP (Haseloff *et al.*, 1997), was generated by cloning annealed oligonucleotides into pGGA1. *xopJ* was recombined into pGWB17 (Nakagawa *et al.*, 2007) using an available pENTR/D-TOPO construct (Thieme *et al.*, 2007). $xopJ_{C235A}$ was derived from *xopJ* by splicing by overlap extension (SOE)-PCR, cloned into pENTR/D-TOPO and recombined into pGWB17 (Nakagawa *et al.*, 2007). *AtSYP121*_Sp2 (Tyrrell *et al.*, 2007) was amplified from *Arabidopsis thaliana* (Col-0) cDNA, cloned into pENTR/D-TOPO and recombined into pGWB17 (Nakagawa *et al.*, 2007). Oligonucleotides are listed in Table S2.

Effector deletion strains

To generate deletions of *xopG*, *xopI*, *xopM*, *xopR*, *xopS* and *xopV*, 0.6–1-kb fragments upstream and downstream of the respective gene were amplified from genomic DNA of *Xcv* 85-10 by PCR using oligonucleotides harboring appropriate restriction sites (Table S2). For the deletion of *xopK*, corresponding fragments were synthesized by Eurofins MWG Operon (Ebersberg,

Germany). Fragments were cloned into the suicide vectors pK18mobsac (Schäfer *et al.*, 1994) (*xopG*, *xopI*, *xopM*), pOK1 (Huguet *et al.*, 1998) (*xopS*) or pOGG2 (*xopK*, *xopR*, *xopV*). The resulting constructs were conjugated into *Xcv* strain 85-10, and mutants were selected by PCR. The *xopB* deletion mutant was available (Noël *et al.*, 2001).

Mesophyll protoplast transient expression assay

Transient expression experiments with *A. thaliana* (Col-0)-derived protoplasts were performed according to Ranf *et al.* (2011). Protoplast samples were co-transformed with the *NHL10* promoter-luciferase construct (Boudsocq *et al.*, 2010; Ranf *et al.*, 2011), *pUBQ10-GUS* (Norris *et al.*, 1993) and either *p35S*-effector gene constructs (*xopB*, $xopB_{A313V}$, *xopS*) or *p35S-H2B* (At5g59910) as a control (10 μg total DNA per 100 μl protoplasts; ratio 1 : 1 : 1).

Electrolyte leakage measurements

Triplicates of five leaf disks each (0.64 cm^2) were harvested at 1 and 2 d post-inoculation (dpi), respectively. Measurements were carried out as described by Szczesny *et al.* (2010a).

Microscopy

Lower epidermal cells of *N. benthamiana* were inspected with a confocal laser scanning microscope LSM 510 and LSM Image Browser software (Carl Zeiss GmbH, Göttingen, Germany) according to the manufacturer's protocol. mCherry Golgi (G-rk, CD3-967) was used for co-localization experiments (Nelson *et al.*, 2007). To visualize plant cell nuclei, leaves were infiltrated with 0.1% (w/v) 4',6-diamidino-2-phenylindole (DAPI) solution 1 h before inspection. GFP was excited with an argon laser at 488 nm, mCherry with an HeNe laser at 543 nm and DAPI with a krypton (UV) laser at 364 nm. The emission filter wavelengths were 505–530 nm for GFP, 560–615 nm for mCherry and 385–470 nm for DAPI.

Transmission electron microscopy was performed as described by Thieme *et al.* (2007) using an EM Libra 120 (Carl Zeiss GmbH).

Results

Gene regulation of *xopB*, *xopG* and six new T3E gene candidates in *Xcv* strain 85-10

For the analysis of effector proteins from *Xcv* strain 85-10, we chose XopB, previously shown to be type III secreted into the medium (Noël *et al.*, 2001), and XopG, a recently identified T3E (Potnis *et al.*, 2011) with homology to the HopH1 family from *Pseudomonas syringae* (Thieme *et al.*, 2005). In addition, we identified six new candidate effectors in *Xcv* strain 85-10 as a result of homology to known effectors (XopK, XopR and XopV), predicted eukaryotic motifs (XopI), indication of gene acquisition by horizontal gene transfer because of significantly lower G + C content (*xopS*) and the presence of a PIP box in the respective promoters (*xopI*, *xopM*, *xopR* and *xopS*) (Table 1). Because the presence of a PIP box suggests the co-regulation of a gene with the T3S system, we performed RT-PCR analyses of *xopG* and the candidate effector genes in the *Xcv* wild-type strain 85-10, its derivative 85*, which expresses a constitutively active HrpG point mutant resulting in constitutive expression of the T3S system (Wengelnik *et al.*, 1999), and the *hrpX* deletion mutant 85*Δ*hrpX* (Noël *et al.*, 2001). When the bacteria were cultivated in complex NYG medium, mRNA of *xopG* was

Table 1 Characteristics of effector genes from *Xanthomonas campestris* pv. *vesicatoria* (*Xcv*) strain 85-10 analyzed in this study

Gene (gene no.)	G + C (%)[a]	Comment(s)[b]	Homolog in[c]					PIP box[d]	Co-reg.[e]	Tr. cl.[f]
			X.	*P.*	*R.*	*A.*	o.			
xopB (XCV0581)	55.54	HopD family (Lindeberg *et al.*, 2005)	+	+	+	+	+[g]	+	+	B
xopG (XCV1298)	52.02	Putative zinc metalloprotease, HopH family (Lindeberg *et al.*, 2005)	+	+	+	+	−	−	−	B
xopI (XCV0806)	65.11	F-box motif	+	−	−	−	−	+	+	B
xopK (XCV3215)	66.60	Homology to XOO1669 (Furutani *et al.*, 2009)	+	−	−	+	+[h]	−	+	B
xopM (XCV0442)	62.76	No homology to known effectors	+	+	−	+	+[i]	+	+	B
xopR (XCV0285)	66.34	Homology to XOO4134 (Furutani *et al.*, 2009)	+	−	−	−	−	+	+	A
xopS (XCV0324)	55.34	No homology to known effectors	+	−	−	−	−	+	+	A
xopV (XCV0657)	61.50	Homology to XOO3803 (Furutani *et al.*, 2009)	+	−	+	+	−	−	+	B

[a]G + C content of the DNA within the coding region (G + C content of the *Xcv* 85-10 chromosome: 64.75% (Thieme *et al.*, 2005)).
[b]Putative function of gene product, eukaryotic motifs and homology to known type III effectors.
[c]Homologs were determined using BLAST algorithms. −, absence; + presence of a (partial) homolog. *X.*, *Xanthomonas* spp.; *P.*, *Pseudomonas* spp.; *R.*, *Ralstonia solanacearum*; *A.*, *Acidovorax* spp.; o., other organisms.
[d]Presence of a PIP and -10 box (TTCGB-N_{15}-TTCGB-$N_{30–32}$-YANNNT; B represents C, G, or T; Y represents C or T) in the respective promoter (Koebnik *et al.*, 2006). +, presence; −, absence of distinct motifs.
[e]HrpG- and HrpX-dependent co-regulation with the T3S system (+, co-regulation; −, constitutive expression).
[f]Translocation class; classification based on HpaB dependence (Büttner *et al.*, 2006).
[g]*Pantoea agglomerans* pv. *gypsophilae*.
[h]*Burkholderia rhizoxinica*.
[i]*Collimonas fungivorans*.

New Phytologist

Research 5

detectable at similar levels in strains 85-10, 85* and 85*Δ*hrpX*, suggesting constitutive expression (Fig. 1a). The transcripts of *xopB*, *xopI*, *xopK*, *xopM*, *xopR*, *xopS* and *xopV* were amplified from strain 85*, suggesting co-expression with T3S genes. As the amounts of amplified transcripts were clearly reduced with RNA preparations from strains 85-10 and 85*Δ*hrpX*, transcription of the candidate genes is presumably controlled by both HrpG and HrpX. The HrpX-dependent induction of *xopR* has been described previously (Koebnik *et al.*, 2006).

Secretion and translocation of the T3Es

To investigate whether the effector candidates are indeed type III dependently secreted and translocated into the plant cell, we generated translational fusions with the reporter protein AvrBs3Δ2, a derivative of the TAL effector AvrBs3 which lacks a T3S and translocation signal (Szurek *et al.*, 2002; Noël *et al.*, 2003). Fusion of a functional T3S signal to AvrBs3Δ2 enables its translocation and thus the induction of the HR in pepper cultivar ECW-30R plants that harbor the corresponding resistance gene *Bs3* (Noël *et al.*, 2003; Thieme *et al.*, 2007). The native promoters and 5′ coding regions of candidate genes (*xopG*, *xopI*, *xopK*, *xopR*, *xopS* and *xopV*) or the complete coding region (*xopM*) were fused to *avrBs3*Δ2. In the case of *xopB*, the 5′ coding region without promoter was used and the fusion construct was expressed from the *lac* promoter. As controls, we used an empty vector and *avrBs3Δ2* alone (Szurek *et al.*, 2002). All plasmids were conjugated into *Xcv* strain 85* and the T3S mutant

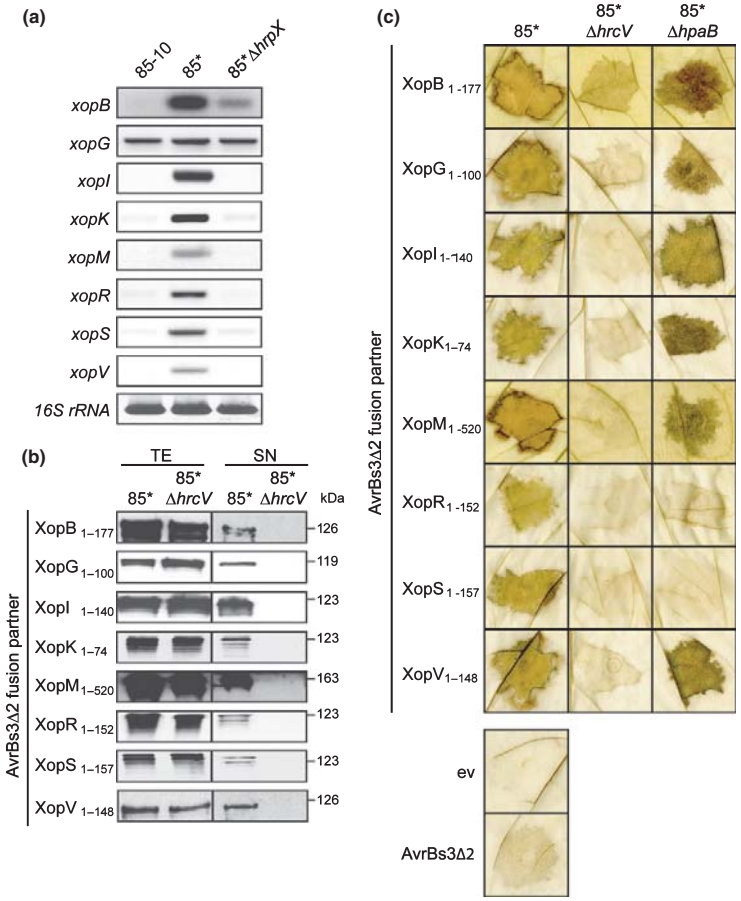

Fig. 1 Regulation of type III effector (T3E) gene expression and type III-dependent transport of XopB, XopG and six new T3Es. (a) Expression studies of effector gene candidates and *xopG* by reverse transcription-polymerase chain reaction (RT-PCR). Gene-specific fragments were amplified from cDNA derived from *Xanthomonas campestris* pv. *vesicatoria* (*Xcv*) strains 85-10, 85* and 85*Δ*hrpX* grown in nutrient yeast glycerol (NYG) medium (Daniels *et al.*, 1984). 16S rRNA was amplified as constitutive control. The amplicons were separated on a 1% agarose gel and stained with ethidium bromide. The experiment was performed three times with similar results. (b) Type III secretion (T3S) assays of AvrBs3Δ2 fusion proteins. Strains 85* and 85*Δ*hrcV* ectopically expressing effector (candidate)-AvrBs3Δ2 fusions were grown in secretion medium. Numbers correspond to the amino acids fused to AvrBs3Δ2. Equal protein amounts of total cell extracts (TE) and culture supernatants (SN) were analyzed by immunoblotting using an AvrBs3-specific antibody. (c) *In planta* translocation assay with effector (candidate)-AvrBs3Δ2 fusions. *Xcv* strains 85*, 85*Δ*hrcV* and 85*Δ*hpaB* expressing the effector gene-*avrBs3Δ2* fusions and 85* carrying an empty vector (ev) or expressing *avrBs3Δ2* alone were inoculated into leaves of AvrBs3-responsive ECW-30R pepper plants. Leaves were harvested at 3 d post-inoculation (dpi) and bleached in ethanol for better visualization of the hypersensitive response (HR).

85*Δ*hrcV*, which lacks an essential inner membrane component of the T3S system (Rossier *et al.*, 2000). When the bacteria were incubated in T3S medium, $XopB_{1–177}$-, $XopG_{1–100}$-, $XopI_{1–140}$-, $XopK_{1–74}$-, $XopM_{1–520}$-, $XopR_{1–152}$-, $XopS_{1–157}$- and $XopV_{1–148}$-AvrBs3Δ2 were detected in the culture supernatant of strain 85*, but not of 85*Δ*hrcV*, by an AvrBs3-specific antibody (Fig. 1b). These results demonstrate that the effector candidates contain functional T3S signals in their N-terminal regions.

To test for type III-dependent translocation, *Xcv* strains 85* and 85*Δ*hrcV* expressing *avrBs3Δ2* or the corresponding effector fusions, as described above, were inoculated into leaves of AvrBs3-responsive pepper plants (ECW-30R) and the near-isogenic susceptible pepper line ECW, which lacks the *Bs3* resistance gene. Derivatives of strain 85* expressing $XopB_{1–177}$-, $XopG_{1–100}$-, $XopI_{1–140}$-, $XopK_{1–74}$-, $XopM_{1–520}$-, $XopR_{1–152}$-, $XopS_{1–157}$- and $XopV_{1–148}$-AvrBs3Δ2 induced the HR in ECW-30R (Fig. 1c), but not in ECW (data not shown). As expected, no HR induction was observed in plants infected with derivatives of strain 85*Δ*hrcV* (Fig. 1c). Taken together, these findings confirm the type III-dependent secretion and translocation of XopB, XopG, XopI, XopK, XopM, XopR, XopS and XopV, and thus their nature as T3Es. In case of XopG, our data confirm a recent publication which showed type III-dependent translocation of the protein using AvrBs2 as reporter (Potnis *et al.*, 2011).

HpaB-dependent translocation of the T3Es

It has been shown previously that the translocation of some T3Es from *Xcv* is dependent on the general T3S chaperone HpaB (Büttner *et al.*, 2004, 2006). To address this question for the *Xcv* effectors analyzed here, we introduced the T3E-AvrBs3Δ2 fusion constructs into strain 85*Δ*hpaB* and inoculated the bacteria into leaves of resistant ECW-30R pepper plants. As shown in Fig. 1(c), $XopB_{1–177}$-, $XopG_{1–100}$-, $XopI_{1–140}$-, $XopK_{1–74}$-, $XopM_{1–520}$- and $XopV_{1–148}$-AvrBs3Δ2 induced the HR even in the absence of HpaB, albeit more or less reduced compared with derivatives of strain 85*. By contrast, $XopR_{1–152}$- and $XopS_{1–157}$-AvrBs3Δ2 failed to induce the HR when analyzed in strain 85*Δ*hpaB*, although both proteins were expressed (Supporting Information, Fig. S1). Thus, according to the published definition (Büttner *et al.*, 2006), XopR and XopS belong to class A, which includes effectors that are not detectably translocated in the absence of HpaB, whereas XopB, XopG, XopI, XopK, XopM and XopV, which are still translocated by the 85*Δ*hpaB* strain, belong to class B (Table 1).

XopB and XopS contribute to the virulence of *Xcv* strain 85-10

To study the contribution of the T3Es to bacterial virulence, all effector genes were individually deleted in *Xcv* strain 85-10, and the mutants were inoculated into leaves of susceptible ECW pepper plants. In addition, induction of the HR in pepper ECW-10R was analyzed, which is based on the recognition of the T3E AvrBs1 by the *Bs1* resistance gene (Cook & Stall, 1963; Ronald & Staskawicz, 1988; Escolar *et al.*, 2001). Bacterial strains carrying deletions of *xopG*, *xopI*, *xopK*, *xopM*, *xopR* and *xopV* showed no difference in the induction of disease symptoms and the HR compared with wild-type strain 85-10 (data not shown). By contrast, deletion of *xopB* or *xopS* led to significantly reduced disease symptoms, whereas the HR induction was not impaired (Fig. 2a,b and data not shown). The mutant phenotypes of 85-10Δ*xopB* and 85-10Δ*xopS* were complemented by ectopic expression of the respective effector gene, suggesting that reduced virulence was not caused by polar effects of the deletions on downstream genes (Fig. 2a,b). Although the growth of both individual effector mutants in ECW plants did not differ significantly from that of the wild-type strain (Fig. S2), multiplication of an 85-10Δ*xopB*Δ*xopS* double mutant was reduced significantly, suggesting that XopB and XopS fulfill redundant functions (Fig. 2c).

XopB and XopS suppress defense gene expression

To test whether the positive effect of XopB and XopS on disease symptoms and bacterial growth can be explained by the suppression of the plant PTI, we analyzed the influence of the effectors on basal and PAMP-induced defense-related gene expression. Therefore, we performed Arabidopsis leaf protoplast assays, a well-established system for PAMP signaling studies (Boudsocq *et al.*, 2010; Ranf *et al.*, 2011). We tested the influence of XopB, a XopB mutant derivative ($XopB_{A313V}$, see the following section) and XopS on the activity of the *A. thaliana NHL10* (*NDR1/HIN1-LIKE 10*) (Zipfel *et al.*, 2004) promoter fused to the firefly luciferase gene (*LUC*) after application of different elicitor-active epitopes of bacterial PAMPs. The luciferase reporter assays showed that the expression of *xopB* and *xopS* decreased the *pNHL10* basal activity significantly, that is, in the absence of an elicitor (Fig. 3a). In addition, both effectors completely inhibited the activation of *pNHL10* by flg22, a bacterial flagellin epitope (Felix *et al.*, 1999), or elf18, a fragment of bacterial EF-Tu (Kunze *et al.*, 2004) (Fig. 3b,c). $XopB_{A313V}$ was only affected slightly in its ability to suppress the elf18-dependent *pNHL10* induction (Fig. 3c). The flg22-mediated induction of *pNHL10* depends, at least in part, on MAPKs (Boudsocq *et al.*, 2010). Therefore, the activation of the MAPKs MPK3, MPK4, MPK6 and MPK11, which are involved in plant immune signaling (Tena *et al.*, 2011; Bethke *et al.*, 2012), might be affected by XopB and XopS. However, immunoblot analysis using an antibody that specifically detects activated kinases revealed no differences in MAPK activity between protoplasts expressing the respective effector genes and protoplasts expressing *CFP* (cyan fluorescent protein) as negative control (Fig. S3; Methods S1). The T3E AvrPto from *P. syringae* served as a positive control (He *et al.*, 2006). Taken together, XopB and XopS suppressed both the basal and PAMP-induced activity of the *NHL10* promoter, but they probably act downstream or independent of MAPK activation (Fig. S2).

XopB, XopG, XopM and XopS trigger cell death in different Solanaceae

To identify additional virulence phenotypes, as well as defense reactions, mediated by the analyzed T3Es, we inoculated leaves

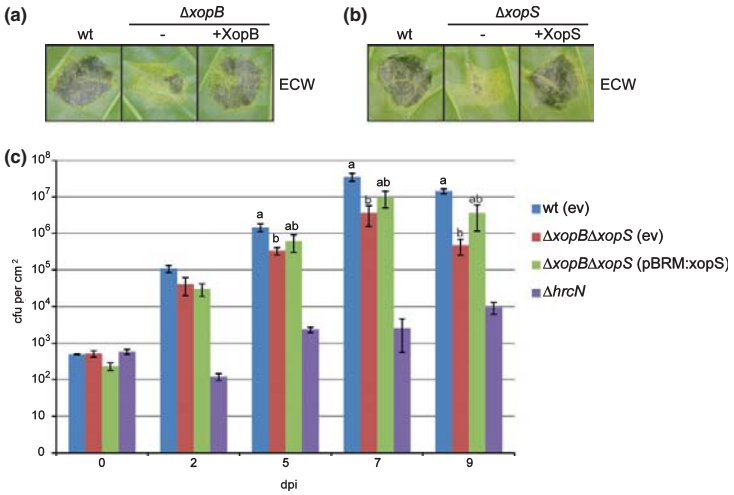

Fig. 2 XopB and XopS contribute to disease symptoms and bacterial growth *in planta*. (a) Leaves of pepper (*Capsicum annuum*) cv ECW plants were inoculated with *Xanthomonas campestris* pv. *vesicatoria* (*Xcv*) strains 85-10, 85-10Δ*xopB* (Δ*xopB*) and an 85-10Δ*xopB* derivative in which *xopB* under control of the *lac* promoter was integrated into the genome (+XopB) (see the Materials and Methods section). Photographs were taken at 7 d post-inoculation (dpi). (b) Pepper ECW plants were inoculated with *Xcv* strains 85-10 and 85-10Δ*xopS* (Δ*xopS*) carrying the empty vector (–) or pBRM:xopS that expresses *xopS* from *plac* (+XopS). Photographs were taken at 7 dpi. (c) Bacterial growth of *Xcv* strains in leaves of susceptible pepper ECW. The following strains were inoculated: *Xcv* 85-10 (wt), 85-10Δ*xopB*Δ*xopS* (Δ*xopB*Δ*xopS*) carrying the empty vector (ev) or pBRM:xopS, and the T3S mutant 85-10Δ*hrcN* (Δ*hrcN*). Bacterial multiplication was monitored over a period of 9 d. Values represent the mean of three samples from three different plants. Error bars indicate standard deviations. Letters a and b indicate statistically significant differences (*t*-test, $P < 0.01$). Experiments were repeated at least three times with similar results.

of pepper ECW, *N. benthamiana* and *N. tabacum*, the latter two being nonhost plants of *Xcv* 85-10, with *Agrobacterium* strains mediating the *in planta* expression of the eight effector genes fused to *GFP*. XopB triggered a cell death reaction in *N. benthamiana* at 5–6 dpi, but not in *N. tabacum* (Fig. 4a). These data are in accordance with recent findings (Salomon *et al.*, 2011). We also tested the transient expression of two *xopB* derivatives with point mutations, accidentally introduced during PCR amplification, for their cell death-inducing activity. Although $XopB_{K455R}$ was still active, $XopB_{A313V}$ did not elicit cell death in *N. benthamiana* (Fig. 4b). Immunoblot analysis of protein extracts from infected plant material, using a GFP-specific antibody, revealed that $XopB_{A313V}$ protein levels were reduced slightly compared with the wild-type protein. We therefore inoculated a dilution series of *Agrobacterium* strains. The *Agrobacterium* strain mediating *xopB* expression triggered cell death even at low density, corresponding to low XopB protein amounts in the plant tissue, whereas *Agrobacterium*-mediated synthesis of $XopB_{A313V}$ did not induce any visible cell death reactions (Fig. S4). This suggests that functional loss rather than a reduced protein level is responsible for the lack of cell death induction by $XopB_{A313V}$.

We also observed a XopG-triggered HR-like cell death in pepper ECW and *N. tabacum* at 2–3 dpi. Furthermore, XopM elicited a cell death reaction in *N. benthamiana* at 3–5 dpi, and XopS caused a weak necrosis (compared with the XopG-triggered reaction) in pepper ECW at 3–4 dpi (Fig. 4a). No distinct plant reactions were observed with the other effectors, although they were expressed, as confirmed by immunoblot analyses of protein extracts from *N. benthamiana* leaves using a GFP-specific antibody (data not shown).

XopB suppresses cell death reactions triggered by XopG and other T3Es

As described above, XopG induces the HR in pepper ECW when transiently expressed *in planta*, whereas *Xcv* 85-10, which naturally expresses XopG, does not. The latter might be caused by other *Xanthomonas* T3Es with cell death suppressing (CDS) activity. Therefore, we tested whether XopB or XopS, which contribute to bacterial virulence (see earlier in the Results section), suppress the XopG-elicited cell death reaction. Co-expression experiments using *Agrobacterium*-mediated gene delivery revealed that the XopG-dependent HR in pepper and *N. tabacum* was strongly reduced or fully abolished in the presence of XopB, but not XopS (Fig. 5a). To validate this finding, we used electrolyte leakage assays, a quantitative measure of early plant cell death (Stall *et al.*, 1974), and found that XopB completely suppressed the XopG HR in *N. tabacum* at early time points (Fig. 5b). Interestingly, no HR suppression was observed with $XopB_{A313V}$, whereas $XopB_{K455R}$ showed wild-type XopB activity (Fig. 5a,b), although the *in planta* expression of both effectors could be detected (Fig. 5c). Hence, the CDS activity in *N. tabacum* and pepper (Fig. 5a,b) and necrosis induction in *N. benthamiana* (Fig. 4b) seem to be functionally linked.

To explore whether the CDS activity of XopB is restricted to XopG-mediated cell death, we transiently co-expressed *xopB* with

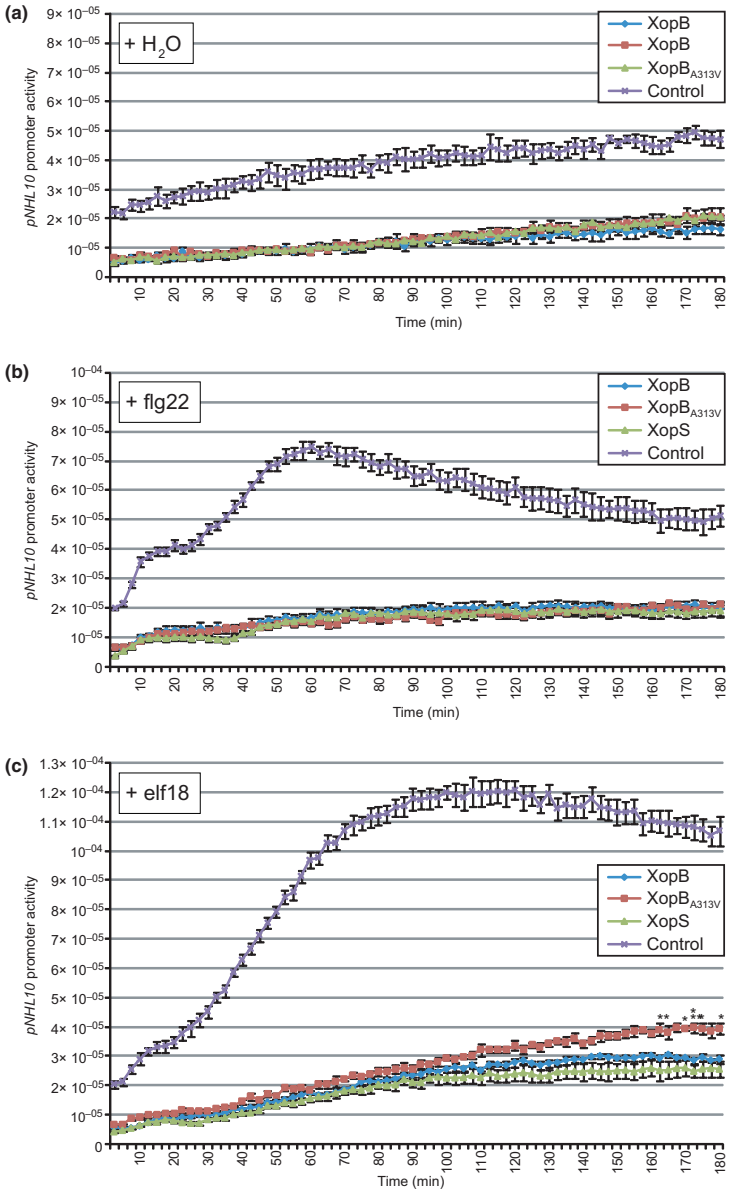

Fig. 3 XopB and XopS inhibit basal and pathogen-associated molecular pattern (PAMP)-induced defense gene expression. *Arabidopsis thaliana* Col-0 protoplasts were co-transformed with *pNHL10-LUC* (luciferase) as a reporter, the indicated *p35S*-effector gene constructs or *p35S-H2B* (control), and *pUBQ10-GUS* (β-glucuronidase) for normalization; 14 h after transformation, protoplasts were treated with (a) H_2O, (b) 100 nM flg22 and (c) 100 nM elf18, and luciferase activity was monitored for 3 h. Results are depicted as LUC/GUS ratios. Asterisks indicate statistically significant differences between XopB and $XopB_{A313V}$ (Kruskal–Wallis/Dunn's post test; *, $P < 0.05$; **, $P < 0.01$). The differences between effector-treated and control samples were statistically significant at every time point (Kruskal–Wallis/Dunn's post test; $P < 0.001$). The experiment was repeated three times with similar results.

avrBs1, *avrBs2*, *avrBsT*, *avrRxv* and *xopJ*, and tested for cell death induction in corresponding resistant plants. XopB suppressed the cell death reactions elicited by AvrBsT, AvrRxv and XopJ in *N. benthamiana* (Fig. 6a). The AvrBs1- and AvrBs2-dependent HRs in pepper ECW-10R and ECW-20R, respectively, were not affected (data not shown). Similar to the effect on XopG-triggered cell death, $XopB_{A313V}$ exhibited no suppression activity, whereas $XopB_{K455R}$ did. Expression of the effector genes was confirmed by immunoblot (Fig. 6b).

To exclude the possibility that the XopB CDS activity is based on unintended cellular changes induced by *Agrobacterium*-mediated overexpression, we analyzed the effect on the

New Phytologist

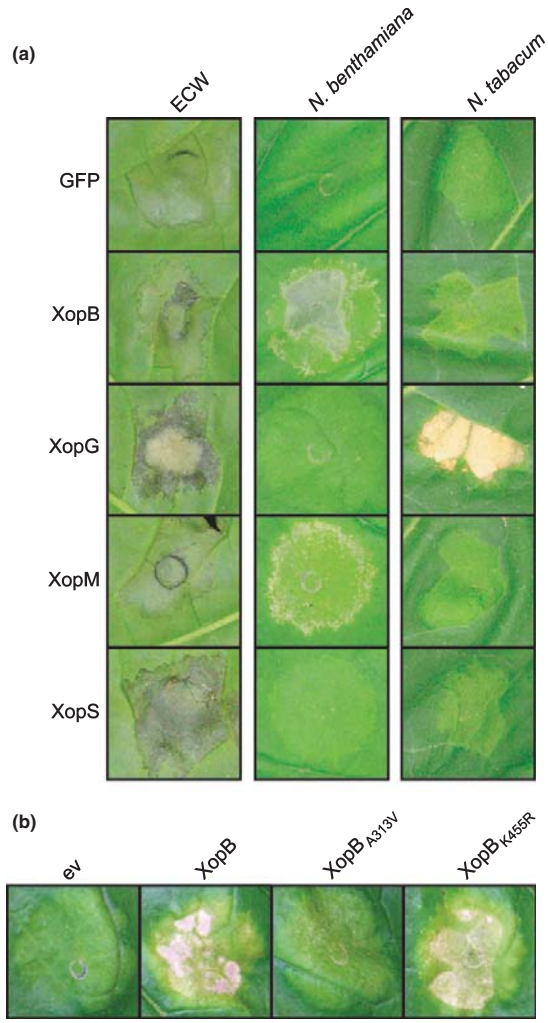

Fig. 4 XopB, XopG, XopM and XopS trigger cell death in different Solanaceae. (a) *Agrobacterium* strains mediating the expression of *GFP*, *xopB::GFP*, *xopG::GFP*, *xopM::GFP* and *xopS::GFP*, under the control of the *35S* promoter, were inoculated into leaves of pepper (*Capsicum annuum*) cv ECW, *Nicotiana benthamiana* and *N. tabacum*. Plant reactions were documented 4 d (ECW) and 6 d (*N. benthamiana*, *N. tabacum*) post-inoculation (dpi). Please note that *Agrobacterium* alone causes a necrotic reaction in pepper that starts at 3–4 dpi.
(b) *Agrobacterium* strains carrying the empty vector (ev) or binary constructs encoding XopB::c-Myc, $XopB_{A313V}$::c-Myc and $XopB_{K455R}$::c-Myc, under the control of the *35S* promoter, were inoculated into *N. benthamiana*. Photographs were taken at 6 dpi.

AvrBsT-dependent HR in pepper using *Xanthomonas* infection. *Xcv*-mediated additional ectopic expression of *xopB*, but not $xopB_{A313V}$, suppressed the HR caused by *Xcv* strain 75-3, which naturally expresses *avrBsT*, in pepper ECW (Fig. 7a,b). This was correlated with increased bacterial growth (Fig. 7c). If *avrBsT* was deleted, strain 75-3 caused no HR and grew significantly better, as expected. In this case, *xopB* overexpression provided no additional growth advantage. This indicates that the positive effect of XopB on bacterial growth is based on the specific suppression of AvrBsT-induced defense responses, and therefore represents a biologically relevant activity of the effector.

XopB localizes to Golgi vesicles and the cytoplasm

Analysis of the subcellular localization of T3Es might provide some clues about their site of action inside the plant cell. To investigate the localization of XopB, we transiently expressed a *xopB::GFP* fusion in *N. benthamiana* using *Agrobacterium*-mediated gene delivery. Subcellular localization was determined by confocal laser scanning microscopy at 24 h post-inoculation (hpi). GFP alone was clearly detectable in the cytoplasm and nuclei (Fig. 8a). By contrast, the fluorescence of XopB::GFP was confined to vesicle-like structures and the cytoplasm, and was not detectable in the nucleus (Fig. 8a). We assumed that the vesicle-like structures might be part of the Golgi system. To test this hypothesis, we transiently co-expressed XopB::GFP with Golgi-mCherry, a fluorescence marker for the Golgi apparatus (Nelson *et al.*, 2007). Both proteins co-localized (Fig. 8a), suggesting that XopB indeed associates with Golgi vesicles. On the ultrastructural level, electron microscopy following immunolabeling showed that, in contrast to free GFP, XopB::GFP predominantly localized to vesicle structures and was strongly under-represented in vesicle-free areas (Fig. 8b).

Furthermore, immunoblot of the subcellular fractionation of *N. benthamiana* extracts confirmed that XopB::c-Myc, similar to Golgi-mCherry, is predominantly associated with the plant membrane fraction (Fig. S5; Methods S1). In addition, intact $XopB_{A313V}$ and $XopB_{K455R}$ were detectable (Fig. S6) and showed a similar localization pattern to the wild-type protein in microscopic as well as fractionation studies (Figs 8a and S5). This suggests that the functional loss of $XopB_{A313V}$ is not caused by mislocalization.

XopB interferes with plant cell protein secretion

The Golgi apparatus provides the cellular basis for intracellular vesicle trafficking, for example protein transport to the plasma membrane and secretion into the apoplast, which plays an important role in plant immunity and has been shown to be targeted by several T3Es (Bartetzko *et al.*, 2009; Frey & Robatzek, 2009). To investigate whether XopB interferes with protein secretion of the plant cell, we used secGFP, a GFP variant that is secreted to the apoplast (Batoko *et al.*, 2000). secGFP only accumulates in a fluorescent form when its transport to a post-Golgi compartment is prevented, for example, by the secretion inhibitor Brefeldin A (BFA). To analyze the influence of XopB on secGFP secretion, both proteins were transiently co-expressed in *N. benthamiana* mediated by *Agrobacterium*. As positive controls, we used BFA and *At*SYP121_Sp2, a cytosolic fragment of a plasma membrane-bound regulator of vesicle trafficking, which has a dominant negative effect on membrane trafficking (Tyrrell *et al.*, 2007), and, in addition, XopJ, a T3E from *Xcv* which suppresses plant cell secretion (Bartetzko *et al.*, 2009). $XopJ_{C235A}$, a XopJ

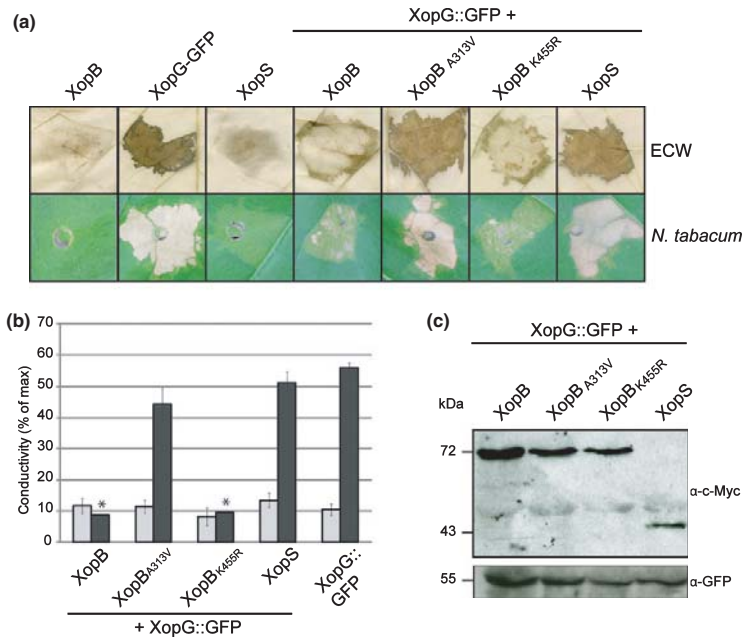

Fig. 5 XopB suppresses XopG-dependent cell death in pepper (*Capsicum annuum*) and tobacco (*Nicotiana tabacum*). (a) *Agrobacterium* strains mediating the transfer of T-DNAs encoding XopB::c-Myc, $XopB_{A313V}$::c-Myc, $XopB_{K455R}$::c-Myc, XopS::c-Myc and XopG::GFP were inoculated into leaves of pepper ECW and *N. tabacum*. For co-expression, the respective strains were mixed before inoculation. Photographs were taken at 4 d post-inoculation (dpi). Pepper leaves were bleached in ethanol for better visualization of cell death reactions. (b) Quantification of XopG-triggered cell death by electrolyte leakage measurements. The inoculation of *N. tabacum* was carried out as described in (a). Leaf tissue of infected plants was harvested at 1 dpi (light gray bars) and 2 dpi (dark gray bars). Bars represent the average conductivity for triplicates of five leaf disks; error bars indicate standard deviations. Asterisks indicate statistically significant differences (*t*-test, $P < 0.01$). (c) Co-expression of XopB and XopS with XopG::GFP in *N. tabacum*. Plants were inoculated as described in (a), and infected leaf tissue was harvested at 24 hpi and analyzed by immunoblotting using c-Myc- and GFP-specific antibodies. All experiments were repeated three times with similar results.

mutant that does not block secretion served as a negative control (Bartetzko *et al.*, 2009). Only weak fluorescence was detectable inside the epidermal cells if secGFP was expressed either alone or together with the negative control (Fig. 9a). By contrast, co-expression of secGFP and XopB resulted in a strong accumulation of GFP fluorescence, forming an intracellular reticulate pattern, comparable with the fluorescence pattern obtained after co-expression of secGFP with *At*SYP121_Sp2 and XopJ or the application of BFA (Fig. 9a). $XopB_{A313V}$ also resulted in the accumulation of intracellular secGFP fluorescence; however, less distinct networks and punctate structures were observed (Fig. 9a). By contrast, $XopB_{K455R}$ caused a fluorescence pattern indistinguishable from that induced by wild-type XopB. Immunoblot analysis showed that differences in secGFP fluorescence were not a result of different protein levels (Fig. 9b).

Discussion

In this study, we analyzed eight *Xcv* effector proteins, six of which were newly identified, so that there are now 23 experimentally verified T3Es in *Xcv* strain 85-10. A major finding is that XopB is a virulence factor that suppresses plant PTI as well as ETI. The T3Es were classified on the basis of whether or not their translocation into plant cells requires the general chaperone HpaB. XopR and XopS belong to *Xcv* translocation class A, comprising T3Es whose translocation into plant cells is completely dependent on HpaB, whereas XopB, XopG, XopI, XopK, XopM and XopV were assigned to class B, because they are still translocated in the absence of HpaB (Büttner *et al.*, 2006). Both new class A effectors lack homology to known proteins or motifs, so that their molecular function remains elusive. By contrast, the class B effectors comprise the putative enzyme XopG, a member of the HopH family (Lindeberg *et al.*, 2005) of putative zinc metalloproteases. Other effectors possess interesting features, for example XopI contains an F-box motif typical for eukaryotic proteins playing a role in the ubiquitin-26S proteasome system (UPS). The UPS controls protein stability in eukaryotes (Willems *et al.*, 2004) and appears to be a favorable target for many T3Es, for example members of the GALA family, which strongly contribute to the virulence of *R. solanacearum* (Angot *et al.*, 2006), and the E3 ubiquitin ligase AvrPtoB from *P. syringae* (Abramovitch *et al.*, 2006; Janjusevic *et al.*, 2006).

As HpaB is essential for pathogenicity, it was speculated that class A effectors play a key role in the establishment of a pathogenic interaction of *Xanthomonas* with the host (Büttner *et al.*, 2004, 2006). Indeed, XopS is involved in the severity of disease

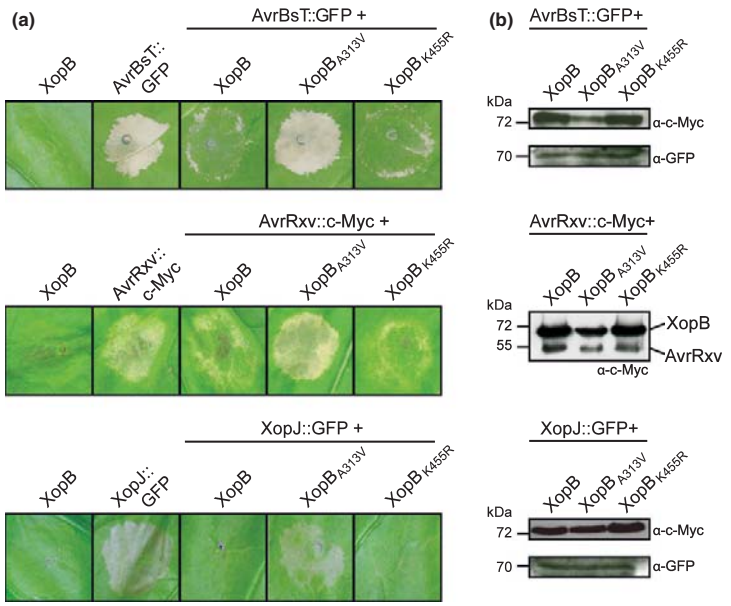

Fig. 6 XopB suppresses cell death reactions induced by XopJ, AvrRxv and AvrBsT. (a) *Agrobacterium* strains mediating the transfer of T-DNA encoding XopB::c-Myc, $XopB_{A313V}$::c-Myc, $XopB_{K455R}$::c-Myc, AvrBsT::GFP, AvrRxv::c-Myc and XopJ::GFP were inoculated into *Nicotiana benthamiana* leaves as indicated. For co-expression, strains were mixed before inoculation. Photographs were taken at 4 d post inoculation (dpi). (b) Expression of the effector genes *in planta*. *N. benthamiana* leaves were inoculated with *Agrobacterium* as described in (a). Infected tissue was harvested at 30 h post-inoculation (hpi) (AvrBsT::GFP) and 40 hpi (AvrRxv::c-Myc and XopJ::GFP), and analyzed by immunoblotting using c-Myc- and GFP-specific antibodies. The experiments were repeated at least twice with similar results.

symptoms, the promotion of bacterial growth and the suppression of PTI, whereas the role of XopR in the virulence of *Xcv* strain 85-10 is probably more subtle. Interestingly, deletion of the *xopR* homolog in *X. oryzae* pv. *oryzae* resulted in reduced virulence on host rice plants (Akimoto-Tomiyama *et al.*, 2012). The fact that individual deletion mutants revealed no major contribution of XopR and most other effectors to the virulence of *Xcv* 85-10 is not unexpected and is probably caused by functional redundancies. Surprisingly, the class B effector XopB clearly contributed to the disease symptoms and bacterial growth of 85-10 on susceptible plants and the suppression of PTI (Figs 2 and 3). This finding differs from our previous study, where no difference in disease symptoms was observed between the wild-type strain and *xopB* mutant (Noël *et al.*, 2001), and may be caused by different environmental conditions (glasshouse, growth chamber). In addition to its effect on PTI, XopB suppressed the ETI-related HR induced by AvrBsT, as well as cell death reactions triggered by XopG, XopJ and AvrRxv (Figs 5 and 6). Although XopB localizes to the Golgi system and the cytoplasm, the inducers of cell death reactions suppressed by XopB localize to different cellular compartments: XopG to the nucleus (Fig. S7), XopJ to the plasma membrane (Thieme *et al.*, 2007), AvrRxv to the cytoplasm (Bonshtien *et al.*, 2005) and AvrBsT to the nucleus and cytoplasm (Szczesny *et al.*, 2010a). As the co-expression of T3Es with XopB did not change their subcellular localization (Fig. S8), XopB probably does not interfere with effector recognition, but rather with downstream signaling.

XopJ, AvrBsT and AvrRxv are members of the YopJ/AvrRxv family from plant and animal pathogens and contain a conserved catalytic triad which is essential for cell death induction (R. Szczesny and U. Bonas, unpublished; Orth *et al.*, 2000; Bonshtien *et al.*, 2005; Cunnac *et al.*, 2007). YopJ/AvrRxv family proteins display acetyltransferase and/or cysteine protease activities (Orth *et al.*, 2000; Ma *et al.*, 2006; Mukherjee *et al.*, 2006; Sweet *et al.*, 2007; Szczesny *et al.*, 2010a). Although a number of bacterial T3Es possess CDS activity (Jackson *et al.*, 1999; Tsiamis *et al.*, 2000; Abramovitch *et al.*, 2003; Espinosa *et al.*, 2003; Jamir *et al.*, 2004; Lopez-Solanilla *et al.*, 2004; Fujikawa *et al.*, 2006; Fu *et al.*, 2007; Guo *et al.*, 2009; Macho *et al.*, 2010), effectors that have successfully been tested for the suppression of several different cell death phenotypes are the exception. To our knowledge, the only known example so far is the sequence-unrelated AvrPtoB from *P. syringae*, which inhibits the HR induced by the T3Es AvrPto, HopA1 and AvrRpm1, the fungal avirulence protein Avr9 and the pro-apoptotic mouse protein Bax (Abramovitch *et al.*, 2003; Guo *et al.*, 2009). Interestingly, AvrPtoB also inhibits PTI and promotes bacterial multiplication *in planta* (Göhre *et al.*, 2008). Suppression of both ETI and PTI depends on the E3 ubiquitin ligase activity of AvrPtoB (Abramovitch *et al.*, 2006; Janjusevic *et al.*, 2006; Göhre *et al.*, 2008; Gimenez-Ibanez *et al.*, 2009), which targets receptor kinases at the plasma membrane (Göhre *et al.*, 2008; Gimenez-Ibanez *et al.*, 2009).

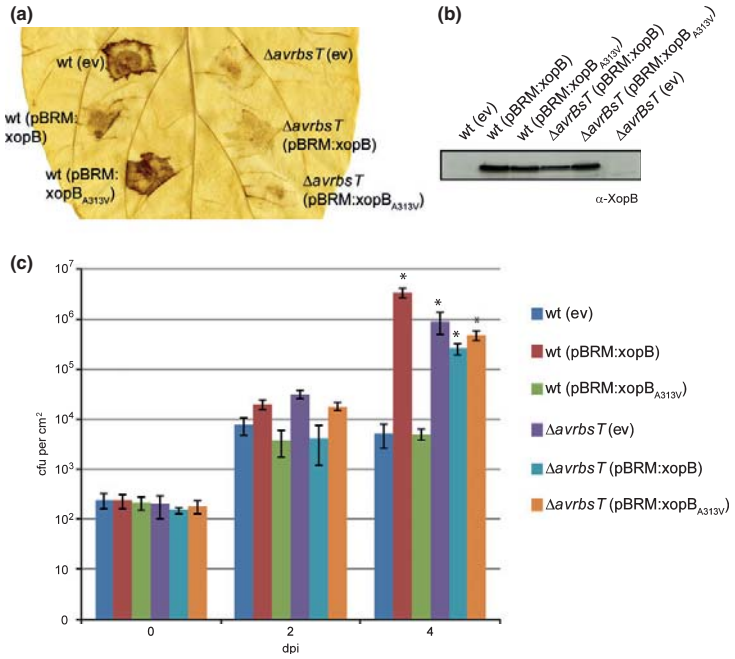

Fig. 7 XopB suppresses the AvrBsT-dependent hypersensitive response (HR) in *Xanthomonas campestris* pv. *vesicatoria* (*Xcv*)-infected pepper. (a) Leaves of pepper (*Capsicum annuum*) cv ECW plants were inoculated with *Xcv* strains 75-3 (wt) and 75-3Δ*avrBsT* (Δ*avrBsT*) carrying the empty vector (ev), pBRM:xopB expressing *xopB* from *plac*, or pBRM:xopB$_{A313V}$. Photographs were taken at 4 d post-inoculation (dpi). (b) Expression of *xopB* and *xopB*$_{A313V}$ in *Xcv* strain 75-3 (wt) and 75-3Δ*avrBsT* (Δ*avrBsT*). Bacteria were grown overnight in liquid nutrient yeast glycerol (NYG) medium and incubated in *hrp* gene-inducing medium for 3.5 h. Similar amounts were analyzed by immunoblotting using a XopB-specific antibody. (c) Bacterial multiplication of the strains described in (a) was monitored over a period of 4 d. Values represent the mean of three samples from three different plants. Error bars indicate standard deviations. Asterisks indicate statistically significant differences when compared with growth of the wild-type strain (*t*-test, $P < 0.05$). The experiments were repeated three times with similar results.

In contrast with AvrPtoB, it is unlikely that XopB acts on top of signaling cascades because it does not inhibit the flg22-triggered activation of MAPKs (Fig. S3) and the CDS activity of XopB is not dependent on membrane-bound receptor kinases because XopG, AvrRxv and AvrBsT are probably not recognized at the plasma membrane (see earlier in the Discussion section). XopB may therefore target a later step of the convergent cellular pathways following T3E recognition. Our studies point to XopB-dependent inhibition of intracellular vesicle trafficking as a possible mode of action to suppress plant immunity. Vesicle trafficking plays an important role in plant defense, for example for the correct localization of PAMP receptors in the plasma membrane. During PTI, genes encoding receptor kinases are induced, including the PAMP receptors themselves (Zipfel *et al.*, 2006; Miya *et al.*, 2007). This results in an increase in receptors and an amplification of the PAMP response (Zipfel *et al.*, 2006). In addition, vesicle transport is involved in the export of antimicrobial molecules, for example PR proteins, phytoalexins and cell wall-bound compounds, and the localization of plasma membrane ABC transporters, which release small antimicrobial molecules to the cell surface (Kwon *et al.*, 2008). Intriguingly, our studies suggest that the inhibition of vesicle transport might explain the XopB effect on PTI, but is insufficient for ETI suppression. XopB$_{A313V}$ completely loses CDS activity, although it still inhibits secGFP secretion and is only slightly affected in PTI suppression (Fig. 3). This suggests that the suppression of PTI and ETI is mediated by separate activities of XopB, and that ETI suppression involves as yet unknown mechanisms.

There are two other T3Es from phytopathogenic bacteria which suppress immunity and interfere with plant protein secretion: (1) HopM1 from *P. syringae*, which is targeted to Arabidopsis endomembranes, suppresses PTI and contributes to disease symptoms and bacterial growth *in planta* (DebRoy *et al.*, 2004; Nomura *et al.*, 2006). HopM1 mediates the UPS-dependent degradation of a key component of the plant vesicle trafficking system (Nomura *et al.*, 2006). (2) XopJ from *Xcv* has been proposed to localize, at least in part, to the Golgi apparatus (Bartetzko *et al.*, 2009). However, the respective analyses were performed in *N. benthamiana*, where XopJ induces necrosis at 3–4 dpi (Thieme *et al.*, 2007), raising the possibility that the occasional localization in punctate structures might be caused by morphological changes induced by ongoing cell death. Nevertheless, XopJ inhibits secGFP secretion and suppresses PTI (Bartetzko *et al.*, 2009). In contrast with XopB, however, HopM1 and XopJ do not appear to affect ETI.

New Phytologist

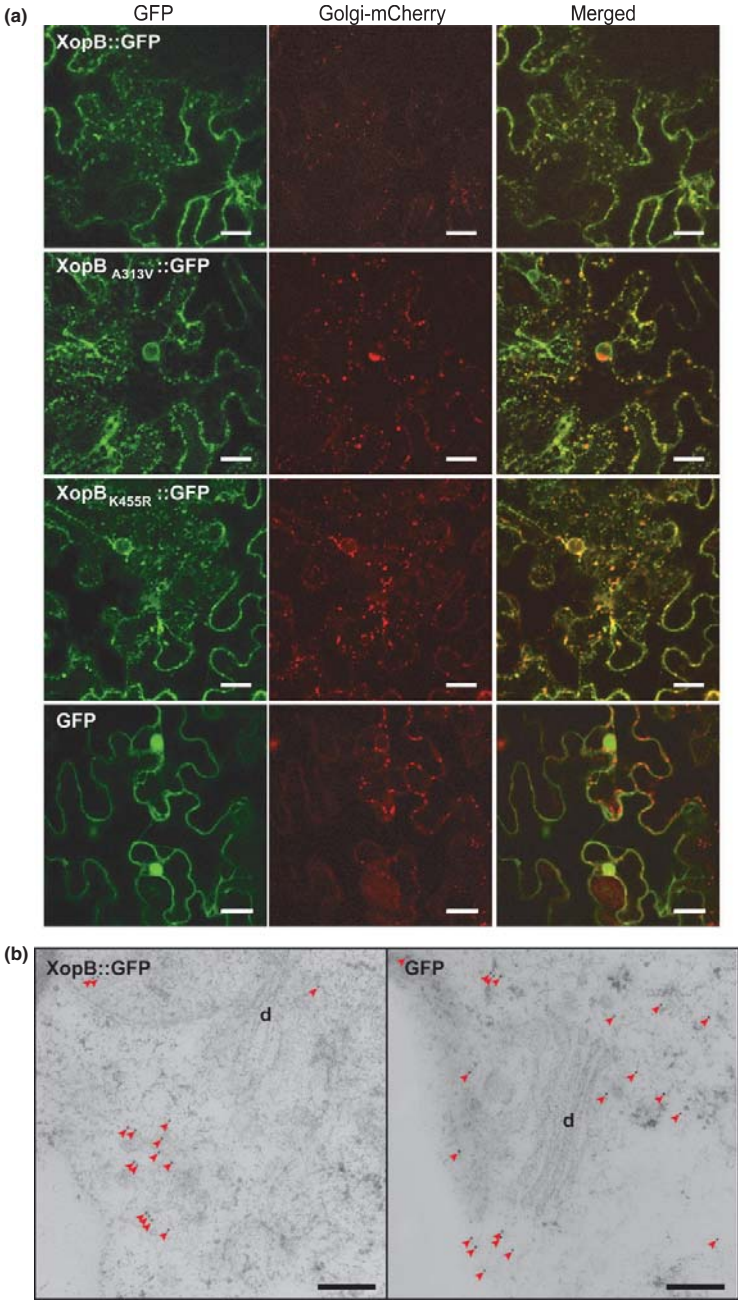

Fig. 8 XopB localizes to the Golgi apparatus and cytoplasm. (a) Confocal laser scanning microscopy of *Nicotiana benthamiana* 24 h after *Agrobacterium*-mediated co-delivery of T-DNAs encoding XopB::GFP, XopB$_{A313V}$::GFP, XopB$_{K455R}$::GFP and GFP with T-DNA encoding Golgi-mCherry. Bars, 20 μm. (b) Ultrastructural localization of GFP fusion proteins by transmission electron microscopy in *N. benthamiana* mesophyll cells 48 h after *Agrobacterium*-mediated transfer of T-DNAs encoding XopB::GFP, XopB$_{A313V}$-GFP and GFP. Tissue samples were cryo-substituted and incubated with a polyclonal GFP-specific antibody and a gold particle-conjugated secondary antibody. For clarity, gold particles are marked with red arrows. Bars, 200 nm. d, dictyosome.

The next challenge is the identification of plant targets, especially of XopB. The putative XopB target appears to be conserved in different plant families as the effector has a virulence activity in pepper, the natural host plant of *Xcv*, and also in the nonhost Brassicaceae *A. thaliana*, as demonstrated by our protoplast assays. That XopB homologs are

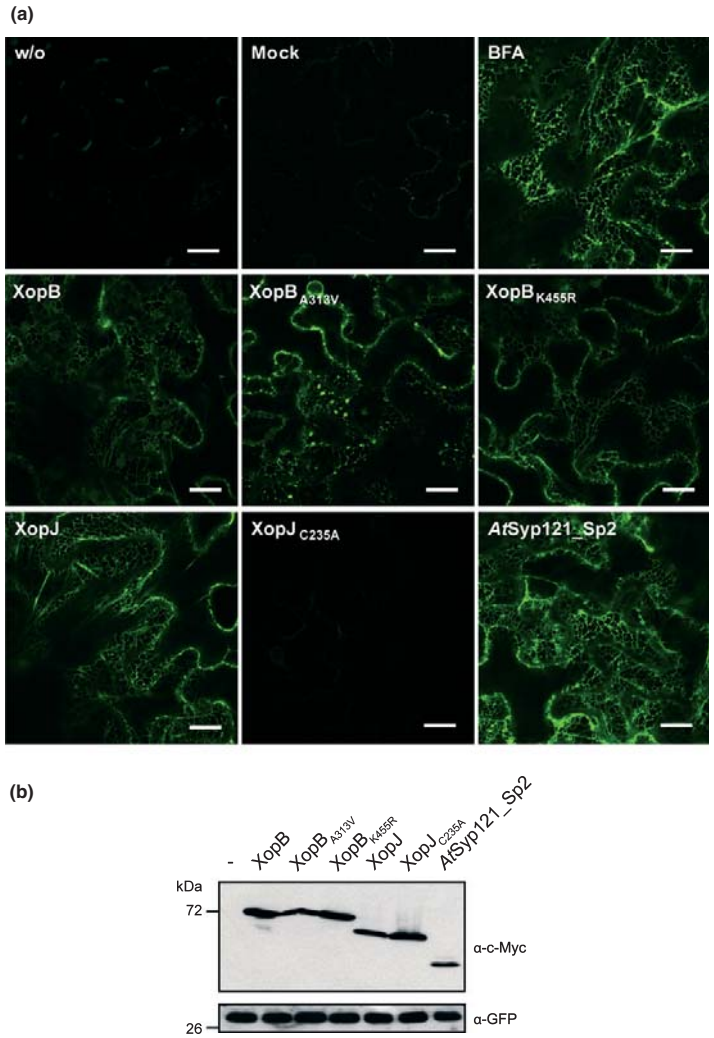

Fig. 9 XopB inhibits plant cell vesicle trafficking. (a) Confocal laser scanning microscopy of *Nicotiana benthamiana* leaves 2 d after *Agrobacterium*-mediated delivery of T-DNA encoding secGFP alone (w/o) or T-DNA encoding the indicated effector proteins fused to a c-Myc tag. XopJ::c-Myc and *At*SYP121_Sp2 served as positive control and $XopJ_{C235A}$::c-Myc as negative control. As additional controls, *secGFP*-expressing leaves were infiltrated with 0.001% dimethyl sulfoxide (DMSO; mock) or brefeldin A (BFA; 10 μg ml^{-1} in 0.001% DMSO) and analyzed 20 min later. Bars, 20 μm. (b) Expression of *secGFP* and effector genes in *N. benthamiana*. Inoculation of *N. benthamiana* leaves was carried out as described in (a). Infected tissue was harvested at 2 d post-inoculation (dpi) and analyzed by immunoblotting using GFP- and c-Myc-specific antibodies. Experiments were repeated twice with similar results.

found in a wide range of plant-pathogenic bacteria (Table 1), infecting various host plants, supports this hypothesis. Interestingly, a recent study has shown that XopB inhibits yeast growth (Salomon *et al.*, 2011). The application of caffeine, which induces cell wall stress, strongly increases the negative effect of XopB on yeast (Salomon *et al.*, 2011). In the light of our results and the fact that vesicle transport is important for yeast cell wall assembly, for example, during budding (Smits *et al.*, 2001), we believe that XopB targets a conserved component of eukaryotic vesicle trafficking.

Acknowledgements

We thank A. Urban, B. Rosinsky, C. Kretschmer, M. Jordan, S. Jahn and N. Bauer for excellent technical assistance. We are grateful to C. Lorenz and H. Berndt for providing unpublished material. This work was funded by grants from the Deutsche Forschungsgemeinschaft to U.B., D.B., J.L. and D.S. (SFB 648 'Molekulare Mechanismen der Informationsverarbeitung in Pflanzen') and from the Bundesministerium für Bildung und Forschung to J.L. and D.S. ('tools, targets & therapeutics – ProNet-T^3').

References

Abramovitch RB, Janjusevic R, Stebbins CE, Martin GB. 2006. Type III effector AvrPtoB requires intrinsic E3 ubiquitin ligase activity to suppress plant cell death and immunity. *Proceedings of the National Academy of Sciences, USA* **103**: 2851–2856.

Abramovitch RB, Kim YJ, Chen S, Dickman MB, Martin GB. 2003. *Pseudomonas* type III effector AvrPtoB induces plant disease susceptibility by inhibition of host programmed cell death. *The EMBO Journal* **22**: 60–69.

Akimoto-Tomiyama C, Furutani A, Tsuge S, Washington EJ, Nishizawa Y, Minami E, Ochiai H. 2012. XopR, a type III effector secreted by *Xanthomonas oryzae* pv. *oryzae*, suppresses microbe-associated molecular pattern-triggered immunity in *Arabidopsis thaliana*. *Molecular Plant–Microbe Interactions* **25**: 505–514.

Angot A, Peeters N, Lechner E, Vailleau F, Baud C, Gentzbittel L, Sartorel E, Genschik P, Boucher C, Genin S. 2006. *Ralstonia solanacearum* requires F-box-like domain-containing type III effectors to promote disease on several host plants. *Proceedings of the National Academy of Sciences, USA* **103**: 14620–14625.

Antony G, Zhou J, Huang S, Li T, Liu B, White F, Yang B. 2010. Rice *xa13* recessive resistance to bacterial blight is defeated by induction of the disease susceptibility gene *Os-11N3*. *Plant Cell* **22**: 3864–3876.

Ausubel FM, Brent R, Kingston RE, Moore DD, Seidman JG, Smith JA, Struhl K. 1996. *Current protocols in molecular biology*. New York, NY, USA: Wiley & Sons.

Bartetzko V, Sonnewald S, Vogel F, Hartner K, Stadler R, Hammes UZ, Börnke F. 2009. The *Xanthomonas campestris* pv. *vesicatoria* type III effector protein XopJ inhibits protein secretion: evidence for interference with cell wall-associated defense responses. *Molecular Plant–Microbe Interactions* **22**: 655–664.

Batoko H, Zheng HQ, Hawes C, Moore I. 2000. A rab1 GTPase is required for transport between the endoplasmic reticulum and golgi apparatus and for normal golgi movement in plants. *Plant Cell* **12**: 2201–2218.

Bethke G, Pecher P, Eschen-Lippold L, Tsuda K, Katagiri F, Glazebrook J, Scheel D, Lee J. 2012. Activation of the *Arabidopsis thaliana* mitogen-activated protein kinase MPK11 by the flagellin-derived elicitor peptide, flg22. *Molecular Plant–Microbe Interactions* **25**: 471–480.

Block A, Alfano JR. 2011. Plant targets for *Pseudomonas syringae* type III effectors: virulence targets or guarded decoys? *Current Opinion in Microbiology* **14**: 39–46.

Boch J, Scholze H, Schornack S, Landgraf A, Hahn S, Kay S, Lahaye T, Nickstadt A, Bonas U. 2009. Breaking the code of DNA binding specificity of TAL-type III effectors. *Science* **326**: 1509–1512.

Bonas U, Schulte R, Fenselau S, Minsavage GV, Staskawicz BJ, Stall RE. 1991. Isolation of a gene cluster from *Xanthomonas campestris* pv. *vesicatoria* that determines pathogenicity and the hypersensitive response on pepper and tomato. *Molecular Plant–Microbe Interactions* **4**: 81–88.

Bonshtien A, Lev A, Gibly A, Debbie P, Avni A, Sessa G. 2005. Molecular properties of the *Xanthomonas* AvrRxv effector and global transcriptional changes determined by its expression in resistant tomato plants. *Molecular Plant–Microbe Interactions* **18**: 300–310.

Boudsocq M, Willmann MR, McCormack M, Lee H, Shan L, He P, Bush J, Cheng SH, Sheen J. 2010. Differential innate immune signalling via Ca^{2+} sensor protein kinases. *Nature* **464**: 418–422.

Büttner D, Bonas U. 2010. Regulation and secretion of *Xanthomonas* virulence factors. *FEMS Microbiology Reviews* **34**: 107–133.

Büttner D, Gürlebeck D, Noël LD, Bonas U. 2004. HpaB from *Xanthomonas campestris* pv. *vesicatoria* acts as an exit control protein in type III-dependent protein secretion. *Molecular Microbiology* **54**: 755–768.

Büttner D, He SY. 2009. Type III protein secretion in plant pathogenic bacteria. *Plant Physiology* **150**: 1656–1664.

Büttner D, Lorenz C, Weber E, Bonas U. 2006. Targeting of two effector protein classes to the type III secretion system by a HpaC- and HpaB-dependent protein complex from *Xanthomonas campestris* pv. *vesicatoria*. *Molecular Microbiology* **59**: 513–527.

Büttner D, Nennstiel D, Klüsener B, Bonas U. 2002. Functional analysis of HrpF, a putative type III translocon protein from *Xanthomonas campestris* pv. vesicatoria. *Journal of Bacteriology* **184**: 2389–2398.

Cook AA, Stall RE. 1963. Inheritance of resistance in pepper to bacterial spot. *Phytopathology* **53**: 1060–1062.

Cunnac S, Wilson A, Nuwer J, Kirik A, Baranage G, Mudgett MB. 2007. A conserved carboxylesterase is a SUPPRESSOR OF AVRBST-ELICITED RESISTANCE in *Arabidopsis*. *Plant Cell* **19**: 688–705.

Daniels MJ, Barber CE, Turner PC, Sawczyc MK, Byrde RJW, Fielding AH. 1984. Cloning of genes involved in pathogenicity of *Xanthomonas campestris* pv. *campestris* using the broad host range cosmid pLAFR1. *EMBO Journal* **3**: 3323–3328.

DebRoy S, Thilmony R, Kwack YB, Nomura K, He SY. 2004. A family of conserved bacterial effectors inhibits salicylic acid-mediated basal immunity and promotes disease necrosis in plants. *Proceedings of the National Academy of Sciences, USA* **101**: 9927–9932.

Engler C, Kandzia R, Marillonnet S. 2008. A one pot, one step, precision cloning method with high throughput capability. *PLoS ONE* **3**: e3647.

Escolar L, Van Den Ackerveken G, Pieplow S, Rossier O, Bonas U. 2001. Type III secretion and *in planta* recognition of the *Xanthomonas* avirulence proteins AvrBs1 and AvrBsT. *Molecular Plant Pathology* **2**: 287–296.

Espinosa A, Guo M, Tam VC, Fu ZQ, Alfano JR. 2003. The *Pseudomonas syringae* type III-secreted protein HopPtoD2 possesses protein tyrosine phosphatase activity and suppresses programmed cell death in plants. *Molecular Microbiology* **49**: 377–387.

Feilner T, Hultschig C, Lee J, Meyer S, Immink RGH, Koenig A, Possling A, Seitz H, Beveridge A, Scheel D *et al.* 2005. High throughput identification of potential Arabidopsis mitogen-activated protein kinases substrates. *Molecular & Cellular Proteomics* **4**: 1558–1568.

Felix G, Duran JD, Volko S, Boller T. 1999. Plants have a sensitive perception system for the most conserved domain of bacterial flagellin. *Plant Journal* **18**: 265–276.

Figurski D, Helinski DR. 1979. Replication of an origin-containing derivative of plasmid RK2 is dependent on a plasmid function provided in trans. *Proceedings of the National Academy of Sciences, USA* **76**: 1648–1652.

Frey NFd, Robatzek S. 2009. Trafficking vesicles: pro or contra pathogens? *Current Opinion in Plant Biology* **12**: 437–443.

Fu ZQ, Guo M, Jeong BR, Tian F, Elthon TE, Cerny RL, Staiger D, Alfano JR. 2007. A type III effector ADP-ribosylates RNA-binding proteins and quells plant immunity. *Nature* **447**: 284–288.

Fujikawa T, Ishihara H, Leach JE, Tsuyumu S. 2006. Suppression of defense responses in plants by the *avrBs3/pthA* gene family of *Xanthomonas* spp. *Molecular Plant–Microbe Interactions* **19**: 342–349.

Furutani A, Takaoka M, Sanada H, Noguchi Y, Oku T, Tsuno K, Ochiai H, Tsuge S. 2009. Identification of novel type III secretion effectors in *Xanthomonas oryzae* pv. *oryzae*. *Molecular Plant–Microbe Interactions* **22**: 96–106.

Gimenez-Ibanez S, Hann DR, Ntoukakis V, Petutschnig E, Lipka V, Rathjen JP. 2009. AvrPtoB targets the LysM receptor kinase CERK1 to promote bacterial virulence on plants. *Current Biology* **19**: 423–429.

Göhre V, Spallek T, Haweker H, Mersmann S, Mentzel T, Boller T, de Torres M, Mansfield JW, Robatzek S. 2008. Plant pattern-recognition receptor FLS2 is directed for degradation by the bacterial ubiquitin ligase AvrPtoB. *Current Biology* **18**: 1824–1832.

Greenberg JT, Yao N. 2004. The role and regulation of programmed cell death in plant–pathogen interactions. *Cellular Microbiology* **6**: 201–211.

Gu K, Yang B, Tian D, Wu L, Wang D, Sreekala C, Yang F, Chu Z, Wang G-L, White FF *et al.* 2005. *R* gene expression induced by a type-III effector triggers disease resistance in rice. *Nature* **435**: 1122–1125.

Guo M, Tian F, Wamboldt Y, Alfano JR. 2009. The majority of the type III effector inventory of *Pseudomonas syringae* pv. *tomato* DC3000 can suppress plant immunity. *Molecular Plant–Microbe Interactions* **22**: 1069–1080.

Hann DR, Gimenez-Ibanez S, Rathjen JP. 2010. Bacterial virulence effectors and their activities. *Current Opinion in Plant Biology* **13**: 388–393.

Haseloff J, Siemering KR, Prasher DC, Hodge S. 1997. Removal of a cryptic intron and subcellular localization of green fluorescent protein are required to

mark transgenic Arabidopsis plants brightly. *Proceedings of the National Academy of Sciences, USA* **94**: 2122–2127.

He P, Shan L, Lin NC, Martin GB, Kemmerling B, Nürnberger T, Sheen J. 2006. Specific bacterial suppressors of MAMP signaling upstream of MAPKKK in Arabidopsis innate immunity. *Cell* **125**: 563–575.

Hotson A, Chosed R, Shu H, Orth K, Mudgett MB. 2003. *Xanthomonas* type III effector XopD targets SUMO-conjugated proteins *in planta*. *Molecular Microbiology* **50**: 377–389.

Hotson A, Mudgett MB. 2004. Cysteine proteases in phytopathogenic bacteria: identification of plant targets and activation of innate immunity. *Current Opinion in Plant Biology* **7**: 384–390.

Huguet E, Hahn K, Wengelnik K, Bonas U. 1998. *hpaA* mutants of *Xanthomonas campestris* pv. *vesicatoria* are affected in pathogenicity but retain the ability to induce host-specific hypersensitive reaction. *Molecular Microbiology* **29**: 1379–1390.

Jackson RW, Athanassopoulos E, Tsiamis G, Mansfield JW, Sesma A, Arnold DL, Gibbon MJ, Murillo J, Taylor JD, Vivian A. 1999. Identification of a pathogenicity island, which contains genes for virulence and avirulence, on a large native plasmid in the bean pathogen *Pseudomonas syringae* pathovar *phaseolicola*. *Proceedings of the National Academy of Sciences, USA* **96**: 10875–10880.

Jamir Y, Guo M, Oh H-S, Petnicki-Ocwieja T, Chen S, Tang X, Dickman MB, Collmer A, Alfano JR. 2004. Identification of *Pseudomonas syringae* type III effectors that can suppress programmed cell death in plants and yeast. *Plant Journal* **37**: 554–565.

Janjusevic R, Abramovitch RB, Martin GB, Stebbins CE. 2006. A bacterial inhibitor of host programmed cell death defenses is an E3 ubiquitin ligase. *Science* **311**: 222–226.

Jones JD, Dangl JL. 2006. The plant immune system. *Nature* **444**: 323–329.

Jones JB, Lacy GH, Bouzar H, Stall RE, Schaad NW. 2004. Reclassification of the xanthomonads associated with bacterial spot disease of tomato and pepper. *Systematic and Applied Microbiology* **27**: 755–762.

Karimi M, De Meyer B, Hilson P. 2005. Modular cloning and expression of tagged fluorescent protein in plant cells. *Trends in Plant Science* **10**: 103–105.

Kay S, Bonas U. 2009. How *Xanthomonas* type III effectors manipulate the host plant. *Current Opinion in Microbiology* **12**: 1–7.

Kay S, Hahn S, Marois E, Hause G, Bonas U. 2007. A bacterial effector acts as a plant transcription factor and induces a cell size regulator. *Science* **318**: 648–651.

Kim JG, Li X, Roden JA, Taylor KW, Aakre CD, Su B, Lalonde S, Kirik A, Chen Y, Baranage G *et al.* 2009. *Xanthomonas* T3S effector XopN suppresses PAMP-triggered immunity and interacts with a tomato atypical receptor-like kinase and TFT1. *Plant Cell* **21**: 1305–1323.

Kim JG, Taylor KW, Hotson A, Keegan M, Schmelz EA, Mudgett MB. 2008. XopD SUMO protease affects host transcription, promotes pathogen growth, and delays symptom development in *Xanthomonas*-infected tomato leaves. *Plant Cell* **20**: 1915–1929.

Klement Z, Goodman RN. 1967. The hypersensitive reaction to infection by bacterial plant pathogens. *Annual Review of Phytopathology* **5**: 17–44.

Knoop V, Staskawicz B, Bonas U. 1991. Expression of the avirulence gene *avrBs3* from *Xanthomonas campestris* pv. vesicatoria is not under the control of *hrp* genes and is independent of plant factors. *Journal of Bacteriology* **173**: 7142–7150.

Koebnik R, Kruger A, Thieme F, Urban A, Bonas U. 2006. Specific binding of the *Xanthomonas campestris* pv. *vesicatoria* AraC-type transcriptional activator HrpX to plant-inducible promoter boxes. *Journal of Bacteriology* **188**: 7652–7660.

Kunze G, Zipfel C, Robatzek S, Niehaus K, Boller T, Felix G. 2004. The N terminus of bacterial elongation factor Tu elicits innate immunity in *Arabidopsis* plants. *Plant Cell* **16**: 3496–3507.

Kwon C, Bednarek P, Schulze-Lefert P. 2008. Secretory pathways in plant immune responses. *Plant Physiology* **147**: 1575–1583.

Lindeberg M, Stavrinides J, Chang JH, Alfano JR, Collmer A, Dangl JL, Greenberg JT, Mansfield JW, Guttman DS. 2005. Proposed guidelines for a unified nomenclature and phylogenetic analysis of type III Hop effector proteins in the plant pathogen *Pseudomonas syringae*. *Molecular Plant–Microbe Interactions* **18**: 275–282.

Lopez-Solanilla E, Bronstein PA, Schneider AR, Collmer A. 2004. HopPtoN is a *Pseudomonas syringae* Hrp (type III secretion system) cysteine protease effector that suppresses pathogen-induced necrosis associated with both compatible and incompatible plant interactions. *Molecular Microbiology* **54**: 353–365.

Lorenz C, Kirchner O, Egler M, Stuttmann J, Bonas U, Büttner D. 2008. HpaA from *Xanthomonas* is a regulator of type III secretion. *Molecular Microbiology* **69**: 344–360.

Ma W, Dong FFT, Stavrinides J, Guttman DS. 2006. Type III effector diversification via both pathoadaptation and horizontal transfer in response to a coevolutionary arms race. *PLoS Genetics* **2**: e209.

Macho AP, Guevara CM, Tornero P, Ruiz-Albert J, Beuzon CR. 2010. The *Pseudomonas syringae* effector protein HopZ1a suppresses effector-triggered immunity. *New Phytologist* **187**: 1018–1033.

Marois E, Van den Ackerveken G, Bonas U. 2002. The *Xanthomonas* type III effector protein AvrBs3 modulates plant gene expression and induces cell hypertrophy in the susceptible host. *Molecular Plant–Microbe Interactions* **15**: 637–646.

Metz M, Dahlbeck D, Morales CQ, Al Sady B, Clark ET, Staskawicz BJ. 2005. The conserved *Xanthomonas campestris* pv. *vesicatoria* effector protein XopX is a virulence factor and suppresses host defense in *Nicotiana benthamiana*. *Plant Journal* **41**: 801–814.

Minsavage GV, Dahlbeck D, Whalen MC, Kearney B, Bonas U, Staskawicz BJ, Stall RE. 1990. Gene-for-gene relationships specifying disease resistance in *Xanthomonas campestris* pv. *vesicatoria*–pepper interactions. *Molecular Plant–Microbe Interactions* **3**: 41–47.

Miya A, Albert P, Shinya T, Desaki Y, Ichimura K, Shirasu K, Narusaka Y, Kawakami N, Kaku H, Shibuya N. 2007. CERK1, a LysM receptor kinase, is essential for chitin elicitor signaling in *Arabidopsis*. *Proceedings of the National Academy of Sciences, USA* **104**: 19613–19618.

Morales CQ, Posada J, Macneale E, Franklin D, Rivas I, Bravo M, Minsavage J, Stall RE, Whalen MC. 2005. Functional analysis of the early chlorosis factor gene. *Molecular Plant–Microbe Interactions* **18**: 477–486.

Mudgett MB, Chesnokova O, Dahlbeck D, Clark ET, Rossier O, Bonas U, Staskawicz BJ. 2000. Molecular signals required for type III secretion and translocation of the *Xanthomonas campestris* AvrBs2 protein to pepper plants. *Proceedings of the National Academy of Sciences, USA* **97**: 13324–13329.

Mukherjee S, Keitany G, Li Y, Wang Y, Ball HL, Goldsmith EJ, Orth K. 2006. *Yersinia* YopJ acetylates and inhibits kinase activation by blocking phosphorylation. *Science* **312**: 1211–1214.

Nakagawa T, Takayuki K, Hino T, Tanaka K, Kawamukai M, Niwa Y, Toyooka K, Matsuoka K, Jinbo T, Kimura T. 2007. Development of series of Gateway binary vectors, pGWBs, for realizing efficient construction of fusion genes for plant transformation. *Journal of Bioscience and Bioengineering* **104**: 34–41.

Nelson BK, Cai X, Nebenfuhr A. 2007. A multicolored set of *in vivo* organelle markers for co-localization studies in Arabidopsis and other plants. *Plant Journal* **51**: 1126–1136.

Noël L, Thieme F, Gäbler J, Büttner D, Bonas U. 2003. XopC and XopJ, two novel type III effector proteins from *Xanthomonas campestris* pv. *vesicatoria*. *Journal of Bacteriology* **185**: 7092–7102.

Noël L, Thieme F, Nennstiel D, Bonas U. 2001. cDNA-AFLP analysis unravels a genome-wide *hrpG*-regulon in the plant pathogen *Xanthomonas campestris* pv. *vesicatoria*. *Molecular Microbiology* **41**: 1271–1281.

Noël L, Thieme F, Nennstiel D, Bonas U. 2002. Two novel type III-secreted proteins of *Xanthomonas campestris* pv. vesicatoria are encoded within the *hrp* pathogenicity island. *Journal of Bacteriology* **184**: 1340–1348.

Nomura K, Debroy S, Lee YH, Pumplin N, Jones J, He SY. 2006. A bacterial virulence protein suppresses host innate immunity to cause plant disease. *Science* **313**: 220–223.

Norris SR, Meyer SE, Callis J. 1993. The intron of *Arabidopsis thaliana* polyubiquitin genes is conserved in location and is a quantitative determinant of chimeric gene expression. *Plant Molecular Biology* **21**: 895–906.

Nürnberger T, Brunner F, Kemmerling B, Piater L. 2004. Innate immunity in plants and animals: striking similarities and obvious differences. *Immunological Reviews* **198**: 249–266.

Orth K, Xu Z, Mudgett MB, Bao ZQ, Palmer LE, Bliska JB, Mangel WF, Staskawicz B, Dixon JE. 2000. Disruption of signaling by *Yersinia* effector YopJ, a ubiquitin-like protein protease. *Science* **290**: 1594–1597.

Parsot C, Hamiaux C, Page AL. 2003. The various and varying roles of specific chaperones in type III secretion systems. *Current Opinion in Microbiology* **6**: 7–14.

Potnis N, Krasileva K, Chow V, Almeida NF, Patil PB, Ryan RP, Sharlach M, Behlau F, Dow JM, Momol M *et al.* 2011. Comparative genomics reveals diversity among xanthomonads infecting tomato and pepper. *BMC Genomics* **12**: 146.

Ranf S, Eschen-Lippold L, Pecher P, Lee J, Scheel D. 2011. Interplay between calcium signalling and early signalling elements during defence responses to microbe- or damage-associated molecular patterns. *Plant Journal* **68**: 100–113.

Roden JA, Belt B, Ross JB, Tachibana T, Vargas J, Mudgett MB. 2004. A genetic screen to isolate type III effectors translocated into pepper cells during *Xanthomonas* infection. *Proceedings of the National Academy of Sciences, USA* **101**: 16624–16629.

Römer P, Hahn S, Jordan T, Strauß T, Bonas U, Lahaye T. 2007. Plant–pathogen recognition mediated by promoter activation of the pepper *Bs3* resistance gene. *Science* **318**: 645–648.

Ronald PC, Staskawicz BJ. 1988. The avirulence gene *avrBs1* from *Xanthomonas campestris* pv. *vesicatoria* encodes a 50-kD protein. *Molecular Plant–Microbe Interactions* **1**: 191–198.

Rossier O, Van den Ackerveken G, Bonas U. 2000. HrpB2 and HrpF from *Xanthomonas* are type III-secreted proteins and essential for pathogenicity and recognition by the host plant. *Molecular Microbiology* **38**: 828–838.

Rossier O, Wengelnik K, Hahn K, Bonas U. 1999. The *Xanthomonas* Hrp type III system secretes proteins from plant and mammalian bacterial pathogens. *Proceedings of the National Academy of Sciences, USA* **96**: 9368–9373.

Salomon D, Dar D, Sreeramulu S, Sessa G. 2011. Expression of *Xanthomonas campestris* pv. *vesicatoria* type III effectors in yeast affects cell growth and viability. *Molecular Plant–Microbe Interactions* **24**: 305–314.

Schäfer A, Tauch A, Jager W, Kalinowski J, Thierbach G, Pühler A. 1994. Small mobilizable multi-purpose cloning vectors derived from the *Escherichia coli* plasmids pK18 and pK19: selection of defined deletions in the chromosome of *Corynebacterium glutamicum*. *Gene* **145**: 69–73.

Smits GJ, van den Ende H, Klis FM. 2001. Differential regulation of cell wall biogenesis during growth and development in yeast. *Microbiology* **147**: 781–794.

Stall RE, Bartz JA, Cook AA. 1974. Decreased hypersensitivity to xanthomonads in pepper after inoculations with virulent cells of *Xanthomonas vesicatoria*. *Phytopathology* **64**: 731–735.

Sweet CR, Conlon J, Golenbock DT, Goguen J, Silverman N. 2007. YopJ targets TRAF proteins to inhibit TLR-mediated NF-κB, MAPK and IRF3 signal transduction. *Cellular Microbiology* **9**: 2700–2715.

Szczesny R, Büttner D, Escolar L, Schulze S, Seiferth A, Bonas U. 2010a. Suppression of the AvrBs1-specific hypersensitive response by the YopJ effector homolog AvrBsT from *Xanthomonas* depends on a SNF1-related kinase. *New Phytologist* **187**: 1058–1074.

Szczesny R, Jordan M, Schramm C, Schulz S, Cogez V, Bonas U, Büttner D. 2010b. Functional characterization of the Xcs and Xps type II secretion systems from the plant pathogenic bacterium *Xanthomonas campestris* pv. *vesicatoria*. *New Phytologist* **187**: 983–1002.

Szurek B, Rossier O, Hause G, Bonas U. 2002. Type III-dependent translocation of the *Xanthomonas* AvrBs3 protein into the plant cell. *Molecular Microbiology* **46**: 13–23.

Tena G, Boudsocq M, Sheen J. 2011. Protein kinase signaling networks in plant innate immunity. *Current Opinion in Plant Biology* **14**: 519–529.

Thieme F, Koebnik R, Bekel T, Berger C, Boch J, Büttner D, Caldana C, Gaigalat L, Goesmann A, Kay S *et al.* 2005. Insights into genome plasticity and pathogenicity of the plant pathogenic bacterium *Xanthomonas campestris* pv. vesicatoria revealed by the complete genome sequence. *Journal of Bacteriology* **187**: 7254–7266.

Thieme F, Szczesny R, Urban A, Kirchner O, Hause G, Bonas U. 2007. New type III effectors from *Xanthomonas campestris* pv. *vesicatoria* trigger plant reactions dependent on a conserved N-myristoylation motif. *Molecular Plant–Microbe Interactions* **20**: 1250–1261.

Tsiamis G, Mansfield JW, Hockenhull R, Jackson RW, Sesma A, Athanassopoulos E, Bennett MA, Stevens C, Vivian A, Taylor JD *et al.* 2000. Cultivar-specific avirulence and virulence functions assigned to *avrPphF* in *Pseudomonas syringae* pv. *phaseolicola*, the cause of bean halo-blight disease. *EMBO Journal* **19**: 3204–3214.

Tyrrell M, Campanoni P, Sutter JU, Pratelli R, Paneque M, Sokolovski S, Blatt MR. 2007. Selective targeting of plasma membrane and tonoplast traffic by inhibitory (dominant-negative) SNARE fragments. *Plant Journal* **51**: 1099–1115.

Vauterin L, Rademaker J, Swings J. 2000. Synopsis on the taxonomy of the genus *Xanthomonas*. *Phytopathology* **90**: 677–682.

Wengelnik K, Bonas U. 1996. HrpXv, an AraC-type regulator, activates expression of five out of six loci in the *hrp* cluster of *Xanthomonas campestris* pv. *vesicatoria*. *Journal of Bacteriology* **178**: 3462–3469.

Wengelnik K, Marie C, Russel M, Bonas U. 1996b. Expression and localization of HrpA1, a protein of *Xanthomonas campestris* pv. *vesicatoria* essential for pathogenicity and induction of the hypersensitive reaction. *Journal of Bacteriology* **178**: 1061–1069.

Wengelnik K, Rossier O, Bonas U. 1999. Mutations in the regulatory gene *hrpG* of *Xanthomonas campestris* pv. vesicatoria result in constitutive expression of all *hrp* genes. *Journal of Bacteriology* **181**: 6828–6831.

Wengelnik K, Van den Ackerveken G, Bonas U. 1996a. HrpG, a key *hrp* regulatory protein of *Xanthomonas campestris* pv. vesicatoria, is homologous to two-component response regulators. *Molecular Plant–Microbe Interactions* **9**: 704–712.

Wilharm G, Dittmann S, Schmid A, Heesemann J. 2007. On the role of specific chaperones, the specific ATPase, and the proton motive force in type III secretion. *International Journal of Medical Microbiology* **297**: 27–36.

Willems AR, Schwab M, Tyers M. 2004. A hitchhiker's guide to the cullin ubiquitin ligases: SCF and its kin. *Biochimica et Biophysica Acta* **1695**: 133–170.

Yang B, Sugio A, White FF. 2006. *Os8N3* is a host disease-susceptibility gene for bacterial blight of rice. *Proceedings of the National Academy of Sciences, USA* **103**: 10503–10508.

Zipfel C, Kunze G, Chinchilla D, Caniard A, Jones JDG, Boller T, Felix G. 2006. Perception of the bacterial PAMP EF-Tu by the receptor EFR restricts *Agrobacterium*-mediated transformation. *Cell* **125**: 749–760.

Zipfel C, Robatzek S, Navarro L, Oakeley EJ, Jones JDG, Felix G, Boller T. 2004. Bacterial disease resistance in Arabidopsis through flagellin perception. *Nature* **428**: 764–767.

Supporting Information

Additional supporting information may be found in the online version of this article.

Fig. S1 XopR- and XopS-AvrBs3Δ2 fusion proteins are expressed in *Xcv* 85*Δ*hpaB*.

Fig. S2 Individual deletion of *xopB* and *xopS* has no influence on bacterial growth.

Fig. S3 XopB and XopS do not suppress mitogen-activated protein kinase (MAPK) activation in Arabidopsis.

Fig. S4 $XopB_{A313V}$ is impaired in cell death induction.

Fig. S5 XopB is associated with the membrane fraction of plant cells.

Fig. S6 Expression of *GFP* and *xopB-GFP* fusions in *Nicotiana benthamiana*.

Fig. S7 Subcellular localization of XopG::GFP.

Fig. S8 Subcellular localization of XopG, AvrBsT, AvrRxv and XopJ is not affected by co-expression of XopB.

Table S1 Bacterial strains and plasmids used in this study

Table S2 Oligonucleotides used in this study

Methods S1 Immunoblot-based detection of mitogen-activated protein kinase (MAPK) activation and membrane fractionation.

Please note: Wiley-Blackwell are not responsible for the content or functionality of any supporting information supplied by the authors. Any queries (other than missing material) should be directed to the *New Phytologist* Central Office.

2.2.1.1 Anlagen zu Publikation 2

SUPPORTING INFORMATION METHODS S1, TABLES S1 & S2 AND FIGS S1-S8

A. thaliana (Col-0) protoplast samples (800 µl each) were transformed with either *p35S*-effector constructs (*xopB*, *xopS*), or *p35S-H2B* (10 µg DNA per 100 µl protoplasts). After about 14 h of incubation (in the dark, 19°C), the protoplasts were elicited with 100 nM flg22 and samples were taken at 15 min post elicitation. Protein extraction and immunoblotting with an pTEpY-specific antibody (α-phospho-p44/42-ERK; CST, http://www.cellsignal.com/) were performed as described (Kroj *et al.*, 2003; Saijo *et al.*, 2009).

Membrane fractionation was modified according to Bartetzko *et al.* (2009). 1 g infected leaf material was ground in 3 ml ice-cold extraction buffer (20 mM HEPES pH 7.5, 100 mM NaCl, 5 mM $MgCl_2$, 1 mM dithiothreitol) and centrifuged at 2,000 x g for 10 min to yield total extract (TE). 1 ml TE was subjected to ultracentrifugation at 100,000 x g for one hour at 4°C. The resulting supernatant (soluble fraction), ultraspeed pellet (membrane fraction) and TE were separated by SDS-PAGE and analyzed by immunoblotting.

Bartetzko V, Sonnewald S, Vogel F, Hartner K, Stadler R, Hammes UZ, Börnke F. 2009. The *Xanthomonas campestris* pv. *vesicatoria* type III effector protein XopJ inhibits protein secretion: evidence for interference with cell wall-associated defense responses. *Molecular Plant-Microbe Interactions* **22**(6): 655-664.

Kroj T, Rudd JJ, Nürnberger T, Gäbler Y, Lee J, Scheel D. 2003. Mitogen-activated protein kinases play an essential role in oxidative burst-independent expression of pathogenesis-related genes in parsley. *Journal of Biological Chemistry* **278**(4): 2256-2264.

Saijo Y, Tintor N, Lu X, Rauf P, Pajerowska-Mukhtar K, Haweker H, Dong X, Robatzek S, Schulze-Lefert P. 2009. Receptor quality control in the endoplasmic reticulum for plant innate immunity. *EMBO Journal* **28**(21): 3439-3449.

SUPPORTING INFORMATION TABLES S1 & S2

Table S1 Bacterial strains and plasmids used in this study

	Relevant characteristics[a]	Reference or source[b]
X. campestris* pv. *vesicatoria		
75-3	Tomato race 1, wild type, Rif^r	(Minsavage *et al.*, 1990)
75-3Δ*avrBsT*	*avrBsT* deletion mutant, derivative of strain 75-3	(Szczesny *et al.*, 2010a)
85-10	Pepper- 2, wild type, Rif^r	(Canteros, 1990; Minsavage *et al.*, 1990)
85-10Δ*hrcN*	*hrcN* deletion mutant, derivative of strain 85-10	(Lorenz & Büttner, 2009)
85-10Δ*xopB*	*xopB* deletion mutant, derivative of strain 85-10	(Noël *et al.*, 2001)
85-10Δ*xopB*Δ*xopS*	*xopBxopS* deletion mutant, derivative of strain 85-10Δ*xopB*	This study
85-10Δ*xopG*	*xopG* deletion mutant, derivative of strain 85-10	This study
85-10Δ*xopI*	*xopI* deletion mutant, derivative of strain 85-10	This study
85-10Δ*xopK*	*xopK* deletion mutant, derivative of strain 85-10	This study
85-10Δ*xopM*	*xopM* deletion mutant, derivative of strain 85-10	This study
85-10Δ*xopR*	*xopR* deletion mutant, derivative of strain 85-10	This study
85-10Δ*xopS*	*xopS* deletion mutant, derivative of strain 85-10	This study
85-10Δ*xopV*	*xopV* deletion mutant, derivative of strain 85-10	This study
85*	85-10 derivative containing the *hrpG** mutation	(Wengelnik *et al.*, 1999)
85*Δ*hpaB*	*hpaB* deletion mutant derivative of strain 85*	(Büttner *et al.*, 2004)
85*Δ*hrcV*	*hrcV* deletion mutant derivative of strain 85*	(Rossier *et al.*, 1999)
A. tumefaciens		
GV3101(pMP90)	Carries Ti plasmid pMP90; Rif^r, Gent^r	(Koncz & Schell, 1986)
E. coli		
Top10	*mcr*A Δ(*mrr-hsd*RMS-*mcr*BC) Φ80*lac*ZΔM15 Δ*lac*X74 *rec*A1 *ara*D139 Δ(*araleu*) 7697 *gal*U *gal*K *rps*L (Str^R) *end*A1 *nup*G	Invitrogen, Karlsruhe, Germany
DH5α λpir	F$^-$ *recA hsdR17*(r_k^-,m_k^+) *Φ80dlacZ DM15 [λpir]*	(Ménard *et al.*, 1993)
Plasmids		
pBGWFS7	Binary expression vector; *att*R1-Cm^r-*ccd*B-*att*R2-*EGFP::uidA*; Sm^r	(Karimi *et al.*, 2005)
pBRM	Golden Gate-compatible derivative of pBBR1MCS-5, *lac* promoter; Gm^r	(Szczesny *et al.*, 2010b)
pDSK602	d-host-range vector; contains triple *lacUV5* promoter; Sm^r	(Murillo *et al.*, 1994)
pENTR/D-TOPO	GATEWAY compatible directional cloning vector; Km^r	Invitrogen
pGGA1	Golden Gate-compatible derivative of pBGWFS7; binary expression vector; 35S promoter-Cm^r-*ccd*B-*EGFP*; Sm^r	This study
pGWB2	Binary expression vector; 35S promoter-*att*R1-Cm^r-*ccd*B-*att*R2; Hm^r, Km^r	(Nakagawa *et al.*, 2007)
pGWB5	Binary expression vector; 35S promoter-*att*R1-Cm^r-*ccd*B-*att*R2-sGFP; Hm^r, Km^r	(Nakagawa *et al.*, 2007)
pGWB17	Binar expression vector; 35S promoter-*att*R1-Cm^r-*ccd*B-*att*R2-4xmyc; Hm^r, Km^r	(Nakagawa *et al.*, 2007)
pK18	suic vector, $oriV_{Ec}$ *oriT sacB*; Km^r	(Schäfer *et al.*, 1994)
pK7FWG2	Bina expression vector; 35S promoter-*att*R1-	(Karimi *et al.*, 2005)

	Cm^r-*ccd*B-*att*R2-eGFP; Sm^r	
pK7WGF2	Binary expression vector; 35S promoter-eGFP-*att*R1-Cm^r-*ccd*B-*att*R2; Sm^r	(Karimi *et al.*, 2005)
pL6GW356	encoding AvrBs3Δ2; Tc^r	(Noël *et al.*, 2003)
pOGG2	den-gate-compatible derivative of pOK1; Sm^r	This study
pOK1	suic vector; *sacB sacQ mobRK2* oriR6K; Sm^r	(Huguet *et al.*, 1998)
pUGW14	Tran expression vector; 35S promoter-*att*R1-Cm^r-*ccd*B-*att*R2-3xHA; Ap^r	(Nakagawa *et al.*, 2007)
pUGW15	Transient expression vector; 35S promoter-3xHA-*att*R1-Cm^r-*ccd*B-*att*R2; Ap^r	(Nakagawa *et al.*, 2007)
Constructs		
pBIN20:ER-rk	Derivative of pBIN20 encoding ER-mCherry; Km^r	(Nelson *et al.*, 2007)
pBIN20:G-rk	Derivative of pBIN20 encoding Golgi-mCherry; Km^r	(Nelson *et al.*, 2007)
pBR356:xopB	Derivative of pBR356 encoding $XopB_{1-177}$-AvrBs3Δ2	This study
pBRM:xopB	Derivative of pBRM encoding XopB-c-Myc	This study
pBRM:$xopB_{A313V}$	Derivative of pBRM encoding $XopB_{A313V}$-c-Myc	This study
pBRM:xopS	Derivative of pBRM encoding XopS-c-Myc	This study
pDONR221:H2B	Derivative of pDONR221 containing *H2B* (At5g59910)	(Feilner *et al.*, 2005)
pDSF356	Derivative of pDSK602 containing *avrBs3Δ2*	(Szurek *et al.*, 2002)
pENTR/D:Atsyp121 sp2	Derivative of pENTR/D-TOPO containing *Atsyp121 sp2*	This study
pENTR/D:Atsyp21 sp2	Derivative of pENTR/D-TOPO containing *Atsyp21 sp2*	This study
pENTR/D:avrBs2	Derivative of pENTR/D-TOPO containing *avrBs2*	This study
pENTR/D:xopB	vative of pENTR/D-TOPO containing *xopB*	This study
pENTR/D:$xopB_{A313V}$	Derivative of pENTR/D-TOPO containing *$xopB_{A313V}$*	This study
pENTR/D:$xopB_{K455R}$	Derivative of pENTR/D-TOPO containing *$xopB_{K455R}$*	This study
pENTR/D:xopG	vative of pENTR/D-TOPO containing *xopG*	This study
pENTR/D:xopI	vative of pENTR/D-TOPO containing *xopI*	This study
pENTR/D:xopJ	vative of pENTR/D-TOPO containing *xopJ*	(Thieme *et al.*, 2007)
pENTR/D:$xopJ_{C235A}$	Derivative of pENTR/D-TOPO containing *$xopJ_{C235A}$*	This study
pENTR/D:xopK	vative of pENTR/D-TOPO containing *xopK*	This study
pENTR/D:xopM	vative of pENTR/D-TOPO containing *xopM*	This study
pENTR/D:xopR	vative of pENTR/D-TOPO containing *xopR*	This study
pENTR/D:xopS	vative of pENTR/D-TOPO containing *xopS*	This study
pENTR/D:xopV	vative of pENTR/D-TOPO containing *xopV*	This study
pGGA1:secGFP	Derivative of pGGA1 containing *sec*GFP	This study
pGWB2:avrBs1	Derivative of pGWB2 containing *avrBs1*	(Gürlebeck *et al.*, 2009)
pGWB2:avrBs2	Derivative of pGWB2 containing *avrBs2*	This study
pGWB5:avrBsT	Derivative of pGWB5 containing *avrBsT*	(Szczesny *et al.*, 2010a)
pGWB5:avrRxv	Derivative of pGWB5 containing *avrRxv*	This study
pGWB5:xopG	Derivative of pGWB5 containing *xopG*	This study
pGWB5:xopJ	Derivative of pGWB5 containing *xopJ*	(Thieme *et al.*, 2007)

pGWB5:xopK	Derivative of pGWB5 containing *xopK*	This study
pGWB5:xopM	Derivative of pGWB5 containing *xopM*	This study
pGWB5:xopV	Derivative of pGWB5 containing *xopV*	This study
pGWB17:Atsyp121_sp2	Derivative of pGWB17 containing *Atsyp121_Sp2*	This study
pGWB17:xopB	Derivative of pGWB17 containing *xopB*	This study
pGWB17:xopB$_{A313V}$	Derivative of pGWB17 containing *xopB$_{A313V}$*	This study
pGWB17:xopB$_{K455R}$	Derivative of pGWB17 containing *xopB$_{K455R}$*	This study
pGWB17:xopJ	Derivative of pGWB17 containing *xopJ*	This study
pGWB17:xopJ$_{C235A}$	Derivative of pGWB17 containing *xopJ$_{C235A}$*	This study
pK18:xopG	Derivative of pK18 carrying flanking regions of *xopG*	This study
pK18:xopI	Derivative of pK18 carrying flanking regions of *xopI*	This study
pK18:xopM	Derivative of pK18 carrying flanking regions of *xopM*	This study
pK7FWG2:xopB	Derivative of pK7FWG2 containing *xopB*	This study
pK7FWG2:xopB$_{A313V}$	Derivative of pK7FWG2 containing *xopB$_{A313V}$*	This study
pK7FWG2:xopB$_{K455R}$	Derivative of pK7FWG2 containing *xopB$_{K455R}$*	This study
pK7FWG2:xopI	Derivative of pK7FWG2 containing *xopI*	This study
pK7FWG2:xopS	Derivative of pK7FWG2 containing *xopS*	This study
pK7WGF2:xopR	Derivative of pK7WGF2 containing *xopR*	This study
pL6GW356:xopG	Derivative of pL6GW356 encoding XopG$_{1-100}$-AvrBs3Δ2	This study
pL6GW356:xopI	vative of pL6GW356 encoding XopI$_{1-140}$-AvrBs3Δ2	This study
pL6GW356:xopK	vative of pL6GW356 encoding XopK$_{1-87}$-AvrBs3Δ2	This study
pL6GW356:xopM	vative of pL6GW356 encoding XopM$_{1-520}$-AvrBs3Δ2	This study
pL6GW356:xopR	Derivative of pL6GW356 encoding XopR$_{1-152}$-AvrBs3Δ2	This study
pL6GW356:xopS	vative of pL6GW356 encoding XopS$_{1-157}$-AvrBs3Δ2	This study
pL6GW356:xopV	vative of pL6GW356 encoding XopG$_{1-187}$-AvrBs3Δ2	This study
pLAND:xopB	Derivative of pLAND containing *xopB*	This study
pLAND:xopB$_{A313V}$	Derivative of pLAND containing *xopB$_{A313V}$*	This study
pNHL10-LUC	Derivative of pFRK1-LUC vector, containing *pNHL10* instead of *pFRK1*	(Boudsocq *et al.*, 2010; Ranf *et al.*, 2011)
pOGG2:xopK	Derivative of pOGG2 carrying flanking regions of xopK	This study
pOGG2:xopR	Derivative of pOGG2 carrying flanking regions of *xopR*	This study
pOGG2:xopV	Derivative of pOGG2 carrying flanking regions of *xopV*	This study
pOK1:xopS	Derivative of pOK1 carrying flanking regions of *xopS*	This study
pUBQ10_GUS	Derivative of pUC119 encoding UBQ10::GUS	(Norris *et al.*, 1993)
pUGW14:xopB	Derivative of pUGW14 containing *xopB*	This study
pUGW14:xopB$_{A313V}$	Derivative of pUGW14 containing *xopB$_{A313V}$*	This study
pUGW14:xopS	Derivative of pUGW14 containing xopS	This study
pUGW15:H2B	Derivative of pUGW15 containing *H2B* (At5g59910)	This study

[a] Ap, ampicillin; Hm, hygromycin; Km, kanamycin; Rif, rifampicin; Sm, spectinomycin; Tc, tetracycline, r, resistant.

[b]Reference

Boudsocq M, Willmann MR, McCormack M, Lee H, Shan L, He P, Bush J, Cheng SH, Sheen J. 2010. Differential innate immune signalling via Ca(2+) sensor protein kinases. *Nature* **464**(7287): 418-422.

Büttner D, Gürlebeck D, Noël LD, Bonas U. 2004. HpaB from *Xanthomonas campestris* pv. *vesicatoria* acts as an exit control protein in type III-dependent protein secretion. *Molecular Microbiology* **54**(3): 755-768.

Canteros BJ. 1990. Diversity of plasmids and plasmid-encoded phenotypic traits in *Xanthomonas campestris* pv. *vesicatoria*. *Ph.D. thesis. University of Florida, Gainesville.*

Feilner T, Hultschig C, Lee J, Meyer S, Immink RGH, Koenig A, Possling A, Seitz H, Beveridge A, Scheel D, Cahill DJ, Lehrach H, Kreutzberger J, Kersten B. 2005. High throughput identification of potential Arabidopsis mitogen-activated protein kinases substrates. *Molecular & Cellular Proteomics* **4**(10): 1558-1568.

Gürlebeck D, Jahn S, Gürlebeck N, Szczesny R, Szurek B, Hahn S, Hause G, Bonas U. 2009. Visualization of novel virulence activities of the *Xanthomonas* type III effectors AvrBs1, AvrBs3 and AvrBs4. *Molecular Plant Pathology* **10**(2): 175-188.

Huguet E, Hahn K, Wengelnik K, Bonas U. 1998. *hpaA* mutants of *Xanthomonas campestris* pv. *vesicatoria* are affected in pathogenicity but retain the ability to induce host-specific hypersensitive reaction. *Molecular Microbiology* **29**(6): 1379-1390.

Karimi M, De Meyer B, Hilson P. 2005. Modular cloning and expression of tagged fluorescent protein in plant cells. *Trends in Plant Science* **10**(3): 103-105.

Koncz C, Schell J. 1986. The promoter of TL-DNA gene *5* controls the tissue-specific expression of chimeric genes carried by a novel type of *Agrobacterium* binary vector. *Molecular and General Genetics* **204**(3): 383-396.

Lorenz C, Büttner D. 2009. Functional characterization of the type III secretion ATPase HrcN from the plant pathogen *Xanthomonas campestris* pv. *vesicatoria*. *Journal of Bacteriology* **191**(5): 1414-1428.

Ménard R, Sansonetti PJ, Parsot C. 1993. Nonpolar mutagenesis of the *ipa* genes defines IpaB, IpaC, and IpaD as effectors of *Shigella flexneri* entry into epithelial cells. *Journal of Bacteriology* **175**: 5899-5906.

Minsavage GV, Dahlbeck D, Whalen MC, Kearney B, Bonas U, Staskawicz BJ, Stall RE. 1990. Gene-for-gene relationships specifying disease resistance in *Xanthomonas campestris* pv. *vesicatoria*-pepper interactions. *Molecular Plant-Microbe Interactions* **3**(1): 41-47.

Murillo J, Shen H, Gerhold D, Sharma A, Cooksey DA, Keen NT. 1994. Characterization of pPT23B, the plasmid involved in syringolide production by *Pseudomonas syringae* pv. *tomato* PT23. *Plasmid* **31**(3): 275-287.

Nakagawa T, Takayuki K, Hino T, Tanaka K, Kawamukai M, Niwa Y, Toyooka K, Matsuoka K, Jinbo T, Kimura T. 2007. Development of series of Gateway binary vectors, pGWBs, for realizing efficient construction of fusion genes for plant transformation. *Journal of Bioscience and Bioengineering* **104**: 34-41.

Nelson BK, Cai X, Nebenführ A. 2007. A multicolored set of in vivo organelle markers for co-localization studies in Arabidopsis and other plants. *Plant Journal* **51**(6): 1126-1136.

Noël L, Thieme F, Gäbler J, Büttner D, Bonas U. 2003. XopC and XopJ, two novel type III effector proteins from *Xanthomonas campestris* pv. vesicatoria. *Journal of Bacteriology* **185**(24): 7092-7102.

Noël L, Thieme F, Nennstiel D, Bonas U. 2001. cDNA-AFLP analysis unravels a genome-wide *hrpG*-regulon in the plant pathogen *Xanthomonas campestris* pv. *vesicatoria*. *Molecular Microbiology* **41**: 1271–1281.

Norris SR, Meyer SE, Callis J. 1993. The intron of *Arabidopsis thaliana* polyubiquitin genes is conserved in location and is a quantitative determinant of chimeric gene expression. *Plant Molecular Biology* **21**(5): 895-906.

Ranf S, Eschen-Lippold L, Pecher P, Lee J, Scheel D. 2011. Interplay between calcium signalling and early signalling elements during defence responses to microbe- or damage-associated molecular patterns. *Plant Journal* **68**(1):100-113.

Rossier O, Wengelnik K, Hahn K, Bonas U. 1999. The *Xanthomonas* Hrp type III system secretes proteins from plant and mammalian bacterial pathogens. *Proceedings of the National Academy of Sciences, USA* **96**: 9368-9373.

Schäfer A, Tauch A, Jager W, Kalinowski J, Thierbach G, Pühler A. 1994. Small mobilizable multi-purpose cloning vectors derived from the *Escherichia coli* plasmids pK18 and pK19: selection of defined deletions in the chromosome of Corynebacterium glutamicum. *Gene* **145**(1): 69-73.

Szczesny R, Büttner D, Escolar L, Schulze S, Seiferth A, Bonas U. 2010a. Suppression of the AvrBs1-specific hypersensitive response by the YopJ effector homolog AvrBsT from *Xanthomonas* depends on a SNF1-related kinase. *New Phytologist* **187**(4): 1058-1074.

Szczesny R, Jordan M, Schramm C, Schulz S, Cogez V, Bonas U, Büttner D. 2010b. Functional characterization of the Xcs and Xps type II secretion systems from the plant pathogenic bacterium *Xanthomonas campestris* pv. *vesicatoria*. *New Phytologist* **187(4)**: 9

Szurek B, Rossier O, Hause G, Bonas U. 2002. Type III-dependent translocation of the *Xanthomonas* AvrBs3 protein into the plant cell. *Molecular Microbiology* **46**(1): 13-23.

Thieme F, Szczesny R, Urban A, Kirchner O, Hause G, Bonas U. 2007. New type III effectors from *Xanthomonas campestris* pv. *vesicatoria* trigger plant reactions dependent on a conserved N-myristoylation motif. *Molecular Plant-Microbe Interactions* **20**(10): 1250-1261.

Wengelnik K, Rossier O, Bonas U. 1999. Mutations in the regulatory gene *hrpG* of *Xanthomonas campestris* pv. *vesicatoria* result in constitutive expression of all *hrp* genes. *Journal of Bacteriology* **181**(21): 6828-6831.

Table S2 Oligonucleotides used in this study

Name	Sequence (5´- 3´)	Purpose
xJ-fe	CACCATGGGTCTATGCGTTTCA	generation of pENTR/DxopJ$_{C235A}$
xJmC-f	CACAGAAGTCTGCAGCGGACGCC	generation of *xopJ$_{C235A}$* (SOE-PCR)
xJmC-r	ATGCAGATCGAACATCAGGGC	generation of *xopJ$_{C235A}$* (SOE-PCR)
xJ-rsl	TGACTGGCGATCAGAGATAGCTGTC	generation of pENTR/DxopJ$_{C235A}$
Arxv-fe	CACCATGTGCGACTCCATAAGAGTG	generation of pENTR/Davrrxv
Arxv.rsl	GGATTCTAAGGCGTGACGGA	generation of pENTR/Davrrxv
xopB_start	CACCATGAAGGCAGAGCTCAC	generation of pENTR/DxopB
xopB_rev	CGGCTCAGGCGCGGGTTGGTGCG	generation of pENTR/DxopB
xopG_start	CACCATGCCAATCAGTCAAAC	generation of pENTR/DxopG
xopG_rev	CATGCCGTGAGGCTTATATT	generation of pENTR/DxopG
xopI_start	CACCATGCCGATCACCCGAAC	generation of pENTR/DxopI
xopI_rev	CATGTCCATATACCTGCGCGACAC	generation of pENTR/DxopI
K_entry_for	CACCATGCGTGTCCAACGATCCACTG	generation of pENTR/DxopK
K_entry_rev	GGCCGTGGACGCAGGGGCCACGGC	generation of pENTR/DxopK
0442 ENTR-ATG	CACCATGACGAAGATCTCTTCAGCCAGTACC	generation of pENTR/DxopM
0442-R2	CTCAGTTCGCGTGCGAGCGCCCTCG	generation of pENTR/DxopM
0285_start	CACCATGCGCCTGACTTCGTTC	generation of pENTR/DxopR
0285_rev	ATAGCCGTTGTTGATCGCCTC	generation of pENTR/DxopR
0324_start	CACCATGGGAGATGTACAAATG	generation of pENTR/DxopS
0324_rev	AGAAATGCCATCGCTGG	generation of pENTR/DxopS
xopV_entry_for	CACCATGAAGATCTCCGGCTCGGCGTCT	generation of pENTR/DxopV
xopV_entry_rev	TTCACCGCTTGGGCTAGGATGCGC	generation of pENTR/DxopV
SYP121_Sp2 fwd	CACCATGAACGATTTGTTTTCCAGCTCATTC	generation of pENTR/DAtsyp121sp2
SYP121_Sp2 rev_no stop	ACATGTCCATTTTCGCGTGTTC	generation of pENTR/DAtsyp121sp2
ab2for	CACCATGCGTATCGGTCCTCTG	generation of pENTR/DavrBs2
ab2rev	TCAATCCGTCTCCGTCTGCCT	generation of pENTR/DavrBs2
secGFP_for	TTTGGTCTCTTATGAAGACTAATCTTTTTCTCTTTCT CATCTTTTCACTTCTCCTATCATTATCCTCGGCC	generation of pGGA1secGFP
secGFP_rev	TTTGGTCTCTCACCGGCCGAGGATAATGATAGGAGAA GTGAAAAGATGAGAAAGAGAAAAAGATTAGTCTTCAT	generation of pGGA1secGFP
XopS_BsaI_for	GCCGGTCTCTTATGGGAGATGTACAAATG	generation of pBRMxopS
XopS_BsaI_rev	ACAGGTCTCTCACCAGAAATGCCATCGC	generation of pBRMxopS
dxopI_a_for	ACTAAGCTTCAGAGCTGCCTGGTGCGTTG	generation of pK18xopI
dxopI_a_rev	TAGAATTCCATCTCGGGTCTCCTGCGGTG	generation of pK18xopI
dxopI_b_for	CGGAATTCTGAGCACTGTTTGATTGAGTG	generation of pK18xopI
dxopI_b_rev	ATAGGATCCAATGCGCGCAGCGTTGCAAC	generation of pK18xopI
0442 F1	AAAGAATTCGGATTATGTCTTGAGTCCGGCAGCAAAC C	generation of pK18xopM
0442 R1	AAATCTAGAGGCTTGTCCTCGCGTTGG	generation of pK18xopM
0442 F2	AAATCTAGAGCGTGGCCGCGCCTGGCG	generation of pK18xopM
0442 R2	GGGAAGCTTGGCAGTGGGAGGCCTCGTCC	generation of pK18xopM

dxopV_left_for	TTTGGTCTCTCGACACTTGCCGGTGCCGTGCCC	generation of pOGG2xopV
dxopV_left_rev	TTTGGATCCTCCACCGTCCACGCGCAT	generation of pOGG2xopV
dxopV_right_for	TTTCCTAGGGCGCGTACTCCTAGAATGCGTGA	generation of pOGG2xopV
dxopV_right_rev	TTTGGTCTCTATGGGTTTACGGCCGCTGATGC	generation of pOGG2xopV
dxopR_left_for	TTTGGTCTCTCGACCAGTAAGTGTTATATAGT	generation of pOGG2xopR
dxopR_left_rev	TTTGGATCCGCGCGTCGTCGTTGCGCGCAAAG	generation of pOGG2xopR
dxopR_right_for	TTTCCTAGGCACAAACTCCCGCGGGAATGCAC	generation of pOGG2xopR
dxopR_right_rev	TTTGGTCTCTATGGCCCATGCATTTTCTGCTGTTT	generation of pOGG2xopR
dXopS_5for	GATAAGCTTGCTTTTCTAAAGCATAGGC	generation of pOK1xopS
dXopS_5rev	ATCGTCGACGCAGTGCACCGTGCCGCAT	generation of pOK1xopS
dXopS_3for	GATAAGCTTAGAGCGAGCCCGCAGAGT	generation of pOK1xopS
dXopS_3rev	CTGTCTAGACATCTGTTCCAGATATGCC	generation of pOK1xopS
xopB_pLAND_for	TTTGGTCTCTTATGAAGGCAGAGCTCACACGATCC	generation of pLANDxopB,pLANDxopB$_{A313V}$ and pBR356xopB
xopB_pLAND_rev	TTTGGTCTCTGGTGCGGCTCAGGCGCGGGTTG	generation of pLANDxopB and pLANDxopB$_{A313V}$
0442_ENTR_999 F	CACCCAGCAAACCGATCAAACTCGCC	generation of pENTR/DxopM+promoter
0442-R2	CTCAGTTCGCGTGCGAGCGCCCTCG	generation of pENTR/DxopM+promoter
xol2fusfw	CACCTGCGAGCGCTTCCTTCAGCAG	generation of pENTR/DxopG+promoter
xol2fusrev	TGCTCTTTCCATAGCGAGCGCTTG	generation of pENTR/DxopG+promoter
xol6fusfw	CACCCGTTCTTCAACCAGTTGCGTG	generation of pENTR/DxopI+promoter
xol6fusrev	CGCTGCAAGCCTTCCGTATC	generation of pENTR/DxopI+promoter
3215-1008 F	CACCGCTATCGGGATGGCATC	generation of pENTR/DxopK+promoter
3215-R	CACGTACTTGGCGACCACGAA	generation of pENTR/DxopK+promoter
0285-998 F	CACCTGCCTGCACACTTCGTT	generation of pENTR/DxopR+promoter
0285-456 R	AAAGCGTTCTGACGCGCGTG	generation of pENTR/DxopR+promoter
0324-1041 F	CACCGCTGTTACCGCAGTGCAC	generation of pENTR/DxopS+promoter
0324-R	CAGCGATATAGCTACCTTC	generation of pENTR/DxopS+promoter
657_p_fw	CACCGAATGCCGACGACCGACGCCAC	generation of pENTR/DxopV+promoter
657_rev	TCCGCGGAACGTCGGGGTGCTC	generation of pENTR/DxopV+promoter
XopB177-Bsarev	TTTGGTCTCTGATCTGTCCGCTCTGAGGAGTTG	generation of pBR356xopB
xopB_RT_for	ATTACGTCGATTACGGCTCAG	RT-PCR on xopB
xopB_RT_rev	CGACAACCGAAGCGGCCATC	RT-PCR on xopB
RTxol6fw	CTGGGATGCTTGCCCGAGGAC	RT-PCR on xopI
RTxol6rev	GAAGGCAGCCTGGCGCACTC	RT-PCR on xopI
RT_xopG forward	CAGCGCTTGAGAAGATTGCAG	RT-PCR on xopG

RT_xopG reverse	CCATGTTCCTGCCTGATGGAG	RT-PCR on xopG
xK-rtf/rob	GATCGAGACCAACGCCTACCTGCAG	RT-PCR on xopK
xK-rtr/rob	GATGCGCAAAGCGGTCGTACTTG	RT-PCR on xopK
0442_1197F	GGTGAACGCGGCCTTGAATGTC	RT-PCR on xopM
0442_1401R	CAAACCGAGCCAGGTGCCAATC	RT-PCR on xopM
xcv0324fw	TGCATGGCACCGCCGAAGCGTC	RT-PCR on xopS
xcv0324rev	ATCGTTCGCTTTTGCAAGATG	RT-PCR on xopS
xcv0657fw	GCGACATGCCCCAGCGGTGTG	RT-PCR on xopV
xcv0657rev	ATGACCAAGCTGCCATTGCTG	RT-PCR on xopV

SUPPORTING INFORMATION FIGS S1-S8

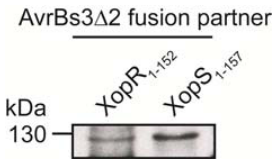

Fig. S1 XopR- and XopS-AvrBs3Δ2 fusion proteins are expressed in *Xcv* 85*Δ*hpaB*. Strains 85*Δ*hpaB* ectopically expressing $XopR_{1-152}$- and $XopS_{1-157}$-AvrBs3Δ2 fusions were grown in minimal medium A. Numbers correspond to the amino acids fused to AvrBs3Δ2. Total cell extracts were analyzed by immunoblotting using an AvrBs3-specific antibody.

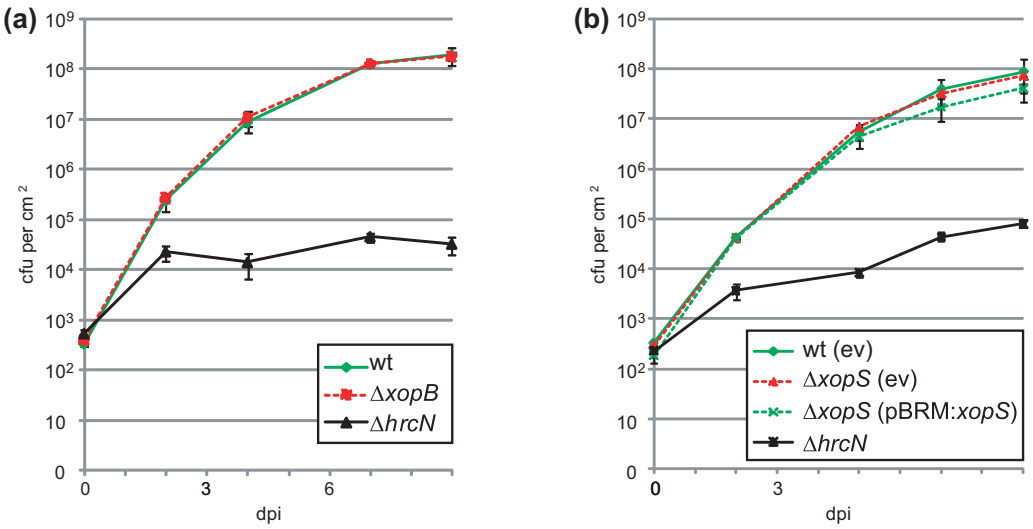

Fig. S2 Individual deletion of *xopB* and *xopS* has no influence on bacterial growth. (a) Bacterial growth of *Xcv* strains 85-10, 85-10Δ*xopB* (Δ*xopB*) and the T3S mutant 85-10Δ*hrcN* (Δ*hrcN*) in leaves of susceptible pepper ECW. Bacterial multiplication was monitored over a period of nine days. Values represent the mean of three samples from three different plants. Error bars indicate standard deviations. (b) Bacterial growth of *Xcv* strains 85-10 and 85-10Δ*xopS* (Δ*xopS*) containing the empty vector (ev) and pBRM:xopS, respectively, in pepper ECW. The experiment was performed as described in panel a). All experiments were performed at least three times with similar results.

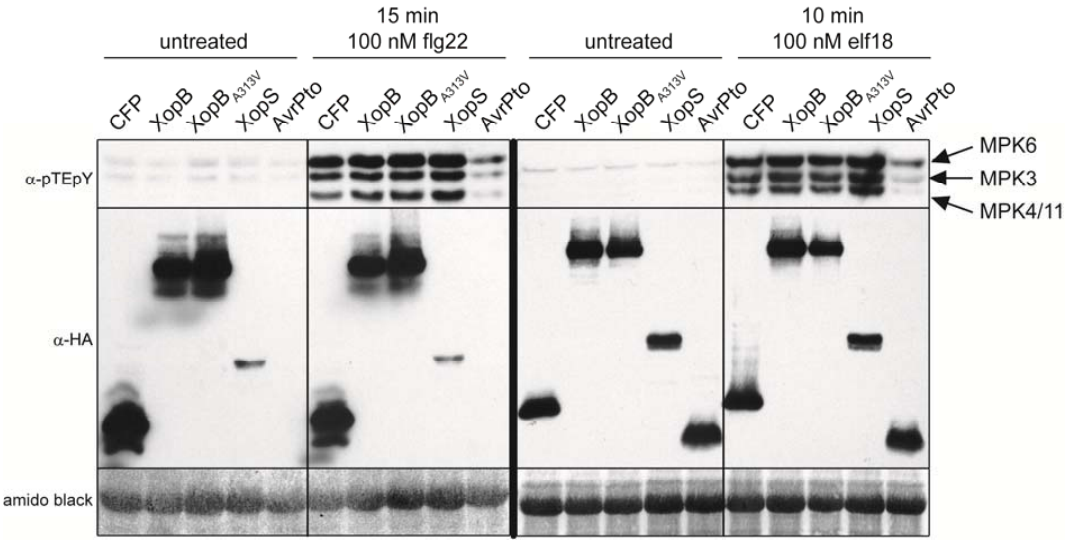

Fig. S3 XopB and XopS do not suppress MAPK activation in Arabidopsis. Protoplasts derived from *A. thaliana* Col-0 were transformed with *p35S-xopB, p35S-xopB*$_{A313V}$*, p35S-xopS* or *p35S-avrPto and p35S-CFP* as positive and negative control, respectively. 14 h after transformation, protoplasts were treated with 100 nM flg22 or elf18 and samples were taken 15 and 10 min later, respectively. Immunoblots were reacted with anti-pTEpY (specific for activated MAP kinases) and HA-specific antibodies (for the epitope-tagged effector proteins). In the experiment using flg22, *avrPto* was expressed without tag. Amido black staining of the large subunit of Rubisco was used as an estimate of equal protein loading. The experiments were performed three times with similar results. MPK3, 4, 6, 11 = mitogen-activated protein kinase 3, 4, 6, 11.

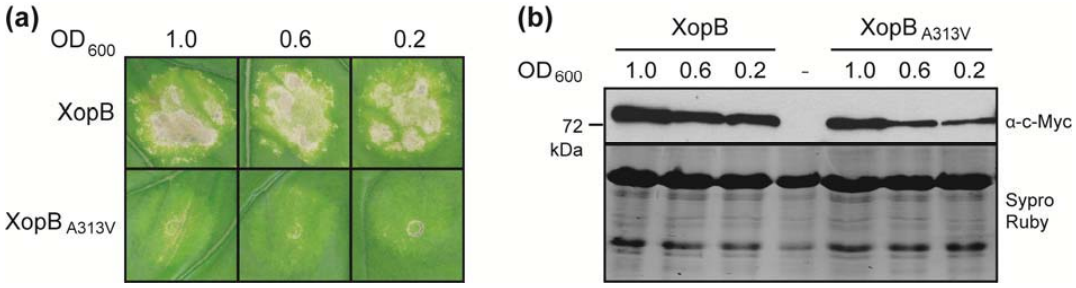

Fig. S4 $XopB_{A313V}$ is impaired in cell death induction. (a) *N. benthamiana* leaves were inoculated with a dilution series of *Agrobacterium* mediating transfer of T-DNA encoding XopB::c-Myc and $XopB_{A313V}$::c-Myc, respectively. OD 1.0 corresponds to 10^9 cfu ml^{-1}, OD_{600}=0.6 to 6×10^8 cfu ml^{-1} and OD_{600}=0.2 to 2×10^8 cfu ml^{-1}. Photographs were taken six dpi. (b) Expression of XopB- and $XopB_{A313V}$-c-Myc fusions *in planta*. Leaves of *N. benthamiana* plants were inoculated as described in (a). Samples of infected (XopB and $XopB_{A313V}$) and uninfected (-) leaf material were analyzed 24 hpi by immunobloting using a c-Myc-specific antibody. To check protein amounts, the SDS-gel was stained with Sypro Ruby solution (BioRad, Hercules, CA, U.S.A.) prior to immunoblotting. The experiments were repeated twice with similar results.

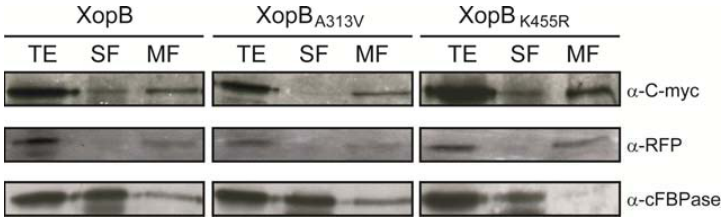

Fig. S5 XopB is associated with the membrane fraction of plant cells. *N. benthamiana* leaves were co-inoculated with *Agrobacterium* strains delivering T-DNA encoding XopB::c-Myc, $XopB_{A313V}$::c-Myc and $XopB_{K455R}$::c-Myc, respectively, with *Agrobacterium* delivering T-DNA encoding Golgi-mCherry. Leaves were harvested two dpi, and total protein extracts were fractionated by ultracentrifugation. Equal volumes of individual fractions representing approximately equal protein amounts were analyzed for the presence of XopB::c-Myc and mutant derivatives and mCherry by immunoblotting using c-Myc- and RFP-specific antibodies, respectively. As control, the blot was reacted with a specific antibody for the cytosolic fructose-1,6-bisphosphatase (cFBPase). TE, total extract; SF, soluble fraction; MF, membrane fraction. The experiments were repeated twice with similar results.

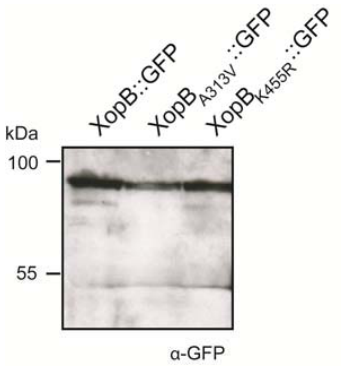

Fig. S6 Expression of *GFP* and *xopB-GFP* fusions in *N. benthamiana*. *N. benthamiana* leaves were co-inoculated with *Agrobacterium* strains mediating delivery of T-DNAs encoding XopB::GFP, XopB$_{A313V}$-GFP, XopB$_{K455R}$-GFP and GFP, respectively, and T-DNA encoding Golgi-mCherry. Infected tissue was harvested 20 hpi. Expression of the effector-GFP fusions was analyzed by immunoblotting using a GFP-specific antibody. The experiments were repeated twice with similar results.

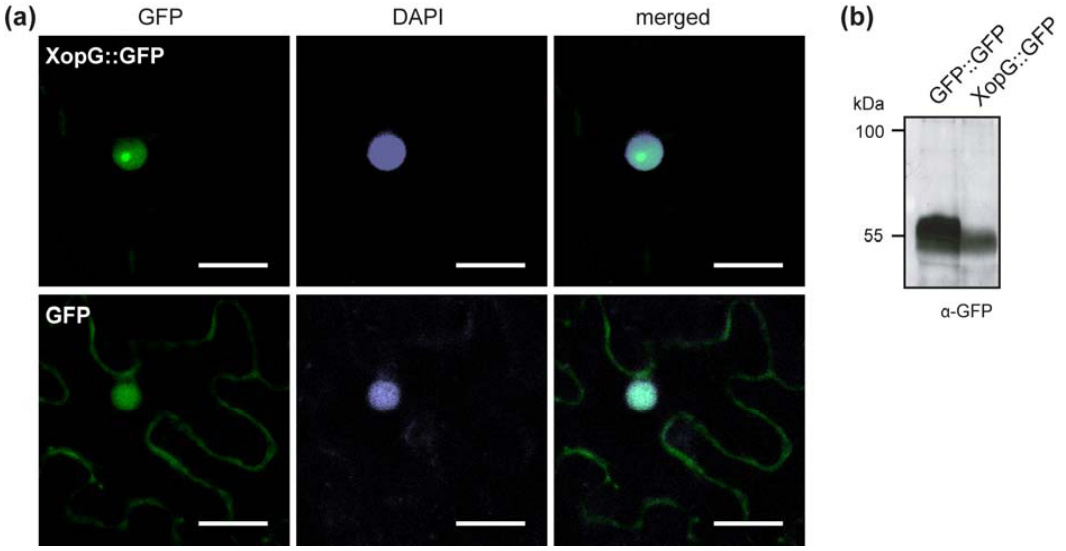

Fig. S7 Subcellular localization of XopG::GFP. (a) Confocal laser scanning microscopy of *N. benthamiana* leaves 18 h after *Agrobacterium*-mediated delivery of *GFP::GFP* and *xopG::GFP*, respectively. 4′,6′-Diamidino-2-phenylindole (DAPI) staining indicates nuclei. Size bars correspond to 5 µm. (b) *N. benthamiana* leaves were inoculated as in (a). Infected tissue was harvested 18 hpi and analyzed by immunoblotting using a GFP-specific antibody. The experiments were repeated twice with similar results.

Confocal laser scanning microscopy revealed a localization of XopG::GFP exclusively to the plant cell nucleus at early time points (18 hpi) after inoculation. However, degradation of XopG::GFP occurred 20-22 hpi leading to fluorescence in the cytoplasm (data not shown).

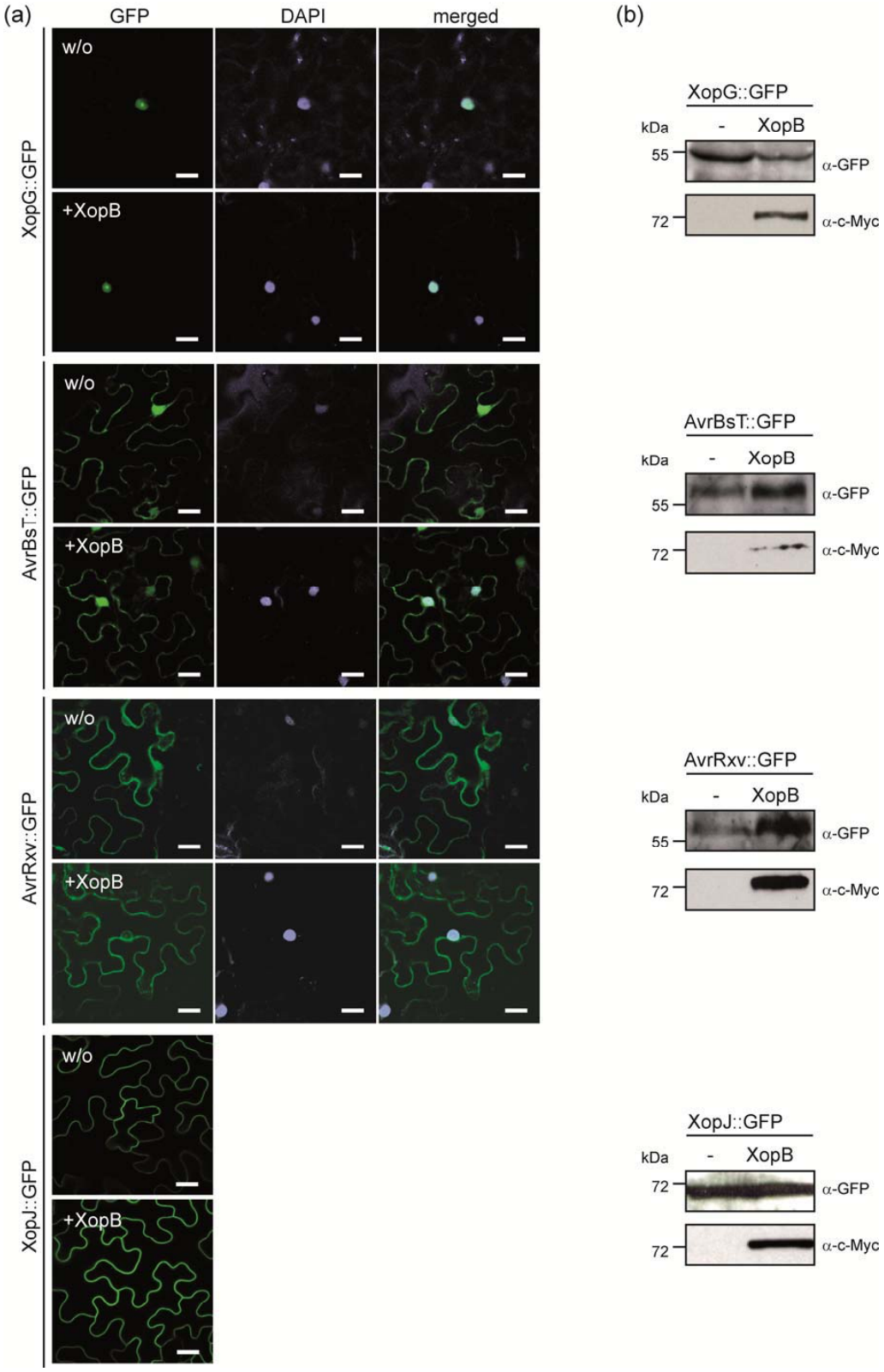
(a)
GFP
DAPI
merged
XopG::GFP
w/o
+XopB
AvrBsT::GFP
w/o
+XopB
AvrRxv::GFP
w/o
+XopB
XopJ::GFP
w/o
+XopB
(b)
XopG::GFP
kDa
-
XopB
55
α-GFP
72
α-c-Myc
AvrBsT::GFP
kDa
-
XopB
55
α-GFP
72
α-c-Myc
AvrRxv::GFP
kDa
-
XopB
55
α-GFP
72
α-c-Myc
XopJ::GFP
kDa
-
XopB
72
α-GFP
72
α-c-Myc

Fig. S8 Subcellular localization of XopG, AvrBsT, AvrRxv and XopJ is not affected by co-expression of XopB. *Agrobacterium* strains mediating expression of XopB::c-Myc, XopG::GFP, AvrbsT::GFP, AvrRxv::GFP and XopJ::GFP were inoculated in leaves of *N. benthamiana*. For co-expression, bacterial suspensions were mixed prior to inoculation. a) Confocal laser-scanning microscopy of inoculated leaf tissue 22 hpi. DAPI staining indicates nuclei. Size bars correspond to 20 µm. b) Expression of effector genes *in planta*. Inoculation of *N. benthamiana* was carried out as described in (a). Tissue was harvested 22 hpi and analyzed by immunolotting using GFP- and c-Myc-specific antibodies. The experiments were repeated twice with similar results.

2.2.1.2 Zusammenfassung der Ergebnisse

In der vorangegangenen Publikation wurden sechs neue T3E (XopI, XopK, XopM, XopR, XopS und XopV) des Stamms *Xcv* 85-10 identifiziert und zusammen mit zwei weiteren Effektoren (XopB und XopG) analysiert. Die Typ III-vermittelte Sekretion und Translokation der T3E in die Pflanzenzelle konnte mit Hilfe des Reporters AvrBs3Δ2 gezeigt werden. Des Weiteren wurde die Translokation in Abhängigkeit vom generellen Typ III-Chaperon HpaB untersucht. Basierend auf diesen Daten wurden die T3E in zwei Klassen unterteilt. Klasse A umfasst Effektoren, die in Abwesenheit von HpaB nicht mehr transloziert werden (XopR und XopS), während Klasse B-Effektoren auch in Abwesenheit von HpaB in die Pflanzenzelle transloziert werden (XopB, XopG, XopI, XopK, XopM, XopV). Alle Effektorgene, außer *xopG* das konstitutiv exprimiert wird, werden abhängig von den Regulatoren des T3S-Systems exprimiert.

Um einen möglichen Beitrag der T3E zur Virulenz von *Xcv* zu untersuchen, wurden Deletionen der einzelnen Effektoren im *Xcv*-Stamm 85-10 erstellt und in Virulenzanalysen *in planta* untersucht. Die Deletionen von *xopG*, *xopI*, *xopK*, *xopM*, *xopR* oder *xopV* hatte im Vergleich zum *Xcv*-Wildtyp-Stamm keinen Einfluss auf die Ausbildung von Krankheitssymptomen nach Inokulation der entsprechenden Stämme in suszeptible Paprikapflanzen. Der Verlust von *xopB* oder *xopS* führte hingegen zu deutlich reduzierten Symptomen, jedoch nicht zu verändertem Wachstum dieser *Xcv*-Stämme in Paprikapflanzen. Stamm 85-10 mit einer Doppeldeletion von *xopB* und *xopS* zeigte hingegen ein geringeres bakterielles Wachstum als der Wildtyp-Stamm, was auf eine redundante Funktion beider Effektoren hinweist.

Dies konnte bestätigt werden: sowohl XopB als auch XopS unterdrückten die Expression pflanzlicher Gene, die an der Immunantwort der PTI beteiligt sind. Beide Effektoren greifen dabei wahrscheinlich nicht in die Erkennung von PAMPs und der daraus resultierenden Signalweiterleitung über MAP-Kinasen ein, da die flg22-induzierte Aktivierung von MAPK-Kaskaden in Gegenwart von XopB und XopS unverändert war.

Des Weiteren supprimiert XopB die durch XopG, XopJ, AvrBsT und AvrRxv induzierten Zelltodreaktionen *in planta*, sowohl nach *Agrobacterium*-vermittelter transienter Koexpression (*xopG*, *xopJ*, *avrBsT* und *avrRxv*), als auch bei Überexpression von *xopB* im *Xcv*-Stamm 75-3, welcher natürlicherweise AvrBsT kodiert. Die Koexpression von *xopB* führte dabei aber nicht zu einer veränderten Lokalisation der Zelltod-auslösenden T3E.

Das Derivat $XopB_{A313V}$ konnte die oben genannten Zelltodreaktionen nicht unterdrücken, supprimierte aber noch die PAMP-induzierte Pflanzenabwehr. XopB und $XopB_{A313V}$ sind im Zytoplasma und Golgi-System der Pflanze lokalisiert und manipulieren die pflanzliche Proteinsekretion. Diese Ergebnisse lassen schlussfolgern, dass die Suppression der PAMP- und Effektor-induzierten Abwehrreaktionen durch XopB auf unterschiedlichen Mechanismen beruht.

2.2.2 Ergänzende Ergebnisse

2.2.2.1 Charakterisierung einzelner Typ III-Effektoren hinsichtlich ihres Beitrags zur Virulenz von *Xcv*

2.2.2.1.1 Generierung von Δ*avrBs2*-Mutanten

Die Deletion von Effektor-kodierenden Genen hat oftmals keinen Einfluss auf die Virulenz von *Xcv*. Zum Einen liegt dies wahrscheinlich an der funktionellen Redundanz der Effektoren (Büttner und Bonas, 2010), zum Anderen könnte ein schwacher Einfluss auf die bakterielle Virulenz makroskopisch nicht erkennbar sein. Deshalb sollte neben den bereits deletierten T3E zusätzlich *avrBs2* deletiert werden. Der T3E AvrBs2 ist in vielen *Xanthomonas* spp. konserviert und löst in resistenten *Bs2*-Pflanzen die HR aus (Minsavage *et al.*, 1990). In anfälligen Pflanzen, die das Resistenzgen *Bs2* nicht besitzen, trägt AvrBs2 erheblich zur Virulenz und Fitness von *Xanthomonas* bei (Kearney und Staskawicz, 1990; Wichmann und Bergelson, 2004).

Daher wurde in dieser Arbeit *avrBs2* in den Genomen der *Xcv*-Stämme 85-10 (Abb. 2-1 a) und 82-8 (Abb. 2-1 b) deletiert. Hierfür wurden Fragmente, die stromaufwärts und stromabwärts von *avrBs2* liegen, per PCR an genomischer DNA von *Xcv* mit spezifischen Primern amplifiziert (s. Anhang). Die Fragmente wurden in den Vektor pOKI (Huguet *et al.*, 1998) kloniert und das daraus resultierende Konstrukt in die Stämme *Xcv* 85-10 und 82-8 konjugiert. Die selektierten Mutanten wurden anschließend mittels PCR identifiziert. Der Stamm 82-8Δ*avrBs2* wurde bereits in früheren Arbeiten charakterisiert (Kearney und Staskawicz, 1990; Minsavage *et al.*, 1990) und wurde in dieser Arbeit als Kontrolle generiert.

Anfällige Paprikapflanzen (ECW) zeigten deutlich reduzierte Krankheitssymptome nach Inokulation von 85-10Δ*avrBs2* bzw. 82-8Δ*avrBs2* im Vergleich zu den entsprechenden Wildtyp-Stämmen (Abb. 2-1). In resistenten Paprikapflanzen (ECW-20R) lösten die *avrBs2*-Mutanten im Gegensatz zum Wildtyp-Stamm keine HR aus (Abb. 2-1). Die Phänotypen der *avrBs2*-Mutanten konnten durch ektopische Expression von *avrBs2* komplementiert werden. Diese Ergebnisse stehen im Einklang mit bereits publizierten Daten (Kearney und Staskawicz, 1990; Minsavage *et al.*, 1990). Der *Xcv*-Stamm 85-10Δ*avrBs2* diente als Ausgangsstamm für die Erstellung weiterer T3E-Deletionsmutanten.

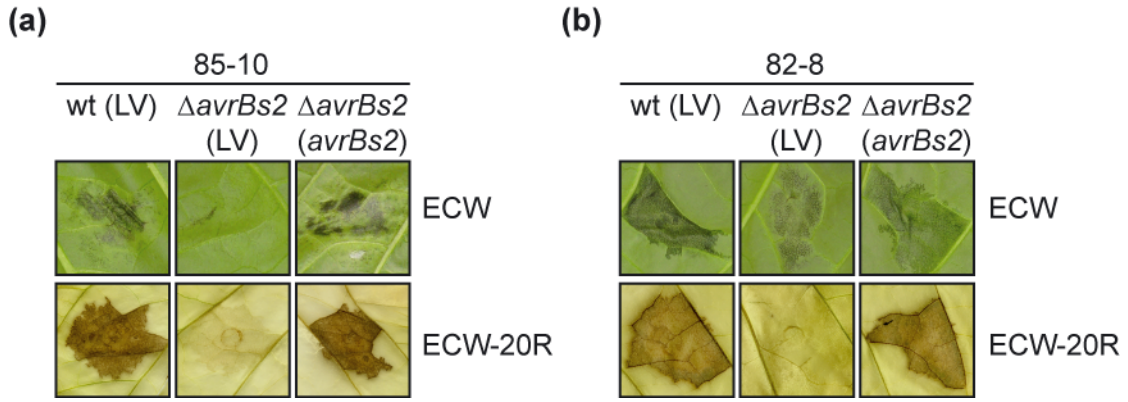

Abbildung 2-1: Analyse der *Xcv*-Stämme 85-10Δ*avrBs2* und 82-8Δ*avrBs2*.
Blätter von anfälligen (ECW) bzw. AvrBs2-responsiven Paprikapflanzen (ECW-20R) wurden mit den Stämmen **(a)** *Xcv* 85-10 (wt) und 85-10Δ*avrBs2*(Δ*avrBs2*) bzw. **(b)** 82-8 (wt) und 82-8Δ*avrBs2*(Δ*avrBs2*) mit einer bakteriellen Dichte von $4x10^8$ KBE/ml inokuliert. Die Stämme tragen den Leervektor pLAFR3 (LV; Staskawicz *et al.*, 1987) oder pLAFR3:avrBs2 (*avrBs2;* Minsavage *et al.*, 1990). Die Phänotypen wurden 4 d nach Inokulation dokumentiert. ECW-20R-Blätter wurden zur besseren Visualisierung der HR in Ethanol gebleicht. Die Experimente wurden zweimal mit ähnlichen Ergebnissen reproduziert.

2.2.2.1.2 Analyse von Mehrfach-Effektormutanten in *Xcv* 85-10Δ*avrBs2*

Die Deletion der Effektorgene *xopK*, *xopR* oder *xopV* hatte keinen makroskopisch sichtbaren Einfluss auf den Krankheitsverlauf nach *Xcv*-Infektion in Paprikapflanzen (Schulze *et al.*, 2012). Um zu untersuchen, ob schwache Virulenzeffekte der T3E eventuell maskiert werden, wurden *xopK*, *xopR* oder *xopV* auch im Stamm *Xcv* 85-10Δ*avrBs2* deletiert. Infektionsstudien in suszeptiblen sowie resistenten Paprikapflanzen ergaben jedoch keine Unterschiede der AvrBs2-Effektor-Doppelmutanten im Vergleich zu 85-10Δ*avrBs2* (Abb. 2-2 a-c). Diese Ergebnisse deuten darauf hin, dass andere Effektoren wahrscheinlich funktionell ähnliche Aufgaben wie XopK, XopR und XopV übernehmen und deshalb kein Beitrag dieser T3E zur Virulenz von *Xcv* beobachtet werden konnte.

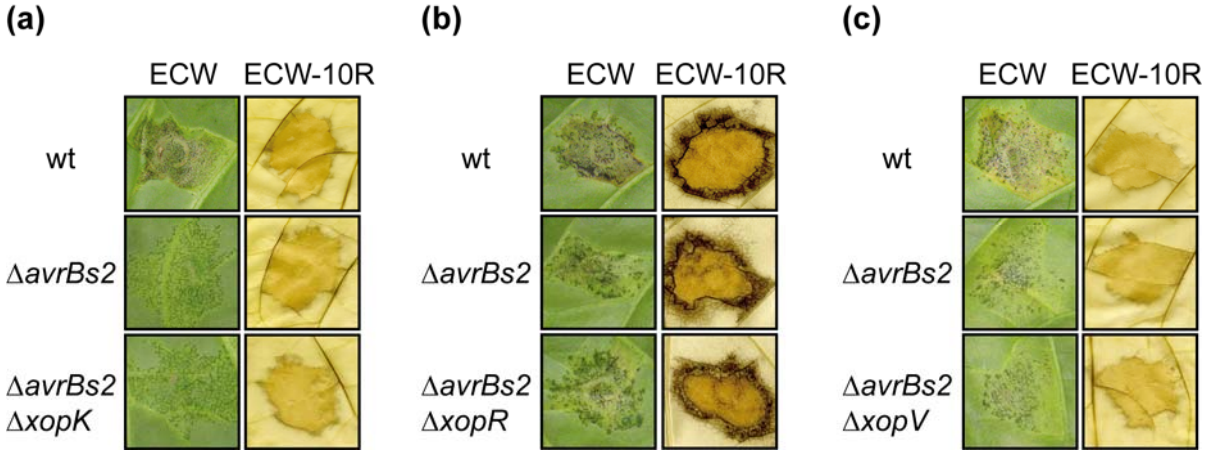

Abbildung 2-2: Phänotypenanalyse nach Inokulation von Effektormutanten in *Xcv* 85-10Δ*avrBs2*.
Die Stämme *Xcv* 85-10 (wt), *Xcv* 85-10Δ*avrBs2* (Δ*avrBs2*), **(a)** 85-10Δ*avrBs2*Δ*xopK* (Δ*avrBs2*Δ*xopK*), **(b)** 85-10Δ*avrBs2*Δ*xopR* (Δ*avrBs2*Δ*xopR*) und **(c)** 85-10Δ*avrBs2*Δ*xopV* (Δ*avrBs2*Δ*xopV*) wurden in anfällige (ECW) und resistente (ECW-10R) Paprikapflanzen inokuliert (10^8 KBE/ml). Die Phänotypen wurden 7 Tage nach Inokulation (ECW), bzw. 2 Tage nach Inokulation (ECW-10R) dokumentiert. Blätter von resistenten Pflanzen wurden zur besseren Visualisierung der HR in Ethanol gebleicht. Die Experimente wurden zweimal mit ähnlichen Ergebnissen reproduziert.

2.2.2.1.3 Subzelluläre Lokalisierung der Effektoren XopK, XopS und XopV

Um XopK, XopS und XopV näher zu charakterisieren, wurden subzelluläre Lokalisierungsstudien mit GFP-Fusionen der entsprechenden Effektoren durchgeführt. Lokalisierungen können ein Hinweis auf den Wirkungsort und somit auf mögliche Zielproteine der Effektoren innerhalb der Pflanze geben. Da die im Folgenden beschriebenen Lokalisierungsmuster der N- als auch C-terminalen GFP-Fusionsproteine vergleichbar waren, werden exemplarisch nur die Ergebnisse für C-terminale GFP-Fusionsproteine gezeigt. *Gfp*, *xopK* und *xopV* in pGWB5 bzw. *xopS* in pK7FWG2 wurden *Agrobacterium*-vermittelt in *N. benthamiana* exprimiert, wobei *gfp* als Kontrolle diente. Abbildung 2-3a zeigt, dass XopK::GFP nahe der pflanzlichen Zellwand akkumulierte. Im Vergleich zu GFP waren keine Zytoplasmastränge für XopK::GFP zu beobachten. Für XopK wurden zwei Transmembrandomänen durch *in silico* Analysen vorhergesagt (http://www.cbs.dtu.dk/services/TMHMM). Dies steht im Einklang mit dem beobachteten Lokalisierungsmuster und lässt die Schlussfolgerung zu, dass XopK::GFP an der pflanzlichen Plasmamembran lokalisiert ist.

XopS::GFP akkumulierte hingegen im Zytoplasma und im Zellkern, ähnlich wie GFP. Für XopV::GFP wurde die GFP-Fluoreszenz hauptsächlich im Zytoplasma beobachtet. Die Synthese der GFP-Fusionsproteine wurde mittels Western-Blot-Analysen nachgewiesen (Abb. 2-3 b).

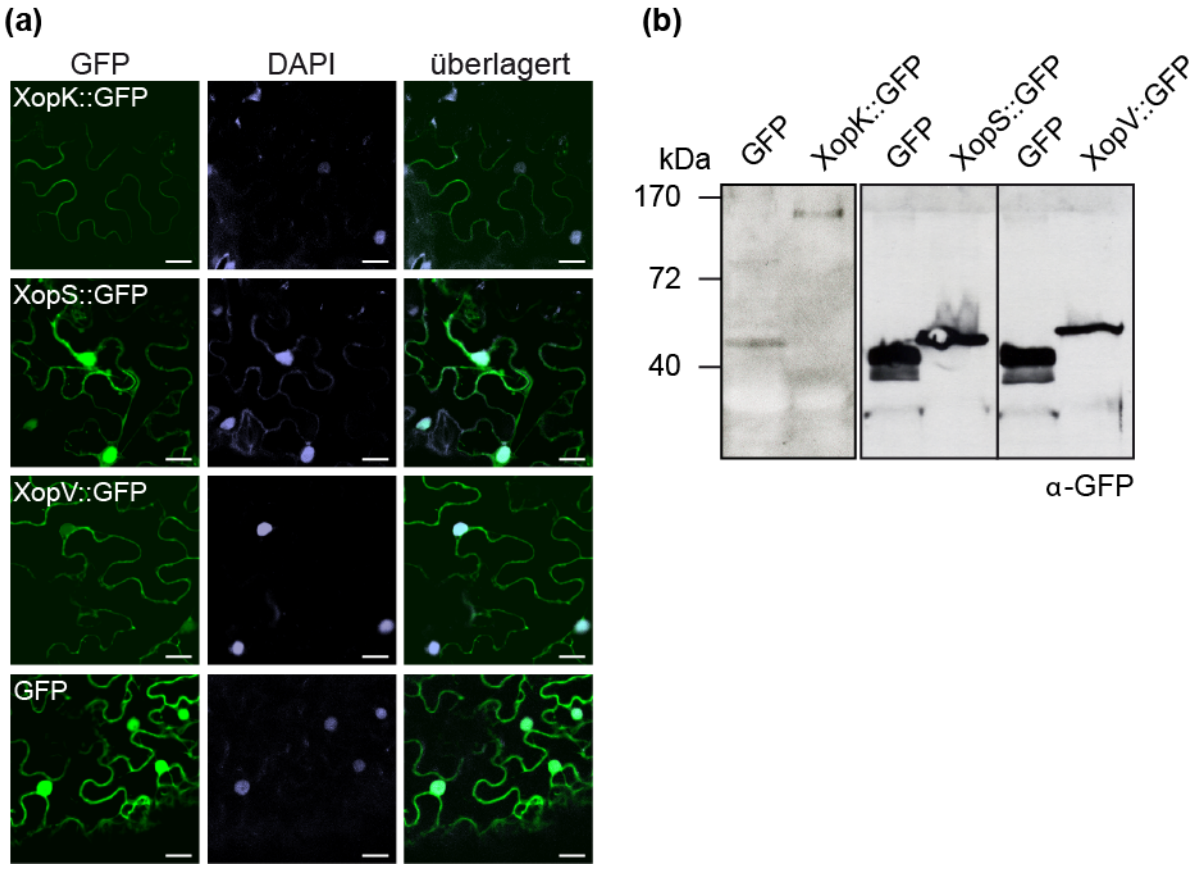

Abbildung 2-3: XopK, XopS und XopV sind in verschiedenen Zellkompartimenten lokalisiert.
Agrobacterium-vermittelte Expression von *xopK::gfp*, *xopS::gfp*, *xopV::gfp* und *gfp* nach Inokulation ($8x10^8$ KBE/ml) in *N. benthamiana*. 30 h nach Inokulation wurden die Blattbereiche mit DAPI infiltriert und mikroskopiert. **(a)** Die GFP-Fluoreszenz in Epidermiszellen ist links, DAPI-gefärbte Zellkerne in der Mitte und die Überlagerung beider Kanäle rechts dargestellt. **(b)** Aus inokuliertem Blattmaterial wurden Proteinextrakte hergestellt, mittels SDS-PAGE aufgetrennt und durch Western-Blot unter Verwendung eines GFP-spezifischen Antikörpers analysiert. Die Experimente wurden zweimal mit ähnlichen Ergebnissen reproduziert.

2.3 Molekulare Analyse des Typ III-Effektors XopL

2.3.1 Publikation 3

OPEN ACCESS Freely available online

PLOS | PATHOGENS

A Pathogen Type III Effector with a Novel E3 Ubiquitin Ligase Architecture

Alexander U. Singer[1,2◑], Sebastian Schulze[3◑], Tatiana Skarina[1,2], Xiaohui Xu[1,2], Hong Cui[1,2], Lennart Eschen-Lippold[4], Monique Egler[3¤], Tharan Srikumar[5], Brian Raught[5], Justin Lee[4], Dierk Scheel[4], Alexei Savchenko[1,2]*, Ulla Bonas[3]*

1 Banting and Best Department for Medical Research, University of Toronto, C.H. Best Institute, Toronto, Ontario, Canada, **2** Department of Chemical Engineering and Applied Chemistry, University of Toronto, Toronto, Ontario, Canada, **3** Department of Genetics, Martin Luther University Halle-Wittenberg, Halle, Germany, **4** Leibniz Institute of Plant Biochemistry, Halle, Germany, **5** Ontario Cancer Institute and Department of Medical Biophysics, University of Toronto, MaRS TMDT 9-805, Toronto, Ontario, Canada

Abstract

Type III effectors are virulence factors of Gram-negative bacterial pathogens delivered directly into host cells by the type III secretion nanomachine where they manipulate host cell processes such as the innate immunity and gene expression. Here, we show that the novel type III effector XopL from the model plant pathogen *Xanthomonas campestris* pv. *vesicatoria* exhibits E3 ubiquitin ligase activity *in vitro* and *in planta*, induces plant cell death and subverts plant immunity. E3 ligase activity is associated with the C-terminal region of XopL, which specifically interacts with plant E2 ubiquitin conjugating enzymes and mediates formation of predominantly K11-linked polyubiquitin chains. The crystal structure of the XopL C-terminal domain revealed a single domain with a novel fold, termed XL-box, not present in any previously characterized E3 ligase. Mutation of amino acids in the central cavity of the XL-box disrupts E3 ligase activity and prevents XopL-induced plant cell death. The lack of cysteine residues in the XL-box suggests the absence of thioester-linked ubiquitin-E3 ligase intermediates and a non-catalytic mechanism for XopL-mediated ubiquitination. The crystal structure of the N-terminal region of XopL confirmed the presence of a leucine-rich repeat (LRR) domain, which may serve as a protein-protein interaction module for ubiquitination target recognition. While the E3 ligase activity is required to provoke plant cell death, suppression of PAMP responses solely depends on the N-terminal LRR domain. Taken together, the unique structural fold of the E3 ubiquitin ligase domain within the *Xanthomonas* XopL is unprecedented and highlights the variation in bacterial pathogen effectors mimicking this eukaryote-specific activity.

Citation: Singer AU, Schulze S, Skarina T, Xu X, Cui H, et al. (2013) A Pathogen Type III Effector with a Novel E3 Ubiquitin Ligase Architecture. PLoS Pathog 9(1): e1003121. doi:10.1371/journal.ppat.1003121

Editor: David Mackey, Ohio State University, United States of America

Received August 10, 2012; **Accepted** November 27, 2012; **Published** January 24, 2013

Funding: This work was supported by National Institutes of Health grant GM074942 and grants from the Deutsche Forschungsgemeinschaft to J.L., D.S. and U.B. (SFB 648 "Molekulare Mechanismen der Informationsverarbeitung in Pflanzen"). L.E.-L. is supported by the BMBF-funded program, ProNet-T3 (03ISO2211B). T. Srikumar was supported by a fellowship from the Canadian Institutes of Health Research (CIHR). B.R. holds the Canada Research Chair in Proteomics and Molecular Medicine. Work in the B.R. lab was supported by CIHR grant MOP119289. The funders had no role in study design, data collection and analysis, decision to publish, or preparation of the manuscript.

Competing Interests: The authors have declared that no competing interests exist.

* E-mail: alexei.savchenko@utoronto.ca (AS); ulla.bonas@genetik.uni-halle.de (UB)

¤ Current address: Scil Proteins GmbH, Halle, Germany.

◑ These authors contributed equally to this work.

Introduction

Most Gram-negative pathogenic bacteria implement the type III secretion system (T3SS) that injects a set of proteins, termed effectors (T3E), directly into the eukaryotic host cell. The effectors' combined function is to subvert the host immune system and to promote bacterial colonization [1,2]. Plant immunity relies on recognition of conserved pathogen-associated molecular patterns (PAMPs) [3], such as flagellin or bacterial elongation factor Tu [4,5]. This defense barrier is termed PAMP-triggered immunity (PTI), is activated upon PAMP recognition at the cell surface by specific receptors, followed by a network of cellular signaling events, such as mitogen-activated protein kinase (MAPK) cascades, that ultimately lead to changes in gene expression [3,6,7]. In contrast, type III effectors manipulate plant cell processes, often leading to subversion of plant immune responses [1,8]. T3Es interfere with key eukaryotic cell functions, such as the cytoskeleton rearrangement [9], transcriptional regulation [10,11] or ubiquitination [12,13]. However, the biochemical function of the majority of T3Es remains elusive.

Ubiquitination is a highly conserved eukaryote-specific post-translational protein modification involving attachment of ubiquitin to the epsilon amine of a lysine residue in the target protein. This modification alters protein activity, protein localization or targets the protein for 26S-proteasome-mediated degradation [14]. Ubiquitination of target proteins involves coupling of ubiquitin to an ubiquitin activating enzyme (E1), transfer to a conjugating enzyme (E2), before an ubiquitin ligase (E3) mediates ubiquitin transfer from an E2 to a target protein [15]. E3 enzymes exhibit high target specificity and differ in the subset of E2s they interact

Author Summary

Numerous bacterial pathogens infecting plants, animals and humans use a common strategy of host colonization, which involves injection of specific proteins termed effectors into the host cell. Identification of effector proteins and elucidation of their individual functions is essential for our understanding of the pathogenesis process. Here, we identify a novel effector, XopL, from *Xanthomonas campestris* pv. *vesicatoria*, which causes disease in tomato and pepper plants. We show that XopL suppresses PAMP-related defense gene expression and further characterize XopL as an E3 ubiquitin ligase. This eukaryote-specific function involves attachment of ubiquitin molecule(s) to a particular protein targeted for degradation or localisation to specific cell compartments. Ubiquitination processes play a central role in cell-cycle regulation, DNA repair, cell growth and immune responses. In the case of XopL this activity triggers plant cell death. Through structural and functional analysis we demonstrate that XopL contains two distinct domains, one of which demonstrates a novel fold never previously observed in E3 ubiquitin ligases. This novel domain specifically interacts with plant ubiquitination system components. Our findings provide the first insights into the function of a previously unknown XopL effector and identify a new member of the growing family of bacterial pathogenic factors hijacking the host ubiquitination system.

with. Eukaryotic E3s fall into two major classes according to the mechanism of ubiquitin transfer: RING/U-box and HECT domain proteins [16]. RING finger/U-box proteins transfer ubiquitin directly from the E2 to the target protein, whereas HECT proteins first form a thioester intermediate with ubiquitin before ligating it to the target. While ubiquitination is absent in prokaryotes, it emerges as a prime eukaryotic host target for bacterial pathogens, which have evolved diverse T3Es to mimic ubiquitination-related functions. In particular, several bacterial T3Es from animal and plant pathogens function as E3 ubiquitin ligases, represented on one hand by the *Pseudomonas syringae* T3E AvrPtoB [12,13] and the NleG family of *E. coli* T3Es [17], which contain typical U-box folds, and on the other hand by the NEL (novel E3 ligase) domains found in the IpaH and SspH2 T3Es of *Shigella* and *Salmonella* spp., respectively [18,19]. The latter contain a novel thioester-forming E3 ligase domain with no structural homology to the HECT domain. This suggests that during co-evolution with their hosts, pathogenic bacteria have employed different solutions to fulfill the otherwise typical eukaryote-specific function of E3 ubiquitin ligases.

Here, we characterized the T3E XopL (*Xanthomonas* outer protein L) from the model plant pathogenic bacterium *Xanthomonas campestris* pv. *vesicatoria* (*Xcv*), which causes disease on tomato and pepper plants. *Xcv* injects a suite of ~30 T3Es into the host cell including the TAL (transcription activator-like) effector AvrBs3, which manipulates plant transcription [10], and the SUMO (small ubiquitin modifier) protease XopD [20]. XopL is a newly identified T3E from *Xcv*, and was found to exhibit E3 ubiquitin ligase activity. Crystal structure determination revealed that the protein contains a novel fold and thus represents a new class of E3 ubiquitin ligases.

Results

Identification of the new type III effector XopL (XCV3220)

The analysis of the genome sequence of *Xcv* strain 85-10 led to the identification of XCV3220 (*xopL*) as a new T3E candidate gene. XCV3220 is conserved in *Xanthomonas* spp. (Figure S1) and contains a PIP box (plant inducible promoter) in its promoter (TTCG-N16-TTCG; genome position 3669238-261). The presence of a PIP box in the *xopL* promoter suggested a co-regulation with the T3S system, which was confirmed by RT-PCR (Figure S2A). The predicted gene product contains leucine-rich repeats (LRRs), which are typically found in eukaryotic proteins and are thus indicative of an effector protein activity. Type III-dependent secretion and translocation of XCV3220 was confirmed by *in vitro* secretion and *in vivo* translocation assays (Figure S2B, C). The protein was therefore renamed XopL (for detailed information see Text S1).

XopL induces cell death and suppresses defense gene expression *in planta*

To investigate a possible virulence function of XopL, we deleted the gene from the genome and analyzed the corresponding deletion mutants by infection studies in pepper plants. However, under the conditions tested XopL had no discernible effect on virulence (Figure S2D) or bacterial growth of *Xcv* (data not shown). To further characterize XopL we expressed *xopL* in different plant species via *Agrobacterium*-mediated transformation. Expression of XopL induced plant cell death (PCD) in leaves of *Nicotiana benthamiana* (Figure 1A), but no macroscopic reaction in pepper or tomato plants (data not shown). PCD was confirmed by quantifying ion leakage, which is used to measure dying plant cells (Figure 1B).

To identify the role of XopL during the infection of plants, we tested if it manipulates plant immunity, as shown previously for several T3Es from *Pseudomonas* and *Xanthomonas*, which specifically suppress the PAMP-triggered immunity (PTI) [21–26]. To analyze this, we performed *Arabidopsis* leaf protoplast assays, a well-established system for PAMP-signaling analysis [25,27,28]. We tested the activity of the *A. thaliana NHL10 (NDR1/HIN1-LIKE 10)* [29,30] promoter fused to the firefly luciferase gene (*LUC*) after application of elicitor-active epitopes of different bacterial PAMPs. The reporter assays showed that the basal activity of *pNHL10* was not affected by XopL (Figure 2A). However, the expression of *xopL* significantly decreased the activation of *pNHL10* by flg22 (a bacterial flagellin epitope) [4] as well as that of elf18 (an 18 amino acid peptide derived from the EF-Tu protein) [5] (Figure 2B, C). Induction of *pNHL10* by flg22 depends, at least partially, on activity of mitogen- activated protein kinases (MAPKs) [27]. Therefore, the activation of the MAPKs MPK3, MPK4, MPK6 and MPK11, which are involved in plant immune signaling [31,32], might be affected by XopL. However, immunoblot analysis using an antibody against activated MAPKs revealed no differences in MAPK activity in protoplasts expressing XopL (or its derivatives; data not shown) compared to CFP (cyan fluorescent protein, negative control) (Figure 2D). AvrPto served as a positive control in both assays as it suppresses PTI by intercepting MAPK signaling pathways [33]. Proteins were stably expressed and protoplasts were still viable during the course of the experiment, confirming that the lack of *pNHL10* expression was not due to ongoing cell death of the protoplasts (Figure S3A, B).

XopL displays E3 ubiquitin ligase activity *in vitro*

The N-terminal LRRs of XopL are reminiscent of the domain architecture of the T3E families IpaH and SspH2 from *Shigella* and *Salmonella*, respectively, that were recently identified as E3 ubiquitin ligases [18,19]. We, therefore, tested XopL for E3 ubiquitin ligase activity *in vitro*. For this, we purified recombinant full-length XopL[aa 1–660] and truncated XopL derivatives XopL[aa 144–660] (lacking the disordered pre-LRR region),

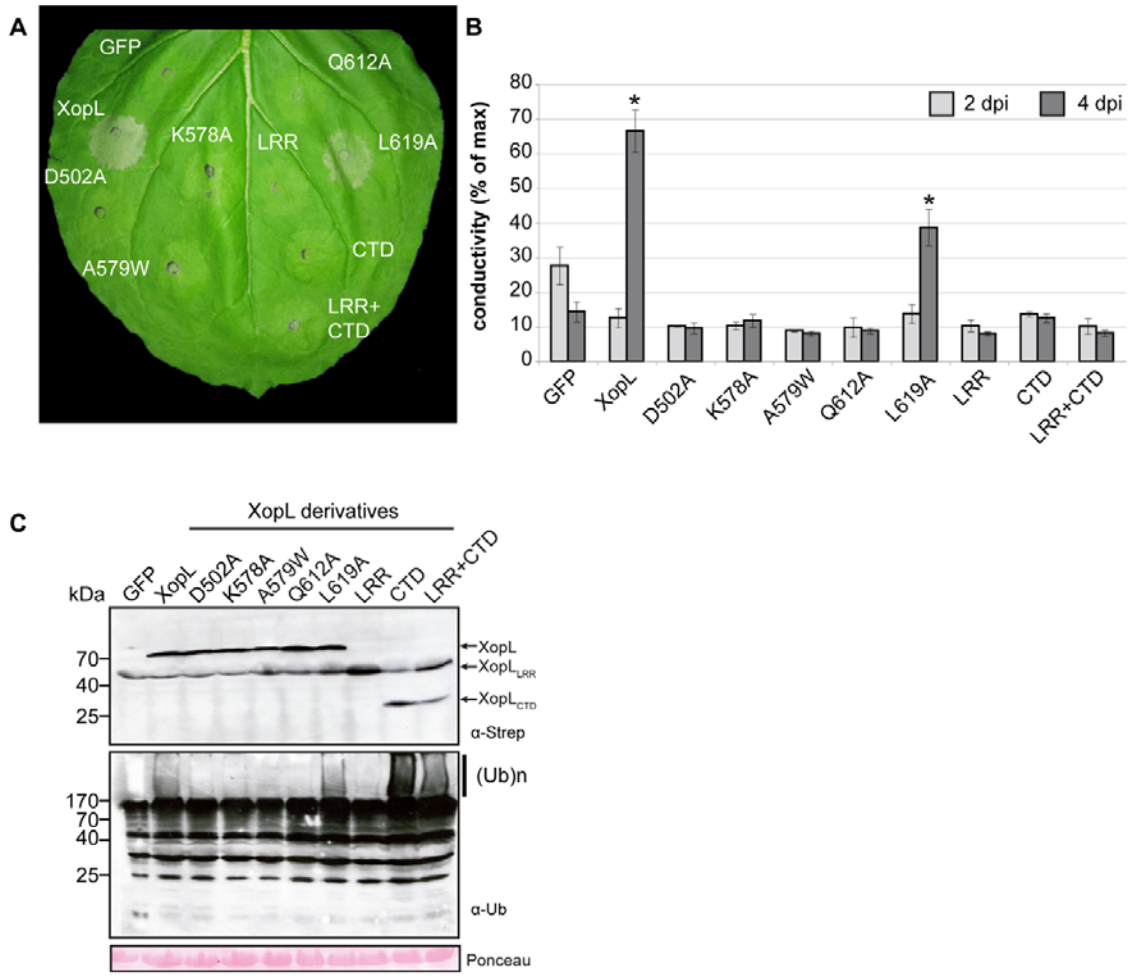

Figure 1. Analysis of cell death induction by XopL in *Nicotiana benthamiana*. *Agrobacterium*-strains carrying binary constructs encoding XopL (WT), $XopL_{D502A}$ (D502A), $XopL_{K578A}$ (K578A), $XopL_{A579W}$ (A579W), $XopL_{Q612A}$ (Q612A), $XopL_{L619A}$ (L619A), XopL[aa 1–449] (leucine-rich repeat, LRR), XopL[aa 450–660] (C-terminal domain, CTD), both XopL[aa 1–449] and XopL[aa 450–660] expressed in trans (LRR+CTD) or GFP under control of the *Cauliflower mosaic virus* (CaMV) 35S promoter, were inoculated into *N. benthamiana* leaves (8×10^8 cfu/ml). (**A**) Phenotypes of the inoculated leaf area were documented 6 days post inoculation (dpi). (**B**) Cell death quantification using electrolyte leakage measurements. Measurements were carried out 2 dpi (light grey bars) and 4 dpi (dark grey bars), respectively. Bars represent the average of triplicates of 5 leaf discs each, error bars represent standard deviations. Asterisks indicate statistically significant differences compared to GFP control (*t*-test, $P<0.01$). (**C**) Leaf tissue was harvested 2 dpi, and protein extracts were analyzsed by western blot using a *Strep*-tag (α-strep) and ubiquitin-specific antibody (α-Ub), respectively. Signals specific for full-length XopL, XopL[aa 1–449] ($XopL_{LRR}$)and XopL[aa 450–660] ($XopL_{CTD}$) are labeled. Polyubiquitination is indicated by $(Ub)_n$. Equal loading is shown by Ponceau staining of Rubisco. The experiments were performed three times with similar results.
doi:10.1371/journal.ppat.1003121.g001

XopL[aa 474–660] (lacking the LRRs) and XopL[aa 86–450] (lacking the C-terminal region).

XopL and its derivatives were tested in ubiquitination assays using human E1 and the ubiquitous human E2 (UBE2D2) or the related plant E2s (AtUBC11 or AtUBC28, both with ~80% sequence identity to UBE2D2) enzymes. In the case of full-length XopL, XopL[aa 144–660] and XopL[aa 474–660], western blot analysis with ubiquitin antibodies revealed a robust time-dependent accumulation of high-molecular-weight polyubiquitinated protein species (Figure 3A, B), which at later time points correlated with consumption of free ubiquitin (Figure 4B). A similar result was also obtained for the more distantly related XopL from *X. c.* pv. *campestris* (Table S1 in Text S1).

Western blot analysis using α-His antibodies (Figure 3A) and Coomassie Blue staining of SDS-PAGE gels (Figure 3B), combined with mass spectrometric analysis of the high-molecular weight species (data not shown) demonstrated minimal modification of the XopL fragments, indicating that the principle product of *in vitro* ubiquitination reactions were unattached ubiquitin chains. In the case of the XopL[aa 86–450] fragment, no polyubiquitinated protein species were detected (Figure 3A), suggesting that polyubiquitination was dependent on the intact XopL C-terminal

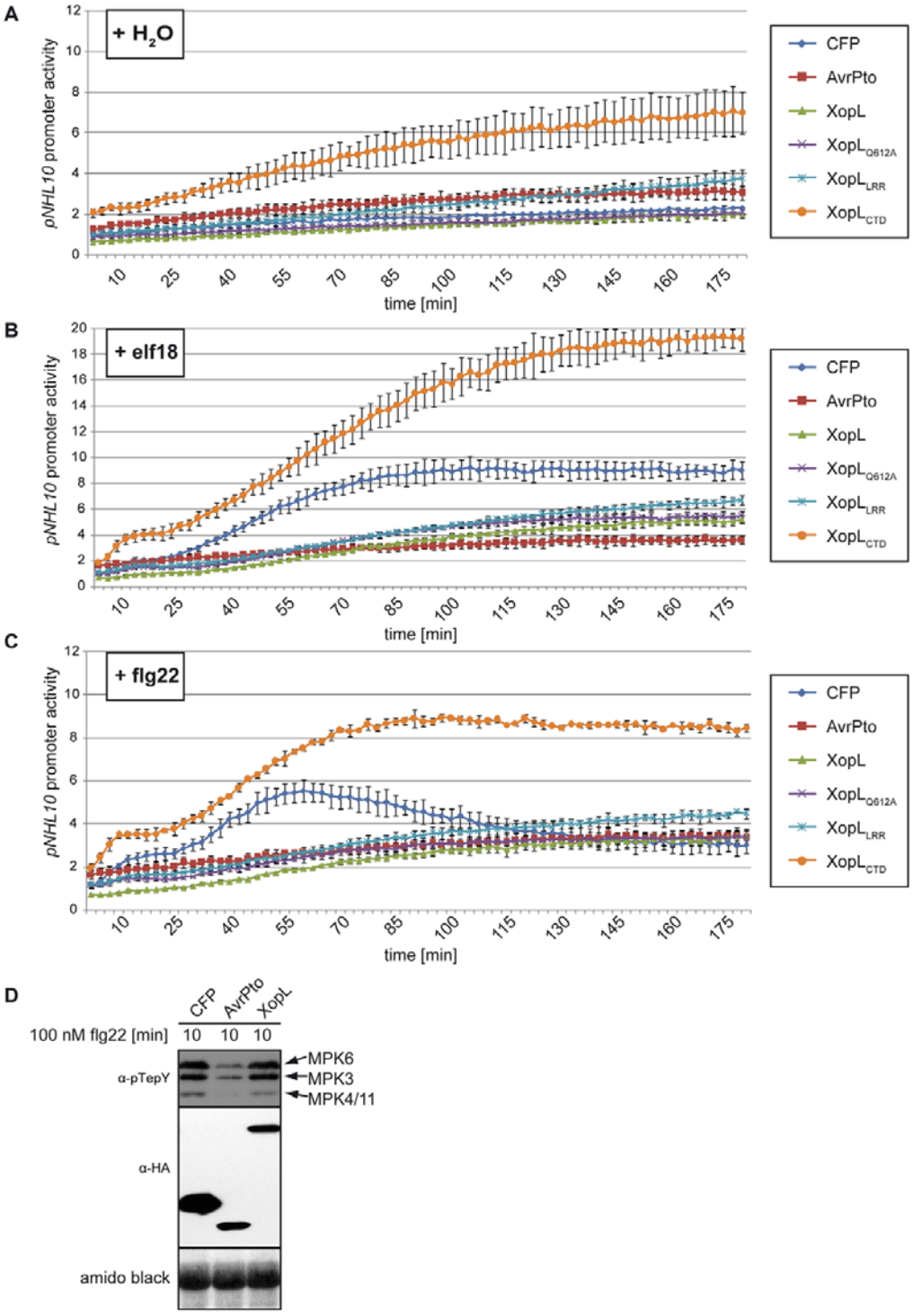
A
+ H2O
pNHL10 promoter activity
time [min]
CFP
AvrPto
XopL
XopLQ612A
XopLLRR
XopLCTD
B
+ elf18
pNHL10 promoter activity
time [min]
CFP
AvrPto
XopL
XopLQ612A
XopLLRR
XopLCTD
C
+ flg22
pNHL10 promoter activity
time [min]
CFP
AvrPto
XopL
XopLQ612A
XopLLRR
XopLCTD
D
CFP
AvrPto
XopL
100 nM flg22 [min]
10
10
10
α-pTepY
MPK6
MPK3
MPK4/11
α-HA
amido black

Figure 2. XopL inhibits pathogen-associated molecular pattern (PTI)-induced defense gene expression. *Arabidopsis thaliana* Col-0 protoplasts were co-transformed with *pNHL10-LUC* (luciferase) as reporter, the *p35S*-effector gene constructs *xopL*, *xopL*$_{Q612A}$, *xopL*$_{LRR}$ and *xopL*$_{CTD}$ or *p35S-cfp* and p*35S-avrPto* (negative and positive control, respectively), and *pUBQ10-GUS* (β-glucuronidase) for normalization. 14 h after transformation, protoplasts were treated with H_2O (**A**), 100 nM elf18 (**B**) and 100 nM flg22 (**C**), and luciferase activity was monitored for 3 h. Results are depicted as LUC/GUS ratios (with the zero timepoint, H_2O-treated sample set at a reference value of one). (**D**) Protein extracts of transformed protoplasts were taken 10 min after treatment and analyzed by immunoblotting using a pTepY-antibody (specific for activated MAP-Kinases) and HA-specific antibodies for detection of HA-tagged effector-or CFP-fusion proteins. MPK3, 4, 6, 11: mitogen activated protein kinase 3, 4, 6, 11. The experiments were performed three times with similar results.
doi:10.1371/journal.ppat.1003121.g002

region. XopL-mediated formation of ubiquitin chains required both E1 and E2 enzymes (Figure 3B), demonstrating that XopL acts similarly to eukaryotic E3 ubiquitin ligases.

Next, we determined the type of ubiquitin linkages preferentially generated by XopL. Ubiquitin contains seven lysine (K) residues (K6, K11, K27, K29, K33, K48 and K63) that can participate in ubiquitin ligation [14]. Therefore, we analyzed the products of the XopL-mediated polyubiquitination reaction using plant AtUBC11, AtUBC28 and human UBE2D2 conjugating enzymes. While the relative amount of distinct ubiquitination linkages detected by this analysis (Table S1 in Text S1) was different depending on which E2 enzyme was used in the reaction, the K11 linkages represented the largest fraction in all cases. More than half of the linkages analyzed in reactions with AtUBC28 and UBE2D2 enzymes were K11, whereas K11 represented ~45% of the linkages in reactions with AtUBC11. The remaining polyubuitination linkages corresponded primarily to K33, K48 and K63 (Table S1 in Text S1). Interestingly, K63-linked polyubiquitin chains were detected in reactions using AtUBC28 and human UBE2D2 but not in reactions with plant AtUBC11, suggesting that these homologous E2 enzymes may contribute to a different preference in linkages that are formed during E3 catalyzed reactions.

In order to confirm the prevalence of the detected linkages in the XopL-mediated reaction we then performed polyubiquitination assays using ubiquitin variants with each individual lysine residue mutated to arginine (Figure 3C). In accordance with mass spectrometry results, the K11R mutation significantly dampened the XopL-mediated formation of polyubiquitin chains in the reaction using the AtUBC11 enzyme. A similar effect was detected in case of K33R and K48R mutations. Interestingly, the K6R mutation also resulted in significant reduction of polyubiquitination, while no K6 linkages were detected among XopL polyubiquitination products. This result suggested that this mutation might have a general deleterious effect on ubiquitination, potentially due to reduced affinity to E1 or E2 enzymes.

XopL interacts with specific plant E2 enzymes

Next, we tested XopL ubiquitin ligase activity with different plant-derived E2s. As stated above, XopL forms ubiquitin chains with AtUBC11 and AtUBC28 (93% sequence identity), which belong to group VI of the 16 E2 classes of this plant [34], and the close human homologue UBE2D2. However, two more distantly related E2s (Table S1 in Text S1), namely AtUBC13 (group V, 34% sequence identity to AtUBC11) and AtUBC19 (group VIII, 43% sequence identity to AtUBC11) did not show any activity in our *in vitro* assays (Figure 4A), suggesting that XopL discriminates between different classes of E2 enzymes, as was described for other E3 ubiquitin ligases [19,35–37].

Interactions between the human UBE2D2 enzyme and E3 ubiquitin ligases have been studied in detail by mutagenesis [38]. Because mutation of conserved residues in UBE2D2 abrogated ubiquitination *in vitro*, we purified the R5A, F62A, K63A and A96D variants of the AtUBC28 E2 enzyme and tested them individually in XopL and XopL[aa 474–660] ubiquitination assays.

The F62A and A96D mutations in AtUBC28 completely abrogated both the XopL[aa 474–660]- and XopL-mediated polyubiquitination reactions (Figure 4B; data not shown), suggesting that F62 and A96 are required for the AtUBC28 interaction with XopL. By contrast, the AtUBC28 R5A and K63A mutants were still very active *in vitro* (Figure 4B).

Taken together, our results demonstrate that XopL is an E3 ubiquitin ligase that selectively recruits plant E2 enzymes.

Structural analysis of the XopL N- and C-terminal domains reveals a novel fold

The XopL C-terminal domain harboring E3 ubiquitin ligase activity lacks significant sequence similarity with previously characterized E3 ligases. To gain further insight into the structural basis of XopL activity, we determined the structure of XopL by X-ray crystallography. While full-length XopL did not crystallize, fragments XopL[aa 144–450] and XopL[aa 474–660] yielded crystals that diffracted to a resolution of 2 Å and 1.8 Å, respectively. In both cases, single-wavelength anomalous dispersion (SAD) data were collected at the selenium peak wavelength from a single selenomethionine-enriched crystal. The final model of XopL[aa 144–450] contained a single molecule in the asymmetric unit corresponding to residues 145 to 437 plus four additional residues from the N-terminal polyhistidine tag. For the XopL[aa 474–660] fragment, three polypeptide chains were found in the asymmetric unit corresponding to residues 474–642 plus up to six residues from the N-terminal polyhistidine tag. Data collection and refinement statistics for both structures are presented in Table 1.

The structure of the XopL[aa 144–450] fragment follows a canonical LRR architecture with ten β-strands and nine complete repeats each folding into an α-helix (single turn)-turn-β-strand motif (Figure 5A). Three α-helices (α1, α2 and α3) and one α-helix (α 4) cap the LRRs at the N- and C-terminus, respectively. This structure is similar to the LRR domain of IpaH3 (PDB 3CVR [39], Figure 5A). Based on the sequence conservation at specific positions in individual repeats, a consensus sequence for the XopL LRRs can be derived that is similar to that of plant derived LRR-containing proteins (Figure 5B).

The structure of the XopL C-terminal region [aa 474–660] represents a four-helix bundle, which can be subdivided into two uneven lobes almost perpendicular to each other (Figure 6A). The smaller lobe contains the N-terminus, α2b and α3 helices and a region C-terminal to the α2b helix (residues 554–562), which adopts a conformation intermediate between a poly-proline type II helix and a β-strand. The two lobes give the XopL[aa 474–660] molecule an "L"-shape, and a large cleft with a net negative charge is formed at the intersection of the two lobes (Figure 6B, C). A search for structural homology using the DALI server (http://ekhidna.biocenter.helsinki.fi/dali_server/, 2012) did not reveal any significant similarity between the XopL[aa 474–660] structure and other structurally characterized proteins including E3

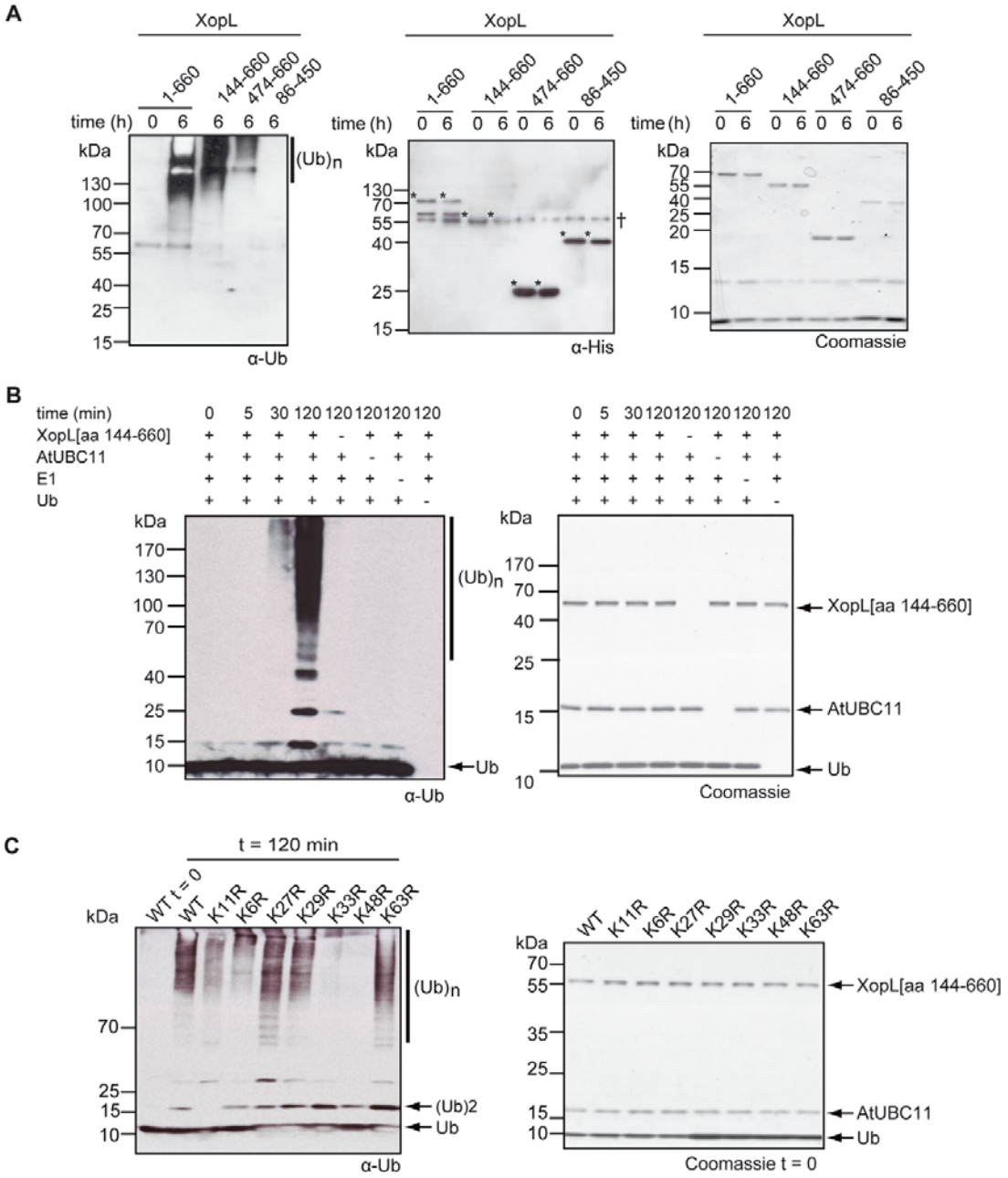

Figure 3. The C-terminal domain of XopL shows E3 ubiquitin ligase activity. (**A**) *In vitro* ubiquitin ligase assay in presence of E1, UBE2D2, ATP, ubiquitin and His_6-XopL full-length protein (1–660) or derivatives thereof (numbers indicate amino acid positions corresponding to full-length protein). The western blots were reacted with antibodies against ubiquitin (α-Ub, left panel) and polyhistidine (α-His, middle panel), respectively, while the right panel shows the reaction mixture via Coomassie Blue staining of the SDS-PAGE. $(Ub)_n$ indicates polyubiquitination. Asterisks indicate His_6-XopL derivatives. Unspecific signals are labeled by †. (**B**) Ubiquitin polymerization reaction at different time points in the presence (+) or absence (−) of E1, AtUBC11 (E2), ubiquitin and His_6-XopL[aa 144–660]. Polyubiquitination was determined by western blot (left panel) using ubiquitin antibodies. The right panel shows the state of modification of the proteins via Coomassie Blue staining of the 10–15% step-gradient SDS-PAGE gel. Components of the reactions (XopL[aa 144–660], ubiquitin (Ub) and AtUBC11) on western blots or Coomassie-stained gels are labeled. (**C**) *In vitro* ubiquitination assay in the presence of ATP, E1, AtUBC11, His_6-XopL[aa 474–660], ubiquitin (WT) and lysine (K) to arginine (R) mutant derivatives thereof. The left panel shows the western blots probed against ubiquitin (α-Ub) of the *in vitro* reactions, run on a 10–15% step-gradient SDS-PAGE

using ubiquitin mutant derivatives in which only the indicated K residues were substituted by R. The right panel shows the starting material of the *in vitro* reactions in the left panel via Coomassie Blue staining of the SDS-PAGE. Polyubiquitination is indicated by $(Ub)_n$; the components of the reactions and the di-ubiquitin (Ub)2 on the western blot or Coomassie-stained SDS-PAGE are labeled.
doi:10.1371/journal.ppat.1003121.g003

ubiquitin ligases. This analysis clearly demonstrates that the XopL C-terminal domain represents a novel fold, which we termed XL-box (XopL E3 ligase box). The XL-box lacks cysteine residues. Therefore, XopL E3 ubiquitin ligase activity appears not to involve the formation of thioester intermediates with ubiquitin as was shown in the case of eukaryotic (HECT-type) and effector (IpaH and SopA) catalytic E3 ubiquitin ligases.

The LRR and XL-box domains play different roles *in planta*

Given that structural analysis defined the presence of two distinct domains in XopL (LRR and XL-box), we tested their individual role in suppressing PAMP-induced gene expression and inducing PCD (see above; Figure 1A). When the N-terminal [aa 1–449] and the C-terminal [aa 450–660] XopL regions were expressed individually or co-expressed in *N. benthamiana*, no PCD was observed (Figure 1A, B) demonstrating that an intact XopL protein is required to provoke PCD, which is consistent with the suggested function of the LRRs in recognition of a plant target protein ubiquitinated by the XL-box. Next, we tested the effect of mutations in the XL-box domain on the ability of XopL to provoke PCD (Figure 1A, B; Figure S5A, B; Table S3 in Text S1). Residues D502, K578, A579, Q612 and L619 co-localize on the surface of the major cleft of the XL-box (Figure 6C), and are

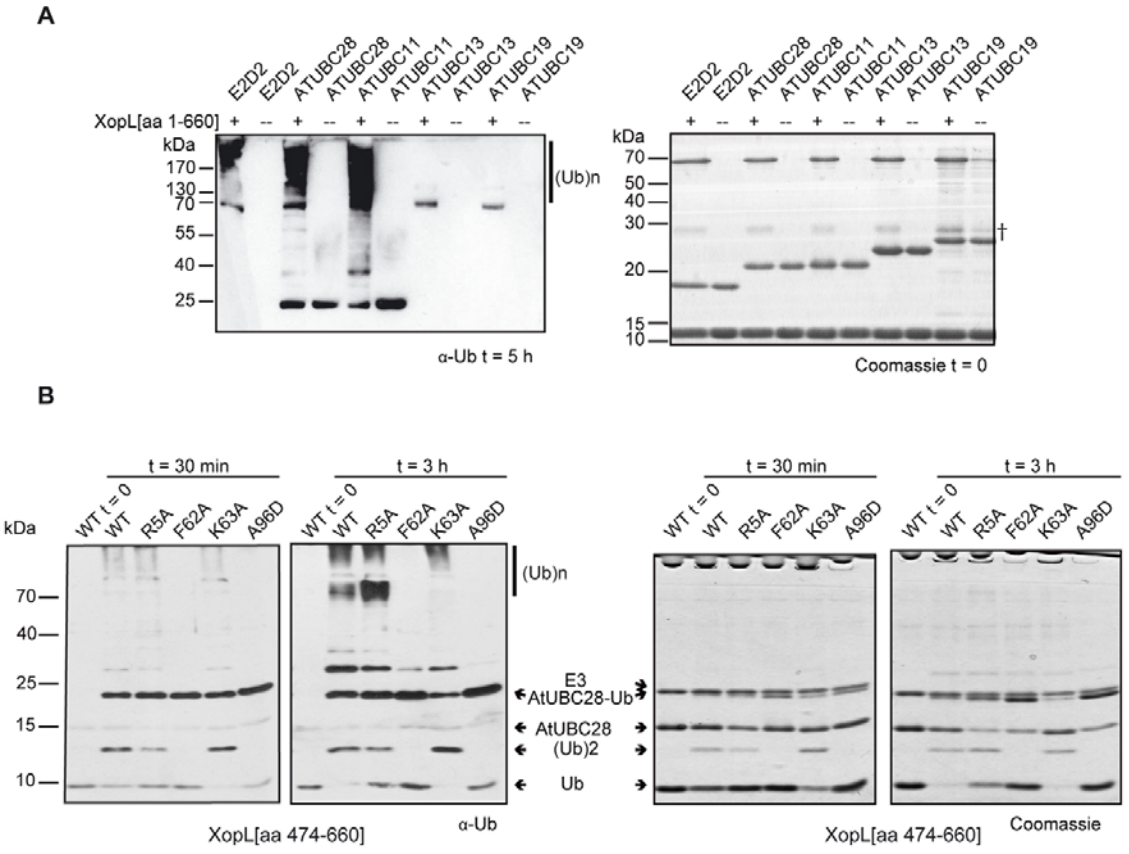

Figure 4. XopL displays E2 specificity *in vitro*. (**A**) *In vitro* ubiquitin ligase assay with ATP, ubiquitin, E1, human UBE2D2 (E2D2) or different *Arabidopsis thaliana* E2s (ATUBC28, 11, 13 or 19) in the presence (+) or absence (−) of His_6-XopL[aa 1–660]. The left panel shows the western blot reacted with ubiquitin antibodies (α-Ub) after 5 hours incubation, while the right panel shows the Coomassie stained gel of the reactants at the start of the reaction. Polyubiquitination is indicated by $(Ub)_n$. A lower-molecular weight impurity or degradation product in the full-length XopL protein purification is denoted by †. (**B**) Ubiquitin ligase assay described in (A) using His_6-XopL[aa 474–660], AtUBC28 and mutant derivatives R5A, F62A, K63A and A96D. Reaction times are indicated. The left panel shows the western blot reacted with ubiquitin antibodies (α-Ub), while the right panel shows the Coomassie-stained gel at the equivalent time points. $(Ub)_n$ indicates polyubiquitination, and positions on the western blot or Coomassie-stained gels corresponding to ubiquitin (Ub), di-ubiquitin (Ub)2, AtUBC28, mono-ubiquitinated AtUBC28 (AtUBC28-Ub) and His_6-XopL[aa 474–660] (E3) are labeled.
doi:10.1371/journal.ppat.1003121.g004

Table 1. Data collection, phasing and refinement statistics for SAD (SeMet) structures.

	XopL[aa 144–450]	XopL[aa 474–660]
Data collection		
Space group	*C2221*	*P32*
Cell dimensions		
a, *b*, *c* (Å)	50.5, 95.2, 115.5	119.2, 38.7
α, β, γ (°)	90, 90, 90	90, 90, 120
	Peak	*Peak*
Wavelength	0.97937	0.97921
Resolution (Å)	50-2.00 (2.03-2.00)*	100-1.8(1.83-1.80)
R_{sym} or R_{merge}[a]	0.072(0.364)	0.063(0.519)
$I/\sigma I$	38.4(4.9)	25.0(1.85)
Completeness (%)	99.9(99.3)	99.4(99.0)
Redundancy	7.3(5.4)	3.2(2.6)
Refinement		
Resolution (Å)	29.9-2.00	28.6-1.80
No. reflections	19119	110283
R_{work}[b]/R_{free}[c]	17.1/22.6	15.2/19.6
No. atoms	2491	4542
Protein	2400	4119
Ligand/ion	23	14
Water	168	409
B-factors		
Protein	30.7	34.3
Ligand/ion	47.3	40.4
Water	37.2	37.0
R.m.s deviations		
Bond lengths (Å)	0.007	0.004
Bond angles (°)	1.1	0.76

*Values in parentheses are for highest-resolution shell.
[a]$R_{merge} = \Sigma|I-<I>|/\Sigma\ I$.
[b]$R_{work} = \Sigma\ |\ F_{obs}-F_{calc}\ |/\Sigma\ |F_{obs}|$, where F_{obs} and F_{calc} are observed and calculated structure factors, respectively.
[c]R_{free} calculated using 5% of total reflections randomly chosen and excluded from the refinement.
doi:10.1371/journal.ppat.1003121.t001

highly conserved (Figure S1). Each of the aforementioned residues was substituted by alanine, except for A579, which was mutated to tryptophan. Transient expression of these XopL variants in *N. benthamiana* revealed that the XopL mutant derivatives were stably synthesized (Figure 1C) and D502A, K578A, A579W or Q612A exchanges abolished the ability of XopL to induce PCD. By contrast, the $XopL_{L619A}$ variant was still active (Figure 1A, B). We then investigated if E3 ubiquitin ligase activity of XopL can be demonstrated in the plant. *N. benthamiana* leaves expressing full-length XopL, XopL[aa 1–450], XopL[aa 450–660] or GFP (green fluorescent protein; control) were analyzed by western blotting using ubiquitin-specific antibodies. Expression of full-length XopL and XopL[aa 450–660], but not XopL[aa 1–450] led to the presence of additional high molecular mass ubiquitinated protein species, that were not detected upon expression of *gfp* (Figure 1C).

Notably, the D502A, K578A, A579W and Q612A mutations that abrogated the ability of XopL to cause PCD also dampened the formation of polyubiquitin chains *in vivo* (Figure 1C, Figure S5C). On the other hand, $XopL_{L619A}$ caused PCD and retained the ability to mediate formation of polyubiquitin chains *in vivo* similarly to the wild type. A similar result was found performing *in vitro* polyubiquitination reactions using the AtUBC11 conjugating enzyme and XopL[aa 474–660] (Figure S6). Taken together these results suggested that PCD is caused by XopL E3 ligase activity, manifested by formation of polyubiquitin products *in vivo* and *in vitro*.

We also tested the effect of the individual domains on suppression of PAMP-induced gene expression relative to full-length XopL (Figure 2, Figure S3). Unexpectedly, the PAMP-suppression activities of XopL are mediated by the N-terminal (residues 1–450) fragment corresponding to the LRR-containing region, which suppressed PAMP-induced gene expression to a similar extent as the full-length XopL. In addition, full-length XopL with a Q612A mutation in the XL-box, which both strongly hinders the ability of XopL to promote PCD and to polyubiquitinate *in vivo* and *in vitro*, retained the ability to inhibit the expression of the reporter gene in the presence of either PAMP elicitor peptides. Finally, the expression of the $XopL_{CTD}$ did not suppress, but rather elevated, the expression of the reporter even in the absence of the PAMP elicitor peptides (Figure 2A–C).

Discussion

In this study, we identified XopL as a new T3E in *Xcv* that induces cell death in *N. benthamiana* and inhibits PTI-related defense gene expression. According to our data, XopL exhibits a robust E3 ubiquitin ligase activity. This activity is associated with its C-terminal region and is required for induction of plant cell death. All ubiquitin ligases known to date including bacterial T3Es with E3 ligase activity belong to the RING/U-box or catalytic (HECT-like) class [16]. RING/U-box proteins act by transferring ubiquitin from E2 directly onto the target protein. T3Es of this class include AvrPtoB from the plant pathogen *P. syringae* [13], and *E. coli* NleG [17]. Both T3Es lack significant sequence similarity with RING/U-box proteins but adapt a protein fold similar to that of U-box proteins. On the other hand, the catalytic HECT E3 ligases first attach ubiquitin from the E2 to a catalytic cysteine residue via a thioester intermediate before ligating it to the target protein. A similar mechanism has been adopted by effector proteins of the IpaH and SopA families of animal pathogens [40,41]. The IpaH and SopA crystal structures are distinct from HECT proteins except for the presence of a catalytic cysteine and certain features of the active site. As XopL lacks cysteine residues in its C-terminal domain, termed XL-box, we hypothesize that it acts by directly transferring ubiquitin from E2 onto a target protein. This is reminiscent of RING/U-box proteins; however, XopL lacks any structural similarity to these E3 ligases.

We found that XopL interacts *in vitro* through its XL-box with a specific family of E2 enzymes, represented by human UBE2D2 and *Arabidopsis* AtUBC11 and AtUBC28. In *Arabidopsis thaliana*, AtUBC11 and AtUBC28 are members of the group VI family of E2 enzymes [34]. Many of the 8 family members are ubiquitously expressed in *Arabidopsis* (including AtUBC28 and AtUBC11) and the three most highly expressed members of this family (AtUBC8, AtUBC10 and AtUBC28; www.genevestigator.com) share 97% sequence similarity with each other. Homologues to these proteins are also found in tomato (*S. lycopersicum* gi|350536447|; 97% identical to AtUBC28) and pepper (*C. annuum* gi|40287554|; 96% identical to AtUBC28). Mutation analyses of AtUBC28 revealed amino acid residues F62 and A96 to be critical for the interaction with the XopL E3 ligase. It is worth noting that residue F62 is essential for E2 interactions with HECT E3 ligases [42], but not for interactions with specific RING/U-box proteins [43]. On the

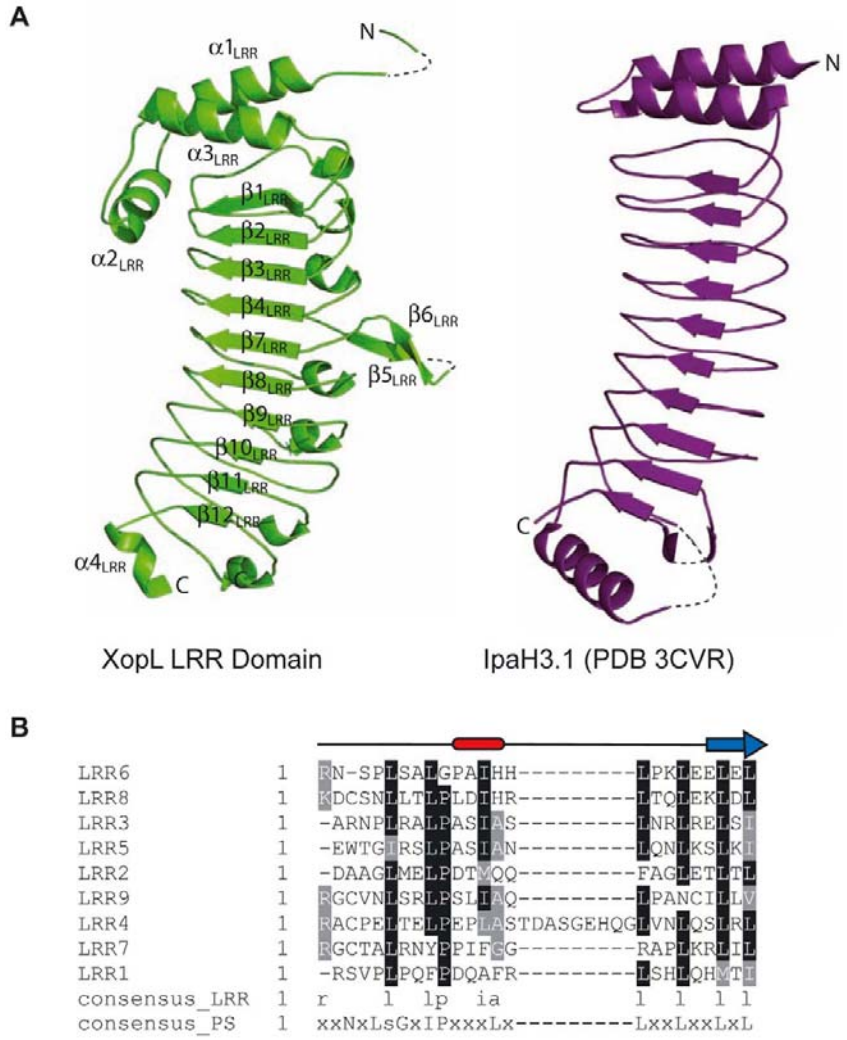

Figure 5. Structure of the N-terminal LRR domain of XopL. (**A**) The left panel shows the ribbon diagram of the XopL[aa 144–450] structure (green). N- and C-termini and the secondary structure elements (see Figure S1) are labeled. In comparison, the IpaH3 LRR domain (PDB code 3CVR), represented by aa residues 25–268, is shown in the right panel as a ribbon diagram (purple) with labeled N- and C-termini. Disordered regions in the protein are represented as grey dashed lines. (**B**) Sequence alignment of the nine leucine-rich repeats of XopL[aa 145–450], showing their consensus and relationship to the plant-specific (PS)-LRR subclass of LRRs. The positions of the helical turn (red box) and β- strand (blue arrow) in the "typical" LRR of XopL are given.
doi:10.1371/journal.ppat.1003121.g005

other hand, residue A96 in E2 enzymes was shown to contribute to interactions with both HECT- and RING-type ligases plus the bacterial effector SspH2 [44]. While this data reveals some molecular details of the XopL interaction with E2 enzymes it cannot be modeled according to previously characterized E3-E2 pairs and requires further structural analysis.

XopL-mediated polyubiquitin chains with preponderance of K11 linkages were detected using both *Arabidopsis* group VI E2 enzymes and the human UBE2D2 enzyme. Ubiquitin contains seven lysine residues that can participate in target protein ubiquitination. Which specific lysine is used is dictated by different E3-E2 enzyme combinations and may trigger different outcomes for a given target protein. Linkage at K48 usually directs target proteins to the proteasome [45], whereas K63-ubiquitination can play a role in signal transduction [46]. The importance of other ubiquitin linkages for cell processes came to light only recently and their physiological role remain largely unknown [47]. A recent report suggested that mixed K11- and K63-linked chains are a virus-internalization signal [48]. In addition, K11-linked ubiquitin chains have been connected to degradation of substrates of the anaphase-promoting complex in cell cycle regulation [49,50]. The *Salmonella* T3E E3 ubiquitin ligase SspH2, which similarly to XopL selectively interacts with the human UBE2D2 enzyme, mediates the formation of primarily K48-linked polyubiquitin chains [44].

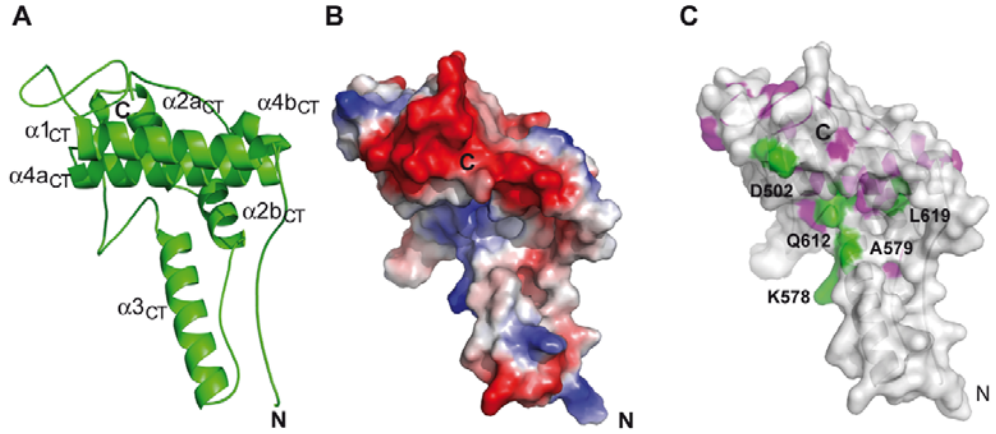

Figure 6. Structure of the XL-box of XopL. (**A**) Ribbon diagram of a single molecule (molecule B) of the 3 molecules in the asymmetric unit of the XopL[aa 474–660] structure. Secondary structure elements (according to the nomenclature in Figure S1) and the N- and C-termini are labeled. (**B**) Electrostatic surface of molecule B from the same structure, using the same view. Electrostatic potential was calculated using the default values from PYMOL (http://www.pymol.org/). (**C**) Same surface as in (B), showing the absolutely conserved residues from the alignment in Figure S1 (colored pink on the semi-transparent surface). The surface is semi-transparent showing a ribbon representation of the structure. Residues absolutely conserved and subject to mutation are colored green and labeled.
doi:10.1371/journal.ppat.1003121.g006

Considering the predominance of K11-linked polyubiquitination in the case of the interaction between XopL and UBE2D2 or its plant homolog we speculate that K11-linked ubiquitin chains may play an important role in plant-pathogen interactions. However, this remains to be elucidated.

Our structural data confirmed that XopL harbors a *bona fide* LRR domain. The LRR domain is a common feature between XopL and the IpaH- and SspH2- effector E3 ubiquitin ligases mentioned above. While the LRR domain in IpaH plays a regulatory role by inhibiting the E3 activity in the absence of the substrate [18,19,51], there is no indication for this kind of mechanism in the case of XopL, as E3 ligase activity is robust in the presence or absence of the LRR domain. However, we were surprised to find that the LRR is involved in suppression of PAMP-elicited gene expression, which we performed using the well-established Arabidopsis protoplast system. According to our data the expression of *pNHL10* following elicitation of protoplasts with either flg22 or elf18 peptides was suppressed by the LRR domain, similarly to full-length XopL. This argues for an adaptor function of the LRR domain in which the LRR domain binds a target downstream of PAMP-receptor binding and either downstream or independent of MAPK cascade-signaling, leading to altered gene expression. These results are reminiscent to those reported for the *Pseudomonas* type III effector AvrPtoB, where suppression of plant immunity by blocking downstream signaling through BAK1-kinase are due exclusively to the two binding domains localized to residues 121–205 and 270–359 [52].

As shown by our *in planta* ubiquitination profiles, the presence of both the LRR and XL-box domains is essential for XopL-induced reactions. While expression of the XL-box domain *in planta* resulted in formation of additional polyubiquitin chains, in line with its *in vitro* activity, only full-length XopL with an intact LRR domain triggered cell death. In addition, expression of the individual XL-box and LRR domain had the opposite effect on expression of the *NHL10* promoter, even in the absence of PAMP-response elicitor. This suggests that the LRR domain functions as a protein-protein interaction module necessary for both the suppression of PAMP-elicited gene expression and the cell death phenotype we observed. Thus, we hypothesize that XopL fulfills multiple functions *in planta* by (i) suppressing PTI via its LRR-region and (ii) ubiquitinating a yet unknown plant substrate(s) whose initial recognition may also require the LRR-region.

In conclusion, characterization of the bacterial pathogen effector XopL uncovered a novel E3 ubiquitin ligase fold that is part of the pathogen repertoire to mimic an otherwise strictly eukaryotic function such as ubiquitination. This underlines the variety of E3 ligases evolved in pathogenic bacteria for subverting host biology. The next challenge is the identification of host targets of XopL that are involved in suppression of plant defenses, as well as determination of the mechanism of action of this unusual E3 ligase.

Materials and Methods

Bacterial strains and growth conditions

Escherichia coli cells were cultivated in lysogeny broth medium (LB) at 37°C. *Agrobacterium tumefaciens* was grown at 30°C in YEB (yeast extract broth) medium and *Xcv* at 30°C in NYG (nutrient yeast glycerol, [53]) or secretion medium (minimal medium A, [54]) supplemented with 10 mM sucrose and 0.3% casamino acids. Plasmids were introduced into *E. coli* and *A. tumefaciens* by electroporation and into *Xcv* by conjugation, using helper plasmid pRK2013 in triparental matings [55].

Plant material and inoculations

The near-isogenic pepper (*Capsicum annuum*) cultivars ECW, ECW-10R and ECW-30R [56] were grown at 23°C with 60% relative humidity and 16 h light and *Nicotiana benthamiana* plants were grown at 22°C with 60% relative humidity and 16 h light. *Xcv* strains were inoculated with a needleless syringe into leaves at 10^8 colony-forming units (cfu)/ml in 10 mM $MgCl_2$. For *in planta* transient expression studies, *A. tumefaciens* strain GV3101 [57] was incubated in inoculation medium (10 mM $MgCl_2$, 5 mM MES,

pH 5.3, 150 µM acetosyringone) and inoculated into leaves at 8×10^8 cfu/ml.

Protein analysis

Xanthomonas in vitro secretion experiments were performed as described [58]. Equal amounts of total bacterial cell extracts and culture supernatants were analyzed by SDS-polyacrylamide gel electrophoresis (PAGE) and immunoblotting following standard protocols. To exclude bacterial lysis, blots were routinely reacted with an antibody specific for the inner membrane lipoprotein HrcJ [59]. To analyze *Agrobacterium*-mediated protein expression, two leaf discs (0.9 cm in diameter) were frozen and ground in liquid nitrogen, resuspended in 100 µl 8 M urea and 50 µl 5× Laemmli buffer, and boiled for 10 min. Proteins were separated by SDS-PAGE and analyzed by immunoblotting. We used polyclonal antibodies for detection of AvrBs3 [60] and ubiquitin (Abcam, Cambridge, U.K.), and a monoclonal *Strep*-tag antibody (IBA GmbH, Göttingen, Germany). Horseradish peroxidase-labeled α-rabbit and α-mouse antibodies (Amersham Pharmacia Biotech, Piscataway, N.J., U.S.A.) were used as secondary antibodies. Antibody reactions were visualized by enhanced chemiluminescence (Amersham Pharmacia Biotech).

RNA analysis

RNA extraction from *Xanthomonas*, cDNA synthesis and reverse transcription polymerase chain reaction (RT-PCR) experiments were performed as described [61].

Generation of a *xopL* deletion strain

To generate a genomic deletion of *xopL* 2 kb and 1.1 kb fragments upstream and downstream of *xopL* were amplified by PCR from genomic DNA of *Xcv* 85-10 using oligonucleotides harboring appropriate restriction sites. PCR-fragments were cloned into the suicide vector pK18mobsac [62]. The resulting constructs were conjugated into *Xcv* strain 85-10 and *xopL* deletion mutants were selected by PCR.

xopL expression constructs

To generate binary expression constructs, the coding sequence of *xopL* was amplified by PCR, fused to a *Strep*-tag-coding sequence, cloned into pENTR/D-TOPO (Invitrogen GmbH, Karlsruhe, Germany) and recombined into pGWB2 [63] using GATEWAY technology (Invitrogen). XopL-derivatives listed in Table S3 (in Text S1) were generated using the Phusion Site-Directed Mutagenesis Kit (Fisher Scientific GmbH, Schwerte, Germany). To generate *avrBs3Δ2*-fusions, the promoter and 5′coding sequence of *xopL* were amplified by PCR, cloned into pENTR/D-TOPO and recombined into pL6GW356 [64]. Sequences of oligonucleotides are available upon request.

Electrolyte leakage measurements and statistical analysis

Triplicates of five leaf discs each (0.9 cm in diameter) were harvested 2 dpi and 4 dpi. Measurements were carried out as described [65]. Values (n = 3) for XopL and each of its derivatives were compared to GFP (control) using unpaired Student's *t*-test.

In vitro E3 ligase assays

In vitro E3 ligase assays were performed as described [17,19]. *Arabidopsis* E2s used in this study were amplified from the CD4-16 cDNA library from the Arabidopsis Biological Resource Centre (ABRC, www.arabidopsis.org/abrc) and cloned into expression plasmid p15Tv-L (gi |134105575|). Plasmids encoding AtUBC28-variants R5A, F62A, K63A and A96D were generated using the Quick Change Site-Directed Mutagenesis II kit (Agilent Technologies Canada, Inc., Mississauga, Canada). The E1-enzyme, ubiquitin and ubiquitin mutants were purchased from Boston Biochem (Cambridge, USA). Ubiquitin- and His antibodies were purchased from EMD Millipore (Billerica, USA) and Qiagen (Toronto, Canada), respectively. His-tagged UBE2D2 was prepared as described [19], and *Arabidopsis* wild-type and mutant His-tagged E2s were purified accordingly. Sequences of oligonucleotides are available upon request.

In vitro ubiquitination reactions were analyzed by LC-MS/MS on OrbitrapVelos as described [66]. Briefly, 20 µl reactions containing 0.029 µM E1, 3 µM E2, 6 µM E3, 25 µM ubiquitin and 10 mM ATP (in 50 mM Tris pH 7.5 buffer, with 0.1 M NaCl, 10 mM $MgCl_2$ and 0.5 mM DTT) were incubated at 25°C for 3 hours. Reactions were stopped by the addition of 2× Laemmli buffer and incubation for 5 minutes at 95°C. Proteins were separated by SDS-PAGE, and the gel band corresponding to >100 kDa excised and trypsinized. 1/10th of each band was analyzed in duplicates.

Protein purification, expression and crystallization

Fragments of Xcv_{XopL} (XCV3220, gi 28872465) and *Xanthomonas campestris* pv. *campestris* str. ATCC 33913 XopL (XCC4186, gi 21233603) were cloned into expression plasmid p15Tv-L, followed by transformation of *E. coli* BL21(DE3)-RIPL (Agilent Technologies Canada, Inc., Mississauga, Canada). After optimizing solubility, *E. coli* cells expressing XopL fragments were cultured in 1 l LB at 37°C to an optical density (600 nm) of approximately 1.2, before IPTG was added to induce protein expression. Selenomethionine-enriched protein was produced following growth and induction of cells in SeMet high-yield media (Shanghai Medicilon, Shanghai, China). After induction, bacteria were incubated overnight on a shaker at 25°C. Cells were harvested by centrifugation, disrupted by sonication, and the insoluble material was removed by centrifugation. XopL fragments were purified using Ni-NTA affinity chromatography and dialyzed at 4°C in 10 mM HEPES (pH 7.5), 500 mM NaCl and 0.5 mM TCEP, concentrated to >15 mg/ml and stored at −70° C.

Crystallization trials were performed at room temperature using hanging-drop vapor diffusion with an optimized sparse matrix crystallization screen [67], with or without limiting amounts of proteases [68] including TEV. XopL[aa 144–450] crystals were grown at 25 mg/ml. The XopL[aa 144–450] crystal used for data collection (see Table 1) was grown from a crystallization liquor containing 0.2 M Potassium Sulfate and 20% PEG3350 monodisperse (Hampton Research, Aliso Viejo, USA) and cryoprotected in a similar buffer containing 10% glycerol and flash-frozen in liquid nitrogen, while the XopL[aa 474–660] crystal was grown using a protein concentration of 26 mg/ml from a crystallization liquor containing 0.1 M Tris pH 8.5, 0.2 M Sodium Acetate, 30% PEG4K and 4% ethylene glycol, cryoprotected using Paratone-N oil (Hampton Research) and flash-frozen in liquid nitrogen.

Data collection, structure determination and refinement

The structure of XopL[aa 144–450] was determined by a crystal derived from selenomethionine-enriched protein with SAD phasing using a peak wavelength of λ = 0.97937 Å. Diffraction data were collected at 100° K at APS beamline 19-BM. Diffraction data were integrated and scaled at the beamline using HKL3000 [69]. Positions of heavy atoms were found using SHELXD [70], followed by solvent flattening using SHELXE [71], which was in turn used to automatically build an initial model using ArpWARP [72], all used within the CCP4 program suite [73]. The model was improved by alternate cycles of manual building and water-picking

using COOT [74] and restrained refinement against a maximum-likelihood target with 5% of the reflections randomly excluded as an R_{free} test set. These refinement steps were performed using REFMAC in the CCP4 program suite. In addition we refined using Phenix.refine from the PHENIX crystallography suite [75,76]. The final model contained a nearly complete chain containing 4 residues in the Ni-affinity tag and residues 145–437, in which the C-terminal Gly residue from the tag, residues 144, 297 and 438–450 were omitted due to protein disorder, and was refined to an R_{work} and R_{free} of 17.1 and 22.6%, respectively, including TLS parameterization [77,78]. The structure of XopL[aa 474–660] was also solved by SAD phasing at peak wavelength ($\lambda = 0.97921$ Å) using a selenomethionine-enriched crystal. Structure solution, model building and refinement followed a similar protocol as for XopL[aa 144–450]. However, during refinement, phenix.xtriage, as part of the PHENIX crystallography suite, we detected merohedral twinning with twin law h, -h-k, -l and a twinning fraction of 0.273. Refinement then proceeded with a newly derived R_{free} set to take the twinning into consideration. As stated above, the final model contained three molecules in the asymmetric unit. Molecule A contains a complete chain involving the 5 most C-terminal residues from the Ni-affinity tag followed by residues 474–639. No electron density for residues 641–660 was observed due to protein disorder. Molecules B and C contained a very similar chain. In addition, in molecule B, the 6 most C-terminal residues of the Ni-affinity tag were modeled as well as residues 640–642. In molecule C, residues 474–476 were not modeled due to protein disorder, but residue 640 was. The final model (to 1.8 Å) was refined to an R_{work} and R_{free} of 15.2 and 19.4%, respectively.

Data collection, phasing and structure refinement statistics for both structures are summarized in Table 1. The Ramachandran plot generated by PROCHECK [79] showed very good stereochemistry overall with 99.6 and 100% of the residues in the most favored and additional allowed regions for XopL[aa 144–450] and XopL[aa 474–660], respectively.

Mesophyll protoplast transient expression assay and immunoblot-based detection of MAPK activity

Transient expression experiments with *A. thaliana* (Col-0)-derived protoplasts were carried out as described [28]. Protoplast samples were co-transformed with the *NHL10* promoter-luciferase construct [27,28], *pUBQ10-GUS* [80] and either *p35S*-effector gene constructs (*xopL*, $xopL_{Q612A}$, $xopL_{CTD[aa450–660]}$) or *p35S-cfp* as control (10 µg total DNA per 100 µl protoplasts; ratio 1:1:1). Activity of MAPKs was determined by protein extraction and immunoblotting using a specific pTepY-antibody as described previously [25]. GUS-activity was determined by measuring the turnover of 4-MUG (4-Methylumbelliferyl-β-D-glucuronide) with a Cytofluor II Platereader (Millipore Corp.; excitation 380 nm, emission 460 nm).

Accession numbers

Coordinates for the XopL LRR domain (XopL[aa 144–450]) and the C-terminal domain (XopL[aa 474–660]) structures were deposited at the Protein Data Bank with accession codes 4FCG and 4FC9, respectively. XCV3220 (XopL) and XCC4186 (XccXopL) are targets APC108260 and APC105826 of the Midwest Center for Structural Genomics, respectively.

Supporting Information

Figure S1 Multiple sequence alignment of XopL homologues. The amino acid sequences of XopL from *Xcv* and homologous proteins from other *Xanthomonas* spp. were aligned by ClustalX [12]. Red cylinders, blue arrows, black lines and dashed black lines represent helical, β-strand, structured loop and disordered regions in XopL, respectively as observed in the XopL[aa 144–450] and XopL[aa 474–660] structures. Cyan lines represent the ordered vector sequences observed in both the XopL[aa 144–450] and XopL[aa 474–660] structures. Mutated residues in the C-terminal domain of XopL, which abrogated PCD are marked with magenta circles or boxes. Mutated residues which elicited cell death similar to wild-type XopL are labeled with blue circles. Secondary structural elements are labeled, but helical regions <5 residues are marked and not labeled, as they may be considered helical loops rather than helices per se. Sequences of XopL and homologous proteins were aligned in the following order: XopL, *X. campestris* pv. *vesicatoria* 85-10 (Xcv), gi|78048776|; PopC, *X. oryzae* pv. *oryzicola* (X. oryzicola), gi|108946646|; PXO016102, *X. oryzae* pv. *oryzae* PXO99A (Xoo_PXO99A), gi|188577374|; XopL, *X. perforans* 91-118 (X. perforans), gi|325925746|; XAC3090, *X. axonopodis* pv. *citri* 306 (Xac_306), gi|77748695|; XopL, *X. fuscans* spp. *aurantifolii* ICPB 11122 (X. fuscans aurant), gi|294627335|;XopL, *X. gardneri* ATCC 19865 (X. gardneri), gi|325919350|; and XCC4186, *X. campestris* pv. *campestris* ATCC 33913 (Xcc), gi|21233603|.
(TIF)

Figure S2 Genetic analysis of the type III effector candidate XopL. (**A**) RT-PCR analysis of the effector gene *xopL*. Fragments were amplified from cDNA derived from *Xcv* strains 85-10, 85* and 85*Δ*hrpX* using specific primers. Genomic DNA, H_2O and 16S rRNA were used as controls. (**B**) Type III secretion assay using the $XopL_{1–92}$-AvrBs3Δ2 reporter fusion. Strains 85* (wt) and 85*Δ*hrcV* (Δ*hrcV*) expressing $xopL_{1–92}$-*avrBs3Δ2* were grown in T3 secretion-inducing medium. Total cell extracts (TE) and culture supernatants (SN) were analyzed by immunoblotting using an AvrBs3-specific antibody. (**C**) *Xcv* strains described in (B), 85-10 and 85*Δ*hpaB* were tested for translocation of $XopL_{1–92}$-AvrBs3Δ2 in AvrBs3-responsive pepper plants (ECW-30R). Leaves were harvested 4 dpi and bleached in ethanol for better visualization of the hypersensitive response (HR). (**D**) Leaves of susceptible (ECW) and resistant (ECW-10R) pepper plants were inoculated with *Xcv* wild-type strain 85-10 (wt) and a genomic deletion mutant of *xopL* (Δ*xopL*) at 10^8 cfu/ml. Pictures of disease symptoms (ECW) were taken 6 dpi. For better visualization of the HR, leaves were bleached in ethanol 2 dpi.
(TIF)

Figure S3 Expression of XopL-HA in protoplasts. (**A**) Total protein extracted from protoplasts described in Figure 2D were subjected to an anti-HA immunoblot to detect expression of CFP, AvrPto, XopL, $XopL_{Q612A}$, $XopL_{LRR}$ and $XopL_{CTD}$. (**B**) To determine viability of the protoplasts, GUS (β-glucuronidase) measurements were carried out at the end of the experiment as explained in Figure 2B. There is no statistically significant difference between the samples (1way ANOVA with Kruskal-Wallis post test; n = 9).
(TIF)

Figure S4 SDS-PAGE of XopL fragments used in this study following protein purification. Note that a persistent contaminant in purified full-length XopL is denoted by an asterisk.
(TIF)

Figure S5 Analysis of cell death induction and ubiquitination by XopL and different derivatives in *Nicotiana benthamiana*. *Agrobacterium*-mediated expression of *gfp*, *xopL* and

constructs encoding the following XopL mutant derivatives: Δ163–185, Δ330–336, D502A, R505A N506A, A512E P513A, K578A, A579W, P517A K519A R520A, H584A L585A G586E, E598A S600A, L619A, XopL[aa 1–449] (LRR), XopL[aa 450–660] (CTD) in leaves of *N. benthamiana* at 8×10^8 cfu/ml. (**A**) Phenotypes of the inoculated leaf area were documented 6 dpi. (**B**) Electrolyte leakage measurements for quantification of cell death reactions 2 dpi (light grey bars) and 4 dpi (dark grey bars), respectively. Bars represent triplicates of 5 leaf discs each and standard deviations thereof. Asterisks indicate statistically significant differences compared to GFP control (*t*-test, $P<0.05$). (**C**) Leaf tissue was harvested 2 dpi and plant protein extracts were analyzed by immunoblotting using *Strep*-tag- (α-Strep) and ubiquitin-specific antibodies (α-Ub), respectively. Signals specific for full length XopL, XopL[aa 1–449] and XopL[aa 450–660] are labeled. $(Ub)_n$ indicates polyubiqutination. Equal loading is demonstrated by Ponceau staining of Rubisco. The experiments were performed three times with similar results.
(TIF)

Figure S6 ***In vitro*** **E3 ligase reaction of the XL-box and various point mutants.** (**A**) Ubiquitination reaction of the wild-type and mutated XL-box fragments. As denoted, ubiquitination reactions were performed for 2 hours, run on a 10–15% SDS-PAGE step gradient gel and probed with anti-ubiquitin antibodies (α-Ub). To demonstrate similar loading, a 15% SDS-PAGE gel was run of the starting material (t = 0) and both stained with Coomassie blue (**B**) or probed with anti-His antibodies (α-His) (**C**).
(TIF)

Text S1 This file includes Supplemental Tables S1, S2, S3 and Supplemental References.
(DOC)

Acknowledgments

We would like to thank all members of the Structural Biology Center beamline (beamline 19) at Argonne National Laboratory, particularly Kemin Tan, as well as Matthew Zimmerman from the laboratory of Wladek Minor (University of Virginia) for help in diffraction data collection and analysis, and B. Rosinsky for greenhouse work. We are grateful to D. Büttner and N. Adlung for critical reading of the manuscript. A.U. Singer, T. Skarina, X. Xu, H. Cui and A. Savchenko are all participants of the Midwest Centre for Structural Genomics (MCSG).

Author Contributions

Conceived and designed the experiments: A.U. Singer, S. Schulze, X. Xu, T. Srikumar, B. Raught, U. Bonas, A. Savchenko, L. Eschen-Lippold, J. Lee, D. Scheel. Performed the experiments: A.U. Singer, S. Schulze. X. Xu, T. Srikumar, H. Cui, M. Egler, T. Skarina, L. Eschen-Lippold. Analyzed the data: A.U. Singer, S. Schulze, T. Skarina, T. Srikumar, M. Egler, B. Raught, U. Bonas, A. Savchenko, L. Eschen-Lippold, J. Lee, D. Scheel. Contributed reagents/materials/analysis tools: X. Xu, H. Cui, B. Raught, J. Lee, D. Scheel. Wrote the paper: A.U. Singer, S. Schulze, U. Bonas, A. Savchenko.

References

1. Block A, Alfano JR (2011) Plant targets for *Pseudomonas syringae* type III effectors: virulence targets or guarded decoys? Curr Opin Microbiol 14: 39–46.
2. Büttner D, Bonas U (2009) Regulation and secretion of *Xanthomonas* virulence factors. FEMS Microbiol Rev 34: 107–133.
3. Jones JD, Dangl JL (2006) The plant immune system. Nature 444: 323–329.
4. Felix G, Duran JD, Volko S, Boller T (1999) Plants have a sensitive perception system for the most conserved domain of bacterial flagellin. Plant J 18: 265–276.
5. Kunze G, Zipfel C, Robatzek S, Niehaus K, Boller T, et al. (2004) The N terminus of bacterial elongation factor Tu elicits innate immunity in Arabidopsis plants. Plant Cell 16: 3496–3507.
6. Asai T, Tena G, Plotnikova J, Willmann MR, Chiu WL, et al. (2002) MAP kinase signalling cascade in *Arabidopsis* innate immunity. Nature 415: 977–983.
7. Boller T, Felix G (2009) A renaissance of elicitors: perception of microbe-associated molecular patterns and danger signals by pattern-recognition receptors. Annu Rev Plant Biol 60: 379–406.
8. White FF, Potnis N, Jones JB, Koebnik R (2009) The type III effectors of *Xanthomonas*. Mol Plant Pathol 10: 749–766.
9. Stevens JM, Galyov EE, Stevens MP (2006) Actin-dependent movement of bacterial pathogens. Nat Rev Microbiol 4: 91–101.
10. Kay S, Hahn S, Marois E, Hause G, Bonas U (2007) A bacterial effector acts as a plant transcription factor and induces a cell size regulator. Science 318: 648–651.
11. Römer P, Hahn S, Jordan T, Strauss T, Bonas U, et al. (2007) Plant pathogen recognition mediated by promoter activation of the pepper *Bs3* resistance gene. Science 318: 645–648.
12. Abramovitch RB, Janjusevic R, Stebbins CE, Martin GB (2006) Type III effector AvrPtoB requires intrinsic E3 ubiquitin ligase activity to suppress plant cell death and immunity. Proc Natl Acad Sci U S A 103: 2851–2856.
13. Janjusevic R, Abramovitch RB, Martin GB, Stebbins CE (2006) A bacterial inhibitor of host programmed cell death defenses is an E3 ubiquitin ligase. Science 311: 222–226.
14. Kerscher O, Felberbaum R, Hochstrasser M (2006) Modification of proteins by ubiquitin and ubiquitin-like proteins. Annu Rev Cell Dev Biol 22: 159–180.
15. Ye Y, Rape M (2009) Building ubiquitin chains: E2 enzymes at work. Nat Rev Mol Cell Biol 10: 755–764.
16. Ardley HC, Robinson PA (2005) E3 ubiquitin ligases. Essays Biochem 41: 15–30.
17. Wu B, Skarina T, Yee A, Jobin MC, Dileo R, et al. (2010) NleG Type 3 effectors from enterohaemorrhagic *Escherichia coli* are U-Box E3 ubiquitin ligases. PLoS Pathog 6: e1000960.
18. Quezada CM, Hicks SW, Galan JE, Stebbins CE (2009) A family of *Salmonella* virulence factors functions as a distinct class of autoregulated E3 ubiquitin ligases. Proc Natl Acad Sci U S A 106: 4864–4869.
19. Singer AU, Rohde JR, Lam R, Skarina T, Kagan O, et al. (2008) Structure of the *Shigella* T3SS effector IpaH defines a new class of E3 ubiquitin ligases. Nat Struct Mol Biol 15: 1293–1301.
20. Hotson A, Chosed R, Shu H, Orth K, Mudgett MB (2003) *Xanthomonas* type III effector XopD targets SUMO-conjugated proteins *in planta*. Mol Microbiol 50: 377–389.
21. Akimoto-Tomiyama C, Furutani A, Tsuge S, Washington EJ, Nishizawa Y, et al. (2012) XopR, a type III effector secreted by *Xanthomonas oryzae* pv. *oryzae*, suppresses microbe-associated molecular pattern-triggered immunity in *Arabidopsis thaliana*. Mol Plant Microbe Interact 25: 505–514.
22. Göhre V, Spallek T, Haweker H, Mersmann S, Mentzel T, et al. (2008) Plant pattern-recognition receptor FLS2 is directed for degradation by the bacterial ubiquitin ligase AvrPtoB. Curr Biol 18: 1824–1832.
23. Guo M, Tian F, Wamboldt Y, Alfano JR (2009) The majority of the type III effector inventory of *Pseudomonas syringae* pv. *tomato* DC3000 can suppress plant immunity. Mol Plant Microbe Interact 22: 1069–1080.
24. Kim JG, Li X, Roden JA, Taylor KW, Aakre CD, et al. (2009) *Xanthomonas* T3S Effector XopN Suppresses PAMP-Triggered Immunity and Interacts with a Tomato Atypical Receptor-Like Kinase and TFT1. Plant Cell 21: 1305–1323.
25. Schulze S, Kay S, Büttner D, Egler M, Eschen-Lippold L, et al. (2012) Analysis of new type III effectors from *Xanthomonas* uncovers XopB and XopS as suppressors of plant immunity. New Phytol 195: 894–911.
26. Feng F, Yang F, Rong W, Wu X, Zhang J, et al. (2012) A *Xanthomonas* uridine 5′-monophosphate transferase inhibits plant immune kinases. Nature 485: 114–118.
27. Boudsocq M, Willmann MR, McCormack M, Lee H, Shan L, et al. (2010) Differential innate immune signalling via Ca(2+) sensor protein kinases. Nature 464: 418–422.
28. Ranf S, Eschen-Lippold L, Pecher P, Lee J, Scheel D (2011) Interplay between calcium signalling and early signalling elements during defence responses to microbe- or damage-associated molecular patterns. Plant J 68: 100–113.
29. Zheng MS, Takahashi H, Miyazaki A, Hamamoto H, Shah J, et al. (2004) Up-regulation of *Arabidopsis thaliana NHL10* in the hypersensitive response to *Cucumber mosaic virus* infection and in senescing leaves is controlled by signalling pathways that differ in salicylate involvement. Planta 218: 740–750.
30. Zipfel C, Robatzek S, Navarro L, Oakeley EJ, Jones JD, et al. (2004) Bacterial disease resistance in *Arabidopsis* through flagellin perception. Nature 428: 764–767.
31. Bethke G, Pecher P, Eschen-Lippold L, Tsuda K, Katagiri F, et al. (2012) Activation of the *Arabidopsis thaliana* mitogen-activated protein kinase MPK11 by the flagellin-derived elicitor peptide, flg22. Mol Plant Microbe Interact 25: 471–480.
32. Tena G, Boudsocq M, Sheen J (2011) Protein kinase signaling networks in plant innate immunity. Curr Opin Plant Biol 14: 519–529.
33. He P, Shan L, Lin NC, Martin GB, Kemmerling B, et al. (2006) Specific bacterial suppressors of MAMP signaling upstream of MAPKKK in *Arabidopsis* innate immunity. Cell 125: 563–575.

34. Kraft E, Stone SL, Ma L, Su N, Gao Y, et al. (2005) Genome analysis and functional characterization of the E2 and RING-type E3 ligase ubiquitination enzymes of Arabidopsis. Plant Physiol 139: 1597–1611.
35. Huang L, Kinnucan E, Wang G, Beaudenon S, Howley PM, et al. (1999) Structure of an E6AP-UbcH7 complex: insights into ubiquitination by the E2-E3 enzyme cascade. Science 286: 1321–1326.
36. Kamadurai HB, Souphron J, Scott DC, Duda DM, Miller DJ, et al. (2009) Insights into ubiquitin transfer cascades from a structure of a UbcH5B approximately ubiquitin-HECT(NEDD4L) complex. Mol Cell 36: 1095–1102.
37. Lin DY, Diao J, Chen J (2012) Crystal structures of two bacterial HECT-like E3 ligases in complex with a human E2 reveal atomic details of pathogen-host interactions. Proc Natl Acad Sci U S A 109: 1925–1930.
38. Sakata E, Satoh T, Yamamoto S, Yamaguchi Y, Yagi-Utsumi M, et al. (2010) Crystal structure of UbcH5b~ubiquitin intermediate: insight into the formation of the self-assembled E2~Ub conjugates. Structure 18: 138–147.
39. Zhu Y, Li H, Hu L, Wang J, Zhou Y, et al. (2008) Structure of a *Shigella* effector reveals a new class of ubiquitin ligases. Nat Struct Mol Biol 15: 1302–1308.
40. Diao J, Zhang Y, Huibregtse JM, Zhou D, Chen J (2008) Crystal structure of SopA, a *Salmonella* effector protein mimicking a eukaryotic ubiquitin ligase. Nat Struct Mol Biol 15: 65–70.
41. Singer AU, Desveaux D, Betts L, Chang JH, Nimchuk Z, et al. (2004) Crystal structures of the type III effector protein AvrPphF and its chaperone reveal residues required for plant pathogenesis. Structure 12: 1669–1681.
42. Nuber U, Scheffner M (1999) Identification of determinants in E2 ubiquitin-conjugating enzymes required for hect E3 ubiquitin-protein ligase interaction. J Biol Chem 274: 7576–7582.
43. Christensen DE, Brzovic PS, Klevit RE (2007) E2-BRCA1 RING interactions dictate synthesis of mono- or specific polyubiquitin chain linkages. Nat Struct Mol Biol 14: 941–948.
44. Levin I, Eakin C, Blanc MP, Klevit RE, Miller SI, et al. (2010) Identification of an unconventional E3 binding surface on the UbcH5~Ub conjugate recognized by a pathogenic bacterial E3 ligase. Proc Natl Acad Sci U S A 107: 2848–2853.
45. Chau V, Tobias JW, Bachmair A, Marriott D, Ecker DJ, et al. (1989) A multiubiquitin chain is confined to specific lysine in a targeted short-lived protein. Science 243: 1576–1583.
46. Deng L, Wang C, Spencer E, Yang L, Braun A, et al. (2000) Activation of the IkappaB kinase complex by TRAF6 requires a dimeric ubiquitin-conjugating enzyme complex and a unique polyubiquitin chain. Cell 103: 351–361.
47. Xu P, Duong DM, Seyfried NT, Cheng D, Xie Y, et al. (2009) Quantitative proteomics reveals the function of unconventional ubiquitin chains in proteasomal degradation. Cell 137: 133–145.
48. Goto E, Yamanaka Y, Ishikawa A, Aoki-Kawasumi M, Mito-Yoshida M, et al. (2010) Contribution of lysine 11-linked ubiquitination to MIR2-mediated major histocompatibility complex class I internalization. J Biol Chem 285: 35311–35319.
49. Rape M (2010) Assembly of K11-linked ubiquitin chains by the anaphase-promoting complex. Subcell Biochem 54: 107–115.
50. Wickliffe KE, Williamson A, Meyer HJ, Kelly A, Rape M (2011) K11-linked ubiquitin chains as novel regulators of cell division. Trends Cell Biol 21: 656–663.
51. Chou YC, Keszei AF, Rohde JR, Tyers M, Sicheri F (2012) Conserved Structural Mechanisms for Autoinhibition in IpaH Ubiquitin Ligases. J Biol Chem 287: 268–275.
52. Cheng W, Munkvold KR, Gao H, Mathieu J, Schwizer S, et al. (2011) Structural analysis of *Pseudomonas syringae* AvrPtoB bound to host BAK1 reveals two similar kinase-interacting domains in a type III Effector. Cell Host Microbe 10: 616–626.
53. Daniels MJ, Barber CE, Turner PC, Sawczyc MK, Byrde RJW, et al. (1984) Cloning of genes involved in pathogenicity of *Xanthomonas campestris* pv. *campestris* using the broad host range cosmid pLAFR1. EMBO J 3: 3323–3328.
54. Ausubel FM, Brent R, Kingston RE, Moore DD, Seidman JG, et al (1996) Current protocols in molecular biology. New York: John Wiley & Sons, Inc.
55. Figurski D, Helinski DR (1979) Replication of an origin-containing derivative of plasmid RK2 dependent on a plasmid function provided *in trans*. Proc Natl Acad Sci USA 76: 1648–1652.
56. Minsavage GV, Dahlbeck D, Whalen MC, Kearny B, Bonas U, et al. (1990) Gene-for-gene relationships specifying disease resistance in *Xanthomonas campestris* pv. *vesicatoria* - pepper interactions. Mol Plant-Microbe Interact 3: 41–47.
57. Koncz C, Schell J (1986) The promoter of T_L-DNA gene 5 controls the tissue specific expression of chimaeric genes carried by a novel type of *Agrobacterium* binary vector. Mol Gen Genet 204: 383–396.
58. Rossier O, Wengelnik K, Hahn K, Bonas U (1999) The *Xanthomonas* Hrp type III system secretes proteins from plant and mammalian pathogens. Proc Natl Acad Sci USA 96: 9368–9373.
59. Rossier O, Van den Ackerveken G, Bonas U (2000) HrpB2 and HrpF from *Xanthomonas* are type III-secreted proteins and essential for pathogenicity and recognition by the host plant. Mol Microbiol 38: 828–838.
60. Knoop V, Staskawicz B, Bonas U (1991) Expression of the avirulence gene *avrBs3* from *Xanthomonas campestris* pv. vesicatoria is not under the control of *hrp* genes and is independent of plant factors. J Bacteriol 173: 7142–7150.
61. Thieme F, Szczesny R, Urban A, Kirchner O, Hause G, et al. (2007) New type III effectors from *Xanthomonas campestris* pv. *vesicatoria* trigger plant reactions dependent on a conserved N-myristoylation motif. Mol Plant Microbe Interact 20: 1250–1261.
62. Schäfer A, Tauch A, Jäger W, Kalinowski J, Thierbach G, et al. (1994) Small mobilizable multi-purpose cloning vectors derived from the *Escherichia coli* plasmids pK18 and pK19: selection of defined deletions in the chromosome of *Corynebacterium glutamicum*. Gene 145: 69–73.
63. Nakagawa T, Kurose T, Hino T, Tanaka K, Kawamukai M, et al. (2007) Development of series of gateway binary vectors, pGWBs, for realizing efficient construction of fusion genes for plant transformation. J Biosci Bioeng 104: 34–41.
64. Noël L, Thieme F, Gabler J, Büttner D, Bonas U (2003) XopC and XopJ, two novel type III effector proteins from *Xanthomonas campestris* pv. vesicatoria. J Bacteriol 185: 7092–7102.
65. Szczesny R, Büttner D, Escolar L, Schulze S, Seiferth A, et al. (2010) Suppression of the AvrBs1-specific hypersensitive response by the YopJ effector homolog AvrBsT from *Xanthomonas* depends on a SNF1-related kinase. New Phytol 187: 1058–1074.
66. Sheng Y, Hong JH, Doherty R, Srikumar T, Shloush J, et al. (2012) A human ubiquitin conjugating enzyme (E2) - HECT E3 ligase structure-function screen. Mol Cell Proteomics 11: 329–41.
67. Kimber MS, Vallee F, Houston S, Necakov A, Skarina T, et al. (2003) Data mining crystallization databases: knowledge-based approaches to optimize protein crystal screens. Proteins 51: 562–568.
68. Dong A, Xu X, Edwards AM, Chang C, Chruszcz M, et al. (2007) *In situ* proteolysis for protein crystallization and structure determination. Nat Methods 4: 1019–1021.
69. Minor W, Cymborowski M, Otwinowski Z, Chruszcz M (2006) *HKL*-3000: the integration of data reduction and structure solution–from diffraction images to an initial model in minutes. Acta Crystallogr D Biol Crystallogr 62: 859–866.
70. Schneider TR, Sheldrick GM (2002) Substructure solution with *SHELXD*. Acta Crystallogr D Biol Crystallogr 58: 1772–1779.
71. Sheldrick GM (2008) A short history of *SHELX*. Acta Crystallogr A 64: 112–122.
72. Perrakis A, Morris R, Lamzin VS (1999) Automated protein model building combined with iterative structure refinement. Nat Struct Biol 6: 458–463.
73. (1994) The *CCP4* suite: programs for protein crystallography. Acta Crystallogr D Biol Crystallogr 50: 760–763.
74. Emsley P, Cowtan K (2004) *Coot*: model-building tools for molecular graphics. Acta Crystallogr D Biol Crystallogr 60: 2126–2132.
75. Adams PD, Afonine PV, Bunkoczi G, Chen VB, Davis IW, et al. (2010) *PHENIX*: a comprehensive Python-based system for macromolecular structure solution. Acta Crystallogr D Biol Crystallogr 66: 213–221.
76. Zwart PH, Afonine PV, Grosse-Kunstleve RW, Hung LW, Ioerger TR, et al. (2008) Automated structure solution with the *PHENIX* suite. Methods Mol Biol 426: 419–435.
77. Winn MD, Murshudov GN, Papiz MZ (2003) Macromolecular TLS refinement in REFMAC at moderate resolutions. Methods Enzymol 374: 300–321.
78. Winn MD, Isupov MN, Murshudov GN (2001) Use of TLS parameters to model anisotropic displacements in macromolecular refinement. Acta Crystallogr D Biol Crystallogr 57: 122–133.
79. Laskowski R A MMW, Moss DS, Thornton J M (1993) *PROCHECK*: a program to check the stereochemical quality of protein structures. J Appl Cryst 26: 283–291.
80. Norris SR, Meyer SE, Callis J (1993) The intron of *Arabidopsis thaliana* polyubiquitin genes is conserved in location and is a quantitative determinant of chimeric gene expression. Plant Mol Biol 21: 895–906.

2.3.1.1 Anlagen zur Publikation 3

Supplemental Text S1

Type III secretion and translocation assays of XopL

The T3S system of *Xcv* is encoded by the 23 kb chromosomal *hrp* (hypersensitive response and pathogenicity) gene cluster, which is essential for bacterial growth and disease symptoms on susceptible plants as well as for induction of the HR in resistant host and nonhost plants [1]. Expression of *hrp* genes is induced *in planta* by the OmpR-family regulator HrpG which controls the expression of a genome-wide regulon [2] including the AraC-type transcriptional activator *hrpX* [3,4]. HrpX binds to *cis*-regulatory PIP (plant-inducible promoter) boxes in the promoter regions of *hrp* and other genes that contribute to virulence [5].

To analyze type III-dependent secretion and translocation of XopL, a 1269 bp fragment containing the native promoter and 276 bp 5' coding sequence (92 aa) was amplified from genomic DNA of *Xcv* 85-10, cloned into the effector reporter plasmid pL6GW356 [6] and conjugated into *Xcv* strain 85-10 and derivatives thereof. Strain 85* is a derivative of strain 85-10 and expresses a constitutively active HrpG protein resulting in constitutive expression of the T3S system. The T3S mutant 85*Δ*hrcV* features the deletion of a gene encoding a conserved inner membrane component of the T3S system [7], and 85*Δ*hpaB* lacks the general T3S-chaperone, which is important for secretion and translocation of certain effectors [8,9]. The native promoter and 5´ coding region of *xopL* was fused to the reporter construct *avrBs3Δ2*, which lacks a T3S signal but retains a functional effector domain [6,10].

In vitro secretion of $XopL_{1-92}$AvrBs3Δ2 clearly depended on a functional T3S system, because $XopL_{1-92}$-AvrBs3Δ2 was detectable in culture supernatants of strain 85* but not in the T3S-deficient strain 85^{*}Δ*hrcV* (Figure S2B). HrcJ, a lipoprotein in the inner membrane of the T3S system [7], was used as lysis control (data not shown). Translocation was tested by inoculation of strains 85-10, 85*, 85*Δ*hrcV* and 85*Δ*hpaB*, all carrying the $XopL_{1-92}$-AvrBs3Δ2 fusion construct, into leaves of pepper ECW-30R plants, that carry the *Bs3*-resistance gene. As shown in Figure S2C, 85-10($XopL_{1-92}$-AvrBs3Δ2) induced the HR. This indicates that *xopL* is expressed during infection of pepper leading to expression and translocation of $XopL_{1-92}$-AvrBs3Δ2. 85* expressing $XopL_{1-92}$-AvrBs3Δ2 also triggered the HR. As expected, no HR was induced by strain 85*Δ*hrcV* expressing $XopL_{1-92}$-AvrBs3Δ2 (Figure S2C). However, $XopL_{1-92}$-AvrBs3Δ2 was also translocated by the Δ*hpaB* strain lacking the T3S chaperone, which is in contrast to the XopL homologue XC_4273 from *X. c.* pv. *campestris* [11].

Table S1. MS/MS analysis of XopL ubiquitination reactions.

				Spectral Counts							
Xanthomonas XopL-derivative (E3 Enzyme)	E2 Enzyme	MS Run	Total Ub Peptides	K6	K11	K27	K29	K33	K48	K63	Total Linkages
Xcv3220_144-660	ATUBC28	1	2712	0	482	0	0	145	54	228	909
Xcv3220_144-660	ATUBC28	2	3700	0	654	0	0	203	58	365	1280
Xcv3220_144-660	hUBE2D2	1	389	0	19	0	0	5	3	3	30
Xcv3220_144-660	hUBE2D2	2	482	0	38	0	0	3	6	3	50
Xcv3220_474-660	hUBE2D2	1	431	0	18	0	0	6	12	3	39
Xcv3220_474-660	hUBE2D2	2	482	0	30	0	0	5	3	6	44
Xcc4186_330-496	ATUBC28	1	830	0	98	0	0	0	3	3	104
Xcc4186_330-496	ATUBC28	2	850	0	108	0	0	0	3	3	114
Xcv3220_144-660	ATUBC11	1*	16	0	0	0	0	0	0	0	0
Xcv3220_144-660	ATUBC11	2*	10	0	0	0	0	0	0	0	0
Xcv3220_144-660	ATUBC11	1	632	0	48	0	0	48	17	0	113
Xcv3220_144-660	ATUBC11	2	649	0	54	0	0	50	15	0	119

				Normalized Linkage Percentage						
Xanthomonas XopL-derivative (E3 Enzyme)	E2 Enzyme	MS Run	Total Ub Peptides	K6	K11	K27	K29	K33	K48	K63
Xcv3220_144-660	ATUBC28	1	2712	0%	57%	0%	0%	16%	5%	22%
Xcv3220_144-660	ATUBC28	2	3700	0%	55%	0%	0%	16%	4%	25%
Xcv3220_144-660	hUBE2D2	1	389	0%	66%	0%	0%	17%	9%	8%
Xcv3220_144-660	hUBE2D2	2	482	0%	79%	0%	0%	6%	10%	5%
Xcv3220_474-660	hUBE2D2	1	431	0%	50%	0%	0%	16%	27%	7%
Xcv3220_474-660	hUBE2D2	2	482	0%	71%	0%	0%	11%	6%	12%
Xcc4186_330-496	ATUBC28	1	830	0%	95%	0%	0%	0%	2%	2%
Xcc4186_330-496	ATUBC28	2	850	0%	96%	0%	0%	0%	2%	2%
Xcv3220_144_660	ATUBC11	1	632	0%	44%	0%	0%	43%	13%	0%
Xcv3220_144_660	ATUBC11	2	649	0%	47%	0%	0%	42%	11%	0%

Spectral counts for each ubiquitin (Ub) linkage type (along with unmodified Ub peptides) identified using the spectral matching algorithm SpectraST [13], with a ubiquitin spectral library ([14]; version Ub_Ubl_v5 (available at raughtlab.ca/resources/msresources.php) in *in vitro* ubiquitination assays using *Xanthomonas* XopL-derivatives (E3), Arabidopsis E2 (ATUBC11 or ATUBC28) or human E2 (hUBE2D2), E1 and ubiquitin. *In vitro* reactions were incubated for 3 hours, except for XopL[aa 144-660] (Xcv3220_144_660) plus ATUBC11, which was stopped immediately at t=0 hours (denoted by a *) or incubated for 2 hours. Reactions were separated via SDS-PAGE, and products migrating at >100 kDa were subjected to in-gel digestion. The resulting peptides were identified using tandem mass spectrometry. Normalized percentages (%) [15] in each reaction are also provided.

Table S2. Arabidopsis E2 ubiquitin conjugating proteins used in E3 ligase assays.

Protein Name	Gene	GI	E2 family[1]	Human homologue
AtUBC11	At3g08690	18398206	VI	UBE2D2
AtUBC13	At3g46460	18408206	V	UBE2G1
AtUBC19	At3g20060	18402475	VIII	UBE2C
AtUBC28	At1g64230	18408001	VI	UBE2D2

[1]Based on the classification of Arabidopsis E2s in Kraft et al (2005).

Table S3. XopL derivatives tested *in vivo* in this study[1].

#	Position of amino acid exchange or deletion	cell death[2]	E3-ligase-activity[3]
	none (XopL wild-type)	+	+
1	LRR-domain (Δ450-660)	-	-
2	Δ163-185	+	+
3	R258A	+	n.a.
4	R280A	+	n.a.
5	W314A	+	n.a.
6	R258A R280A	+	n.a.
7	R258A W314A	+	n.a.
8	R280A W314A	+	n.a.
9	R258A R280A W314A	+	n.a.
10	Δ330-336	-	+
11	K334A	+	n.a.
12	R336A	+	n.a.
13	R359A	+	n.a.
14	K383A	+	n.a.
15	R359A R379A	+	n.a.
16	R359A K383A	+	n.a.
17	R379A K383A	+	n.a.
18	K403A	+	n.a.
19	C-terminal domain (Δ1-449)	-	+
20	D502A	-	-
21	R505A N506A	-	-
22	A512E P513A	-	-
23	K578A	-	-
24	A579W	-	-
25	P517A K519A R520A	-	-
26	H584A L585A G586E	-	-
27	E598A S600A	+	+
28	Q612A	-	-
29	L619A	+	+

[1] XopL derivatives were analyzed by transient expression in *N. benthamiana* regarding their [2]ability to trigger cell death and [3]E3 ligase activity. (+): PCD or E3 ligase activity detectable. (-): PCD or E3 ligase activity not detectable, n.a. not analyzed)

Supplemental References

1. Bonas U, Schulte R, Fenselau S, Minsavage GV, Staskawicz BJ, et al. (1991) Isolation of a gene-cluster from *Xanthomonas campestris* pv. *vesicatoria* that determines pathogenicity and the hypersensitive response on pepper and tomato. Mol Plant-Microbe Interact 4: 81-88.
2. Noël L, Thieme F, Nennstiel D, Bonas U (2001) cDNA-AFLP analysis unravels a genome-wide *hrpG*-regulon in the plant pathogen *Xanthomonas campestris* pv. *vesicatoria*. Mol Microbiol 41: 1271-1281.
3. Wengelnik K, Bonas U (1996) HrpXv, an AraC-type regulator, activates expression of five of the six loci in the *hrp* cluster of *Xanthomonas campestris* pv. vesicatoria. J Bacteriol 178: 3462-3469.
4. Wengelnik K, Van den Ackerveken G, Bonas U (1996) HrpG, a key *hrp* regulatory protein of *Xanthomonas campestris* pv. *vesicatoria* is homologous to two-component response regulators. Mol Plant-Microbe Interact 9: 704-712.
5. Koebnik R, Krüger A, Thieme F, Urban A, Bonas U (2006) Specific binding of the *Xanthomonas campestris* pv. vesicatoria AraC-type transcriptional activator HrpX to plant-inducible promoter boxes. J Bacteriol 188: 7652-7660.
6. Noël L, Thieme F, Gabler J, Büttner D, Bonas U (2003) XopC and XopJ, two novel type III effector proteins from *Xanthomonas campestris* pv. vesicatoria. J Bacteriol 185: 7092-7102.
7. Rossier O, Van den Ackerveken G, Bonas U (2000) HrpB2 and HrpF from *Xanthomonas* are type III-secreted proteins and essential for pathogenicity and recognition by the host plant. Mol Microbiol 38: 828-838.
8. Büttner D, Lorenz C, Weber E, Bonas U (2006) Targeting of two effector protein classes to the type III secretion system by a HpaC- and HpaB-dependent protein complex from *Xanthomonas campestris* pv. *vesicatoria*. Mol Microbiol 59: 513-527.
9. Schulze S, Kay S, Büttner D, Egler M, Eschen-Lippold L, et al. (2012) Analysis of new type III effectors from *Xanthomonas* uncovers XopB and XopS as suppressors of plant immunity. New Phytol.
10. Szurek B, Rossier O, Hause G, Bonas U (2002) Type III-dependent translocation of the *Xanthomonas* AvrBs3 protein into the plant cell. Mol Microbiol 46: 13-23.
11. Jiang W, Jiang BL, Xu RQ, Huang JD, Wei HY, et al. (2009) Identification of six type III effector genes with the PIP box in *Xanthomonas campestris* pv. *campestris* and five of them contribute individually to full pathogenicity. Mol Plant Microbe Interact 22: 1401-1411.
12. Thompson JD, Gibson TJ, Plewniak F, Jeanmougin F, Higgins DG (1997) The CLUSTAL_X windows interface: flexible strategies for multiple sequence alignment aided by quality analysis tools. Nucleic Acids Res 25: 4876-4882.
13. Lam H, Deutsch EW, Eddes JS, Eng JK, Stein SE, et al. (2008) Building consensus spectral libraries for peptide identification in proteomics. Nat Methods 5: 873-875.
14. Srikumar T, Jeram SM, Lam H, Raught B (2010) A ubiquitin and ubiquitin-like protein spectral library. Proteomics 10: 337-342.
15. Sheng Y, Hong JH, Doherty R, Srikumar T, Shloush J, et al. (2012) A human ubiquitin conjugating enzyme (E2) - HECT E3 ligase structure-function screen. Mol Cell Proteomics.

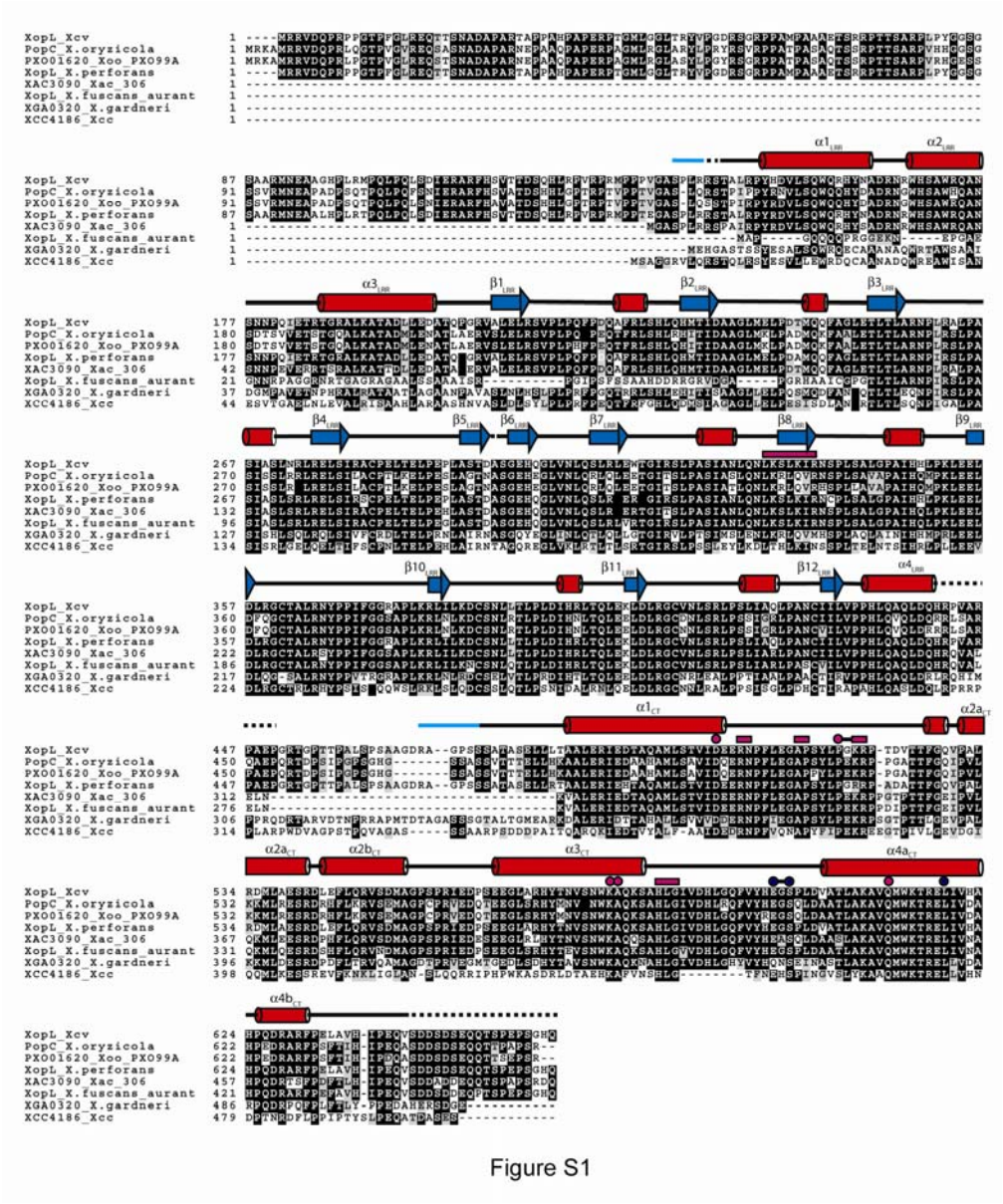

Figure S1

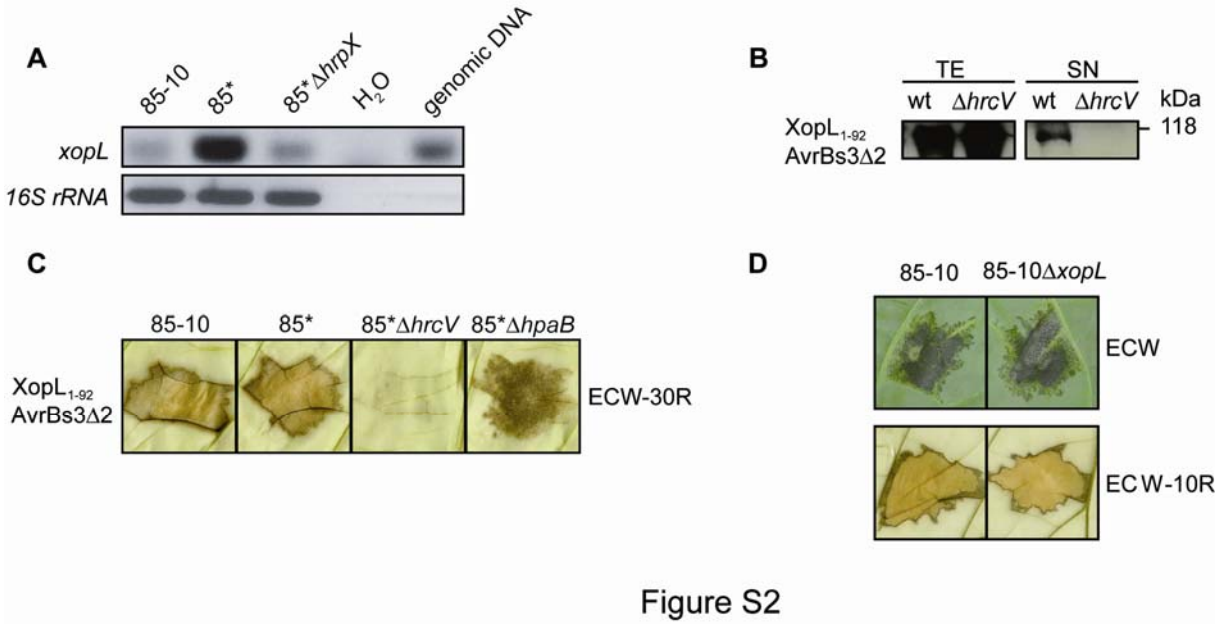

Figure S2

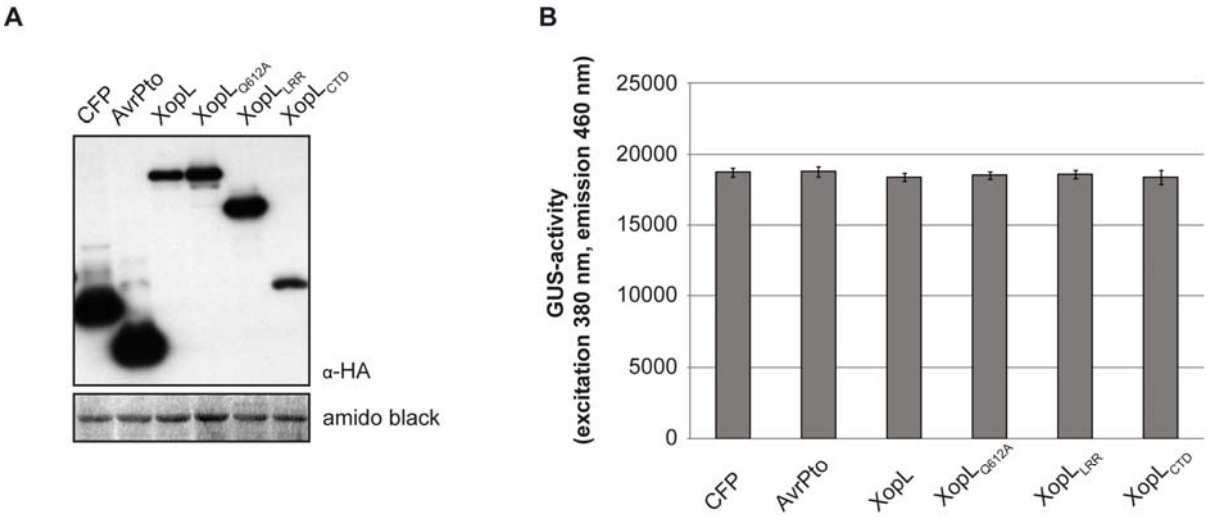

Figure S3

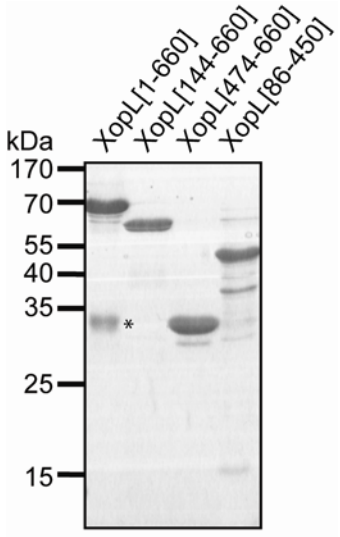

Figure S4

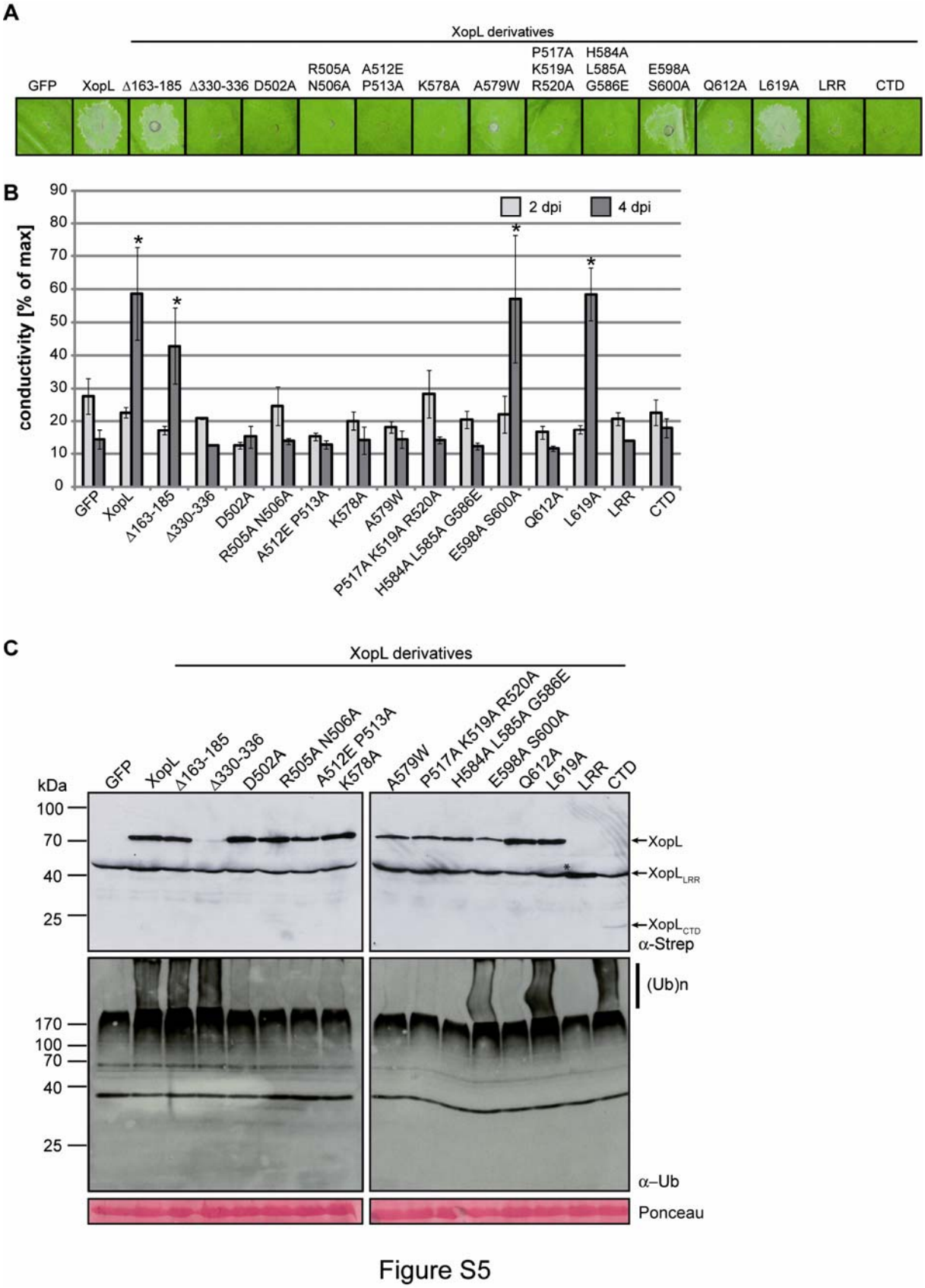
A
XopL derivatives
GFP
XopL
Δ163-185
Δ330-336
D502A
R505A N506A
A512E P513A
K578A
A579W
P517A K519A R520A
H584A L585A G586E
E598A S600A
Q612A
L619A
LRR
CTD
B
2 dpi
4 dpi
conductivity [% of max]
90
80
70
60
50
40
30
20
10
0
GFP
XopL
Δ163-185
Δ330-336
D502A
R505A N506A
A512E P513A
K578A
A579W
P517A K519A R520A
H584A L585A G586E
E598A S600A
Q612A
L619A
LRR
CTD
C
XopL derivatives
kDa
100
70
40
25
170
100
70
40
25
XopL
XopL_LRR
XopL_CTD
α-Strep
(Ub)n
α–Ub
Ponceau

Figure S5

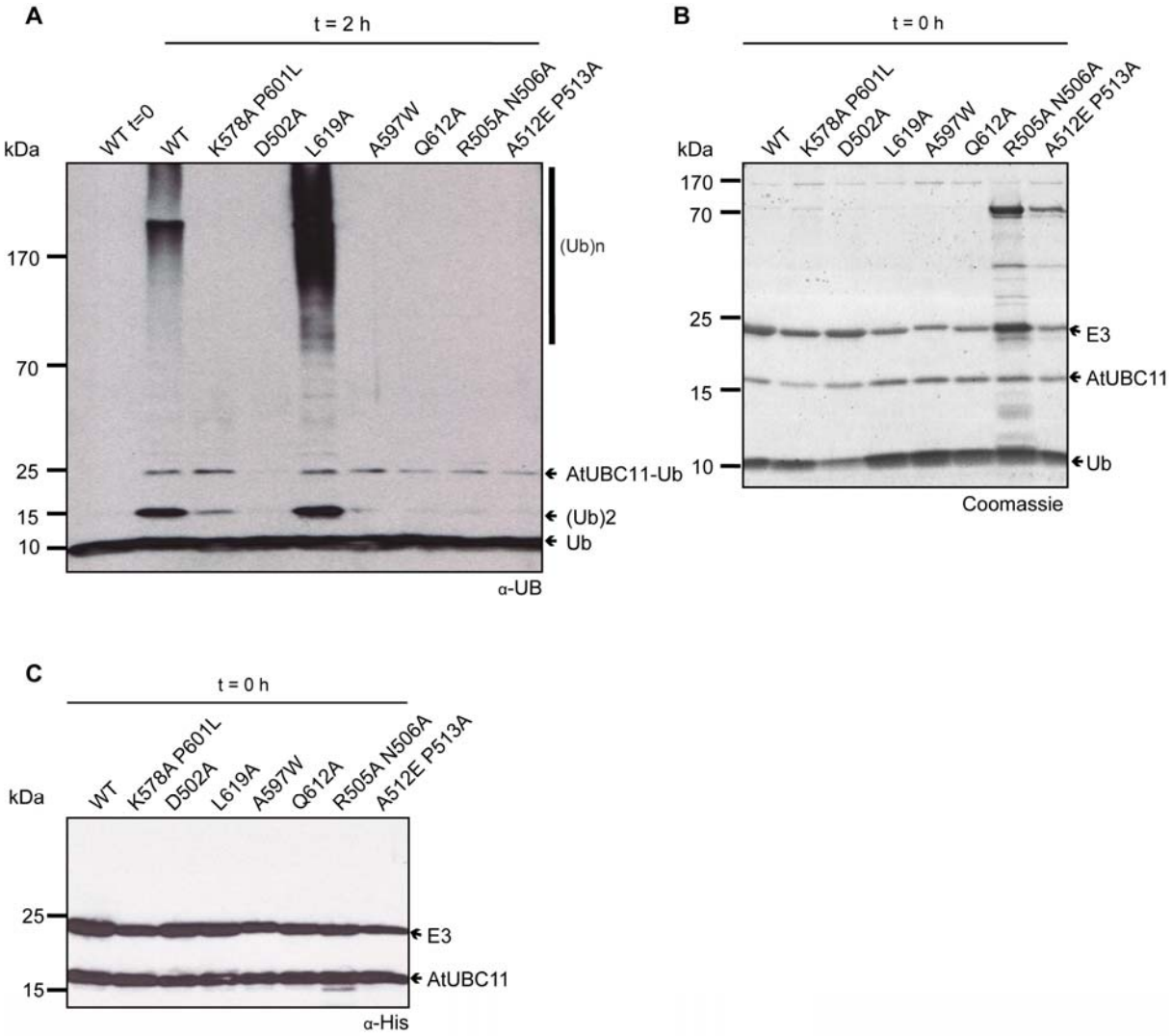
A
t = 2 h
WT t=0
WT
K578A P601L
D502A
L619A
A597W
Q612A
R505A N506A
A512E P513A
kDa
170
70
25
15
10
(Ub)n
AtUBC11-Ub
(Ub)2
Ub
α-UB
B
t = 0 h
WT
K578A P601L
D502A
L619A
A597W
Q612A
R505A N506A
A512E P513A
kDa
170
70
25
15
10
E3
AtUBC11
Ub
Coomassie
C
t = 0 h
WT
K578A P601L
D502A
L619A
A597W
Q612A
R505A N506A
A512E P513A
kDa
25
15
E3
AtUBC11
α-His

Figure S6

2.3.1.2 Zusammenfassung der Ergebnisse

In Publikation 3 wurde der Typ III-Effektor XopL in Kooperation mit der Arbeitsgruppe von A. Savchenko (Universität Toronto) charakterisiert. XopL weist eine LRR in der N-terminalen Hälfte auf, während die C-terminale Region keine Homologie zu bekannten Motiven besitzt.

In diesem Artikel wurde die HrpG- und HrpX-abhängige Aktivierung der Expression des *xopL*-Gens gezeigt. Weiterhin wurde die Typ III-abhängige Sekretion und Translokation von XopL nachgewiesen. Als Reporter diente die AvrBs3-Effektordomäne AvrBs3Δ2.

Um eine mögliche Virulenzfunktion von XopL zu identifizieren, wurde *xopL* aus dem Genom von *Xcv* 85-10 deletiert und die entsprechende Deletionsmutante in Infektionsstudien analysiert. Es konnte jedoch kein Einfluss auf die Virulenz von *Xcv* festgestellt werden. In weiterführenden Studien wurde *xopL Agrobacterium*-vermittelt in verschiedenen Pflanzenspezies exprimiert. Hierbei wurde XopL-induzierter Zelltod in *N. benthamiana* beobachtet. Weiterhin wurde gezeigt, dass XopL die PAMP-induzierte Genexpression in Arabidopsis unterdrückt.

Gereinigtes rekombinantes XopL-Protein zeigte *in vitro* in Gegenwart von E1-und E2-Enzymen, Ubiquitin und ATP E3-Ubiquitin-Ligase-Aktivität. Diese enzymatische Aktivität wurde auch *in planta* nachgewiesen und ist in der C-terminalen Region von XopL lokalisiert. Der zu XopL ähnliche Effektor XCC4186 von *X. campestris* pv. *campestris* ATCC 33913 (44 % Identität bzw. 60 % Ähnlichkeit der Aminosäuresequenz) besitzt ebenfalls E3-Ligase-Aktivität. Massenspektrometrische Untersuchungen und Mutationsanalysen zeigten, dass XopL hauptsächlich Ubiquitinverknüpfungen am Lysin 11 (K11) erstellt. Die Ubiquitinierung erfolgte in Gegenwart des humanen als auch E2-Ubiquitin-konjugierenden Enzymen aus Arabidopsis.

Die Kristallstrukturen der LLR- und der C-terminalen Domäne von XopL wurden gelöst, um weitere Einblicke in die Wirkungsweise von XopL zu erhalten. Die LRR-Region weist strukturelle Homologie zur LRR-Domäne des *Shigella* Effektors IpaH3 auf. Die C-terminale Domäne zeigt hingegen keine Ähnlichkeit zu strukturell charakterisierten Proteinen, einschließlich bekannter E3-Ligasen. Die C-terminale Domäne, XopL E3-Ligase-Box (XL-Box) genannt, weist demnach eine neuartige Faltung auf. Die XL-Box enthält keine Cysteine, was darauf schließen lässt, dass XopL, im Gegensatz zu HECT-E3-Ligasen, keine Thioester-Intermediate mit Ubiquitin bildet. Mit Hilfe von Mutationsanalysen der XL-Box konnte ein direkter Zusammenhang zwischen E3-Ligase-Aktivität und XopL-vermitteltem Pflanzenzelltod nachgewiesen werden. Die Daten der Publikation belegen, dass XopL den ersten Vertreter einer neuen Klasse von E3-Ligasen repräsentiert.

2.3.2 Ergänzende Ergebnisse

2.3.2.1 Charakterisierung des XopL-Derivates $XopL_{\Delta 330-336}$

Die LRR-Domäne von XopL dient möglicherweise als Plattform für die Interaktion mit pflanzlichen Zielproteinen, wie bereits für andere Proteine mit LRRs gezeigt (Kobe und Kajava, 2001). Die LRR-Region von XopL ist für die Suppression der Pflanzenabwehr von Bedeutung (Singer *et al.*, 2013). Um eine LRR-Mutante zu generieren, die nicht mehr funktional ist, wurden umfassende Mutationsanalysen durchgeführt.

Basierend auf der Kristallstruktur wurden positiv-geladene Aminosäuren in der LRR-Region ausgetauscht und Deletionen in der LRR-Region vorgenommen. Allerdings hatten diese Mutationen meist keinen Einfluss auf die Funktionalität von XopL (Singer *et al.*, 2013). Eine Ausnahme stellt das Derivat $XopL_{\Delta 330-336}$, dar, welches eine Deletion von sieben Aminosäuren des 7. β-Faltblatts der LRR-Domäne aufweist (Abb. 2-4 a). Phänotypisch äußerte sich diese Mutation im Verlust des XopL-vermittelten Zelltods in *N. benthamiana*. Im Vergleich zum Wildtyp war $XopL_{\Delta 330-336}$ aber auch deutlich instabiler (Singer *et al.*, 2013) (Abb. 2-4 b).

Ob der Funktionsverlust von $XopL_{\Delta 330-336}$ ein Dosiseffekt ist, sollte in dieser Arbeit geklärt werden. Hierfür wurden Blätter von *N. benthamiana* mit *Agrobacterium*-Stämmen verschiedener Verdünnungsstufen inokuliert. Hohe bakterielle Dichten sollten die Transformationsrate von *N. benthamiana* steigern und zur verstärkten Proteinsynthese von $XopL_{\Delta 330-336}$ führen. Die *Agrobacterium*-vermittelte Expression von *xopL* führte nur bei hohen bakteriellen Dichten (OD_{600}=0,8 oder 0,4) zum pflanzlichen Zelltod. $XopL_{\Delta 330-336}$ induzierte unter den getesteten Bedingungen keinen Zelltod (Abb. 2-4 c, d). Geringere XopL-Proteinmengen korrelierten dabei mit dem Verlust der Zelltod-auslösenden Aktivität von XopL. (Abb. 2-4 b-d).

Die Proteinmengen von $XopL_{\Delta 330-336}$ waren bei hohen Zelldichten vergleichbar mit denen des XopL-Wildtypproteins nach Inokulation mit niedrigen *Agrobacterium*-Dichten. Dies deutet darauf hin, dass die reduzierte Proteinstabilität und nicht die funktionelle Inaktivierung der LRR-Domäne von $XopL_{\Delta 330-336}$ für den Verlust des Phänotyps verantwortlich ist.

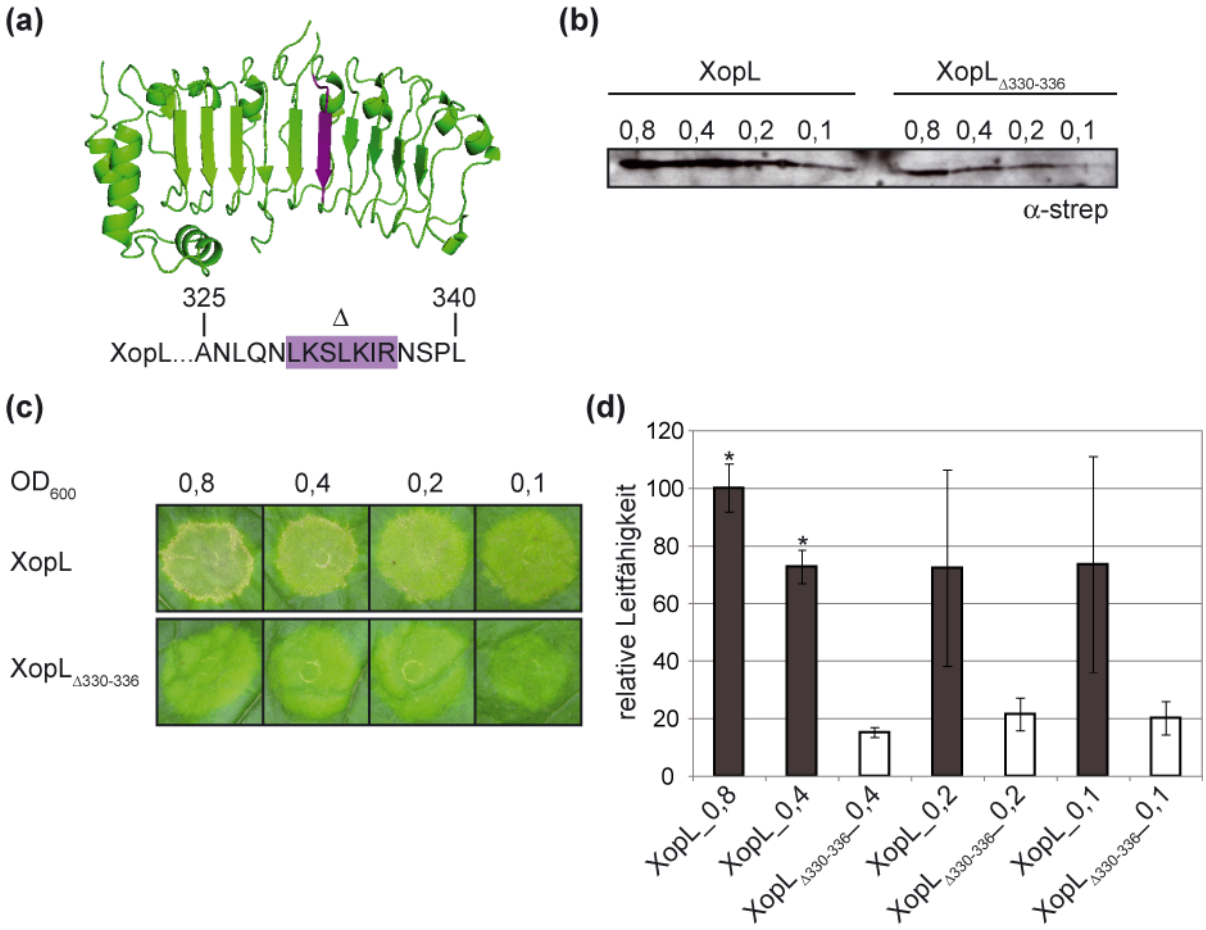

Abbildung 2-4: Deletionen in der LRR-Domäne beeinflussen die Proteinstabilität von XopL.
(a) Schematische Übersicht der Deletion der Aminosäuren 330-336 (violett) in der LRR-Domäne von XopL (grün). Die betroffenen Aminosäuren sind in der Sequenz angegeben. Die *xopL* bzw. *xopL*$_{\Delta 330\text{-}336}$ enthaltenden *Agrobacterium*-Stämme wurden in verschiedenen Konzentrationen in *N. benthamiana* Blätter inokuliert. OD_{600}=0,8 ($8x10^8$ KBE/ml), 0,4 ($4x10^8$ KBE/ml), 0,2 ($2x10^8$ KBE/ml) und 0,1 (10^8 KBE/ml). (**b**) Nachweis der Proteinsynthese von XopL bzw. XopL$_{\Delta 330\text{-}336}$. Proteinextrakte aus inokuliertem Blattmaterial wurden per SDS-PAGE aufgetrennt und mittels Western-Blot und einem *Strep-tag* spezifischen Antikörper analysiert. Die Zahlen weisen auf die verschiedenen optischen Dichten hin. (**c**) Die Phänotypen wurden 6 Tage nach Inokulation in *N. benthamiana* dokumentiert. **(d)** Quantifizierung der XopL-induzierten Zelltodreaktionen. Blätter von *N. benthamiana* wurden wie in (a) beschrieben inokuliert. 4 d nach Inokulation wurden Leitfähigkeitsmessungen durchgeführt. Die Balken entsprechen den Mittelwerten biologischer Triplikate (jeweils 5 Blattscheiben) und deren Standardabweichungen. Sternchen weisen auf signifikante Unterschiede hin (*t*-test, $p<0,05$). Die Experimente wurden zweimal mit ähnlichen Ergebnissen reproduziert.

2.3.2.2 *In vivo* Ubiquitinierungsassay mit weiteren Typ III-Effektoren

Die Deletion von *xopL* hat keinen Einfluss auf die Virulenz von *Xcv*, wie in Publikation 3 gezeigt (siehe 2.3.1). Dies könnte in der funktionellen Redundanz einiger Effektoren begründet sein. Zum Einen supprimieren XopB, XopD, XopN und XopS (Kim *et al.*, 2008; Kim *et al.*, 2009; Schulze *et al.*, 2012) ebenfalls die PTI, wodurch der Virulenzbeitrag von XopL womöglich maskiert wird. Zum Anderen könnten weitere Effektorproteine als E3-Ligasen wirken und die pflanzliche Ubiquitinierung

manipulieren. Um den letztgenannten Punkt zu untersuchen, wurden 16 Effektoren mittels *Agrobacterium* transient in *N. benthamiana* exprimiert. 30 Stunden nach Inokulation wurden Proteinextrakte aus inokuliertem Blattmaterial gewonnen, per SDS-Page aufgetrennt und mittels Western-Blot analysiert.

Neben XopL führte die transiente Expression von XopE1, AvrBsT und AvrRxv zur Akkumulation ubiquitinierter Proteine (Abb. 2-5 a). Die transiente Expression der übrigen 13 Effektoren führte nicht zu einem veränderten Ubiquitinierungsmuster.

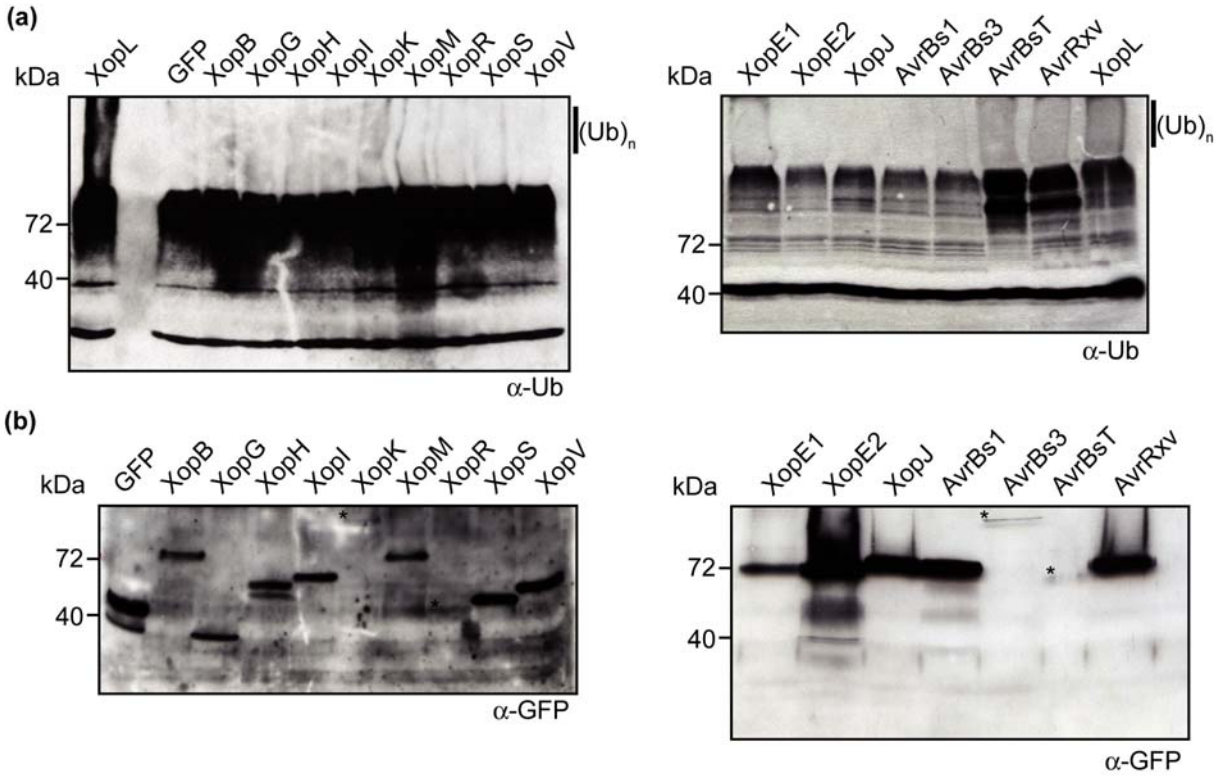

Abbildung 2-5: Einfluss von Typ III-Effektoren aus *Xcv* auf die Ubiquitinierung *in planta*.
Effektor-GFP kodierende Konstrukte wurden mit *Agrobacterium* in *N. benthamiana* transferiert (Inokulation mit $8x10^8$ KBE/ml). 30 h nach Inokulation wurden Proteinextrakte durch SDS-PAGE aufgetrennt und mittels Western-Blot analysiert. **(a)** Die Analyse des Ubiquitinierungsmusters erfolgte mit einem Ubiquitin-spezifischen Antikörper, **(b)** der Nachweis der Effektor-GFP-Fusionsproteine mittels GFP-spezifischem Antikörper. Spezifische Signale für XopK::GFP, XopR::GFP, AvrBs3::GFP und AvrBsT::GFP sind durch ein Sternchen markiert. Die Experimente wurden zweimal mit ähnlichen Ergebnissen reproduziert.

Basierend auf diesen Ergebnissen wurde untersucht, ob ein inaktives Derivat von XopE1 nicht mehr in der Lage ist, das Ubiquitinierungsmuster der Pflanze zu manipulieren, ähnlich wie für XopL gezeigt (Singer *et al.*, 2013). Hierfür wurde das XopE1-Derivat $XopE1_{G113A\ N116A}$ ($XopE1_{mut}$) analysiert, dessen Expression, im Gegensatz zu Wildtyp-XopE1, keinen Zelltod in *N. benthamiana* auslöst (E. Herzfeld und U. Bonas, unpubliziert). Die transiente Expression von $xopE1_{mut}$ führte zur Ausbildung eines Ubiquitinmusters vergleichbar mit XopE1-Wildtyp und XopL (Abb. 2-6 a). Diese Ergebnisse zeigen, dass kein Zusammenhang zwischen zelltodauslösender Aktivität und Manipulation der

Ubiquitinierung durch XopE1 besteht. Die Lokalisation an der Plasmamembran ist hierfür ebenfalls nicht notwendig, da die Fusion von GFP an den N-Terminus von XopE1 dessen Membranlokalisierung verhindert, aber zu einer schnelleren Zelltodreaktion führt (Abb. 2-6 b; F. Thieme und U. Bonas, unpubliziert), ähnlich zum XopE1-Derivat $XopE1_{G2A}$ (Thieme *et al.*, 2007).

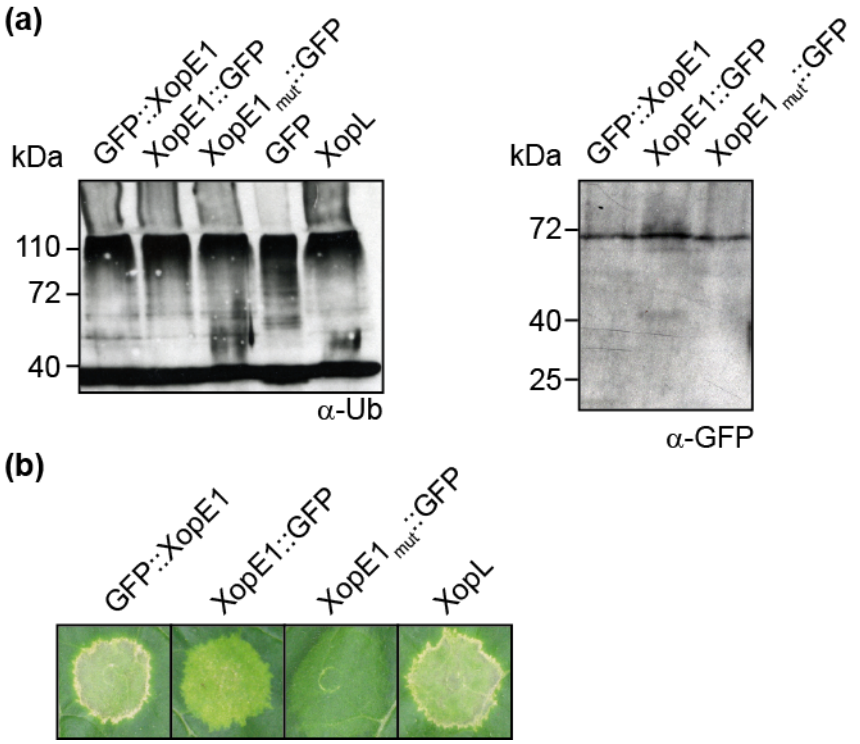

Abbildung 2-6: XopE1-induzierte Ubiquitinmodifikationen in *N. benthamiana*.
Agrobacterium -vermittelte transiente Expression von *gfp*, *xopL*, *xopE1* und $xopE1_{G113A\ N116A}$ ($xopE1_{mut}$) in *N. benthamiana* ($8x10^8$ KBE/ml). **(a)** Proteinextrakte wurden 40 h nach Inokulation per SDS-PAGE aufgetrennt und mittels Western-Blot und einem Ubiquitin-spezifischen (linke Seite) bzw. GFP-spezifischen Antikörper (rechte Seite) analysiert. **(b)** Phänotypen wurden 6 Tage nach Inokulation dokumentiert. Die Experimente wurden zweimal mit ähnlichen Ergebnissen reproduziert.

2.4 Eigenanteil an den Publikationen

Publikation 1, Kapitel 2.1.1

Szczesny, R., Büttner, D., Escolar, L., Schulze, S., Seiferth, A., Bonas, U. 2010. Suppression of the AvrBs1-specific hypersensitive response by the YopJ effector homolog AvrBsT from *Xanthomonas* depends on a SNF1-related kinase. New Phytologist **187(4):**1058-1074.

Eigenanteil: Durchführung und Auswertung der Leitfähigkeitsmessungen nach Planung der Experimente mit R. Szczesny. Die Abbildung 1d wurde von mir erstellt.

Publikation 2, Kapitel 2.2.1 und 2.2.1.1

Schulze, S., Kay, S., Büttner, D., Egler, M., Eschen-Lippold, L., Hause, G., Krüger, A., Lee, J., Müller, O., Scheel, D., Szczesny, R., Thieme, F., Bonas, U. 2012. Analysis of new type III effectors from *Xanthomonas* uncovers XopB and XopS as suppressors of plant immunity. New Phytologist **195(4):** 894-911

Eigenanteil: Selbstständige Planung, Durchführung und Auswertung folgender Experimente: Sekretionstest für XopB und XopV und Translokationsanalysen (alle T3E-Kandidaten); Infektionsstudien und Bestimmung des bakteriellen Wachstums *in planta;* Analysen zur Suppressorwirkung von XopB auf die zelltodauslösende Aktivität von XopG, XopJ, AvrBsT und AvrRxv (Vorarbeiten A. Schonsky (Schonsky, 2013); Durchführung der konfokalen-Laser-Scanning-Mikroskopie zur Analyse der Lokalisation von XopB (Vorarbeit A. Schonsky (Schonsky, 2013) und dessen Derivaten, sowie deren Einfluss auf den Vesikeltransport; Membranfraktionierungsstudien zu XopB. Die Stämme *Xcv* 85-10Δ*xopK*, Δ*xopR*, Δ*xopS*, Δ*xopV* und Δ*xopB*Δ*xopS*, sowie deren Komplementationskonstrukte (pLAND:xopB, pBRM:xopS) wurden von mir erstellt und folgende Binär-Konstrukte kloniert: pGGA1:secGFP, pGWB2:avrBs2, pGWB5:xopG, pGWB5:xopK, pGWB5:xopV, pGWB17:xopB, pGWB17:xopB$_{A313V}$, pGWB17:xopB$_{K455R}$, pGWB17:xopJ, pGWB17:xopJ$_{C235A}$, pK7FWG2:xopB$_{A313V}$, pK7FWG2:xopB$_{K455R}$, pK7FWG2:xopR, pK7FWG2:xopS. Die Effektor:356 Fusionen wurden in Vorarbeit von M. Egler, A. Krüger, O. Müller, R. Szczesny und F. Thieme erstellt und in die Stämme 85* und 85*Δ*hrcV* konjugiert. Die Abbildungen 2, 4, 5, 6, 7, 8a, 9, S1, S4, S5-S8 und Tabelle S1 wurden von mir erstellt.

Publikation 3, Kapitel 2.3.1 und 2.3.1.1

Singer, A. U., Schulze, S., Xu, X., Skarina, T., Cui, H., Eschen-Lippold, L., Egler, M., Srikumar, T., Raught, B., Lee, J., Scheel, D., Savchenko,A., Bonas, U. 2013. A Pathogen Type III Effector with a Novel E3 Ubiquitin Ligase Architecture. PLoS Pathogens **2013 Jan;9(1):**e1003121.

Eigenanteil: Die Planung der Mutationsanalysen von XopL erfolgte in Zusammenarbeit mit A. Singer. Die Durchführung und Auswertung folgender Experimente erfolgte selbstständig: Erstellung der XopL-Derivate durch gerichtete Mutagenese, Klonierung der binären Konstrukte von XopL und dessen Derivaten sowie Analysen *in planta*. Daten in Abb. S2a und c sowie verwendete *Xcv*-Stämme in Abb. S2b und d stammen von M. Egler. Die Abbildungen 1, S2, S5 und Tabelle S3 wurden von mir erstellt. Die Anfertigung des Manuskripts erfolgte in Zusammenarbeit mit A. U. Singer, A. Savchenko und U. Bonas. Geteilte Erstautorenschaft mit A. U. Singer.

3. Diskussion

3.1 Klassifizierung von Effektorproteinen aus *Xcv*

Das T3SS ist für die Pathogenität von *Xcv* essentiell und transloziert mehr als 20 Effektorproteine in das Zytosol der Wirtszelle (Bonas *et al.*, 1991; Roden, JA *et al.*, 2004; Thieme *et al.*, 2005). Einzelne Effektoren sind für sich genommen nicht essentiell, sind in ihrer Gesamtheit jedoch unabdingbar und können oft in Effektorgruppen eingeteilt werden, die gezielt Prozesse in der Pflanze angreifen. (Cunnac *et al.*, 2009; Kay und Bonas, 2009; Cunnac *et al.*, 2011). Die Translokation der Effektoren wird in *Xcv* u. a. durch das Typ III-Chaperon HpaB vermittelt. HpaB bindet Effektoren und fördert deren Sekretion und Translokation (Büttner *et al.*, 2004; Büttner *et al.*, 2006). Interessanterweise unterscheiden sich T3E in ihrer Abhängigkeit von HpaB und wurden deshalb in Klassen eingeteilt (Büttner *et al.*, 2006). Man nimmt an, dass Effektoren der Klasse A, die in Abwesenheit von HpaB nicht mehr transloziert werden, eine Schlüsselrolle in der Interaktion mit der Pflanze spielen und deshalb zuerst transloziert werden (Büttner *et al.*, 2006). Die Translokation der Klasse B-T3E findet hingegen in reduzierter Form auch in Abwesenheit von HpaB statt. Sie sind für die Virulenz womöglich nicht so bedeutend wie Effektoren der Klasse A.

Im Rahmen dieser Arbeit konnten die Effektoren XopR und XopS der Klasse A zugeordnet werden, während XopB, XopG, XopI, XopK, XopL, XopM und XopV zur Klasse B gezählt werden (s. Kapitel 2.2.1 und 2.3.1). Entsprechend des Modells nach Büttner *et al.* (Büttner *et al.*, 2006) sind XopR und XopS besonders wichtig, während XopB, XopG, XopI, XopK, XopL, XopM und XopV für die Interaktion von *Xcv* mit dessen Wirtspflanzen von geringerer Bedeutung sind. Dieses Modell konnte in dieser Arbeit nur teilweise bestätigt werden. Die T3E-kodierenden Gene von *xopG*, *xopI*, *xopK*, *xopL*, *xopM*, und *xopV* sind für die Virulenz von *Xcv* nicht essentiell, wie für Klasse B-Effektoren postuliert (Büttner *et al.*, 2006; Schulze *et al.*, 2012). Einzelne Deletionen Effektor-kodierender Gene im Genom von *Xcv* hatten keinen Einfluss auf den Krankheitsverlauf in Paprikapflanzen (s. Kapitel 2.2.1; (Schulze *et al.*, 2012). Von den Effektoren, die Klasse A zugeordnet werden konnten, trägt jedoch nur XopS zur Ausbildung von Krankheitssymptomen bei. Der Verlust von *xopR* hat keinen nachweisbaren Einfluss auf die Virulenz von *Xcv* (Schulze *et al.*, 2012). Interessanterweise führt die Deletion des x*opR*-Homologen in *X. oryzae* pv. *oryzae* (*Xoo*) zu schlechterem Wachstum der Bakterien in Reispflanzen (Akimoto-Tomiyama *et al.*, 2012). Möglicherweise trägt XopR nur subtil zur Virulenz von *Xcv* bei.

XopB, obwohl als Klasse B-Effektor eingestuft, beeinflusst hingegen die Symptomausprägung ähnlich stark wie XopS. Die Deletion von *xopB* bzw. *xopS* führte aber nicht zu einem veränderten bakteriellen Wachstum im Vergleich zum Wildtyp. Jedoch führte die Doppeldeletion von *xopB* und *xopS* zu reduziertem Wachstum von *Xcv* in Paprikapflanzen (s. auch Kapitel 3.4; Schulze *et al.*, 2012).

Diese Daten zeigen, dass das vorgeschlagene Modell nach Büttner *et al.* (Büttner *et al.*, 2006) in vielen Fällen Gültigkeit besitzt, aber nicht universell anwendbar ist.

3.2 Biochemische und biologische Charakterisierung von T3E

Einige *Xcv*-Effektoren der Klasse B sind auch in *Pseudomonas* und anderen *Xanthomonas*-Spezies konserviert. Während diese T3E nicht zur Virulenz von *Xcv* beitragen, sind die entsprechenden Homologe in *Pseudomonas* und anderen *Xanthomonas* spp. von Bedeutung. Hier sei zunächst XopL genannt, welches für die Virulenz von *Xcv* und *Xoo* vernachlässigbar ist (Song und Yang, 2010; Singer *et al.*, 2013). Der zu XopL homologe Effektor XC_4273 (Aminosäuresequenz ist zu XopL 43 % identisch bzw. 60 % ähnlich) trägt hingegen zur Virulenz und zum Wachsum von *Xcc* bei (Jiang *et al.*, 2009). Es kann nicht ausgeschlossen werden, dass starke Virulenzfaktoren wie XopB und XopS den Effekt von XopL maskieren und sich dessen Deletion daher nicht in verminderter Virulenz äußert. Proteine mit Homologie zu XopB und XopS aus *Xcv* sind nicht im Genom von *Xcc* kodiert (Qian *et al.*, 2005). Möglicherweise wird dadurch die Bedeutung von XC_4273 für die Virulenz von *Xcc* deutlich sichtbar. Ein weiterer Unterschied zwischen XopL von *Xcv* und XopL (XC_4273) aus *Xcc* ist die Abhängigkeit der Translokation vom T3-Chaperon HpaB. Während XopL von *Xcv* auch in Abwesenheit von HpaB tranlsoziert wird (s. Kapitel 2.3.1), kann XC_4273 von einem Δ*hpaB*-Stamm nicht mehr transloziert werden (Jiang *et al.*, 2009).

Auch XopG, XopI, XopK, XopM und XopV tragen nicht nachweisbar zur Infektion von Paprikapflanzen durch *Xcv* bei (Schulze *et al.*, 2012). Obwohl diese T3E in weiteren *Xanthomonas* spp. und anderen phytopathogenen Bakterien konserviert sind, weiß man über deren Rolle in der bakteriellen Virulenz nur sehr wenig. Während XopG für das Wachstum von *Xcv in planta* nicht benötigt wird, trägt der homologe Effektor HopH1 zur Virulenz von *P. syringae* pv. *tomato* DC3000 bei. Die Deletion des Effektorclusters II, bestehend aus *hopH1* und *hopC1,* führt sowohl zu geringeren Krankheitssymptomen, als auch bakteriellem Wachstum in Tomate (Wei *et al.*, 2007). Bisher konnten nur wenige T3E identifiziert werden, die erheblich zur Virulenz und Fitness von *Xanthomonas* beitragen, wie beispielsweise für AvrBs2 oder XopD gezeigt (Kearney und Staskawicz, 1990; Wichmann und Bergelson, 2004; Kim *et al.*, 2008).

Auch die biologischen und/oder biochemischen Aktivitäten der genannten T3E sind weitgehend unbekannt, mit Ausnahme von XopG und XopI. XopG besitzt Homologie zu Zink-Endopeptidasen von *Clostridium botulinum* (Potnis *et al.*, 2011). Proteaseaktivität konnte für XopG aber bislang nicht nachgewiesen werden (A. Krüger und U. Bonas, unpubliziert).

XopI ist in verschiedenen *Xanthomonas* spp. konserviert und besitzt Ähnlichkeit zu F-Box Proteinen (Bogdanove *et al.*, 2011; Schulze *et al.*, 2012). F-Box Proteine sind Teil eines multimeren Komplexes aus Skp, Cullin und F-Box (SCF), der in der Ubiquitin-vermittelten Degradierung von Proteinen involviert ist (Vierstra, 2009). Bisher konnten einige Interaktionspartner von XopI identifiziert

werden, die auf dessen Funktion als F-Box Protein hinweisen (O. Müller und U. Bonas, unpubliziert). Welche Rolle XopI während der Infektion von Paprika- oder Tomatenpflanzen durch *Xcv* spielt, muss in weiterführenden Studien noch untersucht werden.

Eine Möglichkeit um Effektoren zu charakterisieren, ist die *Agrobacterium*-vermittelte Expression der T3E in verschiedenen Pflanzenspezies. Hierdurch hervorgerufene Reaktionen der Pflanzen könnten Hinweise auf eine Aktivität der Effektoren liefern. Die transiente Expression von XopG und XopM führt zu Zelltodreaktionen in Paprika und *N. tabacum* bzw. *N. benthamiana*, während XopI, XopK und XopV keine makroskopischen Veränderungen in verschiedenen *Solanaceen* bewirkten (Schulze *et al.*, 2012). Dies ist ein Hinweis darauf, dass (i) XopG und XopM erkannt werden und eine Abwehrreaktion der Pflanze ausgelösen, oder (ii) XopG und XopM im Zuge starker Überexpression zytotoxisch wirken, was wiederum in enzymatischer Aktivität der T3E begründet sein könnte. Um dies im Detail zu klären, könnten Mutationsstudien durchgeführt werden, um Proteinbereiche zu identifizieren, die für die Aktivität von XopG und XopM von Bedeutung sind. Anschließend könnten diese Mutanten für die Suche von pflanzlichen Interaktionspartnern genutzt werden, da „inaktive T3E" ihre Zielproteine nicht mehr modifizieren bzw. degradieren.

Des Weiteren könnten Transkriptomanalysen nach transienter Expression der Effektoren *in planta* Hinweise auf Signalwege oder Stoffwechselprozesse liefern, die durch die Effektoren verändert werden. Zusätzlich würden Hefe-Dihybrid-Sichtungen die Identifizierung von Interaktionspartner und möglichen Virulenzzielen der Effektoren ermöglichen. Eventuell würden auch Mehrfachdeletionen der Effektor-kodierenden Gene Hinweise geben, ob diese in ihrer Gesamtheit überhaupt für *Xcv* von Bedeutung sind. Für *P. syringae* wurde gezeigt, dass nicht alle T3E für die bakterielle Virulenz nötig sind. Ein minimales Effektor-Repertoire, bestehend aus acht von insgesamt 28 T3E, ist für das Wachstum von *Pseudomonas in planta* ausreichend, während andere Effektoren kaum zur Virulenz beitragen (Cunnac *et al.*, 2011). Ob auch *Xcv* solch ein minimales Effektor-Repertoire besitzt, ist noch unklar. Um diese These zu prüfen, könnte man einen „Null-Effektor-Stamm" generieren, indem alle bekannten Effektor-kodierenden Gene deletiert sind. Anschließend könnte man in diesem Stamm einzelne T3E oder Effektorgruppen ektopisch exprimieren und den Einfluss auf die Virulenz und das bakterielle Wachstum untersuchen.

3.3 XopL repräsentiert eine neue Klasse von E3-Ligasen

In dieser Arbeit wurde XopL zum ersten Mal charakterisiert. Die C-terminale Region von XopL weist *in vitro* und *in vivo* E3-Ubiquitin-Ligase-Aktivität auf. XopL interagiert dabei mit den pflanzlichen E2-konjugierenden Enzymen AtUBC11 und AtUBC28 aus Arabidopsis. Mutationsanalysen an AtUBC28 ergaben, dass die Aminosäuren Phenylalanin und Alanin an den Positionen 62 bzw. 96 für die Interaktion mit XopL essentiell sind. In früheren Studien wurde gezeigt, dass die Aminosäure F62 für die Interaktion mit HECT-E3-Ligasen, jedoch nicht mit RING/U-Box-Proteinen von Bedeutung ist (Nuber und Scheffner, 1999; Christensen *et al.*, 2007), während A96 zur Interaktion mit HECT- und

RING/U-Box-E3-Ligasen beiträgt (Levin *et al.*, 2010). Um weitere Aussagen über die Interaktion zwischen XopL und E2-Enzymen treffen zu können, bedarf es weiterer struktureller Charakterisierungen der XopL-E2-Interaktion. Ähnliche Studien wurden für SopA aus *Salmonella* und NleG aus *E. coli* bereits durchgeführt und lieferten interessante Einblicke in die Interaktion dieser Effektoren mit entsprechenden E2-Enzymen. Trotz struktureller Unterschiede der „Effektor-E3-Ligasen" im Vergleich zu den entsprechenden Enzymen der tierischen Zelle, erfolgt die Bindung an Ubiquitin-konjugierende Enzyme auf eine ähnliche Weise (Lin *et al.*, 2012).

XopL vermittelt Ubiquitinverknüpfungen hauptsächlich an Lysin 11 (K11), aber in geringerem Maße auch an K33, K48 und K63. Über K11-Ubiquitinketten ist bisher sehr wenig bekannt. Sie spielen sowohl im proteolytischen Abbau als auch in der Regulation der Zellteilung eine Rolle (Wickliffe *et al.*, 2011). Der nächste Schritt sollte die Suche nach Interaktionspartnern von XopL sein. Sobald diese identifiziert werden, müsste man analysieren, ob diese durch XopL ubiquitiniert und eventuell proteolytisch abgebaut werden, um weitere Informationen über die Wirkungsweise von XopL zu erhalten.

AvrPtoB aus *Pseudomonas* bedingt den Ubiquitin-vermittelten proteolytischen Abbau der Kinase FLS2 und supprimiert dadurch die Pflanzenabwehr (Göhre *et al.*, 2008). Die Art der Ubiquitin-Verknüpfungen wurde bisher nicht untersucht.

Alle bislang bekannten E3-Ligasen gehören zu den zwei Klassen der RING/U-Box- oder katalytischen HECT-E3-Ligasen und unterscheiden sich im Mechanismus des Ubiquitintransfers (Ardley und Robinson, 2005). HECT-E3-Ligasen besitzen ein katalytisches Cystein, über das Ubiquitin zunächst in Form eines Thioesther-Intermediates gebunden wird, bevor es an das Zielprotein geknüpft wird (Komander und Rape, 2012). E3-Ligasen mit einer RING/U-Box-Domäne interagieren mit E2-Enzymen, bringen diese und das Zielprotein in räumliche Nähe und übertragen Ubiquitin direkt auf das Zielprotein (Ardley und Robinson, 2005). Eine direkte Bindung des Ubiquitins, wie im Fall der HECT-E3-Ligasen, findet demnach nicht statt. Ein weiterer Unterschied zwischen diesen Klassen von E3-Ligasen besteht in der Art der vermittelten Ubiquitinverkettungen. Es wird postuliert, dass die Verknüpfungsspezifität im Fall von RING/U-Box E3-Ligasen durch das konjugierende E2-Enzym festgelegt wird (Ye und Rape, 2009), während HECT-E3-Ligasen die Spezifität selbst bestimmen (Komander und Rape, 2012). XopL enthält selbst kein Cystein in seiner aktiven E3-Ligasedomäne. Die Ubiquitinierung von Zielproteinen erfolgt deshalb wahrscheinlich nicht über Thioesther-Intermediate (Singer *et al.*, 2013), sondern eher indirekt, ähnlich den RING/U-Box E3-Ligasen. Die Kristallstruktur eines XopL-E2-Komplexes könnte Hinweise auf den Mechanismus der Ubiquitinierung von Zielproteinen durch XopL geben. Die Kristallstruktur von XopL lieferte Einblicke in die Architektur des Proteins. Die E3-Ligase-Domäne von XopL besitzt eine neuartige Faltung, XL-Box (XopL-E3-Ligase-Box) genannt, und unterscheidet sich völlig von bisher charakterisierten RING/U-Box-bzw. HECT-E3-Ligasen (Singer *et al.*, 2013). Damit repräsentiert XopL eine neue Klasse von E3-Ligasen und ist zudem erst der zweite Typ III-Effektor

phytopathogener Bakterien, der nachweislich diese für Eukaryoten typische Enzymaktivität besitzt. Wie bereits erwähnt, besitzt auch AvrPtoB von *P. syringae* E3-Ligase-Aktivität und gehört aufgrund struktureller Ähnlichkeit zur Klasse der RING/U-Box-Proteine (Janjusevic *et al.*, 2006).
E3-Ligasen wurden für T3E tierpathogener Bakterien schon häufiger beschrieben. Die Mitglieder der NleG-Effektorfamilie von *E. coli* besitzen ebenfalls RING/U-Box-Motive (Wu *et al.*, 2010), während die T3E IpaH und SopA von *Shigella* bzw. *Salmonella* katalytische Zentren ähnlich denen der HECT-E3-Ligasen aufweisen (Singer *et al.*, 2008; Quezada *et al.*, 2009). IpaH reguliert seine Aktivität selbst, indem die LRR-Region die enzymatische Aktivität der E3-Ligase-Domäne in Abwesenheit des Substrats inhibiert (Singer *et al.*, 2008; Quezada *et al.*, 2009; Chou *et al.*, 2012). Dies trifft für XopL nicht zu, da die Enzymaktivität in An- als auch Abwesenheit der LRR-Region nachzuweisen war (s. Kapitel 2.3.1).

3.3.1 Der Einfluss weiterer Effektoren auf die Ubiquitinierung *in planta*

Im Rahmen dieser Arbeit wurde untersucht, ob die Ubiquitinierung durch weitere Effektoren von *Xcv* manipuliert wird. Wie in Kapitel 2.3.2.2 gezeigt, führt die transiente Expression von XopE1, AvrBsT und AvrRxv zu einem veränderten Ubiquitinierungsmuster, welches dem von XopL ähnlich ist. Ob dieser Effekt indirekt ist oder auf einer enzymatischen E3-Ligase-Aktivität beruht, müsste in zukünftigen Arbeiten geklärt werden. *In vitro* durchgeführte Ubiquitin-Ligase-Analysen mit gereinigten Effektorproteinen in Gegenwart von ATP, Ubiquitin, E1- und E2-Enzymen würden zeigen, ob ein Effektor wirklich diese Enzymaktivität aufweist.
Da für AvrBsT und AvrRxv Cysteinprotease und/oder Acetyltransferase-Aktivität vorhergesagt wird (Lewis *et al.*, 2011), ist die Akkumulation polyubiquitinierter Proteine wahrscheinlich ein indirekter Effekt. AvrBsT interagiert mit der Kinase SnRK1 (s. Kapitel 2.1.1), welche auch mit der 20S-Untereinheit des 26S-Proteasoms interagiert (Farras *et al.*, 2001). Es wird deshalb spekuliert, dass AvrBsT eine 26S-Proteasom-assoziierte Funktion erfüllt und möglicherweise den Proteinabbau am Proteasom stört (Szczesny, 2009). Dieses Modell würde die Akkumulation ubiquitinierter Proteine erklären, die im Zuge der transienten Expression von AvrBsT nachgewiesen wurde.
Die Funktion von XopE1 ist noch nicht bekannt. XopE1 gehört zur HopX-Effektorfamilie putativer Transglutaminasen. Die Transglutaminasen-Proteinfamilie umfasst diverse Enzyme mit verschiedenen Funktionen (Nimchuk *et al.*, 2007; Thieme *et al.*, 2007). Salomon und Kollegen fanden heraus, dass HopX1 MAP-Kinase Signalwege in Hefe im Zuge der Antwort auf osmotischen Stress negativ beeinflusst (Salomon *et al.*, 2012). Durch verschiedene abiotische Stressbedingungen, wie osmotischer oder Hitzestress, kommt es in Eukaryoten zur Anhäufung ent- oder falschgefalteter Proteine, die Ubiquitin-vermittelt über das 26S Proteasom abgebaut werden (Lee und Goldberg, 1998; Lee *et al.*, 2010). Sollte XopE1, ähnlich wie HopX1, negativ auf regulatorische Kreisläufe im Zuge der Stressantwort einwirken, könnte dies eine Erklärung für das verstärkte Auftreten ubiquitinierter

Proteine sein. Diese Hypothese könnte man überprüfen, indem man die von Salomon und Kollegen durchgeführten Studien mit XopE1 durchführt (Salomon *et al.*, 2012).

3.3.2 Die Pflanzenabwehr wird durch XopL unterdrückt

„Effektor-E3-Ligasen" erfüllen unterschiedliche Aufgaben. XopL bindet und ubiquitiniert Zielproteine in *N. benthamiana*. Vermutlich beeinflussen diese Modifikationen bestimmte Stoffwechselprozesse oder regulatorische Signalwege und es kommt zum Absterben der Pflanzenzellen. Dieser Zelltod ist von der E3-Ligase-Aktivität abhängig, da Mutationen an der Oberfläche der XL-Box zum Verlust der enzymatischen Aktivität *in planta* und *in vitro* führen und die entsprechenden XopL-Derivate nicht mehr in der Lage sind Zelltod auszulösen (s. Kapitel 2.3.1; Singer *et al.*, 2013). Die Zielproteine von XopL sind noch unbekannt und sollten durch Hefe-Zwei-Hybrid Sichtungen identifiziert werden.
Die E3-Ligase-Aktivität von AvrPtoB dient der Manipulation der pflanzlichen Immunantwort. Die Kinase Fen wird von AvrPtoB Ubiquitin-vermittelt degradiert, wodurch die ETI inhibiert wird (Abramovitch *et al.*, 2006; Rosebrock *et al.*, 2007). AvrPtoB unterdrückt auch programmierten Zelltod in Hefe und wirkt damit nicht nur in Pflanzen als Zelltodsuppressor (Abramovitch *et al.*, 2003). Ob die ETI durch XopL manipuliert wird, ist bislang nicht bekannt. Allerdings supprimiert XopL die Expression von Abwehrgenen der PAMP-induzierten Abwehr in Arabidopsis. Hierfür ist allein die LRR-Region von XopL verantwortlich (s. Kapitel 2.3.1). Ähnliches wurde auch für AvrPtoB beobachtet. AvrPtoB bindet mit seiner zentralen Region an die Kinase BAK1 und verhindert die Assemblierung von PAMP-Rezeptorkomplexen (Shan *et al.*, 2008). Mutationen in dieser zentralen Region führen zum Verlust der Bindung an BAK1 (Cheng *et al.*, 2011). Es wurde gezeigt, dass die Bindung an BAK1 ausreichend ist, um stromabwärts-gelegene MAPK-Signalwege zu manipulieren und dadurch die PTI zu unterdrücken (Shan *et al.*, 2008; Cheng *et al.*, 2011). Die E3-Ligase-Aktivität von AvrPtoB wird hierfür nicht benötigt. Eine funktionale LRR-Region ist auch für den Effektor AvrAC aus *Xcc* von Bedeutung. AvrAC benötigt für die Interaktion mit den Kinasen RIPK (RPM1 *induced protein kinase*) und BIK1 (*Botrytis-induced kinase* 1) die Kombination aus seiner N-terminalen Domäne und LRR-Region (Feng *et al.*, 2012). Die Kinasen werden anschließend durch die C-terminal-gelegene UMP-Transferase von AvrAC posttranslational modifiziert und dadurch inaktiviert. Dies hat die Unterdrückung der Pflanzenabwehr zur Folge und trägt zur Virulenz von *Xcc* bei (Feng *et al.*, 2012). XopL beeinflusst die Aktivität von MAPKs jedoch nicht und greift vermutlich Proteine der Pflanzenabwehr an, die weiter stromabwärts der Signalkaskade liegen oder anderen regulatorischen Signalwegen zugehörig sind. Die Identifizierung dieser Zielproteine könnte erheblich zum Verständnis der biologischen Wirkung von XopL beitragen.
Bisherige Daten zeigen, dass XopL nicht nachweisbar zum bakteriellen Wachstum von *Xcv* beiträgt. Dies könnte eventuell an der funktionellen Redundanz der Effektoren liegen. Bisher sind fünf weitere T3E aus *Xcv* bekannt, welche die PAMP-induzierte Pflanzenabwehr unterdrücken (Kim *et al.*, 2008;

Bartetzko *et al.*, 2009; Kim *et al.*, 2009; Schulze *et al.*, 2012). Es kann außerdem nicht ausgeschlossen werden, dass weitere Effektor-E3-Ligasen durch *Xcv* transloziert werden, wie bereits in Kapitel 3.2.1 diskutiert. Anhand der Aminosäuresequenz der Effektoren lässt sich eine mögliche E3-Ligase-Aktivität nicht ableiten, so dass entsprechende Experimente nötig sind, um dies zu prüfen (Zhang *et al.*, 2006; Singer *et al.*, 2013).

Zusammenfassend deuten die vorliegenden Daten auf multiple Funktionen von XopL hin, ähnlich wie für AvrPtoB beschrieben (Göhre *et al.*, 2008; Shan *et al.*, 2008). Der N-terminale Bereich beider Effektoren dient nicht nur der Bindung des zu ubiquitinierenden Proteins, sondern zusätzlich auch der Unterdrückung der PTI. Die C-terminale E3-Ligase-Domäne ist ausschließlich für die Ubiquitinierung von Zielproteinen verantwortlich. Ein ähnliches Modell wurde auch für SopA von *Salmonella* postuliert. Die N-terminale Region von SopA ist für den Ausbruch der Bakterien aus der „Salmonella-Vakuole“ in das Zytosol verantwortlich. Die E3-Ligase-Domäne spielt hingegen eine Rolle im Entzündungsprozess während der Infektion (Zhang *et al.*, 2006). Die LRR-Domäne von IpaH9.8 erfüllt sogar regulatorische Aufgaben. Sie ist nicht nur für die Bindung des Substrats Ste7 verantwortlich, sondern inhibiert zusätzlich die Ubiquitinierungsaktivität von IpaH9.8 in Abwesenheit des Substrats (Singer *et al.*, 2008; Quezada *et al.*, 2009). Ste7 ist eine MAPKK (MAP-Kinase Kinase) und wird durch IpaH9.8 in Hefe degradiert (Rohde *et al.*, 2007).

Diese Beispiele verdeutlichen, dass einige Effektoren von Tier-und Pflanzenpathogenen einen ähnlichen modularen Aufbau besitzen und verschiedene Prozesse der Wirtszelle beeinflussen. Der N-terminale Bereich dient der Inaktivierung (Shan *et al.*, 2008; Singer *et al.*, 2013) und/oder Bindung von Virulenzzielen, welche anschließend durch enzymatisch aktive C-terminale Domänen modifiziert werden (Rohde *et al.*, 2007; Diao *et al.*, 2008; Göhre *et al.*, 2008).

3.4 Charakterisierung der Effektoren XopB und XopS

3.4.1 XopB und XopS unterdrücken die Pflanzenabwehr

In dieser Arbeit wurden die Effektorproteine XopB und XopS charakterisiert und als Virulenzfaktoren von *Xcv* identifiziert. Sowohl XopB als auch XopS tragen zur Ausbildung wässriger Läsionen in anfälligen Paprikapflanzen bei. Die Doppeldeletion von *xopB* und *xopS* wirkt sich zudem negativ auf das bakterielle Wachstum aus, der individuelle Verlust hat jedoch keinen Einfluss (s. Kapitel 2.2.1). Diese Beobachtung ließ eine redundante Funktion vermuten und konnte durch weitere Analysen bestätigt werden: XopB und XopS supprimieren die PAMP-induzierte Genexpression von *NHL10* in der Modellpflanze Arabidopsis. Beide Effektoren greifen vermutlich in Abwehrprozesse ein, die nicht von der Aktivierung von MAPK-Kaskaden abhängen oder stromabwärts von diesen liegen. Um dies im Detail zu klären, bedarf es weiterer Analysen. Die Expression von *NHL10* wird durch flg22 induziert und die Aktivität sowohl von MAP-Kinasen als auch Kalzium-abhängigen Proteinkinasen (*calcium-dependent protein kinases*, CDPKs) reguliert (Boudsocq *et al.*, 2010). Um zu prüfen, ob

XopB oder XopS MAPK- oder CDPK-spezifische Signalwege beeinflussen, könnte die Aktivität von spezifisch regulierten Genen in Arabidopsis analysiert werden. So wird die Expression von *FRK1* (*flg22-induced receptor kinase* 1) durch MAPKs reguliert, während die Aktivität von *PHI-1* (*phosphate-induced* 1) CDPK-abhängig ist (Abb. 3-1; (Boudsocq *et al.*, 2010). In weiterführenden Experimenten könnte also untersucht werden, ob die Expression der Reporterkonstrukte *pFRK1-LUC* bzw. *pPHI1-LUC* durch XopB und XopS beeinflusst wird.

CDPKs sind nicht ausschließlich in der Aktivierung der Genexpression involviert, sondern regulieren auch die Produktion reaktiver Sauerstoffspezies (Abb. 3-1; Kobayashi *et al.*, 2007). Es ist durchaus möglich, dass XopB und XopS nicht nur die Genexpression der PTI, sondern auch die ROS-Bildung unterdrücken. Außerdem könnte die reduzierte Expression der Abwehrgene Auswirkungen auf Kalloseablagerungen haben, wie bereits für andere T3E gezeigt (Block und Alfano, 2011). Dies sollte in zukünftigen Arbeiten untersucht werden. Hierfür wäre beispielsweise die Generierung transgener Arabidopsis-bzw. Paprika-Pflanzen sinnvoll, in denen *xopB* oder *xopS* unter Kontrolle eines induzierbaren Promotors stehen. PTI-Analysen durch Behandlung mit PAMPs könnten Hinweise geben, welche Abwehrreaktionen durch XopB oder XopS beeinträchtigt werden (ROS-Produktion, Kalloseablagerungen) und inwieweit Veränderungen im Transkriptom der Pflanzen stattfinden. Die Daten würden Hinweise auf mögliche Zielproteine der Effektoren liefern. Sofern homologe Proteine im Genom von Paprika oder *N. benthamiana* kodiert sind, könnte man diese durch *VIGS* stilllegen und analysieren, ob sich dies auf die Phänotypen nach transienter Expression von XopS bzw. XopB mittels *Agrobacterium* auswirkt. Außerdem müsste man untersuchen, ob die Zielproteine in der Interaktion mit *Xcv* eine Rolle spielen oder die Virulenz von *Xcv* beeinflussen. Falls die Bindung pflanzlicher Zielproteine für XopB- oder XopS-abhängige Virulenz entscheidend ist, sollten reduzierte Expressionslevel der Interaktoren die reduzierten Krankheitssymptome von *Xcv*Δ*xopB* bzw. *Xcv*Δ*xopS* aufheben.

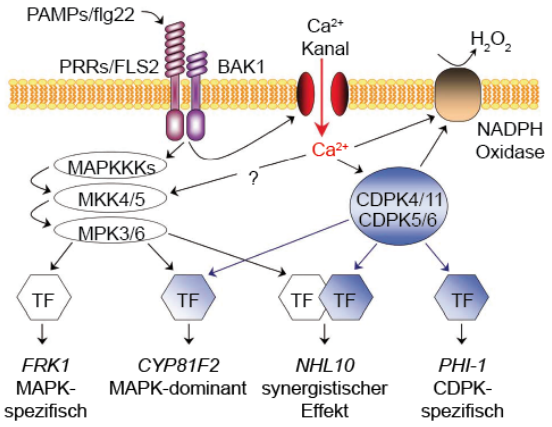

Abbildung 3-1: Modell der Aktivierung von CDPKs und MAPKs in der PAMP-Signalantwort.
Die Erkennung von PAMPs führt zur Signalweiterleitung über MAP-Kinase (MAPK)-Kaskaden oder Kalzium-abhängige Proteinkinasen (CDPK). Beide Signalwege führen zur Aktivierung von Transkriptionsfaktoren (TF), welche die Expression unterschiedlicher Gene spezifisch beeinflussen. MAPK- und CDPK-Signalwege können auch synergistisch wirken. In einigen Fällen wird die Expression einiger Gene zwar durch beide Signalwege induziert, aber deutlich stärker durch MAPKs. CDPKs aktivieren darüber hinaus die NADPH Oxidase und induzieren dadurch die Bildung reaktiver Sauerstoffspezies. Abbildung modifiziert nach Boudsocq *et al.* (2010).

3.4.1.1 Effektoren von *Xanthomonas* manipulieren die PTI

Bislang wurden drei weitere Effektoren von *Xcv* beschrieben, welche PAMP-induzierte Abwehrprozesse unterdrücken. Neben den in dieser Arbeit charakterisierten T3E XopB, XopS und XopL (s. Kapitel 2.2.1 und 2.3.1), unterdrücken auch XopD, XopJ und XopN PTI-induzierte Genexpression bzw. Zellwand-assoziierte Abwehrprozesse (Kim *et al.*, 2008; Bartetzko *et al.*, 2009; Kim *et al.*, 2009).

Die SUMO-Protease XopD aus *Xcv* wirkt im Zellkern der Pflanzenzelle als transkriptioneller Repressor von Abwehrgenen und fördert das bakterielle Wachstum in Tomatenpflanzen. Es wurde gezeigt, dass XopD die Genexpression indirekt beeinflusst, indem es Transkriptionsregulatoren de-sumoyliert und deren Aktivität oder Stabilität beeinflusst (Kim *et al.*, 2008; Kim *et al.*, 2011). Der Transkriptionsfaktor SlERF4 wird durch XopD-vermittelte De-Sumoylierung destabilisiert. Dadurch wird die Ethylen-bedingte Transkription von Genen reprimiert und die pflanzliche Resistenz gegen *Xcv* unterdrückt (Kim *et al.*, 2013). Ein ähnlicher Wirkmechanismus, jedoch mit einem anderen XopD-Interaktor, wurde von Canonne und Kollegen publiziert. Sie zeigten, dass XopD die Aktivität des Transkriptionsfaktors MYB30 aus Arabidopsis hemmt und dadurch Abwehrprozesse unterdrückt (Canonne *et al.*, 2011). Die Funktion von XopD scheint in verschiedenen *Xanthomonas* spp. konserviert zu sein, da XopD des *Xcc*-Stamms B100 ebenfalls mit MYB30 interagiert und die Abwehr in Arabidopsis unterdrückt (Canonne *et al.*, 2011).

Welche Abwehrkomponenten von XopJ und XopN angegriffen werden, ist im Detail noch nicht geklärt. XopJ ist an der Plasmamembran lokalisiert und unterdrückt Kalloseablagerungen nach PAMP-Erkennung, was aber nicht auf die Manipulation der Signalweiterleitung durch MAPK-Kaskaden zurückzuführen ist (Thieme *et al.*, 2007; Bartetzko *et al.*, 2009; Bartetzko, 2012). Bartetzko und Kollegen fanden weiterhin heraus, dass XopJ mit RPT6, einer Komponente der 19S-Untereinheit des 26S-Proteasoms, interagiert und dadurch die Proteasomaktivität reduziert. Vermutlich steht dies im Zusammenhang mit der PTI-Suppression (Bartetzko, 2012). Die Manipulation des Proteasoms erfolgt in Abhängigkeit von der Myristoylierung und der aktiven katalytischen Triade von XopJ. Allerdings konnte die für XopJ vermutete Acetyltransferase-Aktivität bislang nicht gezeigt werden (Bartetzko, 2012).

Der Virulenzfaktor XopN trägt zur Vermehrung von *Xcv* bei und reduziert PAMP-induzierte Genexpression sowie Kalloseablagerungen in Tomatenpflanzen (Kim *et al.*, 2009). XopN interagiert mit der zytosolischen Domäne einer atypischen Rezeptor-ähnlichen Kinase (*tomato atypical receptor-like kinase* 1, TARK1), die partiell für die Resistenz gegen *Xcv* benötigt wird. Außerdem bindet XopN an das 14-3-3 Protein TFT1 (*tomato fourteen-three-three isoform* 1) und fördert die Komplexbildung von TARK1 und TFT1 (Kim *et al.*, 2009; Taylor *et al.*, 2012). *TFT1* wird nicht nur in Folge der PTI verstärkt exprimiert, sondern ist darüber hinaus für die Expression einiger PTI-assoziierter Gene notwendig und inhibiert das bakterielle Wachstum von *Xcv* in anfälligen Tomatenpflanzen (Taylor *et al.*, 2012). XopN-Derivate, die nicht mehr an TFT1 binden, können das Wachstumsdefizit der *Xcv*Δ*xopN* Mutante nicht komplementieren. Diese Daten zeigen, dass die Bindung an TFT1 für die Virulenzwirkung von XopN nötig ist. Bislang ist jedoch nicht genau bekannt, inwiefern die Wirkungsweise von TARK1/TFT1 dadurch beeinflusst wird (Taylor *et al.*, 2012).

XopR aus *Xoo* beeinflusst ebenfalls die Expression von Abwehrgenen. In diesem Fall werden die „frühen" Abwehrgene *CYP81F2* (*cytochrome P450, family* 81, *polypeptide S*2) und *FRK1* vermindert exprimiert (Akimoto-Tomiyama *et al.*, 2012). Aufgrund der Lokalisierung an der Plasmamembran wurde vermutet, dass XopR möglicherweise durch Manipulation von PRRs in frühe Signalwege eingreift (Akimoto-Tomiyama *et al.*, 2012). Allerdings wurde die Aktivität von stromabwärts gelegenen MAPKs noch nicht experimentell untersucht, um diese Theorie zu bestätigen. XopR aus *Xcv* und *Xoo* sind auf Aminosäurebene zu 39 % identisch. Ob beide Effektoren ähnliche Funktionen erfüllen, muss noch geklärt werden. Die bereits erwähnten Protoplastenanalysen könnten zeigen, ob XopR aus *Xcv* einen Einfluss auf die Abwehr in Arabidopsis ausübt. Der bisherige Wissensstand über die Suppression der PTI durch Effektoren aus *Xcv* ist in einem Modell in Abbildung 3-2 zusammengefasst.

Wie Publikationen und Daten dieser Arbeit zeigen, manipulieren XopB, XopD, XopJ, XopL und XopS Abwehrprozesse vermutlich stromabwärts oder unabhängig von MAPK-Kaskaden, im Gegensatz zu zahlreichen Effektoren von *Pseudomonas syringae*.

So greifen AvrPto und AvrPtoB in die PAMP-Erkennung ein, indem sie Rezeptorkinasen degradieren (AvrPtoB) bzw. deren Kinase-Aktivität inhibieren (AvrPto) (Göhre *et al.*, 2008; Shan *et al.*, 2008; Xiang *et al.*, 2008). HopF2 und HopAI1 modifizieren MAP-Kinasen direkt und verhindern dadurch die Signalweiterleitung. MKK5 wird durch HopF2 ribosyliert und inaktiviert (Wang *et al.*, 2010), während HopAI1 MPK3 und 6 dephosphoryliert (Zhang *et al.*, 2007).

Nach den bisherigen Erkenntnissen stellt sich die Frage, ob es weitere T3E aus *Xcv* gibt, die die Pflanzenabwehr manipulieren. Um dies herauszufinden, könnte man alle bekannten T3E einzeln in Arabidopsis-Protoplast-Analysen untersuchen und prüfen, ob ein Effektor die PTI-assoziierte Genexpression unterdrückt. Außerdem könnte man in weiterführenden Arbeiten die bekannten PTI-Suppressoren XopB, XopD, XopJ, XopL, XopN, XopS im Genom von *Xcv* deletieren, um anschließend das *in planta* Wachstum dieses Stamms zu prüfen. Möglicherweise stellen die genannten Effektoren ein Effektor-Repertoire dar, welches für Wachstum und Virulenz von *Xcv* in Paprika-und Tomatenpflanzen essentiell ist. Entsprechendes konnte für einige T3E von *Pseudomonas* gezeigt werden (s. Kapitel 3.1; Cunnac *et al.*, 2011). In diesem Fall würde die Multi-Effektormutante ähnlich wachsen wie ein T3SS-defizienter Stamm. Sollte dies jedoch nicht der Fall sein, wäre das ein Hinweis auf weitere Effektoren, die zur Virulenz von *Xcv* beitragen.

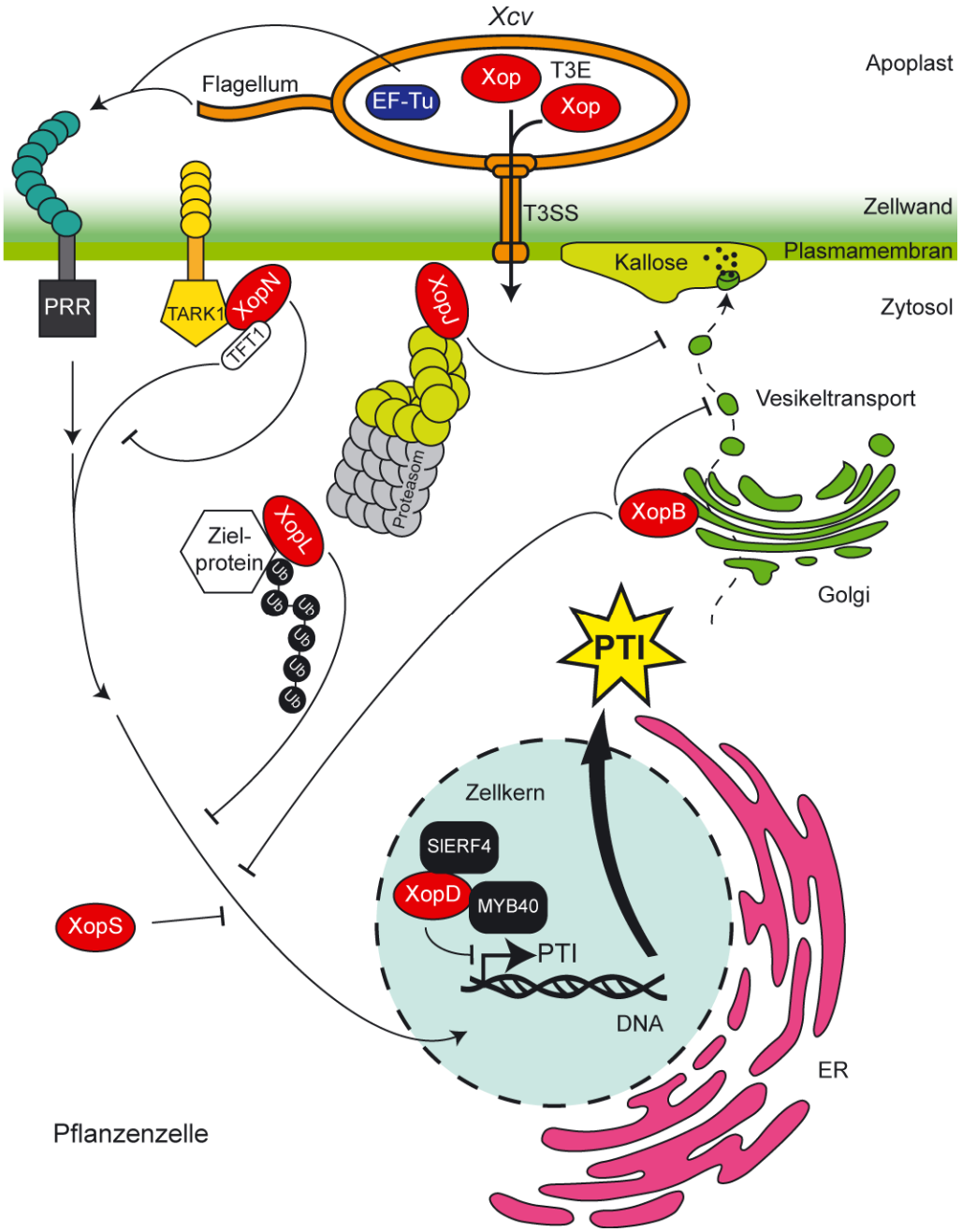

Abbildung 3-2: Modell der PTI-Suppression durch Effektoren von *Xcv* 85-10.
An der Plasmamembran werden konservierte bakterielle PAMPS durch PAMP-Rezeptoren (PRR) erkannt und Abwehrprozesse durch PTI-assoziierte Signalweiterleitung initiiert. Über das Typ III-Sekretionssystem (T3SS) transloziert *Xcv* Effektorproteine (T3E/Xop) in das Zytosol der Pflanzenzelle. Dort greifen einige T3E in Abwehrprozesse ein und fördern die bakterielle Vermehrung im Apoplasten durch Unterdrückung der PTI. XopB, XopL und XopS supprimieren die PAMP-induzierte Genexpression, der genaue Mechanismus ist aber noch ungeklärt. Außerdem greift XopB, genau wie XopJ, in den Vesikeltransport ein. Man spekuliert, dass dies im Fall von XopJ zu reduzierten Kalloseablagerungen führt. XopJ wirkt darüber hinaus störend auf den proteolytischen Abbau von Proteinen. XopN manipuliert die Pflanzenabwehr indem es mit der Kinase TARK1 und dem PTI-assoziierten Protein TFT1 interagiert. XopD greift hingegen die Transkriptionsfaktor SlERF4 und MYB30 im Zellkern an und hemmt deren transkriptionelle Aktivität. Für detaillierte Erläuterungen, siehe Text (Kapitel 3.4.1).

3.4.2 XopB manipuliert die pflanzliche Proteinsekretion

Um einen Einblick in die Wirkungsweise von XopB zu erhalten, wurden subzelluläre Lokalisierungsstudien mit Hilfe von XopB::GFP-Fusionsproteinen durchgeführt. Konfokale Laserabtastungs-Mikroskopie (*confocal laser scanning microscopy,* CLSM) und Elektronenmikroskopische Analysen zeigten, dass XopB im Zytoplasma und am Golgi-Apparat lokalisiert ist (s. Kapitel 2.2.1; Schulze *et al.*, 2012).

Der Golgi-Apparat ist Teil des zellulären Endomembransystems und besonders für den intrazellulären Vesikeltransport von Bedeutung (Glick, 2000). Vesikel werden an der Plasmamembran gebunden und durch Sekretion/Exozytose in den Apoplasten transportiert. Dieser Mechanismus wird durch so genannte SNARE-Komplexe (N-*ethylmaleimide-sensitive factor adaptor protein receptors*) katalysiert (Parlati *et al.*, 2000). SNAREs sind multimere Proteinkomplexe, bestehend aus v-SNAREs (*vesicle-synaptosome-associated protein receptors*) und t-SNAREs (*target-synaptosome-associated protein receptor*), welche wiederum aus Syntaxinen und Synaptosom-assoziierten Proteinen (SNAPs) zusammengesetzt sind (Parsot *et al.*, 2003).

Die Sekretion antimikrobieller Substanzen ist für die Abwehr phytopathogener Mikroorganismen von Bedeutung (s. Kapitel 1.1; Nürnberger und Lipka, 2005). Es konnte nachgewiesen werden, dass Komponenten des SNARE-Komplexes in der Pflanzenabwehr involviert sind und u. a. das Eindringen von Pilzen bzw. Oomyzeten verhindern (Collins *et al.*, 2003; Lipka *et al.*, 2005; Eschen-Lippold *et al.*, 2012). Da phytopathogene Bakterien in der Regel selbst nicht in die Wirtszelle eindringen, sondern sich im Apoplasten vermehren, dient der Vesikeltransport der Exozytose antimikrobieller Substanzen (Kalde *et al.*, 2007). Das Syntaxin SYP132 aus *N. benthamiana* ist an der Sekretion von Vesikeln beteiligt, die antimikrobielle Proteine (PR-Proteine) enthalten. Silencing von *Nb*SYP132 führt zu stark verringerter Akkumulation von PR1a im Apoplasten und ermöglicht *P. syringae* pv. *tabaci* besseres Wachstum in diesen Pflanzen (Kalde *et al.*, 2007). *Nb*SYP132 trägt somit zur Abwehr gegen *Pseudomonas* bei.

Der Vesikeltransport wird dadurch ein Angriffsziel bakterieller Effektoren, die über Manipulation der Proteinsekretion in die Abwehr der Pflanze eingreifen. In dieser Arbeit wurde gezeigt, dass XopB die Sekretion von secGFP supprimiert. Hierbei handelt es sich um ein GFP-Derivat, das eine Signalsequenz enthält, um in den Apoplasten transportiert zu werden. Die Blockierung der Sekretion führt zur intrazellulären Akkumulation des secGFP am endoplasmatischen Retikulum (Haseloff *et al.*, 1997; Batoko *et al.*, 2000). In früheren Studien wurden bereits Effektoren gefunden, die die Sekretion der Pflanze inhibieren. Die T3E HopZ1a und HopM1 von *P. syringae* beeinflussen die Sekretion, tun dies aber auf unterschiedliche Weise (Nomura *et al.*, 2006; Lee, AH *et al.*, 2012). HopZ1a ist ein Vertreter der YopJ/AvrRxv/HopZ-Familie von Cysteinproteasen/Acetyltransferasen. HopZ1a bindet und acetyliert pflanzliches Tubulin und bewirkt dadurch die Zerstörung des eukaryotischen Zytoskeletts (Lee, AH *et al.*, 2012). Dies wirkt sich wiederum negativ auf den Vesikeltransport aus,

führt zu geringeren Kalloseablagerungen im Zuge der PTI und hat letzten Endes ein besseres Wachstum von *P. syringae* zur Folge (Lee, AH *et al.*, 2012).

HopM1 akkumuliert am Golgi-Netzwerk, interagiert dort mit AtMIN7 (*Arabidopsis thaliana* HopM1 *interactor* 7) und vermittelt dessen proteolytischen Abbau (Nomura *et al.*, 2006). AtMIN7 ist einer der acht Vertreter der Familie der ADP-Ribosylierungsfaktoren (ARF) *guanine nucleotide exchange factor* (GEF) Proteine, die eine Schlüsselrolle im Vesikeltransport spielen. AtMIN7 ist in Zellwand-assoziierte Abwehrprozesse involviert und trägt zur PTI von Arabidopsis bei (Nomura *et al.*, 2006). Interessanterweise wird AtMIN7 auch für die ETI benötigt. *Pseudomonas*-Stämme mit verschiedenen Avr-Proteinen können in *atmin7 knockout*-Pflanzen besser wachsen als in Wildtyp-Pflanzen. Außerdem wird der HopM1-vermittelte Abbau von AtMIN7 im Zuge der ETI verhindert (Nomura *et al.*, 2011).

Neben XopB wurde mit XopJ bereits ein Effektor von *Xcv* beschrieben, der Sekretionsprozesse negativ beeinflusst (Bartetzko *et al.*, 2009). Die Suppression durch XopJ ist von dessen katalytischer Triade abhängig, da der Vesikeltransport durch die inaktive Mutante $XopJ_{C235A}$ nicht mehr beeinflusst wird (Bartetzko *et al.*, 2009). XopJ manipuliert auch PTI-assoziierte Abwehrprozesse und unterdrückt dadurch Kalloseablagerungen an der Zellwand (s. Kapitel 3.4.1). Es wird vermutet, dass die Unterdrückung des Vesikeltransports durch XopJ mit der Suppression der PTI in Zusammenhang steht, experimentell wurde dieses Hypothese allerdings noch nicht belegt (Bartetzko *et al.*, 2009). Für XopB wäre ein ähnliches Modell vorstellbar. In der vorliegenden Arbeit konnte mit $XopB_{A313V}$ eine Mutante identifiziert werden, die in ihrer Wirkung als Suppressor der PTI leicht beeinträchtigt ist, die Sekretion von secGFP aber nach wie vor unterdrückt (s. Kapitel 2.2.1). Jedoch konnte bislang kein XopB-Derivat gefunden werden, dass nicht mehr in der Lage ist Sekretion als auch PTI zu unterdrücken. Zukünftige Arbeiten sollten der Identifikation funktioneller Proteinbereiche von XopB dienen, welche für die Unterdrückung der Proteinsekretion und/oder Pflanzenabwehr von Bedeutung sind. Hierfür könnten sukzessive N- bzw. C-terminale Verkürzungen an XopB vorgenommen werden, und die daraus resultierenden Derivate bezüglich subzellulärer Lokalisation, Einfluss auf die secGFP-Sekretion und Unterdrückung der PTI untersucht werden.

3.4.3 Effektor-induzierte Zelltodreaktionen werden durch XopB inhibiert

Neben der Unterdrückung der PAMP-vermittelten Abwehr wirkt XopB zudem als Zelltodsuppressor. Nach transienter Ko-Expression von *avrBsT* und *xopB* in *N. benthamiana* konnte eine deutliche Unterdrückung des AvrBsT-bedingten Zelltods beobachtet werden. Die ist auch nach Überexpression von *xopB* im *Xcv* Stamm 75-3 der Fall. Dieser Stamm kodiert AvrBsT natürlicherweise und löst in AvrBsT-responsiven Paprikapflanzen die HR aus (Escolar *et al.*, 2001), welche durch die Überexpression von *xopB* supprimiert wird (s. Kapitel 2.2.1). Die AvrBsT-induzierte HR wird auch durch ein pflanzeneigenes Protein beeinflusst. Die Carboxylesterase/Phospholipase SOBER1 (*suppressor of AvrBsT-elicited resistance* 1) aus Arabidopsis inhibiert ebenfalls die AvrBsT-induzierte

Resistenz (Cunnac *et al.*, 2007). Im Zuge der Expression von AvrBsT kommt es zu erhöhten Mengen an Phosphatidsäure (PA) *in planta*, deren Anhäufung in Gegenwart von SOBER1 inhibiert wird und wiederum zur Unterdrückung der HR führt (Kirik und Mudgett, 2009). Möglicherweise wirkt XopB ähnlich wie SOBER1 und beeinflusst PA-Mengen innerhalb der Pflanze, was die Unterdrückung der AvrBsT-HR zur Folge hat. Um dies zu prüfen, müsste man die PA-Mengen nach Expression von XopB *in planta* messen und testen, ob XopB an diese Phospholipide binden kann oder aber über Interaktion mit PA-bildenden Enzymen in diesen Stoffwechselweg eingreift (Liscovitch *et al.*, 2000).
Nach transienter Expression wirkt XopB außerdem als Suppressor der Zelltodreaktionen, die durch die T3E XopG, XopJ und AvrRxv ausgelöst werden (s. Kapitel 2.2.1). XopJ und AvrRxv zählen wie AvrBsT zur YopJ/AvrRxv/HopZ-Proteinfamilie. Ob die durch XopJ und AvrRxv ausgelösten Zelltodreaktionen auf ähnlichen biochemischen Mechanismen beruhen wie im Fall von AvrBsT ist jedoch nicht bekannt. Da sich die Lokalisation der genannten T3E nach Ko-Expression mit XopB nicht ändert, greift XopB wahrscheinlich nicht in die Erkennung der T3E ein, sonder eher in stromabwärts gelegene Signalwege.
Der zu XopB ähnliche Effektor HopD1 aus *Pseudomonas* (79 % Identität, 86 % Ähnlichkeit der Aminosäuresequenz) hat eine ähnliche Funktion wie XopB. HopD1 unterdrückt den durch HopA1-induzierten Zelltod partiell und wirkt damit ebenfalls als Zelltodsuppressor (Jamir *et al.*, 2004). Dies ist ein Hinweis, dass beide Effektoren nicht nur Sequenzähnlichkeiten aufweisen, sondern auch funktionell miteinander verwandt sind. Im Gegensatz zu XopB trägt HopD1 jedoch nicht zur Virulenz von *P. syringae* pv. *tomato* DC3000 in Wirtspflanzen bei (Kvitko *et al.*, 2009). HopD1 lokalisiert im Zytoplasma und am endoplasmatischen Retikulum (Munkvold *et al.*, 2008) und könnte daher ebenfalls in den Vesikeltransport der Zelle eingreifen. Diesbezüglich wurden aber noch keine Daten publiziert.
Zelltod-supprimierende Aktivität wurde auch für andere T3E postuliert. So wird die Avirulenzaktivität von AvrPphF aus *P. syringae* pv. *phaseolicola* durch AvrPphC unterdrückt und führt zu Krankheitssymptomen in Bohnenpflanzen (Tsiamis *et al.*, 2000). Die Cysteinprotease HopN1 des *P. syringae* pv. *tomato* DC3000-Stamms wirkt als Zelltodsuppressor in Tomaten- und Nichtwirtspflanzen (Lopez-Solanilla *et al.*, 2004). HopN1 ist in Chloroplasten lokalisiert und inhibiert dort die Aktivität des Photosystems II (PSII) indem es PsbQ, eine Komponente des PSII, degradiert. Es wurde postuliert, dass PsbQ eine Rolle in der Ausbildung des DC3000-bedingten Zelltods in Tabak spielt und daher das Zielprotein darstellt, welches von HopN1 angegriffen wird (Rodriguez-Herva *et al.*, 2012).
Suppressionen von Zelltodreaktionen wurden aber nicht nur für T3E von *Pseudomonas* spp. sondern auch *Xanthomonas* beschrieben. So fanden Fujikawa und Kollegen heraus, dass *Pseudomonas fluorescens* die HR in Tabakpflanzen auslöst und zur Expression von Abwehrgenen führt. Diese Reaktionen werden durch die Effektorproteine AvrXa7 und AvrXa10 aus *Xoo* bzw. Apl1 aus *Xac* unterdrückt (Fujikawa *et al.*, 2006).
Allerdings ist die Suppressorwirkung der genannten Effektorproteine spezifisch. Die Unterdrückung verschiedener Zelltodreaktionen wie durch XopB scheint eine Ausnahme zu sein und wurde bislang

nur für den nicht verwandten Effektor AvrPtoB aus *P. syringae* gezeigt (Abramovitch *et al.*, 2003; Guo *et al.*, 2009). Die genauen molekularen Mechanismen, die der Suppressorwirkung von XopB zugrunde liegen, müssen in nachfolgenden Arbeiten noch untersucht werden.

4. Literaturverzeichnis

1994. The CCP4 suite: programs for protein crystallography. *Acta Crystallogr D Biol Crystallogr* **50**(Pt 5): 760-763.

Abramovitch RB, Janjusevic R, Stebbins CE, Martin GB. 2006. Type III effector AvrPtoB requires intrinsic E3 ubiquitin ligase activity to suppress plant cell death and immunity. *Proc Natl Acad Sci U S A* **103**(8): 2851-2856.

Abramovitch RB, Kim YJ, Chen S, Dickman MB, Martin GB. 2003. *Pseudomonas* type III effector AvrPtoB induces plant disease susceptibility by inhibition of host programmed cell death. *EMBO J* **22**(1): 60-69.

Abramovitch RB und Martin GB. 2004. Strategies used by bacterial pathogens to suppress plant defenses. *Curr Opin Plant Biol* **7**(4): 356-364.

Adams PD, Afonine PV, Bunkoczi G, Chen VB, Davis IW, Echols N, Headd JJ, Hung LW, Kapral GJ, Grosse-Kunstleve RW, McCoy AJ, Moriarty NW, Oeffner R, Read RJ, Richardson DC, Richardson JS, Terwilliger TC, Zwart PH. 2010. PHENIX: a comprehensive Python-based system for macromolecular structure solution. *Acta Crystallogr D Biol Crystallogr* **66**(Pt 2): 213-221.

Ade J, DeYoung BJ, Golstein C, Innes RW. 2007. Indirect activation of a plant nucleotide binding site-leucine-rich repeat protein by a bacterial protease. *Proc Natl Acad Sci U S A* **104**(7): 2531-2536.

Akimoto-Tomiyama C, Furutani A, Tsuge S, Washington EJ, Nishizawa Y, Minami E, Ochiai H. 2012. XopR, a type III effector secreted by *Xanthomonas oryzae* pv. *oryzae*, suppresses microbe-associated molecular pattern-triggered immunity in *Arabidopsis thaliana*. *Mol Plant Microbe Interact* **25**(4): 505-514.

Altschul SF, Madden TL, Schaffer AA, Zhang J, Zhang Z, Miller W, Lipman DJ. 1997. Gapped BLAST and PSI-BLAST: a new generation of protein database search programs. *Nucleic Acids Res* **25**(17): 3389-3402.

Anand A, Krichevsky A, Schornack S, Lahaye T, Tzfira T, Tang Y, Citovsky V, Mysore KS. 2007. Arabidopsis VIRE2 INTERACTING PROTEIN2 is required for Agrobacterium T-DNA integration in plants. *Plant Cell* **19**(5): 1695-1708.

Anderson JC, Pascuzzi PE, Xiao F, Sessa G, Martin GB. 2006. Host-mediated phosphorylation of type III effector AvrPto promotes *Pseudomonas* virulence and avirulence in tomato. *Plant Cell* **18**(2): 502-514.

Angot A, Peeters N, Lechner E, Vailleau F, Baud C, Gentzbittel L, Sartorel E, Genschik P, Boucher C, Genin S. 2006. Ralstonia solanacearum requires F-box-like domain-containing type III effectors to promote disease on several host plants. *Proc Natl Acad Sci U S A* **103**(39): 14620-14625.

Antony G, Zhou J, Huang S, Li T, Liu B, White F, Yang B. 2010. Rice *xa13* recessive resistance to bacterial blight is defeated by induction of the disease susceptibility gene Os-*11N3*. *Plant Cell* **22**(11): 3864-3876.

Ardley HC und Robinson PA. 2005. E3 ubiquitin ligases. *Essays Biochem* **41**: 15-30.

Asai T, Tena G, Plotnikova J, Willmann MR, Chiu WL, Gomez-Gomez L, Boller T, Ausubel FM, Sheen J. 2002. MAP kinase signalling cascade in Arabidopsis innate immunity. *Nature* **415**(6875): 977-983.

Astua-Monge G, Minsavage GV, Stall RE, Vallejos CE, Davis MJ, Jones JB. 2000. *Xv4-vrxv4*: a new gene-for-gene interaction identified between *Xanthomonas campestris* pv. *vesicatoria* race T3 and wild tomato relative Lycopersicon pennellii. *Mol Plant Microbe Interact* **13**(12): 1346-1355.

Ausubel FM, Brent R, Kingston RE, Moore DD, Seidman JG, Smith JA, Struhl K, eds. 1996. *Current protocols in molecular biology*. New York: John Wiley & Sons, Inc.

Axtell MJ, Chisholm ST, Dahlbeck D, Staskawicz BJ. 2003. Genetic and molecular evidence that the *Pseudomonas syringae* type III effector protein AvrRpt2 is a cysteine protease. *Mol Microbiol* **49**(6): 1537-1546.

Badel JL, Charkowski AO, Deng WL, Collmer A. 2002. A gene in the *Pseudomonas syringae* pv. *tomato* Hrp pathogenicity island conserved effector locus, *hopPtoA1*, contributes to efficient formation of bacterial colonies in planta and is duplicated elsewhere in the genome. *Mol Plant Microbe Interact* **15**(10): 1014-1024.

Bartetzko V. 2012. Funktionelle Charakterisierung des Typ III-Effektors XopJ aus *Xanthomonas campestris* pv. *vesicatoria.* Friedrich-Alexander-Universität Erlangen-Nürnberg Erlangen.

Bartetzko V, Sonnewald S, Vogel F, Hartner K, Stadler R, Hammes UZ, Bornke F. 2009. The *Xanthomonas campestris* pv. *vesicatoria* type III effector protein XopJ inhibits protein secretion: evidence for interference with cell wall-associated defense responses. *Mol Plant Microbe Interact* **22**(6): 655-664.

Batoko H, Zheng HQ, Hawes C, Moore I. 2000. A rab1 GTPase is required for transport between the endoplasmic reticulum and golgi apparatus and for normal golgi movement in plants. *Plant Cell* **12**(11): 2201-2218.

Beck T, Krasauskas A, Gruene T, Sheldrick GM. 2008. A magic triangle for experimental phasing of macromolecules. *Acta Crystallogr D Biol Crystallogr* **64**(Pt 11): 1179-1182.

Bender CL, Alarcon-Chaidez F, Gross DC. 1999. *Pseudomonas syringae* phytotoxins: mode of action, regulation, and biosynthesis by peptide and polyketide synthetases. *Microbiol Mol Biol Rev* **63**(2): 266-292.

Bennett-Lovsey RM, Herbert AD, Sternberg MJ, Kelley LA. 2008. Exploring the extremes of sequence/structure space with ensemble fold recognition in the program Phyre. *Proteins* **70**(3): 611-625.

Bent AF und Mackey D. 2007. Elicitors, effectors, and R genes: the new paradigm and a lifetime supply of questions. *Annu Rev Phytopathol* **45**: 399-436.

Bethke G, Pecher P, Eschen-Lippold L, Tsuda K, Katagiri F, Glazebrook J, Scheel D, Lee J. 2012. Activation of the *Arabidopsis thaliana* mitogen-activated protein kinase MPK11 by the flagellin-derived elicitor peptide, flg22. *Mol Plant Microbe Interact* **25**(4): 471-480.

Block A und Alfano JR. 2011. Plant targets for *Pseudomonas syringae* type III effectors: virulence targets or guarded decoys? *Curr Opin Microbiol* **14**(1): 39-46.

Block A, Li G, Fu ZQ, Alfano JR. 2008. Phytopathogen type III effector weaponry and their plant targets. *Curr Opin Plant Biol* **11**(4): 396-403.

Blume B, Nürnberger T, Nass N, Scheel D. 2000. Receptor-mediated increase in cytoplasmic free calcium required for activation of pathogen defense in parsley. *Plant Cell* **12**(8): 1425-1440.

Boch J und Bonas U. 2010. *Xanthomonas* AvrBs3 family-type III effectors: discovery and function. *Annu Rev Phytopathol* **48**: 419-436.

Boch J, Scholze H, Schornack S, Landgraf A, Hahn S, Kay S, Lahaye T, Nickstadt A, Bonas U. 2009. Breaking the code of DNA binding specificity of TAL-type III effectors. *Science* **326**(5959): 1509-1512.

Bogdanove AJ, Beer SV, Bonas U, Boucher CA, Collmer A, Coplin DL, Cornelis GR, Huang HC, Hutcheson SW, Panopoulos NJ, Van Gijsegem F. 1996. Unified nomenclature for broadly conserved *hrp* genes of phytopathogenic bacteria. *Mol Microbiol* **20**(3): 681-683.

Bogdanove AJ, Koebnik R, Lu H, Furutani A, Angiuoli SV, Patil PB, Van Sluys MA, Ryan RP, Meyer DF, Han SW, Aparna G, Rajaram M, Delcher AL, Phillippy AM, Puiu D, Schatz MC, Shumway M, Sommer DD, Trapnell C, Benahmed F, Dimitrov G, Madupu R, Radune D, Sullivan S, Jha G, Ishihara H, Lee SW, Pandey A, Sharma V, Sriariyanun M, Szurek B, Vera-Cruz CM, Dorman KS, Ronald PC, Verdier V, Dow JM, Sonti RV, Tsuge S, Brendel VP, Rabinowicz PD, Leach JE, White FF, Salzberg SL. 2011. Two new complete genome sequences offer insight into host and tissue specificity of plant pathogenic *Xanthomonas* spp. *J Bacteriol* **193**(19): 5450-5464.

Boller T und Felix G. 2009. A renaissance of elicitors: perception of microbe-associated molecular patterns and danger signals by pattern-recognition receptors. *Annu Rev Plant Biol* **60**: 379-406.

Boname JM, Thomas M, Stagg HR, Xu P, Peng J, Lehner PJ. 2010. Efficient internalization of MHC I requires lysine-11 and lysine-63 mixed linkage polyubiquitin chains. *Traffic* **11**(2): 210-220.

Bonas U, Schulte R, Fenselau S, Minsavage GV, Staskawicz BJ, Stall RE. 1991. Isolation of a gene-cluster from *Xanthomonas campestris* pv. *vesicatoria* that determines pathogenicity and the hypersensitive response on pepper and tomato. *Mol Plant-Microbe Interact* **4**(1): 81-88.

Bonshtien A, Lev A, Gibly A, Debbie P, Avni A, Sessa G. 2005. Molecular properties of the *Xanthomonas* AvrRxv effector and global transcriptional changes determined by its expression in resistant tomato plants. *Mol Plant Microbe Interact* **18**(4): 300-310.

Boudsocq M, Willmann MR, McCormack M, Lee H, Shan L, He P, Bush J, Cheng SH, Sheen J. 2010. Differential innate immune signalling via Ca(2+) sensor protein kinases. *Nature* **464**(7287): 418-422.

Bouly JP, Gissot L, Lessard P, Kreis M, Thomas M. 1999. *Arabidopsis thaliana* proteins related to the yeast SIP and SNF4 interact with AKINalpha1, an SNF1-like protein kinase. *Plant J* **18**(5): 541-550.

Brown I, Mansfield J, Bonas U. 1995. *hrp* genes in *Xanthomonas campestris* pv. *vesicatoria* determine ability to suppress papillae deposition in pepper mesophyll cells. *Mol Plant-Microbe Interact* **8**(6): 825-836.

Büttner D und Bonas U. 2002. Getting across-bacterial type III effector proteins on their way to the plant cell. *EMBO J* **21**(20): 5313-5322.

Büttner D und Bonas U. 2006. Who comes first? How plant pathogenic bacteria orchestrate type III secretion. *Curr Opin Microbiol* **9**(2): 193-200.

Büttner D und Bonas U. 2010. Regulation and secretion of *Xanthomonas* virulence factors. *FEMS Microbiol Rev* **34**(2): 107-133.

Büttner D, Gurlebeck D, Noël LD, Bonas U. 2004. HpaB from *Xanthomonas campestris* pv. *vesicatoria* acts as an exit control protein in type III-dependent protein secretion. *Mol Microbiol* **54**(3): 755-768.

Büttner D und He SY. 2009. Type III protein secretion in plant pathogenic bacteria. *Plant Physiol* **150**(4): 1656-1664.

Büttner D, Lorenz C, Weber E, Bonas U. 2006. Targeting of two effector protein classes to the type III secretion system by a HpaC- and HpaB-dependent protein complex from *Xanthomonas campestris* pv. *vesicatoria*. *Mol Microbiol* **59**(2): 513-527.

Büttner D, Nennstiel D, Klüsener B, Bonas U. 2002. Functional analysis of HrpF, a putative type III translocon protein from *Xanthomonas campestris* pv. *vesicatoria*. *J Bacteriol* **184**(9): 2389-2398.

Canonne J, Marino D, Jauneau A, Pouzet C, Briere C, Roby D, Rivas S. 2011. The *Xanthomonas* type III effector XopD targets the Arabidopsis transcription factor MYB30 to suppress plant defense. *Plant Cell* **23**(9): 3498-3511.

Canteros BJ. 1990. Diversity of plasmids and plasmid-encoded phenotypic traits in *Xanthomonas campestris* pv. *vesicatoria.* University of Florida.

Cernadas RA, Camillo LR, Benedetti CE. 2008. Transcriptional analysis of the sweet orange interaction with the citrus canker pathogens *Xanthomonas axonopodis* pv. *citri* and *Xanthomonas axonopodis* pv. *aurantifolii*. *Mol Plant Pathol* **9**(5): 609-631.

Chau V, Tobias JW, Bachmair A, Marriott D, Ecker DJ, Gonda DK, Varshavsky A. 1989. A multiubiquitin chain is confined to specific lysine in a targeted short-lived protein. *Science* **243**(4898): 1576-1583.

Cheng W, Munkvold KR, Gao H, Mathieu J, Schwizer S, Wang S, Yan YB, Wang J, Martin GB, Chai J. 2011. Structural analysis of *Pseudomonas syringae* AvrPtoB bound to host BAK1 reveals two similar kinase-interacting domains in a type III Effector. *Cell Host Microbe* **10**(6): 616-626.

Chinchilla D, Bauer Z, Regenass M, Boller T, Felix G. 2006. The Arabidopsis receptor kinase FLS2 binds flg22 and determines the specificity of flagellin perception. *Plant Cell* **18**(2): 465-476.

Chinchilla D, Zipfel C, Robatzek S, Kemmerling B, Nurnberger T, Jones JD, Felix G, Boller T. 2007. A flagellin-induced complex of the receptor FLS2 and BAK1 initiates plant defence. *Nature* **448**(7152): 497-500.

Chisholm ST, Coaker G, Day B, Staskawicz BJ. 2006. Host-microbe interactions: shaping the evolution of the plant immune response. *Cell* **124**(4): 803-814.

Chou YC, Keszei AF, Rohde JR, Tyers M, Sicheri F. 2012. Conserved Structural Mechanisms for Autoinhibition in IpaH Ubiquitin Ligases. *J Biol Chem* **287**(1): 268-275.

Christensen DE, Brzovic PS, Klevit RE. 2007. E2-BRCA1 RING interactions dictate synthesis of mono- or specific polyubiquitin chain linkages. *Nat Struct Mol Biol* **14**(10): 941-948.

Christie PJ und Cascales E. 2005. Structural and dynamic properties of bacterial type IV secretion systems. *Mol Membr Biol* **22**(1-2): 51-61.

Chung E, Seong E, Kim YC, Chung EJ, Oh SK, Lee S, Park JM, Joung YH, Choi D. 2004. A method of high frequency virus-induced gene silencing in chili pepper (Capsicum annuum L. cv. Bukang). *Mol Cells* **17**(2): 377-380.

Ciesiolka LD, Hwin T, Gearlds JD, Minsavage GV, Saenz R, Bravo M, Handley V, Conover SM, Zhang H, Caporgno J, Phengrasamy NB, Toms AO, Stall RE, Whalen MC. 1999. Regulation of expression of avirulence gene *avrRxv* and identification of a family of host interaction factors by sequence analysis of *avrBsT*. *Mol Plant Microbe Interact* **12**(1): 35-44.

Coaker G, Falick A, Staskawicz B. 2005. Activation of a phytopathogenic bacterial effector protein by a eukaryotic cyclophilin. *Science* **308**(5721): 548-550.

Coaker G, Zhu G, Ding Z, Van Doren SR, Staskawicz B. 2006. Eukaryotic cyclophilin as a molecular switch for effector activation. *Mol Microbiol* **61**(6): 1485-1496.

Collins NC, Thordal-Christensen H, Lipka V, Bau S, Kombrink E, Qiu JL, Huckelhoven R, Stein M, Freialdenhoven A, Somerville SC, Schulze-Lefert P. 2003. SNARE-protein-mediated disease resistance at the plant cell wall. *Nature* **425**(6961): 973-977.

Cook AA und Stall RE. 1963. Inheritance of resistance in pepper to bacterial spot. *Phytopathology* **53**: 1060-1062.

Cox RS. 1966. The role of bacterial spot in tomato production in south Florida. *Plant Dis Reptr* **50**: 699-700.

Cunnac S, Chakravarthy S, Kvitko BH, Russell AB, Martin GB, Collmer A. 2011. Genetic disassembly and combinatorial reassembly identify a minimal functional repertoire of type III effectors in *Pseudomonas syringae*. *Proc Natl Acad Sci U S A* **108**(7): 2975-2980.

Cunnac S, Lindeberg M, Collmer A. 2009. *Pseudomonas syringae* type III secretion system effectors: repertoires in search of functions. *Curr Opin Microbiol* **12**(1): 53-60.

Cunnac S, Wilson A, Nuwer J, Kirik A, Baranage G, Mudgett MB. 2007. A conserved carboxylesterase is a SUPPRESSOR OF AVRBST-ELICITED RESISTANCE in Arabidopsis. *Plant Cell* **19**(2): 688-705.

Dangl JL und Jones JD. 2001. Plant pathogens and integrated defence responses to infection. *Nature* **411**(6839): 826-833.

Daniels MJ, Barber CE, Turner PC, Sawczyc MK, Byrde RJW, Fielding AH. 1984. Cloning of genes involved in pathogenicity of *Xanthomonas campestris* pv. *campestris* using the broad host range cosmid pLAFR1. *EMBO J* **3**: 3323-3328.

Darvill AGA, P. 1984. PHYTOALEXINS AND THEIR ELICITORS-A Defense Against Microbial Infection in Plants. *Annu Rev Plant Physiol* **35**: 243-275.

Davies SP, Hawley SA, Woods A, Carling D, Haystead TA, Hardie DG. 1994. Purification of the AMP-activated protein kinase on ATP-gamma-sepharose and analysis of its subunit structure. *Eur J Biochem* **223**(2): 351-357.

de Torres M, Mansfield JW, Grabov N, Brown IR, Ammouneh H, Tsiamis G, Forsyth A, Robatzek S, Grant M, Boch J. 2006. *Pseudomonas syringae* effector AvrPtoB suppresses basal defence in Arabidopsis. *Plant J* **47**(3): 368-382.

de Wit PJ. 2007. How plants recognize pathogens and defend themselves. *Cell Mol Life Sci* **64**(21): 2726-2732.

DebRoy S, Thilmony R, Kwack YB, Nomura K, He SY. 2004. A family of conserved bacterial effectors inhibits salicylic acid-mediated basal immunity and promotes disease necrosis in plants. *Proc Natl Acad Sci U S A* **101**(26): 9927-9932.

Deng L, Wang C, Spencer E, Yang L, Braun A, You J, Slaughter C, Pickart C, Chen ZJ. 2000. Activation of the IkappaB kinase complex by TRAF6 requires a dimeric ubiquitin-conjugating enzyme complex and a unique polyubiquitin chain. *Cell* **103**(2): 351-361.

Denny TP. 1995. Involvement of bacterial polysaccharide in plant pathogenesis. *Annu Rev Phytopathol* **32**: 173-197.

DeRenzis FA und Schechtman A. 1973. Staining by neutral red and trypan blue in sequence for assaying vital and nonvital cultured cells. *Stain Technol* **48**(3): 135-136.

Deribe YL, Pawson T, Dikic I. 2010. Post-translational modifications in signal integration. *Nat Struct Mol Biol* **17**(6): 666-672.

Deslandes L, Olivier J, Peeters N, Feng DX, Khounlotham M, Boucher C, Somssich I, Genin S, Marco Y. 2003. Physical interaction between RRS1-R, a protein conferring resistance to bacterial wilt, and PopP2, a type III effector targeted to the plant nucleus. *Proc Natl Acad Sci U S A* **100**(13): 8024-8029.

Deslandes L und Rivas S. 2012. Catch me if you can: bacterial effectors and plant targets. *Trends Plant Sci* **17**(11): 644-655.

Dharmapuri S und Sonti RV. 1999. A transposon insertion in the *gumG* homologue of *Xanthomonas oryzae* pv. *oryzae* causes loss of extracellular polysaccharide production and virulence. *FEMS Microbiol Lett* **179**(1): 53-59.

Diao J, Zhang Y, Huibregtse JM, Zhou D, Chen J. 2008. Crystal structure of SopA, a Salmonella effector protein mimicking a eukaryotic ubiquitin ligase. *Nat Struct Mol Biol* **15**(1): 65-70.

Ditta G, Stanfield S, Corbin D, Helinski DR. 1980. Broad host range DNA cloning system for gram-negative bacteria: construction of a gene bank of Rhizobium meliloti. *Proc Natl Acad Sci U S A* **77**(12): 7347-7351.

Dodds PN und Rathjen JP. 2010. Plant immunity: towards an integrated view of plant-pathogen interactions. *Nat Rev Genet* **11**(8): 539-548.

Doidge EM. 1920. A tomato canker. *Ann Appl Biol* **7**: 407-430.

Dominguez C, Bonvin AM, Winkler GS, van Schaik FM, Timmers HT, Boelens R. 2004. Structural model of the UbcH5B/CNOT4 complex revealed by combining NMR, mutagenesis, and docking approaches. *Structure* **12**(4): 633-644.

Dong A, Xu X, Edwards AM, Chang C, Chruszcz M, Cuff M, Cymborowski M, Di Leo R, Egorova O, Evdokimova E, Filippova E, Gu J, Guthrie J, Ignatchenko A, Joachimiak A, Klostermann N, Kim Y, Korniyenko Y, Minor W, Que Q, Savchenko A, Skarina T, Tan K, Yakunin A, Yee A, Yim V, Zhang R, Zheng H, Akutsu M, Arrowsmith C, Avvakumov GV, Bochkarev A, Dahlgren LG, Dhe-Paganon S, Dimov S, Dombrovski L, Finerty P, Jr., Flodin S, Flores A, Graslund S, Hammerstrom M, Herman MD, Hong BS, Hui R, Johansson I, Liu Y, Nilsson M, Nedyalkova L, Nordlund P, Nyman T, Min J, Ouyang H, Park HW, Qi C, Rabeh W, Shen L, Shen Y, Sukumard D, Tempel W, Tong Y, Tresagues L, Vedadi M, Walker JR, Weigelt J, Welin M, Wu H, Xiao T, Zeng H, Zhu H. 2007. In situ proteolysis for protein crystallization and structure determination. *Nat Methods* **4**(12): 1019-1021.

Dowen RH, Engel JL, Shao F, Ecker JR, Dixon JE. 2009. A family of bacterial cysteine protease type III effectors utilizes acylation-dependent and -independent strategies to localize to plasma membranes. *J Biol Chem* **284**(23): 15867-15879.

Driouich A, Jauneau A, Staehelin LA. 1997. 7-Dehydrobrefeldin A, a naturally occurring brefeldin A derivative, inhibits secretion and causes a cis-to-trans breakdown of Golgi stacks in plant cells. *Plant Physiol* **113**(2): 487-492.

Dynek JN, Goncharov T, Dueber EC, Fedorova AV, Izrael-Tomasevic A, Phu L, Helgason E, Fairbrother WJ, Deshayes K, Kirkpatrick DS, Vucic D. 2010. c-IAP1 and UbcH5 promote K11-linked polyubiquitination of RIP1 in TNF signalling. *EMBO J* **29**(24): 4198-4209.

Eitas TK, Nimchuk ZL, Dangl JL. 2008. Arabidopsis TAO1 is a TIR-NB-LRR protein that contributes to disease resistance induced by the *Pseudomonas syringae* effector AvrB. *Proc Natl Acad Sci U S A* **105**(17): 6475-6480.

Emsley P und Cowtan K. 2004. Coot: model-building tools for molecular graphics. *Acta Crystallogr D Biol Crystallogr* **60**(Pt 12 Pt 1): 2126-2132.

Engler C, Kandzia R, Marillonnet S. 2008. A one pot, one step, precision cloning method with high throughput capability. *PLoS One* **3**(11): e3647.

Eschen-Lippold L, Landgraf R, Smolka U, Schulze S, Heilmann M, Heilmann I, Hause G, Rosahl S. 2012. Activation of defense against Phytophthora infestans in potato by down-regulation of syntaxin gene expression. *New Phytol* **193**(4): 985-996.

Escolar L, Van den Ackerveken G, Pieplow S, Rossier O, Bonas U. 2001. Type III secretion and in planta recognition of the *Xanthomonas* avirulence proteins AvrBs1 and AvrBsT. *Mol Plant Pathol* **2**(5): 287–296.

Espinosa A, Guo M, Tam VC, Fu ZQ, Alfano JR. 2003. The *Pseudomonas syringae* type III-secreted protein HopPtoD2 possesses protein tyrosine phosphatase activity and suppresses programmed cell death in plants. *Mol Microbiol* **49**(2): 377-387.

Evdokimov AG, Anderson DE, Routzahn KM, Waugh DS. 2001. Unusual molecular architecture of the Yersinia pestis cytotoxin YopM: a leucine-rich repeat protein with the shortest repeating unit. *J Mol Biol* **312**(4): 807-821.

Farras R, Ferrando A, Jasik J, Kleinow T, Okresz L, Tiburcio A, Salchert K, del Pozo C, Schell J, Koncz C. 2001. SKP1-SnRK protein kinase interactions mediate proteasomal binding of a plant SCF ubiquitin ligase. *EMBO J* **20**(11): 2742-2756.

Feilner T, Hultschig C, Lee J, Meyer S, Immink RG, Koenig A, Possling A, Seitz H, Beveridge A, Scheel D, Cahill DJ, Lehrach H, Kreutzberger J, Kersten B. 2005. High throughput identification of potential Arabidopsis mitogen-activated protein kinases substrates. *Mol Cell Proteomics* **4**(10): 1558-1568.

Feldman MF und Cornelis GR. 2003. The multitalented type III chaperones: all you can do with 15 kDa. *FEMS Microbiol Lett* **219**(2): 151-158.

Felix G und Boller T. 2003. Molecular sensing of bacteria in plants. The highly conserved RNA-binding motif RNP-1 of bacterial cold shock proteins is recognized as an elicitor signal in tobacco. *J Biol Chem* **278**(8): 6201-6208.

Felix G, Duran JD, Volko S, Boller T. 1999. Plants have a sensitive perception system for the most conserved domain of bacterial flagellin. *Plant J* **18**(3): 265-276.

Feng F, Yang F, Rong W, Wu X, Zhang J, Chen S, He C, Zhou JM. 2012. A *Xanthomonas* uridine 5'-monophosphate transferase inhibits plant immune kinases. *Nature* **485**(7396): 114-118.

Figurski D und Helinski DR. 1979. Replication of an origin-containing derivative of plasmid RK2 dependent on a plasmid function provided *in trans*. *Proc Natl Acad Sci USA* **76**: 1648-1652.

Frei dit Frey N und Robatzek S. 2009. Trafficking vesicles: pro or contra pathogens? *Curr Opin Plant Biol* **12**(4): 437-443.

Fu ZQ, Guo M, Jeong BR, Tian F, Elthon TE, Cerny RL, Staiger D, Alfano JR. 2007. A type III effector ADP-ribosylates RNA-binding proteins and quells plant immunity. *Nature* **447**(7142): 284-288.

Fujikawa T, Ishihara H, Leach JE, Tsuyumu S. 2006. Suppression of defense response in plants by the *avrBs3*/*pthA* gene family of *Xanthomonas* spp. *Mol Plant Microbe Interact* **19**(3): 342-349.

Furutani A, Takaoka M, Sanada H, Noguchi Y, Oku T, Tsuno K, Ochiai H, Tsuge S. 2009. Identification of novel type III secretion effectors in *Xanthomonas oryzae* pv. *oryzae*. *Mol Plant Microbe Interact* **22**(1): 96-106.

Galan JE. 2009. Common themes in the design and function of bacterial effectors. *Cell Host Microbe* **5**(6): 571-579.

Galyov EE, Hakansson S, Wolf-Watz H. 1994. Characterization of the operon encoding the YpkA Ser/Thr protein kinase and the YopJ protein of Yersinia pseudotuberculosis. *J Bacteriol* **176**(15): 4543-4548.

Ghosh P. 2004. Process of protein transport by the type III secretion system. *Microbiol Mol Biol Rev* **68**(4): 771-795.

Gimenez-Ibanez S, Hann DR, Ntoukakis V, Petutschnig E, Lipka V, Rathjen JP. 2009. AvrPtoB targets the LysM receptor kinase CERK1 to promote bacterial virulence on plants. *Curr Biol* **19**(5): 423-429.

Glick BS. 2000. Organization of the Golgi apparatus. *Curr Opin Cell Biol* **12**(4): 450-456.

Göhre V und Robatzek S. 2008. Breaking the barriers: microbial effector molecules subvert plant immunity. *Annu Rev Phytopathol* **46**: 189-215.

Göhre V, Spallek T, Haweker H, Mersmann S, Mentzel T, Boller T, de Torres M, Mansfield JW, Robatzek S. 2008. Plant pattern-recognition receptor FLS2 is directed for degradation by the bacterial ubiquitin ligase AvrPtoB. *Curr Biol* **18**(23): 1824-1832.

Gomez-Gomez L, Felix G, Boller T. 1999. A single locus determines sensitivity to bacterial flagellin in *Arabidopsis thaliana*. *Plant J* **18**(3): 277-284.

Goto E, Yamanaka Y, Ishikawa A, Aoki-Kawasumi M, Mito-Yoshida M, Ohmura-Hoshino M, Matsuki Y, Kajikawa M, Hirano H, Ishido S. 2010. Contribution of lysine 11-linked ubiquitination to MIR2-mediated major histocompatibility complex class I internalization. *J Biol Chem* **285**(46): 35311-35319.

Grant SR, Fisher EJ, Chang JH, Mole BM, Dangl JL. 2006. Subterfuge and manipulation: type III effector proteins of phytopathogenic bacteria. *Annu Rev Microbiol* **60**: 425-449.

Greenberg JT und Yao N. 2004. The role and regulation of programmed cell death in plant-pathogen interactions. *Cell Microbiol* **6**(3): 201-211.

Gu K, Yang B, Tian D, Wu L, Wang D, Sreekala C, Yang F, Chu Z, Wang GL, White FF, Yin Z. 2005. *R* gene expression induced by a type-III effector triggers disease resistance in rice. *Nature* **435**(7045): 1122-1125.

Guo M, Tian F, Wamboldt Y, Alfano JR. 2009. The majority of the type III effector inventory of *Pseudomonas syringae* pv. *tomato* DC3000 can suppress plant immunity. *Mol Plant Microbe Interact* **22**(9): 1069-1080.

Gürlebeck D. 2007. Identifizierung und Analyse von Protein-Interaktionen des Typ III-Effektors AvrBs3 aus Xanhomonas campestris pv. vesicatoria. Martin Luther University Halle-Wittenberg Halle, Germany.

Gürlebeck D, Jahn S, Gürlebeck N, Szczesny R, Szurek B, Hahn S, Hause G, Bonas U. 2009. Visualization of novel virulence activities of the Xanthomonas type III effectors AvrBs1, AvrBs3 and AvrBs4. *Mol Plant Pathol* **10**(2): 175-188.

Hajri A, Brin C, Hunault G, Lardeux F, Lemaire C, Manceau C, Boureau T, Poussier S. 2009. A "repertoire for repertoire" hypothesis: repertoires of type three effectors are candidate determinants of host specificity in *Xanthomonas*. *PLoS One* **4**(8): e6632.

Halford NG und Hey SJ. 2009. Snf1-related protein kinases (SnRKs) act within an intricate network that links metabolic and stress signalling in plants. *Biochem J* **419**(2): 247-259.

Hann DR, Gimenez-Ibanez S, Rathjen JP. 2010. Bacterial virulence effectors and their activities. *Curr Opin Plant Biol* **13**(4): 388-393.

Hao L, Wang H, Sunter G, Bisaro DM. 2003. Geminivirus AL2 and L2 proteins interact with and inactivate SNF1 kinase. *Plant Cell* **15**(4): 1034-1048.

Hardie DG. 2007. AMP-activated/SNF1 protein kinases: conserved guardians of cellular energy. *Nat Rev Mol Cell Biol* **8**(10): 774-785.

Haseloff J, Siemering KR, Prasher DC, Hodge S. 1997. Removal of a cryptic intron and subcellular localization of green fluorescent protein are required to mark transgenic Arabidopsis plants brightly. *Proc Natl Acad Sci U S A* **94**(6): 2122-2127.

Hauck P, Thilmony R, He SY. 2003. A *Pseudomonas syringae* type III effector suppresses cell wall-based extracellular defense in susceptible Arabidopsis plants. *Proc Natl Acad Sci U S A* **100**(14): 8577-8582.

He P, Shan L, Lin NC, Martin GB, Kemmerling B, Nürnberger T, Sheen J. 2006. Specific bacterial suppressors of MAMP signaling upstream of MAPKKK in Arabidopsis innate immunity. *Cell* **125**(3): 563-575.

He SY, Nomura K, Whittam TS. 2004. Type III protein secretion mechanism in mammalian and plant pathogens. *Biochim Biophys Acta* **1694**(1-3): 181-206.

Heath MC. 2000. Nonhost resistance and nonspecific plant defenses. *Curr Opin Plant Biol* **3**(4): 315-319.

Hedbacker K und Carlson M. 2008. SNF1/AMPK pathways in yeast. *Front Biosci* **13**: 2408-2420.

Higgins BB. 1922. The bacterial spot of pepper. *Phytopathology* **12**: 501-517.

Holland IB, Schmitt L, Young J. 2005. Type 1 protein secretion in bacteria, the ABC-transporter dependent pathway (review). *Mol Membr Biol* **22**(1-2): 29-39.

Holm L und Rosenstrom P. 2010. Dali server: conservation mapping in 3D. *Nucleic Acids Res* **38**(Web Server issue): W545-549.

Hotson A, Chosed R, Shu H, Orth K, Mudgett MB. 2003. *Xanthomonas* type III effector XopD targets SUMO-conjugated proteins in planta. *Mol Microbiol* **50**(2): 377-389.

Hotson A und Mudgett MB. 2004. Cysteine proteases in phytopathogenic bacteria: identification of plant targets and activation of innate immunity. *Curr Opin Plant Biol* **7**(4): 384-390.

Hu CD, Chinenov Y, Kerppola TK. 2002. Visualization of interactions among bZIP and Rel family proteins in living cells using bimolecular fluorescence complementation. *Mol Cell* **9**(4): 789-798.

Huang L, Kinnucan E, Wang G, Beaudenon S, Howley PM, Huibregtse JM, Pavletich NP. 1999. Structure of an E6AP-UbcH7 complex: insights into ubiquitination by the E2-E3 enzyme cascade. *Science* **286**(5443): 1321-1326.

Huguet E, Hahn K, Wengelnik K, Bonas U. 1998. *hpaA* mutants of *Xanthomonas campestris* pv. *vesicatoria* are affected in pathogenicity but retain the ability to induce host-specific hypersensitive reaction. *Mol Microbiol* **29**(6): 1379-1390.

Jackson RW, Athanassopoulos E, Tsiamis G, Mansfield JW, Sesma A, Arnold DL, Gibbon MJ, Murillo J, Taylor JD, Vivian A. 1999. Identification of a pathogenicity island, which contains genes for virulence and avirulence, on a large native plasmid in the bean pathogen *Pseudomonas syringae* pathovar *phaseolicola*. *Proc Natl Acad Sci USA* **96**(19): 10875-10880.

Jamir Y, Guo M, Oh HS, Petnicki-Ocwieja T, Chen S, Tang X, Dickman MB, Collmer A, Alfano JR. 2004. Identification of *Pseudomonas syringae* type III effectors that can suppress programmed cell death in plants and yeast. *Plant J* **37**(4): 554-565.

Janjusevic R, Abramovitch RB, Martin GB, Stebbins CE. 2006. A bacterial inhibitor of host programmed cell death defenses is an E3 ubiquitin ligase. *Science* **311**(5758): 222-226.

Jiang BL, He YQ, Cen WJ, Wei HY, Jiang GF, Jiang W, Hang XH, Feng JX, Lu GT, Tang DJ, Tang JL. 2008. The type III secretion effector XopXccN of *Xanthomonas campestris* pv. *campestris* is required for full virulence. *Res Microbiol* **159**(3): 216-220.

Jiang W, Jiang BL, Xu RQ, Huang JD, Wei HY, Jiang GF, Cen WJ, Liu J, Ge YY, Li GH, Su LL, Hang XH, Tang DJ, Lu GT, Feng JX, He YQ, Tang JL. 2009. Identification of six type III effector genes with the PIP box in *Xanthomonas campestris* pv. *campestris* and five of them contribute individually to full pathogenicity. *Mol Plant Microbe Interact* **22**(11): 1401-1411.

Jones JB, Lacy GH, Bouzar H, Stall RE, Schaad NW. 2004. Reclassification of the xanthomonads associated with bacterial spot disease of tomato and pepper. *Syst Appl Microbiol* **27**(6): 755-762.

Jones JB, Stall RE, Bouzar H. 1998. Diversity among xanthomonads pathogenic on pepper and tomato. *Annu Rev Phytopathol* **36**: 41-58.

Jones JD und Dangl JL. 2006. The plant immune system. *Nature* **444**(7117): 323-329.

Kajava AV, Anisimova M, Peeters N. 2008. Origin and evolution of GALA-LRR, a new member of the CC-LRR subfamily: from plants to bacteria? *PLoS One* **3**(2): e1694.

Kalde M, Nuhse TS, Findlay K, Peck SC. 2007. The syntaxin SYP132 contributes to plant resistance against bacteria and secretion of pathogenesis-related protein 1. *Proc Natl Acad Sci U S A* **104**(28): 11850-11855.

Kamadurai HB, Souphron J, Scott DC, Duda DM, Miller DJ, Stringer D, Piper RC, Schulman BA. 2009. Insights into ubiquitin transfer cascades from a structure of a UbcH5B approximately ubiquitin-HECT(NEDD4L) complex. *Mol Cell* **36**(6): 1095-1102.

Karimi M, De Meyer B, Hilson P. 2005. Modular cloning in plant cells. *Trends Plant Sci* **10**(3): 103-105.

Kay S und Bonas U. 2009. How *Xanthomonas* type III effectors manipulate the host plant. *Curr Opin Microbiol* **12**(1): 37-43.

Kay S, Hahn S, Marois E, Hause G, Bonas U. 2007. A bacterial effector acts as a plant transcription factor and induces a cell size regulator. *Science* **318**(5850): 648-651.

Kearney B und Staskawicz BJ. 1990. Widespread distribution and fitness contribution of *Xanthomonas campestris* avirulence gene *avrBs2*. *Nature* **346**(6282): 385-386.

Keen NT und Buzzell RI. 1991. New disease resistance genes in soybean against *Pseudomonas syringae* pv. glycinea - evidence that one of them interacts with a bacterial elicitor. *Theor Appl Genet* **81**(1): 133-138.

Kelley LA, MacCallum RM, Sternberg MJ. 2000. Enhanced genome annotation using structural profiles in the program 3D-PSSM. *J Mol Biol* **299**(2): 499-520.

Kelley LA und Sternberg MJ. 2009. Protein structure prediction on the Web: a case study using the Phyre server. *Nat Protoc* **4**(3): 363-371.

Kerscher O, Felberbaum R, Hochstrasser M. 2006. Modification of proteins by ubiquitin and ubiquitin-like proteins. *Annu Rev Cell Dev Biol* **22**: 159-180.

Kim DW, Lenzen G, Page AL, Legrain P, Sansonetti PJ, Parsot C. 2005. The Shigella flexneri effector OspG interferes with innate immune responses by targeting ubiquitin-conjugating enzymes. *Proc Natl Acad Sci U S A* **102**(39): 14046-14051.

Kim HT, Kim KP, Lledias F, Kisselev AF, Scaglione KM, Skowyra D, Gygi SP, Goldberg AL. 2007. Certain pairs of ubiquitin-conjugating enzymes (E2s) and ubiquitin-protein ligases (E3s) synthesize nondegradable forked ubiquitin chains containing all possible isopeptide linkages. *J Biol Chem* **282**(24): 17375-17386.

Kim JG, Li X, Roden JA, Taylor KW, Aakre CD, Su B, Lalonde S, Kirik A, Chen Y, Baranage G, McLane H, Martin GB, Mudgett MB. 2009. *Xanthomonas* T3S Effector XopN Suppresses PAMP-Triggered Immunity and Interacts with a Tomato Atypical Receptor-Like Kinase and TFT1. *Plant Cell* **21**(4): 1305-1323.

Kim JG, Stork W, Mudgett MB. 2013. *Xanthomonas* Type III Effector XopD Desumoylates Tomato Transcription Factor SlERF4 to Suppress Ethylene Responses and Promote Pathogen Growth. *Cell Host Microbe* **13**(2): 143-154.

Kim JG, Taylor KW, Hotson A, Keegan M, Schmelz EA, Mudgett MB. 2008. XopD SUMO protease affects host transcription, promotes pathogen growth, and delays symptom development in xanthomonas-infected tomato leaves. *Plant Cell* **20**(7): 1915-1929.

Kim JG, Taylor KW, Mudgett MB. 2011. Comparative analysis of the XopD type III secretion (T3S) effector family in plant pathogenic bacteria. *Mol Plant Pathol* **12**(8): 715-730.

Kim MG, da Cunha L, McFall AJ, Belkhadir Y, DebRoy S, Dangl JL, Mackey D. 2005. Two *Pseudomonas syringae* type III effectors inhibit RIN4-regulated basal defense in Arabidopsis. *Cell* **121**(5): 749-759.

Kim NH, Choi HW, Hwang BK. 2010. *Xanthomonas campestris* pv. *vesicatoria* effector AvrBsT induces cell death in pepper, but suppresses defense responses in tomato. *Mol Plant Microbe Interact* **23**(8): 1069-1082.

Kim SH, Kwon SI, Saha D, Anyanwu NC, Gassmann W. 2009. Resistance to the *Pseudomonas syringae* effector HopA1 is governed by the TIR-NBS-LRR protein RPS6 and is enhanced by mutations in SRFR1. *Plant Physiol* **150**(4): 1723-1732.

Kim YJ, Lin NC, Martin GB. 2002. Two distinct *Pseudomonas* effector proteins interact with the Pto kinase and activate plant immunity. *Cell* **109**(5): 589-598.

Kimber MS, Vallee F, Houston S, Necakov A, Skarina T, Evdokimova E, Beasley S, Christendat D, Savchenko A, Arrowsmith CH, Vedadi M, Gerstein M, Edwards AM. 2003. Data mining crystallization databases: knowledge-based approaches to optimize protein crystal screens. *Proteins* **51**(4): 562-568.

Kirik A und Mudgett MB. 2009. SOBER1 phospholipase activity suppresses phosphatidic acid accumulation and plant immunity in response to bacterial effector AvrBsT. *Proc Natl Acad Sci U S A* **106**(48): 20532-20537.

Kitajima S und Sato F. 1999. Plant pathogenesis-related proteins: molecular mechanisms of gene expression and protein function. *J Biochem* **125**(1): 1-8.

Kleinow T, Bhalerao R, Breuer F, Umeda M, Salchert K, Koncz C. 2000. Functional identification of an Arabidopsis snf4 ortholog by screening for heterologous multicopy suppressors of snf4 deficiency in yeast. *Plant J* **23**(1): 115-122.

Klement Z. GR. 1967. The hypersensitive reaction to infection by bacterial plant pathogens. *Annual Review of Phytopathology* **5**: 17-44.

Knoop V, Staskawicz B, Bonas U. 1991. Expression of the avirulence gene *avrBs3* from *Xanthomonas campestris* pv. *vesicatoria* is not under the control of *hrp* genes and is independent of plant factors. *J Bacteriol* **173**(22): 7142-7150.

Kobayashi M, Ohura I, Kawakita K, Yokota N, Fujiwara M, Shimamoto K, Doke N, Yoshioka H. 2007. Calcium-dependent protein kinases regulate the production of reactive oxygen species by potato NADPH oxidase. *Plant Cell* **19**(3): 1065-1080.

Kobe B und Kajava AV. 2001. The leucine-rich repeat as a protein recognition motif. *Curr Opin Struct Biol* **11**(6): 725-732.

Koch E und Slusarenko A. 1990. Arabidopsis is susceptible to infection by a downy mildew fungus. *Plant Cell* **2**(5): 437-445.

Koebnik R, Krüger A, Thieme F, Urban A, Bonas U. 2006. Specific binding of the *Xanthomonas campestris* pv. vesicatoria AraC-type transcriptional activator HrpX to plant-inducible promoter boxes. *J Bacteriol* **188**(21): 7652-7660.

Komander D und Rape M. 2012. The ubiquitin code. *Annu Rev Biochem* **81**: 203-229.

Koncz C und Schell J. 1986. The promoter of T_L-DNA gene 5 controls the tissue specific expression of chimaeric genes carried by a novel type of *Agrobacterium* binary vector. *Mol. Gen. Genet.* **204**: 383-396.

Kousik CS und Ritchie DE. 1999. Development of bacterial spot on near-isogenic lines of bell pepper carrying gene pyramids composed of defeated major resistance genes. *Phytopathology* **89**(11): 1066-1072.

Kraft E, Stone SL, Ma L, Su N, Gao Y, Lau OS, Deng XW, Callis J. 2005. Genome analysis and functional characterization of the E2 and RING-type E3 ligase ubiquitination enzymes of Arabidopsis. *Plant Physiol* **139**(4): 1597-1611.

Kroj T, Rudd JJ, Nurnberger T, Gabler Y, Lee J, Scheel D. 2003. Mitogen-activated protein kinases play an essential role in oxidative burst-independent expression of pathogenesis-related genes in parsley. *J Biol Chem* **278**(4): 2256-2264.

Kunze G, Zipfel C, Robatzek S, Niehaus K, Boller T, Felix G. 2004. The N terminus of bacterial elongation factor Tu elicits innate immunity in *Arabidopsis* plants. *Plant Cell* **16**(12): 3496-3507.

Kvitko BH, Park DH, Velasquez AC, Wei CF, Russell AB, Martin GB, Schneider DJ, Collmer A. 2009. Deletions in the repertoire of *Pseudomonas syringae* pv. *tomato* DC3000 type III secretion effector genes reveal functional overlap among effectors. *PLoS Pathog* **5**(4): e1000388.

Kwon C, Bednarek P, Schulze-Lefert P. 2008. Secretory pathways in plant immune responses. *Plant Physiol* **147**(4): 1575-1583.

Lagaert S, Belien T, Volckaert G. 2009. Plant cell walls: Protecting the barrier from degradation by microbial enzymes. *Semin Cell Dev Biol* **20**(9): 1064-1073.

Lakatos L, Klein M, Hofgen R, Banfalvi Z. 1999. Potato StubSNF1 interacts with StubGAL83: a plant protein kinase complex with yeast and mammalian counterparts. *Plant J* **17**(5): 569-574.

Lam H, Deutsch EW, Eddes JS, Eng JK, Stein SE, Aebersold R. 2008. Building consensus spectral libraries for peptide identification in proteomics. *Nat Methods* **5**(10): 873-875.

Laskowski R A MMW, Moss D S & Thornton J M 1993. PROCHECK: a program to check the stereochemical quality of protein structures. *J. Appl. Cryst.* **26**: 283-291.

Lee AH, Hurley B, Felsensteiner C, Yea C, Ckurshumova W, Bartetzko V, Wang PW, Quach V, Lewis JD, Liu YC, Bornke F, Angers S, Wilde A, Guttman DS, Desveaux D. 2012. A bacterial acetyltransferase destroys plant microtubule networks and blocks secretion. *PLoS Pathog* **8**(2): e1002523.

Lee CC, Wood MD, Ng K, Andersen CB, Liu Y, Luginbuhl P, Spraggon G, Katagiri F. 2004. Crystal structure of the type III effector AvrB from *Pseudomonas syringae*. *Structure* **12**(3): 487-494.

Lee DH und Goldberg AL. 1998. Proteasome inhibitors: valuable new tools for cell biologists. *Trends Cell Biol* **8**(10): 397-403.

Lee J, Teitzel GM, Munkvold K, del Pozo O, Martin GB, Michelmore RW, Greenberg JT. 2012. Type III secretion and effectors shape the survival and growth pattern of *Pseudomonas syringae* on leaf surfaces. *Plant Physiol* **158**(4): 1803-1818.

Lee SH, Park Y, Yoon SK, Yoon JB. 2010. Osmotic stress inhibits proteasome by p38 MAPK-dependent phosphorylation. *J Biol Chem* **285**(53): 41280-41289.

Levin I, Eakin C, Blanc MP, Klevit RE, Miller SI, Brzovic PS. 2010. Identification of an unconventional E3 binding surface on the UbcH5 ~ Ub conjugate recognized by a pathogenic bacterial E3 ligase. *Proc Natl Acad Sci U S A* **107**(7): 2848-2853.

Lewis JD, Abada W, Ma W, Guttman DS, Desveaux D. 2008. The HopZ family of *Pseudomonas syringae* type III effectors require myristoylation for virulence and avirulence functions in *Arabidopsis thaliana*. *J Bacteriol* **190**(8): 2880-2891.

Lewis JD, Guttman DS, Desveaux D. 2009. The targeting of plant cellular systems by injected type III effector proteins. *Semin Cell Dev Biol* **20**(9): 1055-1063.

Lewis JD, Lee A, Ma W, Zhou H, Guttman DS, Desveaux D. 2011. The YopJ superfamily in plant-associated bacteria. *Mol Plant Pathol* **12**(9): 928-937.

Lin DY, Diao J, Chen J. 2012. Crystal structures of two bacterial HECT-like E3 ligases in complex with a human E2 reveal atomic details of pathogen-host interactions. *Proc Natl Acad Sci U S A* **109**(6): 1925-1930.

Lin DY, Diao J, Zhou D, Chen J. 2011. Biochemical and structural studies of a HECT-like ubiquitin ligase from Escherichia coli O157:H7. *J Biol Chem* **286**(1): 441-449.

Lindeberg M, Stavrinides J, Chang JH, Alfano JR, Collmer A, Dangl JL, Greenberg JT, Mansfield JW, Guttman DS. 2005. Proposed guidelines for a unified nomenclature and phylogenetic analysis of type III Hop effector proteins in the plant pathogen *Pseudomonas syringae*. *Mol Plant Microbe Interact* **18**(4): 275-282.

Lipka V, Dittgen J, Bednarek P, Bhat R, Wiermer M, Stein M, Landtag J, Brandt W, Rosahl S, Scheel D, Llorente F, Molina A, Parker J, Somerville S, Schulze-Lefert P. 2005. Pre- and postinvasion defenses both contribute to nonhost resistance in Arabidopsis. *Science* **310**(5751): 1180-1183.

Liscovitch M, Czarny M, Fiucci G, Tang X. 2000. Phospholipase D: molecular and cell biology of a novel gene family. *Biochem J* **345 Pt 3**: 401-415.

Liu Y, Schiff M, Dinesh-Kumar SP. 2002a. Virus-induced gene silencing in tomato. *Plant J* **31**(6): 777-786.

Liu Y, Schiff M, Marathe R, Dinesh-Kumar SP. 2002b. Tobacco Rar1, EDS1 and NPR1/NIM1 like genes are required for N-mediated resistance to tobacco mosaic virus. *Plant J* **30**(4): 415-429.

Long SR und Staskawicz BJ. 1993. Prokaryotic plant parasites. *Cell* **73**(5): 921-935.

Lopez-Solanilla E, Bronstein PA, Schneider AR, Collmer A. 2004. HopPtoN is a *Pseudomonas syringae* Hrp (type III secretion system) cysteine protease effector that suppresses pathogen-induced necrosis associated with both compatible and incompatible plant interactions. *Mol Microbiol* **54**(2): 353-365.

Lorenz C und Buttner D. 2009. Functional characterization of the type III secretion ATPase HrcN from the plant pathogen *Xanthomonas campestris* pv. *vesicatoria*. *J Bacteriol* **191**(5): 1414-1428.

Lorenz C, Kirchner O, Egler M, Stuttmann J, Bonas U, Buttner D. 2008a. HpaA from *Xanthomonas* is a regulator of type III secretion. *Mol Microbiol* **69**(2): 344-360.

Lorenz C, Schulz S, Wolsch T, Rossier O, Bonas U, Buttner D. 2008b. HpaC controls substrate specificity of the *Xanthomonas* type III secretion system. *PLoS Pathog* **4**(6): e1000094.

Losada LC und Hutcheson SW. 2005. Type III secretion chaperones of *Pseudomonas syringae* protect effectors from Lon-associated degradation. *Mol Microbiol* **55**(3): 941-953.

Lukasik E und Takken FL. 2009. STANDing strong, resistance proteins instigators of plant defence. *Curr Opin Plant Biol* **12**(4): 427-436.

Lumbreras V, Alba MM, Kleinow T, Koncz C, Pages M. 2001. Domain fusion between SNF1-related kinase subunits during plant evolution. *EMBO Rep* **2**(1): 55-60.

Ma W, Dong FF, Stavrinides J, Guttman DS. 2006. Type III effector diversification via both pathoadaptation and horizontal transfer in response to a coevolutionary arms race. *PLoS Genet* **2**(12): e209.

Macho AP, Guevara CM, Tornero P, Ruiz-Albert J, Beuzon CR. 2010. The *Pseudomonas syringae* effector protein HopZ1a suppresses effector-triggered immunity. *New Phytol* **187**(4): 1018-1033.

Mackey D, Belkhadir Y, Alonso JM, Ecker JR, Dangl JL. 2003. Arabidopsis RIN4 is a target of the type III virulence effector AvrRpt2 and modulates RPS2-mediated resistance. *Cell* **112**(3): 379-389.

Mackey D, Holt BF, 3rd, Wiig A, Dangl JL. 2002. RIN4 interacts with *Pseudomonas syringae* type III effector molecules and is required for RPM1-mediated resistance in Arabidopsis. *Cell* **108**(6): 743-754.

Marois E, Van den Ackerveken G, Bonas U. 2002. The *Xanthomonas* type III effector protein AvrBs3 modulates plant gene expression and induces cell hypertrophy in the susceptible host. *Mol Plant Microbe Interact* **15**(7): 637-646.

Ménard R, Sansonetti PJ, Parsot C. 1993. Nonpolar mutagenesis of the ipa genes defines IpaB, IpaC, and IpaD as effectors of Shigella flexneri entry into epithelial cells. *J Bacteriol* **175**(18): 5899-5906.

Metz M, Dahlbeck D, Morales CQ, Al Sady B, Clark ET, Staskawicz BJ. 2005. The conserved *Xanthomonas campestris* pv. *vesicatoria* effector protein XopX is a virulence factor and suppresses host defense in *Nicotiana benthamiana*. *Plant J* **41**(6): 801-814.

Minor W, Cymborowski M, Otwinowski Z, Chruszcz M. 2006. HKL-3000: the integration of data reduction and structure solution--from diffraction images to an initial model in minutes. *Acta Crystallogr D Biol Crystallogr* **62**(Pt 8): 859-866.

Minsavage GV, Dahlbeck D, Whalen MC, Kearny B, Bonas U, Staskawicz BJ, Stall RE. 1990. Gene-for-gene relationships specifying disease resistance in *Xanthomonas campestris* pv. *vesicatoria* - pepper interactions. *Mol Plant-Microbe Interact* **3**(1): 41-47.

Misumi Y, Miki K, Takatsuki A, Tamura G, Ikehara Y. 1986. Novel blockade by brefeldin A of intracellular transport of secretory proteins in cultured rat hepatocytes. *J Biol Chem* **261**(24): 11398-11403.

Mitchelhill KI, Stapleton D, Gao G, House C, Michell B, Katsis F, Witters LA, Kemp BE. 1994. Mammalian AMP-activated protein kinase shares structural and functional homology with the catalytic domain of yeast Snf1 protein kinase. *J Biol Chem* **269**(4): 2361-2364.

Miya A, Albert P, Shinya T, Desaki Y, Ichimura K, Shirasu K, Narusaka Y, Kawakami N, Kaku H, Shibuya N. 2007. CERK1, a LysM receptor kinase, is essential for chitin elicitor signaling in Arabidopsis. *Proc Natl Acad Sci U S A* **104**(49): 19613-19618.

Mohr TJ, Liu H, Yan S, Morris CE, Castillo JA, Jelenska J, Vinatzer BA. 2008. Naturally occurring nonpathogenic isolates of the plant pathogen *Pseudomonas syringae* lack a type III secretion system and effector gene orthologues. *J Bacteriol* **190**(8): 2858-2870.

Morales CQ, Posada J, Macneale E, Franklin D, Rivas I, Bravo M, Minsavage J, Stall RE, Whalen MC. 2005. Functional analysis of the early chlorosis factor gene. *Mol Plant Microbe Interact* **18**(5): 477-486.

Mudgett MB, Chesnokova O, Dahlbeck D, Clark ET, Rossier O, Bonas U, Staskawicz BJ. 2000. Molecular signals required for type III secretion and translocation of the *Xanthomonas campestris* AvrBs2 protein to pepper plants. *Proc Natl Acad Sci U S A* **97**(24): 13324-13329.

Mukherjee S, Hao YH, Orth K. 2007. A newly discovered post-translational modification--the acetylation of serine and threonine residues. *Trends Biochem Sci* **32**(5): 210-216.

Mukherjee S, Keitany G, Li Y, Wang Y, Ball HL, Goldsmith EJ, Orth K. 2006. Yersinia YopJ acetylates and inhibits kinase activation by blocking phosphorylation. *Science* **312**(5777): 1211-1214.

Munkvold KR, Martin ME, Bronstein PA, Collmer A. 2008. A survey of the *Pseudomonas syringae* pv. *tomato* DC3000 type III secretion system effector repertoire reveals several effectors that are deleterious when expressed in *Saccharomyces cerevisiae*. *Mol Plant Microbe Interact* **21**(4): 490-502.

Murillo J, Shen H, Gerhold D, Sharma A, Cooksey DA, Keen NT. 1994. Characterization of pPT23B, the plasmid involved in syringolide production by *Pseudomonas syringae* pv. *tomato* PT23. *Plasmid* **31**(3): 275-287.

Murshudov GN, Vagin AA, Dodson EJ. 1997. Refinement of macromolecular structures by the maximum-likelihood method. *Acta Crystallogr D Biol Crystallogr* **53**(Pt 3): 240-255.

Nakagawa T, Kurose T, Hino T, Tanaka K, Kawamukai M, Niwa Y, Toyooka K, Matsuoka K, Jinbo T, Kimura T. 2007. Development of series of gateway binary vectors, pGWBs, for realizing efficient construction of fusion genes for plant transformation. *J Biosci Bioeng* **104**(1): 34-41.

Napoli C und Staskawicz B. 1987. Molecular characterization and nucleic acid sequence of an avirulence gene from race 6 of *Pseudomonas syringae* pv. *glycinea*. *J Bacteriol* **169**(2): 572-578.

Nelson BK, Cai X, Nebenfuhr A. 2007. A multicolored set of in vivo organelle markers for co-localization studies in Arabidopsis and other plants. *Plant J* **51**(6): 1126-1136.

Ni S, Sheldrick GM, Benning MM, Kennedy MA. 2009. The 2A resolution crystal structure of HetL, a pentapeptide repeat protein involved in regulation of heterocyst differentiation in the cyanobacterium Nostoc sp. strain PCC 7120. *J Struct Biol* **165**(1): 47-52.

Nimchuk ZL, Fisher EJ, Desveaux D, Chang JH, Dangl JL. 2007. The HopX (AvrPphE) family of *Pseudomonas syringae* type III effectors require a catalytic triad and a novel N-terminal domain for function. *Mol Plant Microbe Interact* **20**(4): 346-357.

Nino-Liu DO, Ronald PC, Bogdanove AJ. 2006. *Xanthomonas oryzae* pathovars: model pathogens of a model crop. *Mol Plant Pathol* **7**(5): 303-324.

Noël L, Thieme F, Gabler J, Büttner D, Bonas U. 2003. XopC and XopJ, two novel type III effector proteins from *Xanthomonas campestris* pv. *vesicatoria*. *J Bacteriol* **185**(24): 7092-7102.

Noël L, Thieme F, Nennstiel D, Bonas U. 2001. cDNA-AFLP analysis unravels a genome-wide *hrpG*-regulon in the plant pathogen *Xanthomonas campestris* pv. *vesicatoria*. *Mol Microbiol* **41**(6): 1271-1281.

Noël L, Thieme F, Nennstiel D, Bonas U. 2002. Two novel type III-secreted proteins of *Xanthomonas campestris* pv. *vesicatoria* are encoded within the *hrp* pathogenicity island. *J Bacteriol* **184**(5): 1340-1348.

Nomura K, Debroy S, Lee YH, Pumplin N, Jones J, He SY. 2006. A bacterial virulence protein suppresses host innate immunity to cause plant disease. *Science* **313**(5784): 220-223.

Nomura K, Mecey C, Lee YN, Imboden LA, Chang JH, He SY. 2011. Effector-triggered immunity blocks pathogen degradation of an immunity-associated vesicle traffic regulator in Arabidopsis. *Proc Natl Acad Sci U S A* **108**(26): 10774-10779.

Nomura K, Melotto M, He SY. 2005. Suppression of host defense in compatible plant-*Pseudomonas syringae* interactions. *Curr Opin Plant Biol* **8**(4): 361-368.

Norris SR, Meyer SE, Callis J. 1993. The intron of Arabidopsis thaliana polyubiquitin genes is conserved in location and is a quantitative determinant of chimeric gene expression. *Plant Mol Biol* **21**(5): 895-906.

Ntoukakis V, Mucyn TS, Gimenez-Ibanez S, Chapman HC, Gutierrez JR, Balmuth AL, Jones AM, Rathjen JP. 2009. Host inhibition of a bacterial virulence effector triggers immunity to infection. *Science* **324**(5928): 784-787.

Nuber U und Scheffner M. 1999. Identification of determinants in E2 ubiquitin-conjugating enzymes required for hect E3 ubiquitin-protein ligase interaction. *J Biol Chem* **274**(11): 7576-7582.

Nürnberger T, Brunner F, Kemmerling B, Piater L. 2004. Innate immunity in plants and animals: striking similarities and obvious differences. *Immunol Rev* **198**: 249-266.

Nürnberger T und Lipka V. 2005. Non-host resistance in plants: new insights into an old phenomenon. *Mol Plant Pathol* **6**(3): 335-345.

Nürnberger T und Scheel D. 2001. Signal transmission in the plant immune response. *Trends Plant Sci* **6**(8): 372-379.

Orth K. 2002. Function of the Yersinia effector YopJ. *Curr Opin Microbiol* **5**(1): 38-43.

Orth K, Xu Z, Mudgett MB, Bao ZQ, Palmer LE, Bliska JB, Mangel WF, Staskawicz B, Dixon JE. 2000. Disruption of signaling by Yersinia effector YopJ, a ubiquitin-like protein protease. *Science* **290**(5496): 1594-1597.

Otwinowski Z und Minor W 1997. Processing of X-ray Diffraction Data Collected in Oscillation Mode. *Methods in Enzymology*, 307-326.

P. D. Adams PVA, G. Bunkóczi, V. B. Chen, I. W. Davis, N. Echols, J. J. Headd, L.-W. Hung, G. J. Kapral, R. W. Grosse-Kunstleve, A. J. McCoy, N. W. Moriarty, R. Oeffner, R. J. Read, D. C. Richardson, J. S. Richardson, T. C. Terwilliger and P. H. Zwart 2010. PHENIX: a comprehensive Python-based system for macromolecular structure solution. *Acta Cryst.* **D66**: 213-221.

P. H. Zwart PVA, R. W. Grosse-Kunstleve, L.-W. Hung, T. R. Ioerger, A. J. McCoy, E. McKee, N. W. Moriarty, R. J. Read, J. C. Sacchettini, N. K. Sauter, L. C. Storoni, T. C. Terwilliger, P. D. Adams 2008. Automated Structure Solution with the PHENIX Suite. *Methods in Molecular Biology* **426**: 419-435.

Pal A, Debreczeni JE, Sevvana M, Gruene T, Kahle B, Zeeck A, Sheldrick GM. 2008. Structures of viscotoxins A1 and B2 from European mistletoe solved using native data alone. *Acta Crystallogr D Biol Crystallogr* **64**(Pt 9): 985-992.

Pal A, Kraetzner R, Gruene T, Grapp M, Schreiber K, Gronborg M, Urlaub H, Becker S, Asif AR, Gartner J, Sheldrick GM, Steinfeld R. 2009. Structure of tripeptidyl-peptidase I provides insight into the molecular basis of late infantile neuronal ceroid lipofuscinosis. *J Biol Chem* **284**(6): 3976-3984.

Parlati F, McNew JA, Fukuda R, Miller R, Sollner TH, Rothman JE. 2000. Topological restriction of SNARE-dependent membrane fusion. *Nature* **407**(6801): 194-198.

Parsot C, Hamiaux C, Page AL. 2003. The various and varying roles of specific chaperones in type III secretion systems. *Curr Opin Microbiol* **6**(1): 7-14.

Perrakis A, Morris R, Lamzin VS. 1999. Automated protein model building combined with iterative structure refinement. *Nat Struct Biol* **6**(5): 458-463.

Pfoh R, Laatsch H, Sheldrick GM. 2008. Crystal structure of trioxacarcin A covalently bound to DNA. *Nucleic Acids Res* **36**(10): 3508-3514.

Pitzschke A, Schikora A, Hirt H. 2009. MAPK cascade signalling networks in plant defence. *Curr Opin Plant Biol* **12**(4): 421-426.

Pohronezny K, Moss MA, Dankers W, Schenk J. 1990. Dispersal and Management of *Xanthomonas campestris* pv. *vesicatoria*. During Thinning of Direct-Seeded Tomato. *Plant Dis* **74**: 800-805.

Potnis N, Krasileva K, Chow V, Almeida NF, Patil PB, Ryan RP, Sharlach M, Behlau F, Dow JM, Momol M, White FF, Preston JF, Vinatzer BA, Koebnik R, Setubal JC, Norman DJ, Staskawicz BJ, Jones JB. 2011. Comparative genomics reveals diversity among xanthomonads infecting tomato and pepper. *BMC Genomics* **12**: 146.

PyMOL. 2006. (The PyMOL Molecular Graphics System, Version 1.5) (Schrödinger, LLC, version 0.99, 2006).

Qian W, Jia Y, Ren SX, He YQ, Feng JX, Lu LF, Sun Q, Ying G, Tang DJ, Tang H, Wu W, Hao P, Wang L, Jiang BL, Zeng S, Gu WY, Lu G, Rong L, Tian Y, Yao Z, Fu G, Chen B, Fang R, Qiang B, Chen Z, Zhao GP, Tang JL, He C. 2005. Comparative and functional genomic analyses of the pathogenicity of phytopathogen *Xanthomonas campestris* pv. *campestris*. *Genome Res* **15**(6): 757-767.

Quezada CM, Hicks SW, Galan JE, Stebbins CE. 2009. A family of Salmonella virulence factors functions as a distinct class of autoregulated E3 ubiquitin ligases. *Proc Natl Acad Sci U S A* **106**(12): 4864-4869.

Ranf S, Eschen-Lippold L, Pecher P, Lee J, Scheel D. 2011. Interplay between calcium signalling and early signalling elements during defence responses to microbe- or damage-associated molecular patterns. *Plant J* **68**(1): 100-113.

Rape M. 2010. Assembly of k11-linked ubiquitin chains by the anaphase-promoting complex. *Subcell Biochem* **54**: 107-115.

Ray SK, Rajeshwari R, Sharma Y, Sonti RV. 2002. A high-molecular-weight outer membrane protein of *Xanthomonas oryzae* pv. *oryzae* exhibits similarity to non-fimbrial adhesins of animal pathogenic bacteria and is required for optimum virulence. *Mol Microbiol* **46**(3): 637-647.

Records AR. 2011. The type VI secretion system: a multipurpose delivery system with a phage-like machinery. *Mol Plant Microbe Interact* **24**(7): 751-757.

Robert-Seilaniantz A, Shan L, Zhou JM, Tang X. 2006. The *Pseudomonas syringae* pv. *tomato* DC3000 type III effector HopF2 has a putative myristoylation site required for its avirulence and virulence functions. *Mol Plant Microbe Interact* **19**(2): 130-138.

Rock KL, Gramm C, Rothstein L, Clark K, Stein R, Dick L, Hwang D, Goldberg AL. 1994. Inhibitors of the proteasome block the degradation of most cell proteins and the generation of peptides presented on MHC class I molecules. *Cell* **78**(5): 761-771.

Roden J, Eardley L, Hotson A, Cao Y, Mudgett MB. 2004. Characterization of the *Xanthomonas* AvrXv4 effector, a SUMO protease translocated into plant cells. *Mol Plant Microbe Interact* **17**(6): 633-643.

Roden JA, Belt B, Ross JB, Tachibana T, Vargas J, Mudgett MB. 2004. A genetic screen to isolate type III effectors translocated into pepper cells during *Xanthomonas* infection. *Proc Natl Acad Sci U S A* **101**(47): 16624-16629.

Rodriguez-Herva JJ, Gonzalez-Melendi P, Cuartas-Lanza R, Antunez-Lamas M, Rio-Alvarez I, Li Z, Lopez-Torrejon G, Diaz I, Del Pozo JC, Chakravarthy S, Collmer A, Rodriguez-Palenzuela P, Lopez-Solanilla E. 2012. A bacterial cysteine protease effector protein interferes with photosynthesis to suppress plant innate immune responses. *Cell Microbiol* **14**(5): 669-681.

Rodriguez MC, Petersen M, Mundy J. 2010. Mitogen-activated protein kinase signaling in plants. *Annu Rev Plant Biol* **61**: 621-649.

Rohde JR, Breitkreutz A, Chenal A, Sansonetti PJ, Parsot C. 2007. Type III secretion effectors of the IpaH family are E3 ubiquitin ligases. *Cell Host Microbe* **1**(1): 77-83.

Römer P, Hahn S, Jordan T, Strauss T, Bonas U, Lahaye T. 2007. Plant pathogen recognition mediated by promoter activation of the pepper *Bs3* resistance gene. *Science* **318**(5850): 645-648.

Ronald PC und Staskawicz BJ. 1988. The avirulence gene *avrBs1* from *Xanthomonas campestris* pv. *vesicatoria* encodes a 50-kD protein. *Mol Plant Microbe Interact* **1**(5): 191-198.

Rosebrock TR, Zeng L, Brady JJ, Abramovitch RB, Xiao F, Martin GB. 2007. A bacterial E3 ubiquitin ligase targets a host protein kinase to disrupt plant immunity. *Nature* **448**(7151): 370-374.

Rossier O, Van den Ackerveken G, Bonas U. 2000. HrpB2 and HrpF from *Xanthomonas* are type III-secreted proteins and essential for pathogenicity and recognition by the host plant. *Mol Microbiol* **38**(4): 828-838.

Rossier O, Wengelnik K, Hahn K, Bonas U. 1999. The *Xanthomonas* Hrp type III system secretes proteins from plant and mammalian pathogens. *Proc Natl Acad Sci USA* **96**(16): 9368-9373.

Rytkonen A, Poh J, Garmendia J, Boyle C, Thompson A, Liu M, Freemont P, Hinton JC, Holden DW. 2007. SseL, a Salmonella deubiquitinase required for macrophage killing and virulence. *Proc Natl Acad Sci U S A* **104**(9): 3502-3507.

Saijo Y, Tintor N, Lu X, Rauf P, Pajerowska-Mukhtar K, Haweker H, Dong X, Robatzek S, Schulze-Lefert P. 2009. Receptor quality control in the endoplasmic reticulum for plant innate immunity. *EMBO J* **28**(21): 3439-3449.

Sakata E, Satoh T, Yamamoto S, Yamaguchi Y, Yagi-Utsumi M, Kurimoto E, Tanaka K, Wakatsuki S, Kato K. 2010. Crystal structure of UbcH5b~ubiquitin intermediate: insight into the formation of the self-assembled E2~Ub conjugates. *Structure* **18**(1): 138-147.

Salomon D, Bosis E, Dar D, Nachman I, Sessa G. 2012. Expression of *Pseudomonas syringae* type III effectors in yeast under stress conditions reveals that HopX1 attenuates activation of the high osmolarity glycerol MAP kinase pathway. *Microbiology*.

Salomon D, Dar D, Sreeramulu S, Sessa G. 2011. Expression of *Xanthomonas campestris* pv. *vesicatoria* type III effectors in yeast affects cell growth and viability. *Mol Plant Microbe Interact* **24**(3): 305-314.

Sandkvist M. 2001. Biology of type II secretion. *Mol Microbiol* **40**(2): 271-283.

Schäfer A, Tauch A, Jäger W, Kalinowski J, Thierbach G, Pühler A. 1994. Small mobilizable multi-purpose cloning vectors derived from the *Escherichia coli* plasmids pK18 and pK19: selection of defined deletions in the chromosome of *Corynebacterium glutamicum*. *Gene* **145**(1): 69-73.

Schlicker C, Fokina O, Kloft N, Grune T, Becker S, Sheldrick GM, Forchhammer K. 2008. Structural analysis of the PP2C phosphatase tPphA from Thermosynechococcus elongatus: a flexible flap subdomain controls access to the catalytic site. *J Mol Biol* **376**(2): 570-581.

Schneider TR und Sheldrick GM. 2002. Substructure solution with SHELXD. *Acta Crystallogr D Biol Crystallogr* **58**(Pt 10 Pt 2): 1772-1779.

Scholze H und Boch J. 2011. TAL effectors are remote controls for gene activation. *Curr Opin Microbiol* **14**(1): 47-53.

Schonsky A. 2013. Molekulare Charakterisierung neuer Typ III Effektorproteine sowie des Effektors XopB aus *Xanthomonas campestris* pv. *vesicatoria.* PhD thesis, Martin-Luther-Universität Halle-Wittenberg Halle.

Schulze S, Kay S, Büttner D, Egler M, Eschen-Lippold L, Hause G, Krüger A, Lee J, Müller O, Scheel D, Szczesny R, Thieme F, Bonas U. 2012. Analysis of new type III effectors from *Xanthomonas* uncovers XopB and XopS as suppressors of plant immunity. *New Phytol* **195**(4): 894-911.

Sels J, Mathys J, De Coninck BM, Cammue BP, De Bolle MF. 2008. Plant pathogenesis-related (PR) proteins: a focus on PR peptides. *Plant Physiol Biochem* **46**(11): 941-950.

Sevvana M, Vijayan V, Zweckstetter M, Reinelt S, Madden DR, Herbst-Irmer R, Sheldrick GM, Bott M, Griesinger C, Becker S. 2008. A ligand-induced switch in the periplasmic domain of sensor histidine kinase CitA. *J Mol Biol* **377**(2): 512-523.

Shan L, He P, Li J, Heese A, Peck SC, Nurnberger T, Martin GB, Sheen J. 2008. Bacterial effectors target the common signaling partner BAK1 to disrupt multiple MAMP receptor-signaling complexes and impede plant immunity. *Cell Host Microbe* **4**(1): 17-27.

Shao F, Golstein C, Ade J, Stoutemyer M, Dixon JE, Innes RW. 2003. Cleavage of Arabidopsis PBS1 by a bacterial type III effector. *Science* **301**(5637): 1230-1233.

Sheldrick GM. 2008. A short history of SHELX. *Acta Crystallogr A* **64**(Pt 1): 112-122.

Sheng Y, Hong JH, Doherty R, Srikumar T, Shloush J, Avvakumov GV, Walker JR, Xue S, Neculai D, Wan JW, Kim SK, Arrowsmith CH, Raught B, Dhe-Paganon S. 2012. A human ubiquitin conjugating enzyme (E2) - HECT E3 ligase structure-function screen. *Mol Cell Proteomics*.

Shrestha R, Tsuchiya K, Baek S, Bae H, Hwang I, Hur J, Lim C. 2005. Identification of the dspEF, hrpW, and hrpN loci and characterization of the hrpNEP gene in Erwinia pyrifoliae. *Journal of General Plant Pathology* **71**: 211-220.

Simpson AJReinach FCArruda PAbreu FAAcencio MAlvarenga RAlves LMAraya JEBaia GSBaptista CSBarros MHBonaccorsi EDBordin SBove JMBriones MRBueno MRCamargo AACamargo LECarraro DMCarrer HColauto NBColombo CCosta FFCosta MCCosta-Neto CMCoutinho LLCristofani MDias-Neto EDocena CEl-Dorry HFacincani APFerreira AJFerreira VCFerro JAFraga JSFranca SCFranco MCFrohme MFurlan LRGarnier MGoldman GHGoldman MHGomes SLGruber AHo PLHoheisel JDJunqueira MLKemper ELKitajima JPKrieger JEKuramae EELaigret FLambais MRLeite LCLemos EGLemos MVLopes SALopes CRMachado JAMachado MAMadeira AMMadeira HMMarino CLMarques MVMartins EAMartins EMMatsukuma AYMenck CFMiracca ECMiyaki CYMonteriro-Vitorello CBMoon DHNagai MANascimento ALNetto LENhani A, Jr.Nobrega FGNunes LROliveira MAde Oliveira MCde Oliveira RCPalmieri DAParis APeixoto BRPereira GAPereira HA, Jr.Pesquero JBQuaggio RBRoberto PGRodrigues Vde MRAJde Rosa VE, Jr.de Sa RGSantelli RVSawasaki HEda Silva ACda Silva AMda Silva FRda Silva WA, Jr.da Silveira JFSilvestri MLSiqueira WJde Souza AAde Souza APTerenzi MFTruffi DTsai SMTsuhako MHVallada HVan Sluys MAVerjovski-Almeida SVettore ALZago MAZatz MMeidanis J und Setubal JC. 2000. The genome sequence of the plant pathogen Xylella fastidiosa. The *Xylella fastidiosa* Consortium of the Organization for Nucleotide Sequencing and Analysis. *Nature* **406**(6792): 151-159.

Singer AU, Desveaux D, Betts L, Chang JH, Nimchuk Z, Grant SR, Dangl JL, Sondek J. 2004. Crystal structures of the type III effector protein AvrPphF and its chaperone reveal residues required for plant pathogenesis. *Structure* **12**(9): 1669-1681.

Singer AU, Rohde JR, Lam R, Skarina T, Kagan O, Dileo R, Chirgadze NY, Cuff ME, Joachimiak A, Tyers M, Sansonetti PJ, Parsot C, Savchenko A. 2008. Structure of the Shigella T3SS effector IpaH defines a new class of E3 ubiquitin ligases. *Nat Struct Mol Biol* **15**(12): 1293-1301.

Singer AU, Schulze S, Skarina T, Xu X, Cui H, Eschen-Lippold L, Egler M, Srikumar T, Raught B, Lee J, Scheel D, Savchenko A, Bonas U. 2013. A Pathogen Type III Effector with a Novel E3 Ubiquitin Ligase Architecture. *PLoS Pathog* **9**(1): e1003121.

Smits GJ, van den Ende H, Klis FM. 2001. Differential regulation of cell wall biogenesis during growth and development in yeast. *Microbiology* **147**(Pt 4): 781-794.

Song C und Yang B. 2010. Mutagenesis of 18 type III effectors reveals virulence function of XopZ(PXO99) in *Xanthomonas oryzae* pv. *oryzae*. *Mol Plant Microbe Interact* **23**(7): 893-902.

Speth EB, Lee YN, He SY. 2007. Pathogen virulence factors as molecular probes of basic plant cellular functions. *Curr Opin Plant Biol* **10**(6): 580-586.

Srikumar T, Jeram SM, Lam H, Raught B. 2010. A ubiquitin and ubiquitin-like protein spectral library. *Proteomics* **10**(2): 337-342.

Stall R, Bartz J, AA. C. 1974. Decreased hypersensitivity to xanthomonads in pepper after inoculations with virulent cells of *Xanthomonas vesicatoria*. *Phytopathology* **64**: 731-735.

Stall RE, Jones JB, Minsavage GV. 2009. Durability of resistance in tomato and pepper to xanthomonads causing bacterial spot. *Annu Rev Phytopathol* **47**: 265-284.

Stall RE und Minsavage GV 1996. Methods for screening for bacterial spot resistance genes, Bs1, Bs2 and Bs3, in a single pepper plant.In. *National pepper conference*. Naples.

Staskawicz B, Dahlbeck D, Keen N, Napoli C. 1987. Molecular characterization of cloned avirulence genes from race 0 and race 1 of *Pseudomonas syringae* pv. *glycinea*. *J Bacteriol* **169**(12): 5789-5794.

Stevens JM, Galyov EE, Stevens MP. 2006. Actin-dependent movement of bacterial pathogens. *Nat Rev Microbiol* **4**(2): 91-101.

Strange RN. 2007. Phytotoxins produced by microbial plant pathogens. *Nat Prod Rep* **24**(1): 127-144.

Sunter G, Sunter JL, Bisaro DM. 2001. Plants expressing tomato golden mosaic virus AL2 or beet curly top virus L2 transgenes show enhanced susceptibility to infection by DNA and RNA viruses. *Virology* **285**(1): 59-70.

Sweet CR, Conlon J, Golenbock DT, Goguen J, Silverman N. 2007. YopJ targets TRAF proteins to inhibit TLR-mediated NF-kappaB, MAPK and IRF3 signal transduction. *Cell Microbiol* **9**(11): 2700-2715.

Szczesny R. 2009. Molekulare und funktionelle Charakterisierung der Typ-III-Effektoren AvrBs1, AvrBsT und XopJ aus *Xanthomonas campestris* pv. *vesicatoria.* PhD thesis, Martin-Luther-Universität Halle-Wittenberg Halle.

Szczesny R, Büttner D, Escolar L, Schulze S, Seiferth A, Bonas U. 2010a. Suppression of the AvrBs1-specific hypersensitive response by the YopJ effector homolog AvrBsT from *Xanthomonas* depends on a SNF1-related kinase. *New Phytol* **187**(4): 1058-1074.

Szczesny R, Jordan M, Schramm C, Schulz S, Cogez V, Bonas U, Buttner D. 2010b. Functional characterization of the Xcs and Xps type II secretion systems from the plant pathogenic bacterium *Xanthomonas campestris* pv *vesicatoria*. *New Phytol* **187**(4): 983-1002.

Szurek B, Rossier O, Hause G, Bonas U. 2002. Type III-dependent translocation of the *Xanthomonas* AvrBs3 protein into the plant cell. *Mol Microbiol* **46**(1): 13-23.

Tampakaki AP, Fadouloglou VE, Gazi AD, Panopoulos NJ, Kokkinidis M. 2004. Conserved features of type III secretion. *Cell Microbiol* **6**(9): 805-816.

Tao Y, Xie Z, Chen W, Glazebrook J, Chang HS, Han B, Zhu T, Zou G, Katagiri F. 2003. Quantitative nature of Arabidopsis responses during compatible and incompatible interactions with the bacterial pathogen *Pseudomonas syringae*. *Plant Cell* **15**(2): 317-330.

Taylor KW, Kim JG, Su XB, Aakre CD, Roden JA, Adams CM, Mudgett MB. 2012. Tomato TFT1 is required for PAMP-triggered immunity and mutations that prevent T3S effector XopN from binding to TFT1 attenuate *Xanthomonas* virulence. *PLoS Pathog* **8**(6): e1002768.

Tena G, Boudsocq M, Sheen J. 2011. Protein kinase signaling networks in plant innate immunity. *Curr Opin Plant Biol* **14**(5): 519-529.

Thieme F, Koebnik R, Bekel T, Berger C, Boch J, Büttner D, Caldana C, Gaigalat L, Goesmann A, Kay S, Kirchner O, Lanz C, Linke B, McHardy AC, Meyer F, Mittenhuber G, Nies DH, Niesbach-Klosgen U, Patschkowski T, Ruckert C, Rupp O, Schneiker S, Schuster SC, Vorholter FJ, Weber E, Puhler A, Bonas U, Bartels D, Kaiser O. 2005. Insights into genome plasticity and pathogenicity of the plant pathogenic bacterium *Xanthomonas campestris* pv. *vesicatoria* revealed by the complete genome sequence. *J Bacteriol* **187**(21): 7254-7266.

Thieme F, Szczesny R, Urban A, Kirchner O, Hause G, Bonas U. 2007. New type III effectors from *Xanthomonas campestris* pv. *vesicatoria* trigger plant reactions dependent on a conserved N-myristoylation motif. *Mol Plant Microbe Interact* **20**(10): 1250-1261.

Thilmony R, Underwood W, He SY. 2006. Genome-wide transcriptional analysis of the *Arabidopsis thaliana* interaction with the plant pathogen *Pseudomonas syringae* pv. *tomato* DC3000 and the human pathogen *Escherichia coli* O157:H7. *Plant J* **46**(1): 34-53.

Thompson JD, Gibson TJ, Plewniak F, Jeanmougin F, Higgins DG. 1997. The CLUSTAL_X windows interface: flexible strategies for multiple sequence alignment aided by quality analysis tools. *Nucleic Acids Res* **25**(24): 4876-4882.

Thordal-Christensen H. 2003. Fresh insights into processes of nonhost resistance. *Curr Opin Plant Biol* **6**(4): 351-357.

Toth IK und Birch PR. 2005. Rotting softly and stealthily. *Curr Opin Plant Biol* **8**(4): 424-429.

Tsiamis G, Mansfield JW, Hockenhull R, Jackson RW, Sesma A, Athanassopoulos E, Bennett MA, Stevens C, Vivian A, Taylor JD, Murillo J. 2000. Cultivar-specific avirulence and virulence functions assigned to avrPphF in *Pseudomonas syringae* pv. *phaseolicola*, the cause of bean halo-blight disease. *EMBO J* **19**(13): 3204-3214.

Tyrrell M, Campanoni P, Sutter JU, Pratelli R, Paneque M, Sokolovski S, Blatt MR. 2007. Selective targeting of plasma membrane and tonoplast traffic by inhibitory (dominant-negative) SNARE fragments. *Plant J* **51**(6): 1099-1115.

Van den Ackerveken G, Marois E, Bonas U. 1996. Recognition of the bacterial avirulence protein AvrBs3 occurs inside the host plant cell. *Cell* **87**(7): 1307-1316.

van Dijk K, Tam VC, Records AR, Petnicki-Ocwieja T, Alfano JR. 2002. The ShcA protein is a molecular chaperone that assists in the secretion of the HopPsyA effector from the type III (Hrp) protein secretion system of *Pseudomonas syringae*. *Mol Microbiol* **44**(6): 1469-1481.

Van Larebeke N, Engler G, Holsters M, Van den Elsacker S, Zaenen I, Schilperoort RA, Schell J. 1974. Large plasmid in Agrobacterium tumefaciens essential for crown gall-inducing ability. *Nature* **252**(5479): 169-170.

van Ooijen G, van den Burg HA, Cornelissen BJ, Takken FL. 2007. Structure and function of resistance proteins in solanaceous plants. *Annu Rev Phytopathol* **45**: 43-72.

VanDemark AP, Hofmann RM, Tsui C, Pickart CM, Wolberger C. 2001. Molecular insights into polyubiquitin chain assembly: crystal structure of the Mms2/Ubc13 heterodimer. *Cell* **105**(6): 711-720.

Vauterin L, Rademaker J, Swings J. 2000. Synopsis on the taxonomy of the genus *xanthomonas*. *Phytopathology* **90**(7): 677-682.

Vieira J und Messing J. 1987. Production of single-stranded plasmid DNA. *Methods Enzymol* **153**: 3-11.

Vierstra RD. 2009. The ubiquitin-26S proteasome system at the nexus of plant biology. *Nat Rev Mol Cell Biol* **10**(6): 385-397.

Vivian A, Arnold, DL. 2000. Bacterial effector genes and their role in host pathogen interactions. *Journal of Plant Pathology* **82**: 163-178.

Walter M, Chaban C, Schutze K, Batistic O, Weckermann K, Nake C, Blazevic D, Grefen C, Schumacher K, Oecking C, Harter K, Kudla J. 2004. Visualization of protein interactions in living plant cells using bimolecular fluorescence complementation. *Plant J* **40**(3): 428-438.

Wang W, Vinocur B, Shoseyov O, Altman A. 2004. Role of plant heat-shock proteins and molecular chaperones in the abiotic stress response. *Trends Plant Sci* **9**(5): 244-252.

Wang Y, Li J, Hou S, Wang X, Li Y, Ren D, Chen S, Tang X, Zhou JM. 2010. A *Pseudomonas syringae* ADP-ribosyltransferase inhibits Arabidopsis mitogen-activated protein kinase kinases. *Plant Cell* **22**(6): 2033-2044.

Waterfield NR, Daborn PJ, Dowling AJ, Yang G, Hares M, ffrench-Constant RH. 2003. The insecticidal toxin makes caterpillars floppy 2 (Mcf2) shows similarity to HrmA, an avirulence protein from a plant pathogen. *FEMS Microbiol Lett* **229**(2): 265-270.

Weber E, Ojanen-Reuhs T, Huguet E, Hause G, Romantschuk M, Korhonen TK, Bonas U, Koebnik R. 2005. The type III-dependent Hrp pilus is required for productive interaction of *Xanthomonas campestris* pv. *vesicatoria* with pepper host plants. *J Bacteriol* **187**(7): 2458-2468.

Wei CF, Kvitko BH, Shimizu R, Crabill E, Alfano JR, Lin NC, Martin GB, Huang HC, Collmer A. 2007. A *Pseudomonas syringae* pv. *tomato* DC3000 mutant lacking the type III effector HopQ1-1 is able to cause disease in the model plant *Nicotiana benthamiana*. *Plant J* **51**(1): 32-46.

Wengelnik K und Bonas U. 1996. HrpXv, an AraC-type regulator, activates expression of five of the six loci in the *hrp* cluster of *Xanthomonas campestris* pv. vesicatoria. *J Bacteriol* **178**(12): 3462-3469.

Wengelnik K, Marie C, Russel M, Bonas U. 1996a. Expression and localization of HrpA1, a protein of *Xanthomonas campestris* pv. *vesicatoria* essential for pathogenicity and induction of the hypersensitive reaction. *J Bacteriol* **178**(4): 1061-1069.

Wengelnik K, Rossier O, Bonas U. 1999. Mutations in the regulatory gene *hrpG* of *Xanthomonas campestris* pv. *vesicatoria* result in constitutive expression of all *hrp* genes. *J Bacteriol* **181**(21): 6828-6831.

Wengelnik K, Van den Ackerveken G, Bonas U. 1996b. HrpG, a key *hrp* regulatory protein of *Xanthomonas campestris* pv. *vesicatoria* is homologous to two-component response regulators. *Mol Plant-Microbe Interact* **9**: 704-712.

Whalen M, Richter T, Zakhareyvich K, Yoshikawa M, Al-Azzeh D, Adefioye A, Spicer G, Mendoza LL, Morales CQ, Klassen V, Perez-Baron G, Toebe CS, Tzovolous A, Gerstman E, Evans E, Thompson C, Lopez M, Ronald PC. 2008. Identification of a host 14-3-3 Protein that Interacts with *Xanthomonas* effector AvrRxv. *Physiol Mol Plant Pathol* **72**(1-3): 46-55.

Whalen MC, Wang JF, Carland FM, Heiskell ME, Dahlbeck D, Minsavage GV, Jones JB, Scott JW, Stall RE, Staskawicz BJ. 1993. Avirulence gene *avrRxv* from *Xanthomonas campestris* pv. *vesicatoria* specifies resistance on tomato line Hawaii 7998. *Mol Plant Microbe Interact* **6**(5): 616-627.

White FF, Potnis N, Jones JB, Koebnik R. 2009. The type III effectors of *Xanthomonas*. *Mol Plant Pathol* **10**(6): 749-766.

Wichmann G und Bergelson J. 2004. Effector genes of *Xanthomonas axonopodis* pv. *vesicatoria* promote transmission and enhance other fitness traits in the field. *Genetics* **166**(2): 693-706.

Wickliffe KE, Williamson A, Meyer HJ, Kelly A, Rape M. 2011. K11-linked ubiquitin chains as novel regulators of cell division. *Trends Cell Biol* **21**(11): 656-663.

Wilharm G, Dittmann S, Schmid A, Heesemann J. 2007. On the role of specific chaperones, the specific ATPase, and the proton motive force in type III secretion. *Int J Med Microbiol* **297**(1): 27-36.

Willems AR, Schwab M, Tyers M. 2004. A hitchhiker's guide to the cullin ubiquitin ligases: SCF and its kin. *Biochim Biophys Acta* **1695**(1-3): 133-170.

Williams JW, Langer JS, Northrop DB. 1975. A spectrophotometric assay for gentamicin. *J Antibiot (Tokyo)* **28**(12): 982-987.

Wilton M, Subramaniam R, Elmore J, Felsensteiner C, Coaker G, Desveaux D. 2010. The type III effector HopF2Pto targets Arabidopsis RIN4 protein to promote *Pseudomonas syringae* virulence. *Proc Natl Acad Sci U S A* **107**(5): 2349-2354.

Winn MD, Isupov MN, Murshudov GN. 2001. Use of TLS parameters to model anisotropic displacements in macromolecular refinement. *Acta Crystallogr D Biol Crystallogr* **57**(Pt 1): 122-133.

Winn MD, Murshudov, G.N. & Papiz, M.Z. 2003. Macromolecular TLS refinement in REFMAC at moderate resolutions. *Methods Enzymol.* , 300-321

Wood DW, Setubal JC, Kaul R, Monks DE, Kitajima JP, Okura VK, Zhou Y, Chen L, Wood GE, Almeida NF, Jr., Woo L, Chen Y, Paulsen IT, Eisen JA, Karp PD, Bovee D, Sr., Chapman P, Clendenning J, Deatherage G, Gillet W, Grant C, Kutyavin T, Levy R, Li MJ, McClelland E, Palmieri A, Raymond C, Rouse G, Saenphimmachak C, Wu Z, Romero P, Gordon D, Zhang S, Yoo H, Tao Y, Biddle P, Jung M, Krespan W, Perry M, Gordon-Kamm B, Liao L, Kim S, Hendrick C, Zhao ZY, Dolan M, Chumley F, Tingey SV, Tomb JF, Gordon MP, Olson MV, Nester EW. 2001. The genome of the natural genetic engineer *Agrobacterium tumefaciens* C58. *Science* **294**(5550): 2317-2323.

Wu B, Skarina T, Yee A, Jobin MC, Dileo R, Semesi A, Fares C, Lemak A, Coombes BK, Arrowsmith CH, Singer AU, Savchenko A. 2010. NleG Type 3 effectors from enterohaemorrhagic Escherichia coli are U-Box E3 ubiquitin ligases. *PLoS Pathog* **6**(6): e1000960.

Xiang T, Zong N, Zhang J, Chen J, Chen M, Zhou JM. 2011. BAK1 is not a target of the *Pseudomonas syringae* effector AvrPto. *Mol Plant Microbe Interact* **24**(1): 100-107.

Xiang T, Zong N, Zou Y, Wu Y, Zhang J, Xing W, Li Y, Tang X, Zhu L, Chai J, Zhou JM. 2008. *Pseudomonas syringae* effector AvrPto blocks innate immunity by targeting receptor kinases. *Curr Biol* **18**(1): 74-80.

Xu P, Duong DM, Seyfried NT, Cheng D, Xie Y, Robert J, Rush J, Hochstrasser M, Finley D, Peng J. 2009. Quantitative proteomics reveals the function of unconventional ubiquitin chains in proteasomal degradation. *Cell* **137**(1): 133-145.

Yang B, Sugio A, White FF. 2006. *Os8N3* is a host disease-susceptibility gene for bacterial blight of rice. *Proc Natl Acad Sci U S A* **103**(27): 10503-10508.

Ye Y und Rape M. 2009. Building ubiquitin chains: E2 enzymes at work. *Nat Rev Mol Cell Biol* **10**(11): 755-764.

Zhang J, Shao F, Li Y, Cui H, Chen L, Li H, Zou Y, Long C, Lan L, Chai J, Chen S, Tang X, Zhou JM. 2007. A *Pseudomonas syringae* effector inactivates MAPKs to suppress PAMP-induced immunity in plants. *Cell Host Microbe* **1**(3): 175-185.

Zhang Y, Higashide WM, McCormick BA, Chen J, Zhou D. 2006. The inflammation-associated Salmonella SopA is a HECT-like E3 ubiquitin ligase. *Mol Microbiol* **62**(3): 786-793.

Zhao B, Dahlbeck D, Krasileva KV, Fong RW, Staskawicz BJ. 2011. Computational and biochemical analysis of the *Xanthomonas* effector AvrBs2 and its role in the modulation of *Xanthomonas* type three effector delivery. *PLoS Pathog* **7**(12): e1002408.

Zheng MS, Takahashi H, Miyazaki A, Hamamoto H, Shah J, Yamaguchi I, Kusano T. 2004. Up-regulation of *Arabidopsis thaliana NHL10* in the hypersensitive response to Cucumber mosaic virus infection and in senescing leaves is controlled by signalling pathways that differ in salicylate involvement. *Planta* **218**(5): 740-750.

Zhou JM und Chai J. 2008. Plant pathogenic bacterial type III effectors subdue host responses. *Curr Opin Microbiol* **11**(2): 179-185.

Zhu Y, Li H, Hu L, Wang J, Zhou Y, Pang Z, Liu L, Shao F. 2008. Structure of a Shigella effector reveals a new class of ubiquitin ligases. *Nat Struct Mol Biol* **15**(12): 1302-1308.

Zipfel C. 2008. Pattern-recognition receptors in plant innate immunity. *Curr Opin Immunol* **20**(1): 10-16.

Zipfel C, Kunze G, Chinchilla D, Caniard A, Jones JD, Boller T, Felix G. 2006. Perception of the bacterial PAMP EF-Tu by the receptor EFR restricts Agrobacterium-mediated transformation. *Cell* **125**(4): 749-760.

Zipfel C, Robatzek S, Navarro L, Oakeley EJ, Jones JD, Felix G, Boller T. 2004. Bacterial disease resistance in Arabidopsis through flagellin perception. *Nature* **428**(6984): 764-767.

Zwart PH, Afonine PV, Grosse-Kunstleve RW, Hung LW, Ioerger TR, McCoy AJ, McKee E, Moriarty NW, Read RJ, Sacchettini JC, Sauter NK, Storoni LC, Terwilliger TC, Adams PD. 2008. Automated structure solution with the PHENIX suite. *Methods Mol Biol* **426**: 419-435.

5. Anhang

Verwendete Oligonukleotide

Name	Sequenz (5´- 3´)	Bemerkung
xopL_entr_for	CACCATGCGACGCGTCGATCAACC	Generierung von pENTR/DxopL und pENTR/Dlrr
3220_strep_rev	CTATTTTTCGAACTGCGGGTGGCTCCACTGATGGCCT	Generierung von pENTR/DxopL und pENTR/Dcdom
L_D502A_for	AGCACGGTCATCGCAGAAGAAAGAAAT	Generierung von pENTR/DxopLD502A
L_D502A_rev	CAGCATGGCCTGTGCGGTGTCTTC	Generierung von pENTR/DxopLD502A
L_K578A_for	GTCAGCAACTGGGCAGCGCAGAAGAGC	Generierung von pENTR/DxopLK578A
L_K578A_rev	TGGCGTGTAGTGGCGGGCGAGGCC	Generierung von pENTR/DxopLK578A
L_A579W_for	AGCAACTGGAAGTGGCAGAAGAGCGCA	Generierung von pENTR/DxopLA579W
L_A579W_rev	GACGTTCGTGTAGTGGCGGGCGAG	Generierung von pENTR/DxopLA579W
L_Q612A_for	GCCAAGGCAGTGGCAATGTGGAAGACC	Generierung von pENTR/DxopLQ612A
L_Q612A_rev	CAATGTCGCTACGTCGAGCGGGCT	Generierung von pENTR/DxopLQ612A
L_L619A_for	AAGACCCGTGAGGCAATCGTCCACGCA	Generierung von pENTR/DxopLL619A
L_L619A_rev	CCACATCTGCACTGCCTTGGCCAA	Generierung von pENTR/DxopLL619A
L_d163_185_for	ACAGGCCGGGCGCTGAAGGCGACAGCC	Generierung von pENTR/DxopLΔ163-185
L_d163_185_rev	GTTGTAGTGGCGTTGCCATTGCGACAG	Generierung von pENTR/DxopLΔ163-185
3220-F1-Eco(2)	AAAGAATTCGCACAGGCAAGCATGGCG	Generierung von pK18xopL
3220 R1-BamHI	AAAGGATCCCGCATTCCTCGTCTTGGCTG	Generierung von pK18xopL
3220 F2-BamHI	AAAGGATCCAGAGCCAACGCGACAGGC	Generierung von pK18xopL
3220 R2-XbaI	AAATCTAGACTGATCCGTCGCAAGCCG	Generierung von pK18xopL
3220-F993 entry	CACCCGCGGCCCGCAGCAATGGCAGACAC	Generierung von pENTR/DxopL+Promotor
3220-R276	GTTCATCCGCGCGGCGCTGC	Generierung von pENTR/DxopL+Promotor
xopL_RT_for	CGACCAGGCATTCCGTCTTTCG	RT-PCR
xopL_RT_rev	TGACGGAACTTCCCGAACCCCT	RT-PCR
3220_LRR_strep_rev	CTATTTTTCGAACTGCGGGTGGCTCCATTCGGCGGGG	Generierung von pENTR/Dlrr
3220_CDOM-for	CACCATGCCAGGGCGGACCGGACCG	Generierung von pENTR/Dcdom
R311for	GGATCGATCGCTTCCGGCGTCCA	Generierung von pENTR/DxopLR311A
R311rev	CGGTCCATTCCAGTGCTAGGCTCTG	Generierung von pENTR/DxopLR311A
W314for	CTACGGCTGGAAGCAACCGGGATCAGAT	Generierung von pENTR/DxopLW314A

W314rev	GCTCTGCAGGTTGACCAAG CCCTGGTGC	Generierung von pENTR/DxopLW314A
R280for	GAGCTCTCCATCGCAGCCT GCCCGGAATT	Generierung von pENTR/DxopLR280A und pENTR/DxopLR280AW314A
R280rev	GCGTAATCGGTTGAGGCTT GCGATG	Generierung von pENTR/DxopLR280A und pENTR/DxopLR280AW314A
R258for	CTCACGCTCGCAGCCAATC CGCTTCGCGCG	Generierung von pENTRD/xopLR280A, pENTR/DxopLR258AR280A und pENTR/DxopLR258AR280AW314A
R258rev	TGTTTCCAGGCCCGCAAAT TGCTGCATGGT	Generierung von pENTRD/xopLR280A, pENTR/DxopLR258AR280A und pENTR/DxopLR258AR280AW314A
K334for	CTGAAAAGCCTGGCAATAC GCAACTCGC	Generierung von pENTR/DxopLK334A
K334rev	ATTTTGCAGGTTGGCGATG GACGCCGGA	Generierung von pENTR/DxopLK334A
R336for	AGCCTGAAGATAGCAAACT CGCCGCTGT	Generierung von pENTR/DxopLR336A
R336rev	TTTCAGATTTTGCAGGTTGG CGATGGAC	Generierung von pENTR/DxopLR336A
R379for	GCGCCACTGAAGGCACTGA ATCTGAAAG	Generierung von pENTR/DxopLR359AR379A und pENTR/DxopLR379AK383A
R379rev	ACGGCCGCCGAAAATCGGC GGATAGTTG	Generierung von pENTR/DxopLR359AR379A und pENTR/DxopLR379AK383A
R359for	GAGCTTGATTTGGCAGGCT GTACCGCGCTG	Generierung von pENTR/DxopLR359A, pENTR/DxopLR359AK383A
R359rev	CTCCAACTTTGGCAGGTGA TGGATGGCCG	Generierung von pENTR/DxopLR359A, pENTR/DxopLR359AK383A
K383for	GCGACTGATTCTGGCAGAC TGCAGCAACCT	Generierung von pENTR/DxopLK383A
K383rev	TTCAGTGGCGCACGGCCGC CGAAAATCGGC	Generierung von pENTR/DxopLK383A
d330-336_XopL_for	AACTCGCCGCTGTCCGCCC TTGGCCCG	Generierung von pENTR/DxopLΔ330-336
d330-336_XopL_rev	ATTTTGCAGGTTGGCGATG GACGC	Generierung von pENTR/DxopLΔ330-336
E598S600_AA_for	TTCGTTTATCACGCAGGAG CCCCGCTCGACGTAGC	Generierung von pENTR/DxopLE598S600AA
E598S600_AA_rev	CTGCCCGAGATGATCGACG ATGCC	Generierung von pENTR/DxopLE598S600AA
A512P513_EA_for	CCCTTTCTGGAAGGTGAAG CATCCTATCTCCCAG	Generierung von pENTR/DxopLA512P513EA
A512P513_EA_rev	ATTTCTTTCTTCATCGATGA CCGT	Generierung von pENTR/DxopLA512P513EA
R505N506_AA_for	GTCATCGATGAAGAAGCAG CTCCCTTTCTGGAAGGTG	Generierung von pENTR/DxopLR505N506AA
R505N506_AA_rev	CGTGCTCAGCATGGCCTGT GCGGT	Generierung von pENTR/DxopLR505N506AA
H584L585G586AAE_for	CAGAAGAGCGCAGCCGCG GAGATCGTCGATCAT	Generierung von pENTR/DxopLH584L585G586AAE
H584L585G586AAE_rev	CGCCTTCCAGTTGCTGACG TTCGTGTAGTG	Generierung von pENTR/DxopLH584L585G586AAE
P518K19R520AAA_for	TCCATCCTATCTCGCAGGA GCAGCCCCTACCGATGTCA CC	Generierung von pENTR/DxopLP518K519R520AAA
P518K19R520AAA_rev	GCACCTTCCAGAAAGGGAT TTCTTTC	Generierung von pENTR/DxopLP518K519R520AAA

dAb2_5f	GATTGTCGACATAACTTCC GATCAC	Generierung von pOKIΔavrBs2
dAb2_5r	GATAAGCTTGATGACCTCG AAAACGCGG	Generierung von pOKIΔavrBs2
dAb2_3f	ACGAAGCTTACCTTCCAAT CACGGCTTC	Generierung von pOKIΔavrBs2
dAb2_3r	CTGTCTAGAGCGATTCCCA CCGAGGCGC	Generierung von pOKIΔavrBs2

Danksagung

Ulla, ich danke Ihnen für die Aufnahme in Ihre Arbeitsgruppe, die Bereitstellung des spannenden Themas und für die Unterstützung bei praktischen und theoretischen Problemen. Ich danke Ihnen auch für die zahlreichen fachlichen Diskussionen, die erheblich zu unseren gemeinsamen Publikationen und dem Voranschreiten dieser Arbeit beigetragen haben.

Ich bedanke mich weiterhin bei allen Mitarbeitern der Arbeitsgruppe (present and past), insbesondere Labor 222, für die angenehme Arbeitsatmosphäre und gegenseitige Unterstützung. Es hat ´ne Menge Spaß gemacht mit euch zu arbeiten.
Ein großes Dankeschön geht auch an Simone Hahn, Cornelius Schmidtke, Sabine Thieme und Robert Szczesny für die zahlreichen fachlichen Diskussionen im Büro, Labor und während der Kaffepausen.

Ein besonderer Dank gebührt meiner Familie und meinen Freunden für die vielseitige Unterstützung und die schöne gemeinsame Zeit. Ein „Extra-Dankeschön“ geht an Steve für die tolle Zeit - we ride together, we die together - since 2001.

Aber was hätte ich nur ohne die beste Frau der Welt gemacht? Nadine - dein Vertrauen, deine Geduld, dein Zuspruch und deine Liebe haben entscheidend zu meinem Leben und meiner Arbeit beigetragen. Ich danke dir!

Zu guter Letzt danke ich Ihnen für das Lesen dieser Arbeit. Danke!

Lebenslauf

Name:	Sebastian Schulze
Anschrift:	Eichendorffstraße 32 in 06114 Halle
Geburtsdatum:	23.04.1982
Geburtsort:	Sangerhausen
Familienstand:	ledig
Staatsangehörigkeit:	deutsch

Ausbildung

1988-1992	Grundschule Sangerhausen
1992-2000	Geschwister Scholl Gymnasium, Sangerhausen Abschluss: Abitur
2001-2007	Studium der Biologie an der Martin-Luther-Universität Halle-Wittenberg
2007-2008	Diplomarbeit in der Abteilung Stress- und Entwicklungsbiologie des Leibniz-Instituts für Pflanzenbiochemie mit dem Thema: „Untersuchung eines Gens für ein Lektin-ähnliches Protein aus *Arabidopsis thaliana*“ Abschluss: Diplom-Biologe
2008-2012	Promotionsarbeit im Fachbereich Genetik am Institut für Biologie der Naturwissenschaftlichen Fakultät I der Martin-Luther-Universität Halle-Wittenberg
seit 2013	wissenschaftlicher Mitarbeiter der NOMAD Bioscience GmbH, Halle/Saale

Publikationen

Teile dieser Arbeit wurden bereits in Fachzeitschriften publiziert:

Szczesny R, Büttner D, Escolar L, Schulze S, Seiferth A, Bonas U. 2010. Suppression of the AvrBs1-specific hypersensitive response by the YopJ effector homolog AvrBsT from *Xanthomonas* depends on a SNF1-related kinase. *New Phytol* **187**(4): 1058-1074.

Schulze S, Kay S, Büttner D, Egler M, Eschen-Lippold L, Hause G, Krüger A, Lee J, Müller O, Scheel D, Szczesny R, Thieme F, Bonas U. 2012. Analysis of new type III effectors from *Xanthomonas* uncovers XopB and XopS as suppressors of plant immunity. *New Phytol* **195**(4): 894-911.

Singer AU, Schulze S, Skarina T, Xu X, Cui H, Eschen-Lippold L, Egler M, Srikumar T, Raught B, Lee J, Scheel D, Savchenko A, Bonas U. 2013. A Pathogen Type III Effector with a Novel E3 Ubiquitin Ligase Architecture. *PLoS Pathog* **9**(1): e1003121.

Nicht in diese Arbeit eingegangene Publikationen:

Eschen-Lippold L, Landgraf R, Smolka U, Schulze S, Heilmann M, Heilmann I, Hause G, Rosahl S. 2012. Activation of defense against *Phytophthora infestans* in potato by down-regulation of syntaxin gene expression. *New Phytol* **193**(4): 985-996.

Erklärung

Hiermit erkläre ich, dass ich die vorliegende wissenschaftliche Arbeit selbstständig und ohne fremde Hilfe verfasst habe. Ich erkläre weiterhin, dass andere als die von mir angegebenen Quellen und Hilfsmittel nicht benutzt, und die den benutzten Werken wörtlich oder inhaltlich entnommenen Stellen als solche kenntlich gemacht wurden. Mit dieser Arbeit bewerbe ich mich erstmals um die Erlangung des Doktorgrades.

Halle, 01. Mai 2013

Sebastian Schulze